FLIGHT TEST AND HANDLING QUALITIES ANALYSIS OF

A LONGITUDINAL FLIGHT CONTROL SYSTEM USING

MULTIOBJECTIVE TECHNIQUES

THESIS
John R. Anderson
Captain, USAF

AFIT/GAE/ENY/98M-01

19980423 068

The views expressed in this thesis are those of the author and do not reflect the official policy or

position of the department of defense or the U.S. Government

**This Document Contains Missing
Page/s That Are Unavailable In
The Original Document**

FLIGHT TEST AND HANDLING QUALITIES ANALYSIS OF

A LONGITUDINAL FLIGHT CONTROL SYSTEM

USING MULTIOBJECTIVE CONTROL DESIGN TECHNIQUES

THESIS

Presented to the Faculty of the School of Engineering

of the Air Force Institute of Technology

Air University

In Partial Fulfillment of the

Requirements for a Degree of

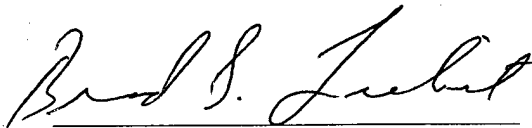Master of Science

John R. Anderson, B.S.

Captain, USAF

March 1998

FLIGHT TEST AND HANDLING QUALITIES ANALYSIS OF

A LONGITUDINAL FLIGHT CONTROL SYSTEM USING

MULTIOBJECTIVE TECHNIQUES

John R. Anderson, B.S.
Captain, USAF

Approved:

_____
Dr. Brad S. Liebst - Advisor

2-11-98
Date

_____
Maj Thomas Buter

2/12/98
Date

_____
Capt Sharon A. Heise

2/17/98
Date

Acknowledgements

This research could have not been completed without the help of many people along the way. I would first like to thank the Have Infinity II test team; Eric Boe, Maurizio Cantiello, Mark Spillman, Mike Stephens, and Jon Stevenson. They were instrumental in helping me prepare and conduct the flight test. Mark Spillman and Mike Stephens provide an invaluable "sanity" check on technical issues while the pilots took care of defining the tasks and running down logistics. It was truly a team effort.

My fellow Joint AFIT/TPS students, Lars Hoffman and Brian Ernisse were also extremely helpful throughout the program. They provided mutual support and motivation throughout this lengthy and intense program.

I would like to thank the pilots, engineers, and support personnel from Calspan Corporation, specifically Scott Buethe and Russ Easter. There dedication and outstanding support from the days of the analytical research at AFIT, implementation sims at Buffalo, and finally keeping the Learjet flying through a very demanding test schedule was truly appreciated and made for a successful flight test program.

I would like to thank my advisors, Dr. Brad Liebst and Dr. Brett Ridgely. Dr. Ridgely was the genesis of this research. This work would have not been possible without his outstanding instruction and motivation during the research phase. I wish to thank Dr. Brad Leibst for stepping in and taking the position upon Dr. Ridgely's departure for the private sector. I would also like to thank the members of my research committee, Capt Sharon Heise, and Maj Tom Buter. Their insight, constructive criticism, and willingness to review my research was truly appreciated.

An enormous debt of gratitude goes to my wife, Diane, and son Matthew. There patience, encouragement, and sacrifice for the sake of this whole joint AFIT/TPS program is something that could never be measured, nor repayed.

Table of Contents

List of Figures

ix

List of Tables

List of Abbreviations

Abbreviation	Definition
ADI	Attitude-Direction Indicator
AFB	Air Force Base
AFIT	Air Force Institute of Technology
AGL	Above Ground Level
AoA	Angle of Attack
C-H	Cooper-Harper Handling Qualities Scale
CTF	Combined Test Force
FCS	Flight Control System
HQDT	Handling Qualities During Tracking
ILS	Instrument Landing System
KIAS	Knots Indicated Airspeed
LHP	Left Half Plane
LQG	Linear Quadratic Gaussian
MOP	Measure of Performance
MWTD	Main Wheel Touchdown
PIO	Pilot in-the-Loop Oscillation
PTI	Programmed Test Input
RHP	Right Half Plane
RTO	Responsible Test Organization
SQP	Sequential Quadratic Programming
TC	Test Conductor
TPS	Test Pilot School

AFIT/GAE/ENY/98M-01

Abstract

This thesis addresses the application of optimal, multiobjective control theory control theory to flight control design for the approach and landing phase of flight. Five flight control systems were designed using classical, H_2, H_∞, and Mixed H_2/H_∞ methods. The MATLAB™ MUTOOLS™ and AFIT MXTOOLS toolboxes were used to produce the optimal, multiobjective designs. These designs were implemented for flight test on the Calspan VSS I Learjet, simulating the unstable longitudinal dynamics of an F-16 type aircraft. A limited handling qualities investigation was performed. Model following was used in the design phase to meet handling qualities specifications. The designs were successfully implemented and verified on the Calspan Learjet prior to flight test. An unmodeled aircraft mode was discovered just prior to flight test that made three of the designs slightly unstable. However, all of the designs achieved Level II or better Cooper-Harper handling qualities ratings for the landing tasks performed illustrating that the optimal multiobjective methods used can give acceptable or better handling qualities.

Flight Test and Handling Qualities Analysis of a Longitudinal Flight Control System Using Multiobjective Control Design Techniques

I. Introduction

1.1 Motivation/Background

All aircraft control system designs are based on a mathematical model of the aircraft at a specific flight condition (altitude, airspeed, weight, load factor, and gear/flap configuration). Usually, this model is not perfect. There will, in general, be many underlying assumptions made to develop the aircraft model. These assumptions include such things as: approximation of stability derivatives not easily measured, linearization of the aircraft equations of motion, and various other simplifications that make the control design problem tractable. The end result is a model which may be far from reality in its representation of the aircraft.

Classical control design techniques, such as root locus, are limited in the sense that they offer no way to incorporate allowances for the assumptions made about the aircraft model. If the actual aircraft model is significantly different from the design model, the designer is forced to go back and adjust control gains or possibly redesign the entire control law if the response is not as desired. This tuning process becomes cumbersome and time consuming for any sort of complex, multiple loop control scheme. Even at a specific flight condition where a good aircraft model exists, there are in-flight factors such as wind changes, pressure changes, temperature changes, and weight change due to fuel consumption which will alter the aircraft model. Finally, the controller will receive measurements that are corrupted by different types and levels of noise. All of these things can be looked at as uncertainties that affect the aircraft model. If there was a

way of incorporating these aircraft model, environmental, and noise uncertainties into the problem setup, it should be possible to design a more capable controller.

Multiobjective control design techniques offer the promise of addressing these uncertainties that root locus techniques cannot. These techniques allow the designer to incorporate different types of weightings to account for things like wind disturbances, sensor noise distortion, and unmodeled or changing aircraft dynamics into the design. Therefore multiobjective controllers should produce better performance for a larger range of flight conditions (i.e. they are more robust) than the classical controller .

Two classes of multiobjective control techniques that allow the designer to incorporate the types of weightings previously discussed are H_2 optimal control, and H_∞ optimal control. H_2 optimal control was derived to design for noise rejection. H_2 optimization minimizes the energy of a system's response with respect to exogenous noise disturbances that are modeled as zero-mean, unit intensity white Gaussian noises, by minimizing the specified transfer function two-norm. For example, an H_2 control design in an aircraft might minimize the noise on a pitch rate (q) signal due to turbulence and pitch rate sensor noise inputs. H_∞ optimization minimizes the energy output of a system due to an unknown, but bounded energy, input by minimizing the specified transfer function infinity-norm. An example here would be to include a weight in the design to account for unmodeled aircraft dynamics but still require tight tracking of the control command. There is a third class of optimal control called μ optimal control that was considered in this research. It is closely related to H_∞ optimal control. The difference between μ and H_∞ optimization is that μ optimal control handles multiple uncertainty constraints better than H_∞ methods. Designs that included μ optimal control techniques did not make it to Phase II of this research for reasons that will be apparent in Chapter IV.

In a realistic aircraft control design problem, there are **both** stochastic noise sources and uncertainties related to unmodeled aircraft dynamics. Therefore, there might be an advantage to designing a controller that leverages the benefits of both H_2 and H_∞ optimization.

1.2 The Mixed-Norm Problem

One of the earliest formulations of a mixed H_2 / H_∞ problem was derived by Bernstein and Haddad [1] in 1989. Their approach minimized an overbound to the H_2 norm of one transfer function and also satisfied an H_∞ constraint for a related transfer function. The inputs to each transfer function were required to be the same while the outputs could be different. In other words, there existed a controller that provided a tradeoff between robustness and noise rejection. Ridgely, et al, [2, 3] showed in 1992 that the general mixed H_2 / H_∞ problem, where no overbound to the H_2 norm is used and the subject transfer function need not be related, could not be solved analytically. They also proposed a numerical solution to the problem for a fixed order controller. This solution required unique solutions to Lyapunov equations and stabilizing solutions to Riccati equations. Although Ridgely, et al, developed a numerical solution to the problem, the implementation still did not lend itself to efficient controller design because of the large number of iterations required to solve the Lyapunov and Riccati equations. Walker [4] improved on Ridgely's method in 1994 . He re-cast Ridgely's original problem formulation as a convex optimization problem. However, this formulation did not address the problem of actually finding the optimal solution. Further work by Megretski [5] in this area indicates that the optimal solution is not rational. It can only be expressed as an infinite dimensional compensator. Thus, using the actual optimal compensator would not be practical from an applications standpoint.

For this reason, Walker reformulated the problem as a Lagrange multiplier problem so that it could be solved numerically. The ultimate result of the work begun by Walker was the creation of MXTOOLS for MATLAB^{TM} by Jacques, Canfield, and Ridgely [6]. This is a public domain toolbox that efficiently solves the mixed norm control problem for a fixed order controller. The toolbox is geared toward quick design of a mixed norm controller, where an H_2 objective function is constrained by an H_∞, μ, or ℓ_1 constraint (ℓ_1 constraints will not be considered in this thesis). The program also allows for multiple constraints. The user is only required to provide the plant model and the constraint model(s) to be included in the problem formulation. The toolbox then forms the problem, checks whether or not any constraints are active, and iterates until a solution is found. The program uses a Sequential Quadratic Programming (SQP) algorithm to find the optimal solution. An advantage of this type of algorithm is that it is efficient at solving constrained optimization problems.

Edwards [7] was the first to use MXTOOLS to create a mixed H_2 / H_∞ control design that was flight tested. He also flight tested three other designs: an H_2 optimal control design, an H_∞ optimal control design, and a classic control law designed using root-locus methods. All of the designs used a 4th order, unstable F-16 short period and phugoid aircraft model provided by Calspan SRL Corporation. The mixed H_2 / H_∞ control was a combination (via MXTOOLS) of the flight test H_2 and H_∞ optimal control designs. The H_2 optimal control design included weights for turbulence rejection and command tracking. The H_∞ optimal control design included weights to account for model uncertainty through maximizing stability margins and tracking a command input. Because of the setup of the H_2 and H_∞ designs, the mixed H_2 / H_∞ design included good command tracking, stability margins, and turbulence rejection. The classic control law was designed using angle of attack (α) and pitch rate (q) feedback gains.

Handling qualities predictions for all of these designs were checked using Hoh's Bandwidth Criteria for the landing phase of flight. This criteria is defined in MIL-STD-1797A, *Flying Qualities of Piloted Aircraft* [8]. All control designs are desired to have Level 1 handling qualities predictions based on the Cooper-Harper aircraft handling qualities rating scale. This rating scale is presented in Appendix A. All of the designs used by Edwards in flight test had Level 1 handling qualities predictions.

Edwards' flight test program was named HAVE INFINITY by the USAF Test Pilot School. Each HAVE INFINITY flight control system was evaluated by four pilots during the approach and landing phase of flight in the Calspan Variable Stability Learjet 24. Several straight-in and horizontal offset landings were made by each pilot to evaluate all four flight control systems. The horizontal offset landings were performed primarily to raise the pilot's gains, which would expose any potential handling qualities "cliffs" in the flight control systems. HAVE INFINITY used all of the handling qualities ratings for each type of landing to come up with an overall level rating for each flight control design. The evaluation pilots also gave a Pilot-In-the-Loop-Oscillation (PIO) rating using the scale defined in [8]. The PIO rating gives a measure of the flight control system's susceptibility to PIO for a given task. This rating scale along with an explanatory decision tree are also presented in Appendix A. All PIO ratings were between 2 and 5. The classical controller was rated Level II on the Cooper-Harper (C-H) Rating Scale, and the H_2, H_∞, and mixed H_2/H_∞ designs all received Level III C-H ratings. The Level III C-H ratings were primarily attributed to an uncommanded pitch up in the landing flare. The HAVE INFINITY test team concluded that the pitch up problem may have been related to problems in the implementation of the HAVE INFINITY optimal control laws. It turned out that the H_2, H_∞, and mixed H_2/H_∞ designs contained high frequency and unstable modes internal to the control laws. This made the designs very difficult to implement on the Calspan Learjet.

Subsequent model verification and validation testing revealed that predicted time and frequency responses did not match the actual time and frequency responses. The HAVE INFINITY test team felt that the dubious nature of the implementation and the potential negative impact on handling qualities rendered the results inconclusive as to the potential benefits of the multiobjective design techniques used.

Due to the HAVE INFINITY test results, the decision was made to continue the multiobjective flight control research in hopes of producing a definitive answer about their utility with regard to handling qualities. This decision was in lieu of testing some of the potential advantages of the methods such as turbulence rejection and stability robustness, as had been originally planned. It was felt that getting good handling qualities using the optimal methods had to be accomplished before more advanced testing could take place.

1.3 Research Objectives

The overall objective of this thesis was to perform an inflight handling qualities evaluation of several multiobjective, optimal flight control designs. Specifically, this research focused on the development, simulation, and flight test of several H_2 and mixed-norm control designs during the approach and landing phase of flight. The designs were flight tested on the Calspan Variable Stability Learjet simulating the F-16 handling characteristics. All designs were evaluated using Hoh's Bandwidth Criteria for predicting pilot opinion of aircraft handling qualities. This research was conducted in two phases. Phase I was conducted at AFIT. Phase I assumed the F-16 longitudinal dynamics could be accurately approximated on the Calspan Learjet by a second order short period transfer function. Phase I specific objectives were to formulate, synthesize, and simulate:

1. The H_2 model-following subproblem to determine the optimal H_2 controller that provided the best possible noise rejection while following the ideal model.

2. The H_∞ model-following subproblem to determine the optimal H_∞ controller that provided good command tracking in addition to stability robustness.

3. The μ subproblem to determine the optimal controller to handle multiple uncertainties.

4. The mixed H_2 with multiple H_∞ constraints problem(s) to tradeoff noise rejection with separate tracking, input model uncertainty, and output stability margin constraints.

5. The mixed H_2 / μ problem to tradeoff noise rejection and robust performance for multiple uncertainties.

6. Determine the best designs to use in phase II based on analytical analysis and simulation.

Phase II specific objectives of this research were:

1. Perform flight test evaluation of selected control designs from Phase I that satisfies Objective 6.

2. Obtain and evaluate qualitative and quantitative pilot opinion and Cooper-Harper Pilot Ratings of the flight control designs selected for flight test evaluation.

3. Compare flight test handling qualities ratings to those predicted in Phase I.

4. Draw conclusions with regards to apparent trends in Objective 3, Phase II.

5. Collect and archive data for future use by AFIT and USAF TPS.

1.4 Thesis Organization

Chapters II-IV cover the analytical phase (Phase I) of this research and chapters V and VI cover the flight test phase (Phase II). Chapter VII is a summary chapter. Specifically, Chapter II contains the theory for H_2, H_∞ and mixed H_2 / H_∞ control design. This chapter II also describes the complex structured singular value, μ, in terms of analysis, synthesis, and

mixed H_2 / μ. Chapter III contains the setup and synthesis for the various mixed norm control designs. The design examples use a short period, longitudinal state space model for the Calspan Variable Stability Learjet simulating an F-16 in the landing phase. The results of the design synthesis and simulation accomplished during Phase I are then presented in Chapter IV. Flight control design implementation, flight test techniques used, flight test structure, and model verification/validation are described in Chapter V. Handling qualities results for each flight control design flight tested are presented in Chapter VI. Finally, Chapter VII brings the analytical and flight test phases together and makes conclusions and recommendations for further research.

II. Theoretical Preliminaries

This chapter first focuses on the single norm optimization methods that will be used: H_2, H_∞, and μ. The last portion of the chapter provides a brief overview of fixed-order mixed H_2 / H_∞ control optimization and fixed-order mixed H_2 / μ control optimization.

2.1 H_2 Optimal Control

2.1.1 The H_2 space.

H_2 is defined as the space of all transfer function matrices which are stable (all eigenvalues in the open-left half complex plane) and have a bounded two-norm. The two-norm, α, is defined as:

$$\alpha = \|T_{zw}\|_2 = \left(\frac{1}{2\pi} \int_{-\infty}^{\infty} tr[T_{zw}(j\omega)T_{zw}(j\omega)]d\omega \right)^{\frac{1}{2}} \tag{2.1}$$

The subspace $\Re H_2$ is defined as the space of rational functions with real coefficients in H_2. Equation 2.1 is not easy to compute. Fortunately, there is an easier method for computing the two-norm of a transfer function (see [9] for a more detailed explanation). Consider the transfer function

$$G(s) = \left[\begin{array}{c|c} A & B \\ \hline C & 0 \end{array} \right] \in \Re H_2 \tag{2.2}$$

where the above notation represents $G(s) = C(sI - A)^{-1}B + 0$. Assuming the real part of all the eigenvalues of A are less than zero, we can find the controllability and observability

grammians, L_c and L_o, which are the positive semidefinite solutions to the Lyapunov equations

$$AL_c + L_c A^T + BB^T = 0 \qquad (2.3)$$

$$L_o A + A^T L_o + C^T C = 0 \qquad (2.4)$$

From here we can easily compute the two-norm, which is given by

$$\|G(s)\|_2^2 = tr(CL_c C^T) = tr(B^T L_o B) \qquad (2.5)$$

2.1.2 H_2 Optimization.

The H_2 optimal control problem is described by the block diagram in Figure 2.1. This notation is known as a lower Linear Fractional Transformation (LFT) of P and K, denoted $F_\ell(P,K)$. The exogenous input to the system, w, is zero-mean, unit intensity, white Gaussian noise. Typically, these noise inputs would model wind gust disturbances and sensor noise in an aircraft. The output, z, is whatever the control designer wishes to have minimized with respect to w. The plant model is designated P and can include weights on parameters that the designer wishes to emphasize or de-emphasize in certain frequency ranges. An example would be a weight on control use to account for actual aircraft limits of control deflection. The goal then is to determine the feedback controller, K, using the method described in this section. The measurements, y, are the outputs of P that are fed back to K. The control law, u, is the output of K that is fed into P.
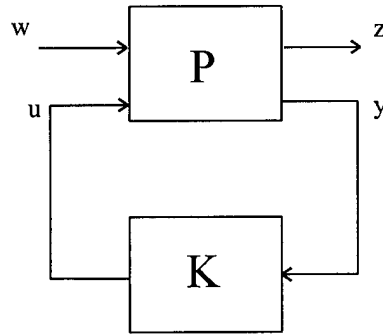
Figure 2.1 Block Diagram for H_2 Problem

The objective of H_2 control optimization is to find a stabilizing controller that minimizes the rms energy, or two-norm, of z, given the noise inputs, w, described previously. H_2 optimization is performed by solving two Algebraic Riccati Equations (ARE's) and is a generalization of the standard Linear Quadratic Gaussian (LQG) problem. This generalization allows noise inputs and desired outputs to be placed anywhere in the problem formulation. Dynamic weightings of outputs and inputs are also allowed. See Section B.1, Appendix B for further mathematical development.

2.2 H_∞ Optimal Control

2.2.1 The H_∞ Space.

H_∞ is defined as the space of all transfer function matrices which are stable (all eigenvalues in the open-left half complex plane) and have a bounded infinity-norm. The infinity-norm can be looked at as the maximum possible energy gain of a system. Thus, to minimize the energy to a deterministic, but unknown, bounded energy input (e.g. a pulse), we must minimize the infinity-norm of the associated transfer function. Analogous to the H_2 space, $\Re H_\infty$ is the

subspace of all real, rational H_∞ functions. The infinity-norm is an induced norm and is defined as

$$\gamma = \left\| T_{ed} \right\|_\infty \qquad (2.6)$$

$$= \sup_{d \neq 0} \frac{\left\| T_{ed} d \right\|_2}{\left\| d \right\|_2} \qquad (2.7)$$

$$= \sup_{\left\| d \right\|_2 \leq 1} \left\| e \right\|_2 \qquad (2.8)$$

$$= \sup_{\omega} \bar{\sigma}[T_{ed}(j\omega)] \qquad (2.9)$$

where T_{ed} is a closed loop transfer function whose meaning will be clarified later.

An important characteristic of the infinity-norm is that since it is an induced operator norm, it has a sub-multiplicative property [10]; given $F, G \in H_\infty$ then

$$\left\| FG \right\|_\infty \leq \left\| F \right\|_\infty \left\| G \right\|_\infty \qquad (2.10)$$

The easiest way to calculate the infinity-norm of a transfer function is to calculate its maximum singular values over a sufficiently large range of frequencies and select the maximum value. However, this approach may not be numerically practical since the frequency at which the maximum singular value will be attained is not known *a priori*. A more precise approach is based on the eigenvalues of a Hamiltonian matrix associated with a state space realization of a proper stable transfer function [10].

Consider the transfer function

$$G(s) = \left[\begin{array}{c|c} A & B \\ \hline C & D \end{array}\right]$$

(2.11)

The associated *Hamiltonian* is

$$H = \begin{bmatrix} A + BR^{-1}D^T C & BR^{-1}B^T \\ -C^T(I + DD^T)^{-1}C & -(A + BR^{-1}D^T C)^T \end{bmatrix}$$

(2.12)

where $R := \gamma^2 I - D^T D$. The infinity-norm of the transfer function is the smallest value of γ such that H has no eigenvalues on the imaginary axis.

2.2.2 H_∞ Optimization.

Consider the block diagram in Figure 2.2. This is the same setup as Figure 2.2 except that the inputs and outputs have been defined differently. The input, *d*, is an unknown but deterministic bounded energy signal. The task is then to find the controller, K, that minimizes the output, e, with respect to d.
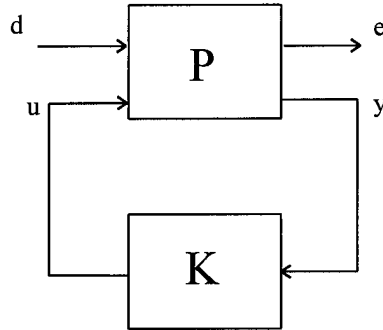
Figure 2.2 Block Diagram for the H_∞ Problem

The plant P can be partitioned as

$$P = \begin{bmatrix} P_{ed} & P_{eu} \\ P_{yd} & P_{yu} \end{bmatrix}$$

(2.13)

such that

$$e = P_{ed}d + P_{eu}u \qquad (2.14)$$

$$y = P_{yd}d + P_{yu}u \qquad (2.15)$$

This is equivalent to minimizing the infinity-norm of the closed loop transfer function, T_{ed}.

Further mathematical development on H_∞ control optimization can be found in Section B.2,

Appendix B.

2.3 The Complex Structured Singular Value

The next optimal control tool of interest is the *structured singular value, μ*. This

section will introduce μ and how to find an upper bound on it through H_∞ optimization

techniques. The application of μ-synthesis to the F-16 landing problem as a means of ensuring

robust stability and robust performance is presented in Chapter III. The reader is invited to see

[11] for a tutorial on the complex structured singular value. Consider the problem represented

in Figure 2.3.
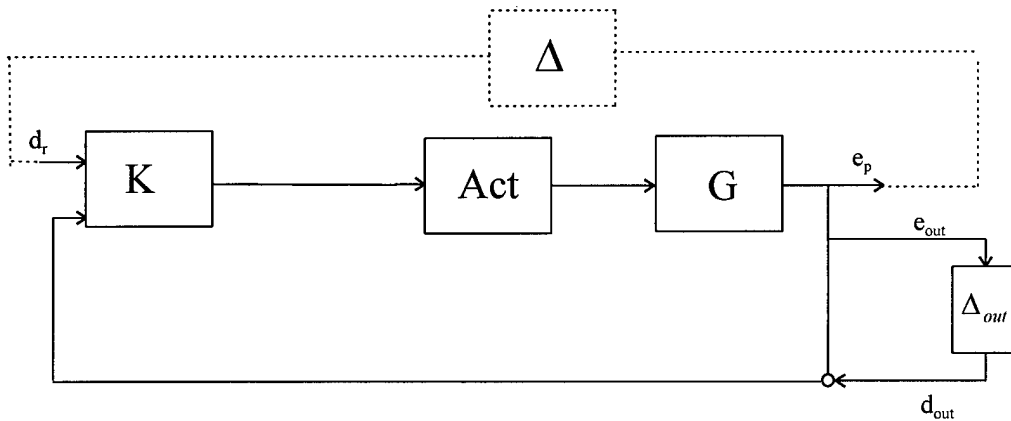
Figure 2.3 System with Multiple Uncertainties

In this figure, d_r is the reference input, e_p is the controlled output, *Act* is the actuator, G is the core plant, and K is the controller. The system has an uncertainty at the output of the plant. These uncertainties include frequency weights for such things as neglected high frequency dynamics or uncertain parameters in the system. The structure in the uncertainty is apparent from the figure. There is an uncertainty for the actuator and another for the plant output and these uncertainties occur at different places in the system. μ allows us to use this structure to combine the two uncertainties into a single structured uncertainty, and come up with a robust design that is less conservative than the standard H_∞ design would be in this case. The mathematical development for the structured singular value is found in Section B.3, Appendix B.

2.4 Mixed H_2 / H_∞ Control

2.4.1 Background.

Recall that both H_2 and H_∞ optimization minimize the energy of the chosen output(s). However, the input(s) for H_2 are characterized by white Gaussian noise (wind gusts and sensor noise, for example), and the inputs for H_∞ are unknown, but bounded energy deterministic inputs (unmodelled dynamics, etc.). Since each type of control optimization is designed for a different type of input, there may be some advantage to mixing the two in a problem where both types of inputs are present. However, we must also realize that mixing these two different types of control designs will often produce competing objectives. If our H_2 design is optimized for noise rejection and our H_∞ design is optimized to provide good tracking by minimizing output sensitivity, we can expect to tradeoff noise rejection performance for tracking performance.

Ridgely [2,3] and Walker [4] have both developed techniques to handle mixed norm control optimization using the H_2 subproblem as the objective function to be minimized, and append one or more H_∞ subproblem(s) as constraints. Note that we are not doing H_∞ control optimization here but rather constraining the infinity-norm to some level specified by the designer. This process can be formally stated as follows

$$\inf_{K_{adm}} \|T_{zw}\|_2, \quad \text{subject to} \quad \|T_{ed}\|_\infty \leq \gamma \tag{2.16}$$

The details of the mathematical development of Walker's mixed H_2 / H_∞ control method is found in Section B.4, Appendix B. The results of Walker's work provided the basis for a reliable numerical method for mixed H_2 / H_∞ control optimization.

2.4.2 Numerical Approach.

The method developed by Jacques, Canfield, Ridgely, and Spillman [6] uses a gradient based Sequential Quadratic Programming (SQP) numerical optimization routine to solve the mixed H_2 / H_∞ problem. This approach uses inequality rather than equality constraints. The main reason for this is that inequality constraint approaches overcome the numerical drawbacks associated with using equality constraints. The approach can be expressed mathematically as

$$\min_{K_{stabilizing}} \|T_{zw}\|_2^2$$
$$\text{subject to} \tag{2.17}$$
$$\|T_{ed}\|_\infty - \gamma \leq 0$$

Now define the parameter vector X as

$$X = \begin{bmatrix} a_{c_1}^T \dots a_{c_n}^T & b_{c_1}^T \dots b_{c_p}^T & c_{c_1}^T \dots c_{c_n}^T \end{bmatrix}^T \tag{2.18}$$

where a_{c_j}, b_{c_j}, and c_{c_j} are the columns of the closed loop state space matrices A_C, B_C, and C_C, respectively. We can now use the SQP algorithm to minimize the performance index of this program defined above. A feature of this algorithm is that it is able to search over both feasible and infeasible solutions. Since the only solutions of interest are stable ones, a stability constraint and penalty function was added to keep the algorithm from getting lost in an unstable region. The stability constraint is stated as

$$g_s(K) = \left(\max_i \left\{ \Re \left[\lambda_i \left(A_c \right) \right] \right\} \right) < 0 \qquad (2.19)$$

where $\lambda_i \left(A_c \right)$ denotes the ith eigenvalue of the closed-loop system. The penalty function added to the objective function is simply the square of the stability constraint. This assures continuous derivatives at the stability boundary. The analytical gradients of the objective as well as the constraints are derived in Jacques, *et al* [6]. The normal approach is to compute the H_2 optimal controller which gives us a starting point on the Pareto curve (see App. B, page B-26). We then step to the left on the curve by decrementing γ until we approach $\underline{\gamma}$. At each γ step, SQP will determine the controller which minimizes α subject to the constraint γ. When α is minimized as much as possible the controller is saved and $\left(\gamma^*, \alpha^* \right)$ is plotted on the Pareto curve. It should be noted here that this method is not guaranteed to converge to a global minimum at each γ step. This approach is implemented in MATLAB™ through the MXTOOLS™ Toolbox and is available via anonymous ftp at the Air Force Institute of Technology.

2.5 Mixed H_2 / μ Control Optimization.

This is just an extension of the mixed H_2 / H_∞ theory already discussed. It follows the theoretical framework for H_2 / H_∞ control optimization that was developed in section B.4, Appendix B. H_2 optimization is done as before, but now the H_∞ part of the problem is modified by the D matrices discussed in Section B.3, Appendix B. First, μ synthesis is done on the portion of the problem dealing with the uncertainties. Instead of being interested in the resulting controller, we are now interested in the D scales. They will be absorbed into the open loop P of the H_∞ problem, and that will become our new H_∞ problem. Our new P is calculated using the formula

$$P = DP_\infty D^{-1} \tag{2.20}$$

Now $\left\| T_{ed} \right\|_\infty$ in Figure B6 becomes $\left\| DT_{ed}D^{-1} \right\|_\infty$. Other than this modification, there is no difference from the H_2 / H_∞ optimization techniques previously discussed in Appendix B.

III. Problem Formulation

Now that the mathematical theory has been established, the design application that is used in the rest of this thesis can be outlined. However, before the details of the design process are discussed, it is instructive to review the longitudinal parameters of interest during the landing phase of flight. Section 3.1 contains a brief overview of how a pilot normally accomplishes a landing. The rest of the chapter details all of the problem formulations that were used to produce the design results discussed in the next chapter. The initial system definitions are those common to all of the problem formulations. Then the single norm subproblem setups will be discussed $\left(H_2, H_\infty, \text{ and } \mu\right)$ followed by the H_2 / H_∞ and H_2 / μ problems. The last part of the chapter will summarize significant findings relating to the setup phase as a prelude to the design results.

3.1 Background on Landing Phase

MIL-STD-1797A [8] defines the landing phase as those maneuvers which require precise flight path control using gradual maneuvers during the terminal phases of flight. Precise tracking tasks generally require high open loop (here, open loop refers to the aircraft and flight control system without the pilot) system stability and high short period damping, ζ_{sp}. This enables the pilot to track high frequency inputs and reject disturbances without unacceptable oscillations due to low ζ_{sp} in the system [15]. In the initial stage of the approach, the pilot adjusts pitch angle, θ, to control the flight path angle, γ. Throttle position is used to control airspeed. As the pilot nears the touchdown point, the throttle is moved to idle. The control

inputs now affect the flight path angle, γ. The pilot's goal is to smoothly transition γ to zero at touchdown[16]. Figure 1 show the definitions of pitch attitude angle and flight path angle.
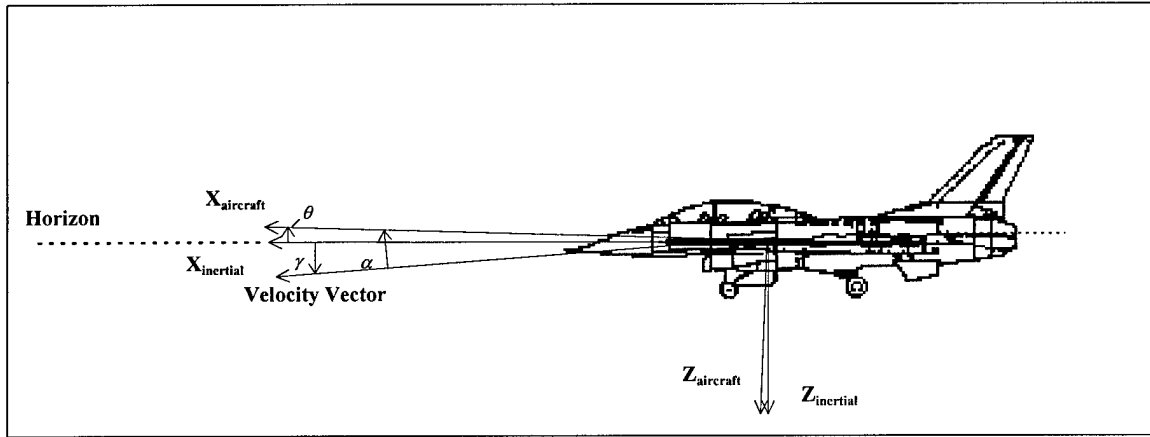
Figure 3.1. Aircraft Axis System

3.2 System Definitions

The plant model used throughout this thesis is a short period model of the Calspan Variable Stability Learjet simulating an F-16. The state space model is defined as

$$\dot{x}_g = \begin{bmatrix} -0.3722 & 0.7593 \\ 1 & -0.822 \end{bmatrix} \begin{bmatrix} q \\ \alpha \end{bmatrix} + \begin{bmatrix} -2.7768 \\ -0.0397 \end{bmatrix} \delta_e$$
$$y_g = \begin{bmatrix} 1 & 0 \\ 0 & 1 \end{bmatrix} \begin{bmatrix} q \\ \alpha \end{bmatrix} + \begin{bmatrix} 0 \\ 0 \end{bmatrix} \delta_e$$

(3.1)

where the pitch rate, q, is in deg/sec, and angle of attack, α, elevator input, δ_e, are in degrees.

This plant system can also be represented in terms of the following transfer function

$$G_g(s) \equiv \left[\begin{array}{c|c} A_g & B_g \\ \hline C_g & D_g \end{array} \right]$$

(3.2)

A short period only model was used because Calspan's experience indicated that the phugoid mode did not have a significant effect on the handling qualities. The second order plant model also offered the advantage of keeping the resulting control laws lower order. The second order model for the actuator dynamics was also supplied by Calspan and the state space model is given by

$$\dot{x}_{act} = \begin{bmatrix} -17.915 & -49.154 \\ 49.154 & -66.085 \end{bmatrix} x_{act} + \begin{bmatrix} -4.9575 \\ 4.9575 \end{bmatrix} \delta_{ec}$$

$$y_{act} = \begin{bmatrix} -4.9575 & -4.9575 \end{bmatrix} x_{act} + \begin{bmatrix} 0 \end{bmatrix} \delta_{ec}$$

(3.3)

The actuator system is also referred to as G_{act} and is defined as

$$G_{act}(s) = \begin{bmatrix} A_{act} & B_{act} \\ \hline C_{act} & D_{act} \end{bmatrix}$$

(3.4)

The next system definition common to all of the design problems is the weight on the reference input, W_r. It was not desired to shape the frequency content of the reference input in the design process so W_r was set equal to 1.

The final element that is common to all designs is the "ideal" closed-loop model that is used in the model following portion of the problem. The reference input to the controller for this problem is a pitch rate command. So we will need to choose a desired closed loop model of the pitch rate to commanded-pitch-rate transfer function to follow. In this case, good handling qualities predictions and good tracking of a pitch rate input were the primary figures of merit in the selection of an ideal model. It was also desired to keep the order of the model as low as possible so the order of the resulting controller would not get too large for practical implementation in the flight test phase. A first order model was found that satisfied all of these requirements and is defined as

3-3

$$W_m = \frac{q}{q_c} = \frac{6}{s+6} = \left[\begin{array}{c|c} A_m & B_m \\ \hline C_m & D_m \end{array}\right] \qquad (3.5)$$

3.3 H_2 Problem

The H_2 problem is an LQG design that minimizes the output states (q and α), elevator

control rate usage, elevator usage, and pitch rate tracking error to wind disturbances and sensor

noise. The problem setup is depicted in Figure 3.2.
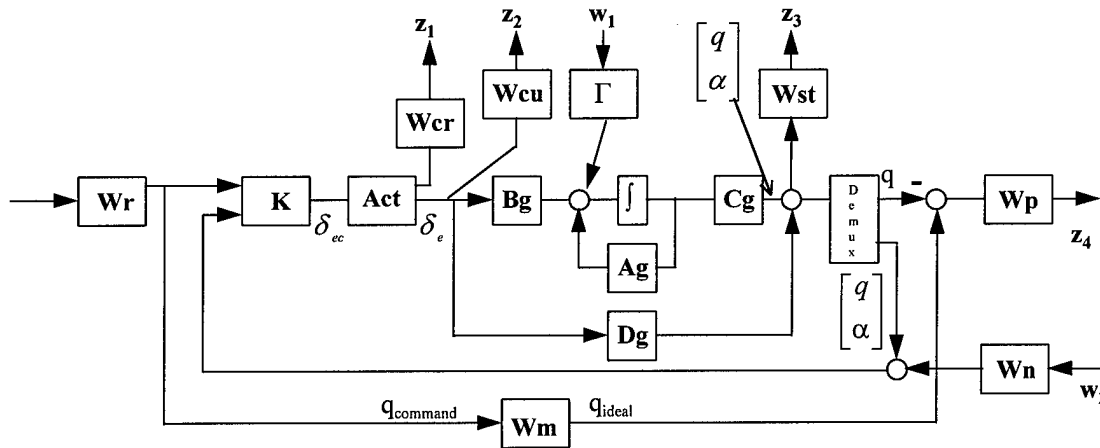
Figure 3.2. H_2 Problem Setup

It is important to now spend some time discussing the various weight selections that

were used in this H_2 problem. These weights determine what performance measures are

emphasized in the resulting controller (tracking vs. noise rejection, for instance). It turns out that

the choices of the control rate weight, W_{cr}, and the tracking weight, W_p, have a significant

impact on handling qualities predictions. The control rate weight selection directly impacted the

bandwidth of the resulting closed-loop system. In general, larger control rate weights produced

closed-loop

systems with smaller bandwidth that rolled off rapidly in phase at frequencies above the bandwidth frequency. This means that the pilot has less ability to increase the bandwidth of the system through increasing his gain (i.e. he can't aggressively track without causing instability in the system). Continuing to increase the control weight rate will eventually decrease the bandwidth and increase the phase rolloff to the point where level 1 handling qualities predictions are no longer possible. This will be illustrated further in Chapter 4 when looking at the H_2 problem results. A potential solution to this problem would be to select a very small weight on control rate use. There are two problems with this approach. First, a very small weight on control use will usually cause rate limiting of control actuators, which can lead to instability. Second, widening the bandwidth of the system will increase its susceptibility to sensor noise corruption.

The tracking weight had a more indirect effect on the bandwidth of the closed-loop system. The higher the DC gain of this weight, the better the tracking performance of the closed-loop system. However, the price to be paid for this good tracking was rate limit saturation of the actuators. In order to rid the system of the rate limit saturation, the control rate use weight had to be increased. This narrowed the bandwidth of the system, and increased phase rolloff, which produced a degradation in handling qualities predictions. The bottom line is that there ends up being a trade-off between tracking performance and handling qualities in the selection of these weights. With this in mind, the tracking weight is defined as

$$W_p = \frac{s + 40}{s + 4} \qquad (3.6)$$

The smallest corresponding rate limit weight that just prevents the system from rate limiting for a 5 deg, 4 sec pulse input is

$$W_{cr} = \begin{bmatrix} 0.000667 & 0 \\ 0 & .000667 \end{bmatrix} \qquad (3.7)$$

The control usage weight W_{cu} had very little effect on the output of the overall system because the rate limit constraint was more restrictive for this flight condition and control input. However, this weight needs to be included because the rate limit may not always be the dominant constraint depending on flight condition and control input. The saturation limit of the elevator on an F-16 is +/- 25 degrees. Therefore the control use weight was set at the inverse of this and is given by

$$W_{cu} = 1/25 \qquad (3.8)$$

The next weight that was chosen was the state weighting on the outputs q and α. Since one of the objectives here is to minimize the states given wind and sensor noise inputs, we want to just minimize the outputs of the states themselves. For this reason W_{st} was chosen as an identity matrix.

$$W_{st} = \begin{bmatrix} 1 & 0 \\ 0 & 1 \end{bmatrix} \qquad (3.8)$$

The next set of weights to be discussed are those associated with the wind turbulence and sensor noise. Wind turbulence manifests itself as an angle of attack disturbance in an aircraft. For this reason it makes sense to weight the angle of attack states in the plant A-matrix. It was found through iteration (while holding other weights fixed) that a representative turbulence noise is produced by introducing the following weight as an angle of attack disturbance:

$$\Gamma = 0.0316 \times A_g(:,2) \qquad (3.9)$$

3-6

The sensor noise weightings corrupted the state feedback measurements, q and α, and effectively simulates the noise that is present on those measurements. A static weight was used here and was again found by iteration (again, while holding other weights fixed). The sensor noise weight is given by

$$W_n = \begin{bmatrix} .1 & 0 \\ 0 & 1 \end{bmatrix} \begin{bmatrix} q \\ \alpha \end{bmatrix} \tag{3.10}$$

This says that the noise affects the pitch rate measurement, q, by 10% over all frequencies and the angle-of-attack measurement, α, by 100% over all frequencies. It is worth spending a moment discussing these extremely conservative weights. Although sensor noise is mainly a high frequency disturbance, static weights were found to work well and had the added benefit of keeping the order of the H_2 problem down (This will become important later in the mixed H_2 / H_∞ problem). The magnitude of the sensor noise weights were given the values above to optimize the noise rejection performance of the H_2 design. One way to get better noise rejection performance from an LQG design is to input a higher level (magnitude and frequency) of noise than the system would actually expect to experience. However, the improvement in noise rejection usually comes at the expense of other performance specifications like command tracking. For this design the values of W_n provided excellent noise rejection with no appreciable degradation in tracking.

3.4 H_∞ Problem

The H_∞ problem formulation included three different objectives; command tracking, maximizing output stability margins, and making the system robust to uncertainty at the input to

the plant by accounting for neglected high frequency plant dynamics and other modeling errors

that may be present in the plant. A block diagram of this setup is shown in Figure 3.3
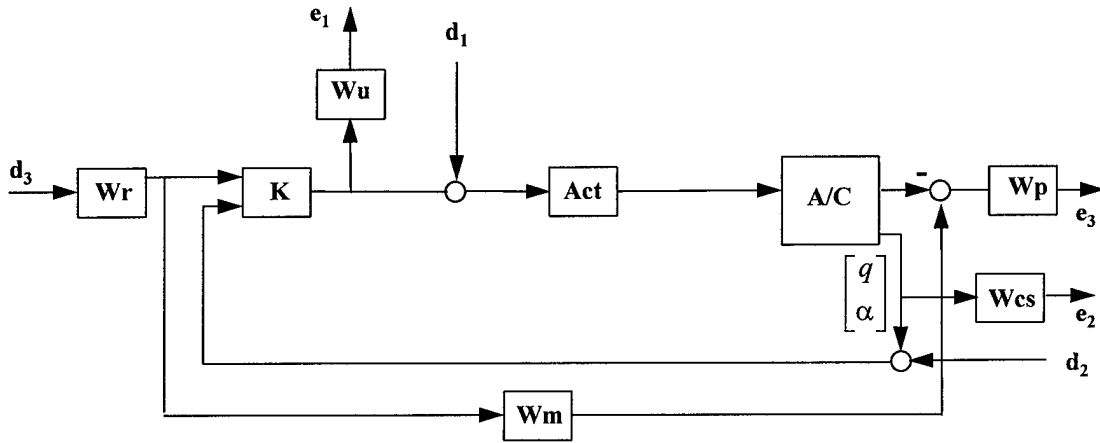
Figure 3.3. H_∞ Problem Setup

The tracking objective is controlled by minimizing the transfer function of the weighted

output e_3 and input d_3. The output stability margins are addressed by the minimizing the

weighted complimentary sensitivity transfer function, e_2d_2. Finally, the uncertainty robustness

objective is contained in the e_1d_1 transfer function. The weights associated with each of these

outputs will now be discussed.

The tracking weight for the H_∞ problem was much more stringent than in the H_2

problem. As mentioned previously, the tracking weight had an effect on the handling qualities

predictions in the H_2 problem by affecting the bandwidth of the closed-loop system. This is not

the case in this work because the H_∞ problem is used only as a constraint in the mixed H_2 / H_∞

problem. It was found in this work that the handling qualities predictions were almost

completely influenced by the H_2 problem. Therefore, no tradeoff between handling qualities

and the various weight selections had to be made in the H_∞ problem. Thus the tracking weight is defined as

$$W_p = \frac{s+40}{s+.004} \tag{3.11}$$

The output vector stability margins are maximized by minimizing the weighted complementary sensitivity of the measurement outputs of the plant. The reader is invited to see Franklin, *et al.* [17] for a detailed discussion of vector stability margins. There was no need to frequency weight the output measurements in order to minimize complementary sensitivity, so this weight was set to identity and is expressed as

$$W_{cs} = \begin{bmatrix} 1 & 0 \\ 0 & 1 \end{bmatrix} \tag{3.12}$$

The input uncertainty weight was chosen to account for neglected high frequency dynamics and modeling errors in the actuator and plant. By minimizing this objective, the designer should be able to improve the controller performance for an "off-nominal" plant. The uncertainty weight is expressed as

$$W_u = \frac{3s+30}{s+250} \tag{3.13}$$

The final item that needs to be addressed with regards to this H_∞ problem is the absence of control rate and control use weights. Recall from Chapter 2/Appendix B, that the constraints in the mixed H_2 / H_∞ problem come only from the H_∞ portion of the problem. Therefore the rate limit and control use constraints do not need to be included in the H_∞ setup because they are taken care of by the H_2 problem.

3.5 μ Problem

The μ problem is setup exactly the same as the H_∞ problem discussed in section 3.3 other than the "D" scales associated with the uncertainty structure, Δ (see Figure 3.2). Recall from Chapter 2, that μ has the advantage of handling multiple uncertainties less conservatively than the H_∞ problem. μ also has the advantage of guaranteeing robust performance for values of $\mu < 1$, see [1]. This means that performance specifications can be met while remaining robustly stable for all perturbations contained in the structure of Δ. For this problem setup, the Δ structure contains the tracking, output stability margins, and input uncertainty objectives.

3.6 Mixed H_2 / H_∞ Problem

Recall the mixed H_2 / H_∞ problem can be expressed as

$$\inf_{K_{adm}} \|T_{zw}\|_2 \text{, subject to } \|T_{ed}\|_\infty \leq \gamma \tag{3.14}$$

where K_{adm} is the set of stabilizing controllers of some fixed order. This problem can have a single constraint transfer function or multiple constraint transfer functions. Allowing the problem to be set up with a single or multiple constraints gives the designer great flexibility to tailor the problem to whatever objective(s) are important for a particular application. For example, a control engineer has an LQG tracking design that produces good command following and noise rejection, but insufficient output stability margins. An H_∞ constraint minimizing output sensitivity or output complementary sensitivity could be employed in a mixed H_2 / H_∞ problem formulation to correct the stability margin deficiency of the H_2 problem. The reader is reminded that these constraints are allowed to be singular as all of the regularity constraints (i.e. certain matrices must have a nonzero determinant) are handled by the H_2 portion of the problem.

The setup of the mixed H_2 / H_∞ problem is provided in Figure 3.4. The inputs to the system are

w (unit intensity white Gaussian noise), and d, an unknown but bounded energy input. The

outputs z and e are the signals whose two-norms are either minimized or constrained. All of the

weights used in the mixed H_2 / H_∞ problem are carried over from the single norm problem

formulations.
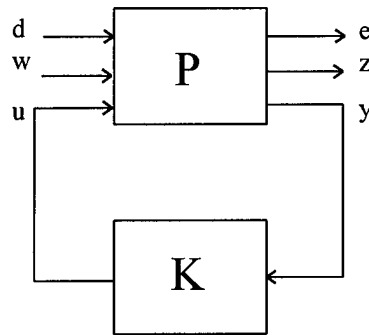
Figure 3.4. Mixed H_2 / H_∞ Problem Setup

3.7 Mixed H_2 / μ Problem

Analogous to the single norm case, the mixed H_2 / μ is setup the same way as the mixed

H_2 / H_∞ problem. However μ-synthesis must now be performed to determine the optimal "D"

scales to include in the μ constraint. We are not interested in the controller generated by μ-

synthesis, only the "D" scales. In essence we still have a mixed H_2 / H_∞ problem that now

includes scalings associated with uncertainty structure of the H_∞ constraint. The problem setup,

minus the "D" scales is shown in Figure 3.3.

3.8 Summary

This chapter detailed the single norm subproblem setups $\left(H_2, H_\infty, \text{ and } \mu \right)$ followed by

the mixed H_2 / H_∞ and H_2 / μ problems. The transfer function matrices common to all problems

and the weights on various objectives of each problem formulation were also presented. These will be used to build the system matrices that are utilized in the design and simulation results discussed in Chapter 4.

The most significant finding from this chapter is that the control rate usage and tracking performance weights appears to influence the handling qualities predictions of a control design by controlling the bandwidth of the closed loop system.

Also, of note, is that the LQG problem can be "tricked" into providing better noise rejection by increasing the weight on the noise signals being input to the system. However, this comes at the price of reduced performance from other objectives and a tradeoff must be made by the designer.

In order to allow the reader to easily track the evolution of the control designs (and methods) through the flight test, design summary tables will be provided at the end of each chapter from this point forward.

TABLE 3.1

SUMMARY OF DESIGN METHODS AND NUMBERS TO BE PRODUCED
FOR FLIGHT TEST CONSIDERATION

Control Design Method	Number of Designs
H_2	1
H_∞	1
μ	1
H_2 / H_∞	1
H_2 / μ	1

IV. Design and Simulation Results

This chapter presents the phase I control designs that are candidates for flight testing in phase II. There are five pitch rate designs, and two angle of attack control designs. There was also a modification made to the simulation that converted the five pitch rate designs to angle of attack designs. This will be discussed further when the angle of attack designs are presented. Some of the twenty other designs that were not good enough to be flight test candidates will also be mentioned where appropriate to help illustrate and support the analytical findings contained herein. It should also be noted here that time and financial constraints may only allow flight testing of 3-4 of the flight test candidate designs. However, all seven are included for the sake of analytical completeness. The angle of attack designs were added very late in Phase I. Discussions with Calspan engineers indicated that the pitch rate command following designs may exhibit deficient handling qualities when the pilot is required to be tightly in the control loop (e.g., turbulent air), and that an angle of attack system would be preferable. However, a test program conducted by the F-16 Combined Test Force (CTF) indicates that pilots preferred a pitch rate system for landing [18]. Because rejection of wind turbulence is included directly in the pitch rate designs, it is hypothesized that the presence of turbulence will not greatly affect these designs. For these reasons, both the pitch rate and angle of attack designs will be represented in Phase II. It is hoped that there will be some discrimination in phase II as to which type of design is preferable. The pitch rate designs, simulations, and handling qualities predictions will be discussed first. Next, the angle of attack designs, simulations, and handling qualities will be discussed. Finally, a summary of Phase I findings along with a summary of the designs picked for flight test will be given as a prelude to Phase II and Chapter V.

4.1 Pitch Rate Design Results

The five pitch rate control designs that will be discussed consist of: a single norm H_2 design, three mixed $H_2 / T_{e_1 d_1} / T_{e_2 d_2} / T_{e_3 d_3}$ designs, and one mixed $H_2 / \mu / T_{e_1 d_1}$ design. The following table defines the constraints and objectives used in the mixed-norm designs

TABLE 4. 1

SUMMARY OF H_∞ CONSTRAINTS AND OBJECTIVES FOR THE MIXED NORM PROBLEMS

Constraint	Objective
$T_{e_3 d_3}$	Command tracking performance
$T_{e_1 d_1}$	Plant Input Uncertainty Robustness
$T_{e_2 d_2}$	Output Stability Margins
μ	Combination of $T_{e_3 d_3}$ and $T_{e_2 d_2}$

The objectives in Table 4.1 were handled separately in the mixed H_2 / H_∞ design because the resulting design was better than trying to include all three objectives in one H_∞ constraint. There are two of reasons for this. First, the reader will recall that H_∞ problem formulations are guaranteed to only handle one uncertainty in a nonconservative manner. The objectives in Table 4.1 can be looked at as uncertainties. So by virtue of including all three objectives in one H_∞ constraint, the resulting design may be too restrictive. Second, the objectives may have the same frequency ranges in which they compete. By breaking our multiple objective H_∞ constraint into three single objectives, we can see, and control, where the conservativeness is introduced by tightening or relaxing the individual constraints. In the case where all the objectives are together, the most difficult one to achieve will limit the performance of the others. A good example of this will be illustrated in the mixed $H_2 / \mu / T_{e_1 d_1}$ design.

Tables 4.2 and 4.3 summarize the results of the five pitch rate designs. Table 4.2 compares the 2-norms and ∞-norms of the various designs while Table 4.3 compares input and output vector gain and phase stability margins [18]. Following the tables, there are discussions of each design.

TABLE 4.2

PITCH RATE DESIGN DATA- $\|T_{zw}\|_2$ vs. TRACKING,
INPUT ROBUSTNESS, AND OUTPUT STABILITY CONSTRAINTS

Case	Design Type	$\|T_{zw}\|_2$	$\|T_{e_3d_3}\|_\infty$	$\|T_{e_1d_1}\|_\infty$	$\|T_{e_2d_2}\|_\infty$
1-1	H_2	2.518	528.970	13.280	2.950
1-2	$H_2 / T_{e_1d_1} / T_{e_2d_2} / T_{e_3d_3}$	5.022	1.400	4.000	1.650
1-3	$H_2 / T_{e_1d_1} / T_{e_2d_2} / T_{e_3d_3}$	5.810	1.400	2.800	1.650
1-4	$H_2 / T_{e_1d_1} / T_{e_2d_2} / T_{e_3d_3}$	3.940	1.400	9.925	1.650
1-5	$H_2 / \mu / T_{e_1d_1}$	8.410	34.220	.990	1.613

TABLE 4.3

PITCH RATE DESIGN DATA - STABILITY MARGIN COMPARISON

Case	Complement. Sensitivity Vector Gain Margins(dB) Input of Plant	Sensitivity Vector Gain Margins (dB) Input of Plant	Phase Margins (deg) Input of Plant	Complement. Sensitivity Vector Gain Margins (dB) Output of Plant	Sensitivity Vector Gain Margins (dB) Output of Plant	Phase Margins (deg) Output of Plant
1-1	[-6.53, 3.68]	[-5.88, 29.72]	57.85	[-3.62, 2.55]	[-2.84, 4.24]	22.26
1-2	[-20.11, 5.58]	[-5.13, 14.20]	53.57	[-14.59, 5.17]	[-5.11, 14.02]	48.01
1-3	[-21.62, 5.65]	[-4.79, 11.61]	54.59	[-14.94, 5.21]	[-4.78, 11.52]	48.47
1-4	[-16.25, 5.32]	[-5.46, 18.06]	51.89	[-14.18, 5.13]	[-4.99, 13.07]	47.44
1-5	[-10.56, 4.63]	[-4.97, 12.84]	45.42	[-8.35, 4.18]	[-4.78, 11.52]	43.10

4.1.1   The H2 Design (Case 1-1)

This design is included as a flight test candidate because it is the basis for all of the

mixed H_2 / H_∞ and H_2 / μ designs that follow. The large value of $\|T_{e_3d_3}\|_\infty$ in Table 4.2

indicates that this design does not track pitch rate command inputs well at all. Additionally, the value of $\left\|T_{e_1 d_1}\right\|_\infty$ indicates that this control design is not robustly stable to input perturbations in the class included in the H_∞ problem formulation because the infinity-norm is not less than 1. We would not expect this as we did not include this type of weighting in the H_2 problem formulation. The final deficiency of this design can be seen in Table 4.2. The output stability margins are unacceptably low. Good stability margins for aircraft applications are [-6.0,12.0]dB of Gain Margin and +/- 30 deg of Phase Margin [19]. The tracking and output stability margin problems must be addressed in order to have a good design while the input uncertainty weighting is an artificial constraint that falls into the "nice to have" category for this problem. The first question to ask is how to improve tracking and output stability margin performance? Tracking performance might be improved by simply tightening the tracking constraint in the original H_2 problem formulation. Likewise, the sensor noise weights could be adjusted to improve our output stability margins. Both of these approaches were evaluated and resulted in a significant degradation in noise rejection performance which led to unsatisfactory results. Another approach would be to include these performance objectives in constraints that are part of a multiobjective tradeoff such as the H_2 / H_∞ problem discussed next.

4.1.2 The $H_2 / T_{e_1 d_1} / T_{e_2 d_2} / T_{e_3 d_3}$ Designs (Cases 1-2 through 1-4).

These designs represent varying tradeoffs between noise rejection performance quantified by $\left\|T_{zw}\right\|_2$ and input uncertainty robustness quantified by $\left\|T_{e_1 d_1}\right\|_\infty$. The reader will note that the norms for the tracking and output stability margin constraints are all the same for each case. It was found that these norm values produced good tracking and output stability

margins. These constraints were then "frozen" while trying to minimize the input uncertainty

constraint. As in the H_2 design, robust input stability is not guaranteed for any of these designs.

The singular value plots of each closed loop constraint (where the H_2 optimal controller is used

to close the loop) in Figure 4.1 show why there are problems optimizing the robust stability
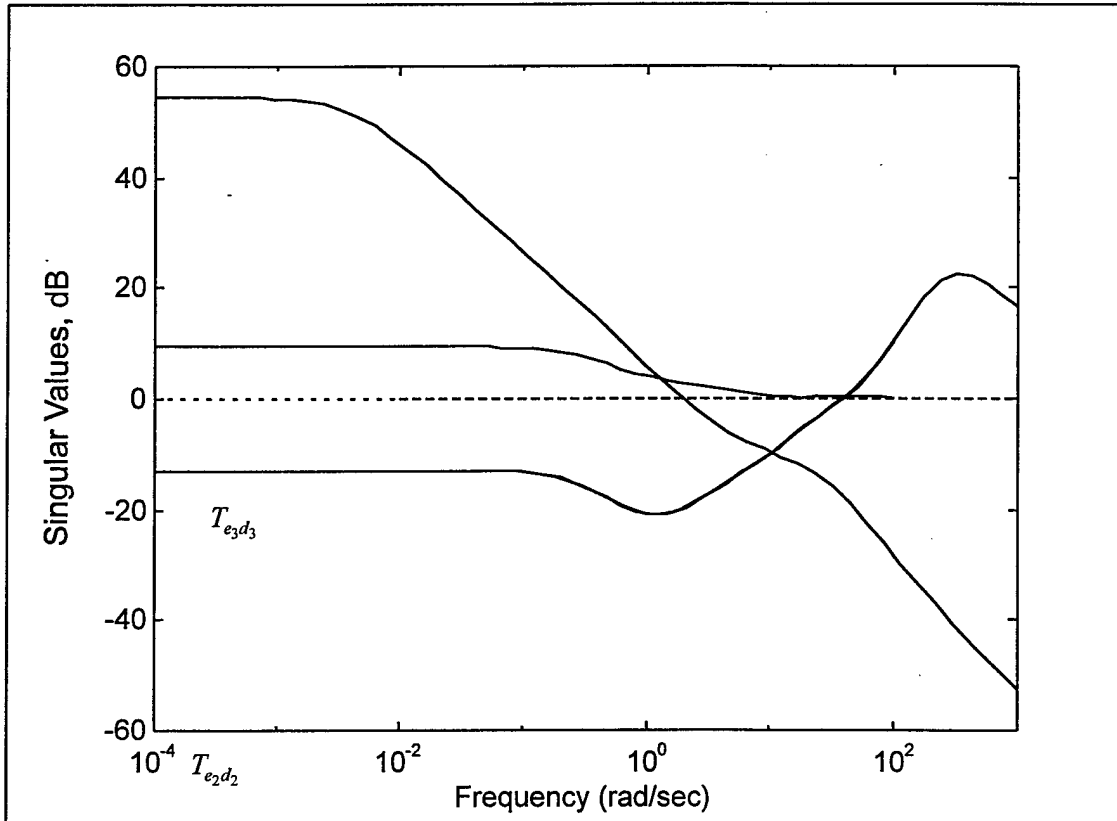
$T_{e_1 d_1}$ Figure 4.1. Singular Value Plots of Constraints

constraint. The tracking and output stability margin constraints ($T_{e_3 d_3}$ and $T_{e_2 d_2}$) are composed of

low frequency dynamics while the input robustness constraint ($T_{e_1 d_1}$) is composed of high

frequency dynamics. This competition between objectives indicates that we cannot get robust

input stability, at 90 rad/sec and above, without sacrificing tracking and/or output stability

margin performance. A technique to potentially improve these designs is discussed next.

4.1.3 The Mixed $H_2 / T_{e_1 d_1} / \mu$ Design (Case 1-5).

This design was developed to try to improve the results obtained in cases 1-2 through 1-4. The approach was to combine the two low frequency constraints in a μ- problem formulation while leaving the robust input stability constraint separate. Then a mixed $H_2 / T_{e_1 d_1}$ design was developed that guaranteed robust input stability. The value of $\left\| T_{e_1 d_1} \right\|_\infty = 0.2$ resulted from the μ design. This is well below the 0.99 requirement to guarantee robust input stability. Now this μ- constraint was appended to the $H_2 / T_{e_1 d_1}$ problem to account for the command tracking and output stability margin objectives (The reader is reminded that this is not an explicit μ constraint, but rather an H_∞ constraint that is optimally scaled through μ-synthesis). The approach was then to relax the robust input stability constraint ∞-norm to .99 while minimizing the μ-constraint ∞-norm to produce a design that meets the tracking, output stability margin, and robust input stability objectives. The potential advantage of this formulation vs. the three individual constraints was that the μ constraint would trade off the included performance objectives in an optimal manner, rather than requiring the designer to tradeoff the objectives individually as had to be done on the previous cases. The design results did support the hypothesis of this problem formulation. Table 4.2 shows that while we have robust input stability, our command input tracking is not as good as what we were able to get in the previous designs. This goes back to the fact that no matter how you set up this problem, the robust stability objective competes with tracking and output stability margin objectives. The bottom line is that tracking and/or output stability margin performance is going to have to be sacrificed to guarantee robust input stability. However, the simulations show that this design does indeed produce good command tracking. Unfortunately, this controller had one pole in the Right-Half Complex Plane (RHP) and was disqualified as a flight test design based on the problems HAVE

INFINITY had with implementing control laws with poles in the RHP. An option here would be to pick a controller that is "lower" on the Edgeworth-Pareto curve (see Appendix B) in Figure 4.2 that has all Left-Half Complex Plane (LHP) poles.
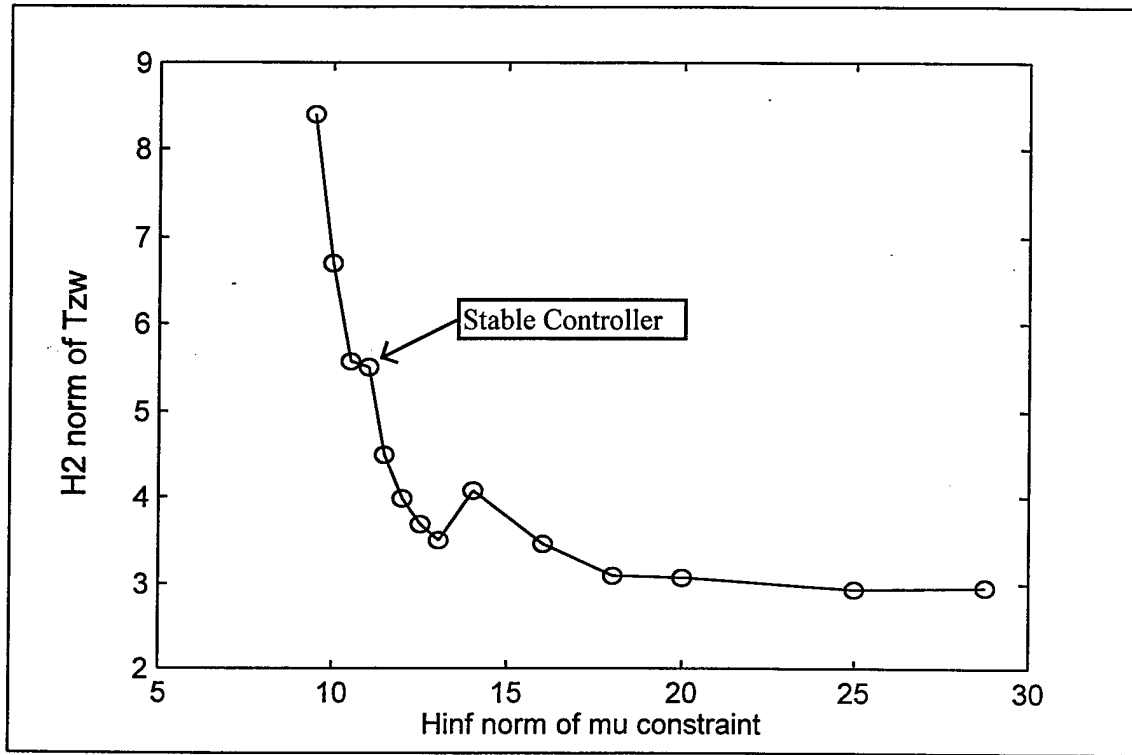
Figure 4.2. Edgeworth-Pareto Curve for mixed H_2 / μ problem

The point that corresponds to this type of controller is the marked point on the left side of the Pareto curve in Figure 4.2. Note that the curve shown in Figure 4.2 is not monotonically increasing in T_{zw} as the theory dictates. Since the stabilizing control law is found iteratively, the SQP algorithm can get 'lost' from one solution point to the next and not necessarily produce the best solution from a theoretical point of view. Multiple runs of the algorithm would be required to eliminate this problem. Since the control laws of interest in this case were not contained in the non-monotonic region, the optimization was not re-accomplished.

The norms and vector margins of this controller are

$$\left\|T_{zw}\right\|_2 = 5.4891, \quad \left\|T_{e_3 d_{31}}\right\|_\infty = 48.99, \quad \left\|T_{e_1 d_1}\right\|_\infty = .99, \text{ and } \left\|T_{e_2 d_2}\right\|_\infty = 1.7240$$

Case	Complement. Sensitivity Vector Gain Margins (dB) Input of Plant	Sensitivity Vector Gain Margins (dB) Input of Plant	Phase Margins (deg) Input of Plant	Complement. Sensitivity Vector Gain Margins (dB) Output of Plant	Sensitivity Vector Gain Margins (dB) Output of Plant	Phase Margins (deg) Output of Plant
1-5a	[-22.61, 5.69]	[-4.89, 12.24]	55.16	[-11.55, 4.79]	[-4.88, 12.16]	44.27

The stability margins of this controller are excellent, but there is degradation in tracking performance as indicated by the increase in $T_{e_3 d_3}$. The next step would be to evaluate this design's tracking performance to see if it is an acceptable design. This is accomplished in the following section.

4.1.4   Simulations.

Several simulations were carried out to validate the short period longitudinal controller designs. Unfortunately, the nonlinear aircraft/atmospheric model of the Calspan LearF-16 was not available to perform dynamic simulations and validation of the controller designs. Therefore, Matlab's[TM] simulation toolbox SIMULINK[TM] [20] was used. The simulations that were performed were "static" in that the controllers were tested only at the design points. For small changes in pitch rate (which we would expect in the approach and landing phase, and is an assumption of the linearized equations of motion), these simulations should provide a realistic transient response as long as the state and input variables remain relatively small. Figure 4.3 illustrates the SIMULINK[TM] setup used to test the control designs developed in cases 1-1 through 1-5a. As illustrated, the simulation included wind and measurement noises, as well as rate and saturation limiters on elevator deflection. A Dryden wind model [21] was fed by white

noise to produce moderate turbulence conditions in approach and landing as specified in [8].

The measurement noise inputs consisted of both filtered additive and multiplicative components

that were fed by white noise. The breakdown was 98% multiplicative and 2% additive. The

magnitude of multiplicative noise on the measurement increased as the magnitude of the output

signal increased. However, when there was no output signal, there was no multiplicative

component of measurement noise. There was **always** additive noise present in the system

representing the steady state inaccuracies of measurement devices. The high-pass Butterworth

Figure 4.3. SIMULINK™ Setup for Pitch Rate Control Design Evaluation
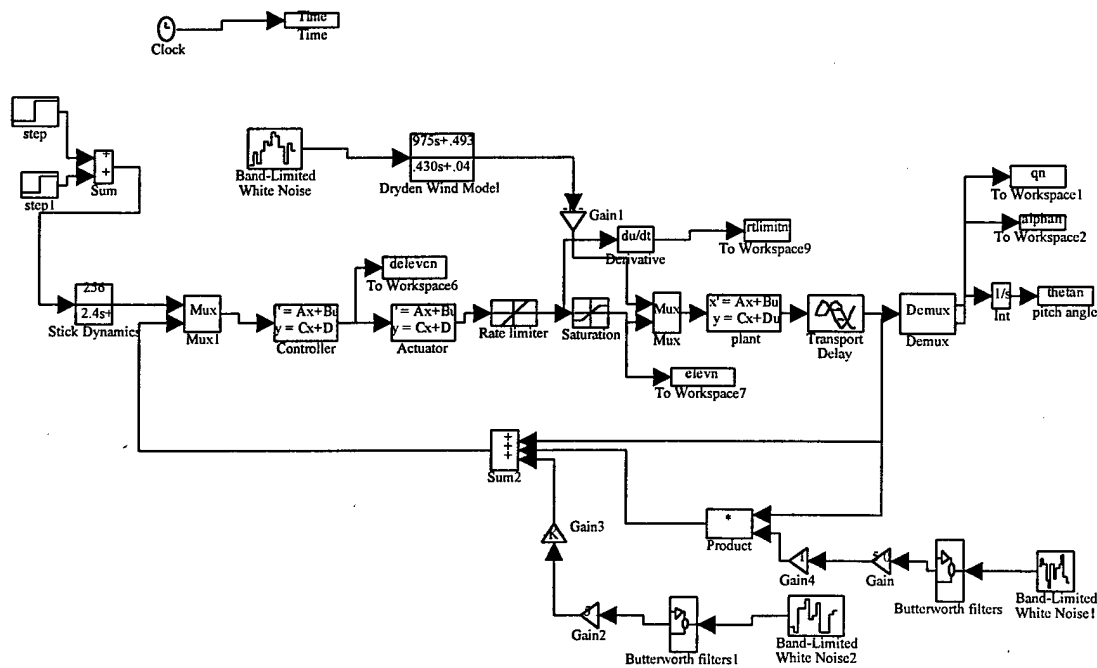
filters were included because measurement noise is substantially a high frequency phenomenon.

The "gain" blocks immediately following the Butterworth Filters contain the various gains used

to produce the correct amount of sensor noise on each measurement $(q$ and $\alpha)$. Very little data

is available in academic texts on typical sensor measurement accuracies. The data used in these simulations was obtained from McClean [22] and USAF TPS flight test data for their aircraft. The final elements included in the simulation to add realism are a pure transport delay of 0.016 seconds and a stick dynamics model. The delay accounts for overall system delays in signal processing, etc., while the stick dynamics model accounts for pilot interface delays with the flight control system. The delay was chosen based on an sensor sample rate of 63 Hz for an operational Block 30+ F-16. Finally, the simulation model includes only short period dynamics. This was done on the advice of Calspan engineers, because a good phugoid model for the LearF16 was not available and flight test experience with this model has shown that the phugoid mode is an insignificant factor in influencing handling qualities. The handling qualities prediction for each design is plotted in Figure 4.16 following the simulation plots. Comments regarding handling qualities will be made as the simulations are discussed for each design.

The time responses in Figures 4.4 and 4.5 show that the H_2 controller does not track the command exactly, as predicted, however the error is only on the order of 7% and the noise rejection performance is excellent. This design predicts level 1 handling qualities even with its tracking deficiencies because it has good phase rolloff and bandwidth characteristics. Figures 4.6 and 4.7 represent case 1-2 and show that this design provides excellent tracking with only a small sacrifice in noise rejection performance. However the handling qualities are predicted level 2 for this design. In order to get this excellent tracking, the bandwidth has decreased and hence induced excessive phase rolloff. Figures 4.8 and 4.9 are the simulations for case 1-3. A small amount of tracking performance has been sacrificed here to move the handling qualities back to the level 1/2 border. Figures 4.10 and 4.11 show the simulations for case 1-4. Tracking performance has been further sacrificed. But this small sacrifice has resulted in solid level 1 handling qualities predictions. Finally, Figures 4.12-4.15 cover cases 1-5 and 1-5a. Case 1-5a is

not shown on the handling qualities plot because it results in the same prediction as case 1-5. However these figures illustrate a fairly noticeable loss in tracking performance if we are constrained to a controller that has all of its poles in the LHP. Overall, the results for the pitch rate command designs were very good. However, discussions with Calspan test pilots and engineers close to the end of phase I revealed that these types of designs may exhibit some undesirable handling qualities in the approach and landing phase based on their flight test experience [23]. This will be addressed next in the angle of attack design results.

4.2 Angle of Attack Design Results

The angle of attack designs are included to address potential handling qualities deficiencies in the pitch rate designs [23]. The main problem with the pitch rate designs for the approach and landing phase can be seen by looking at the pitch angle (θ), and flight path angle (γ) plots in Figures 4.4 - 4.15. Note that there is a steady state value for both θ and γ after the control is removed. This may give pilots the sensation they are "floating", and will require them to push forward on the stick with a pulse type input in the flare to land the airplane. This characteristic of these designs is caused by an integral closed loop pole at the origin. This suggests that putting a closed loop zero at the origin might be a way to fix this problem. Two approaches to doing this are discussed. The first involves adding a washout filter and a lead filter to the pitch rate simulations. Note that the control designs are the same ones from the previous section. The command signal is being filtered to produce a specific type of response. The specifics of the filter structure and utility will be discussed in the next section. This approach was implemented mainly because of severe time constraints remaining in Phase I of this research. Figure 4.17 shows the simulation setup for this approach. The second approach

involves actually designing a new controller that eliminates the steady state characteristics of the pitch and flight path responses. This will produce an angle of attack following system which should be more desirable for the landing task. Again, because of the severe time limitations, only two designs were completed. However these designs are promising and will be discussed along with the necessary changes in the problem setup to produce them.
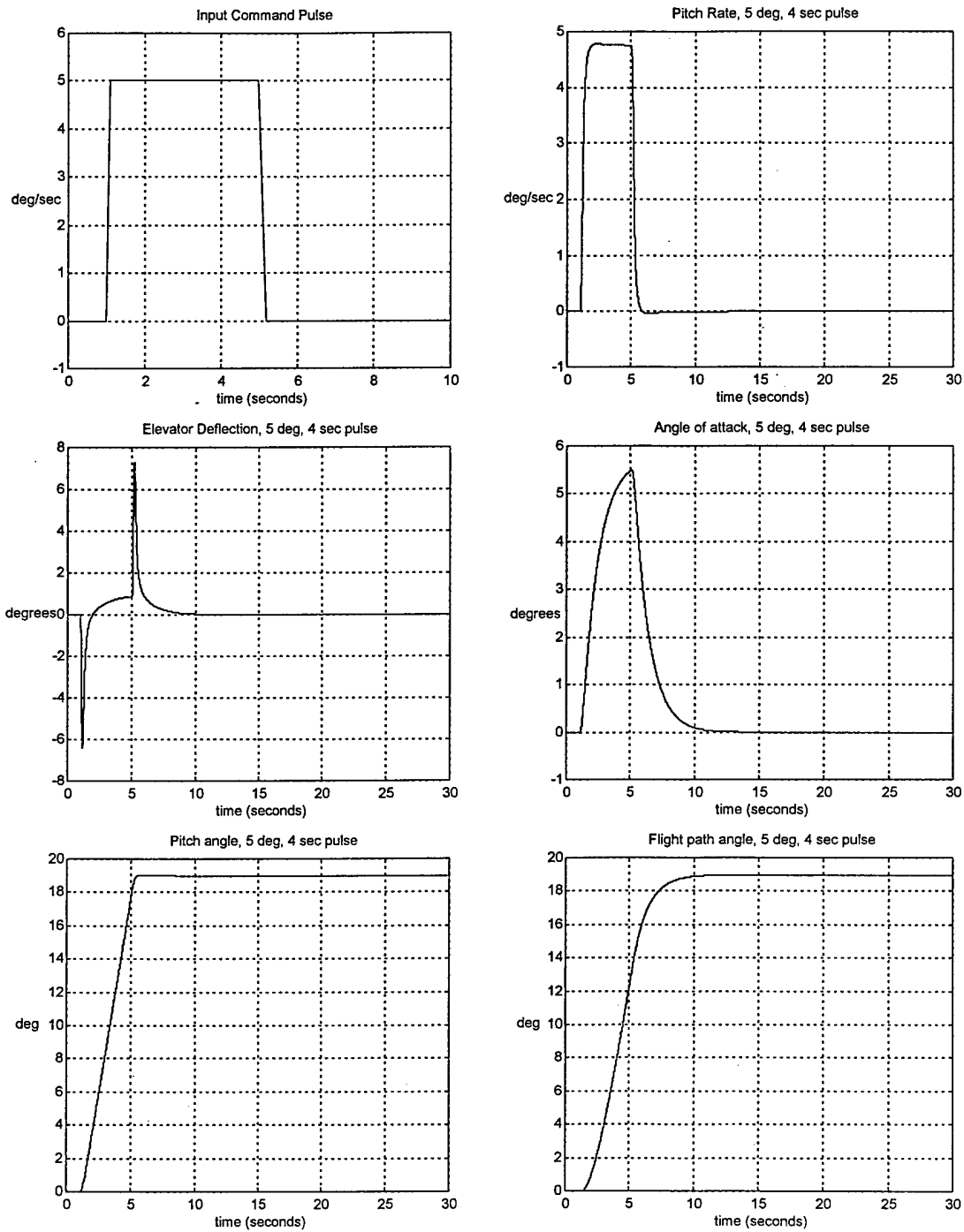
Figure 4.4. Short Period Simulations for Case 1-1 - Noises off
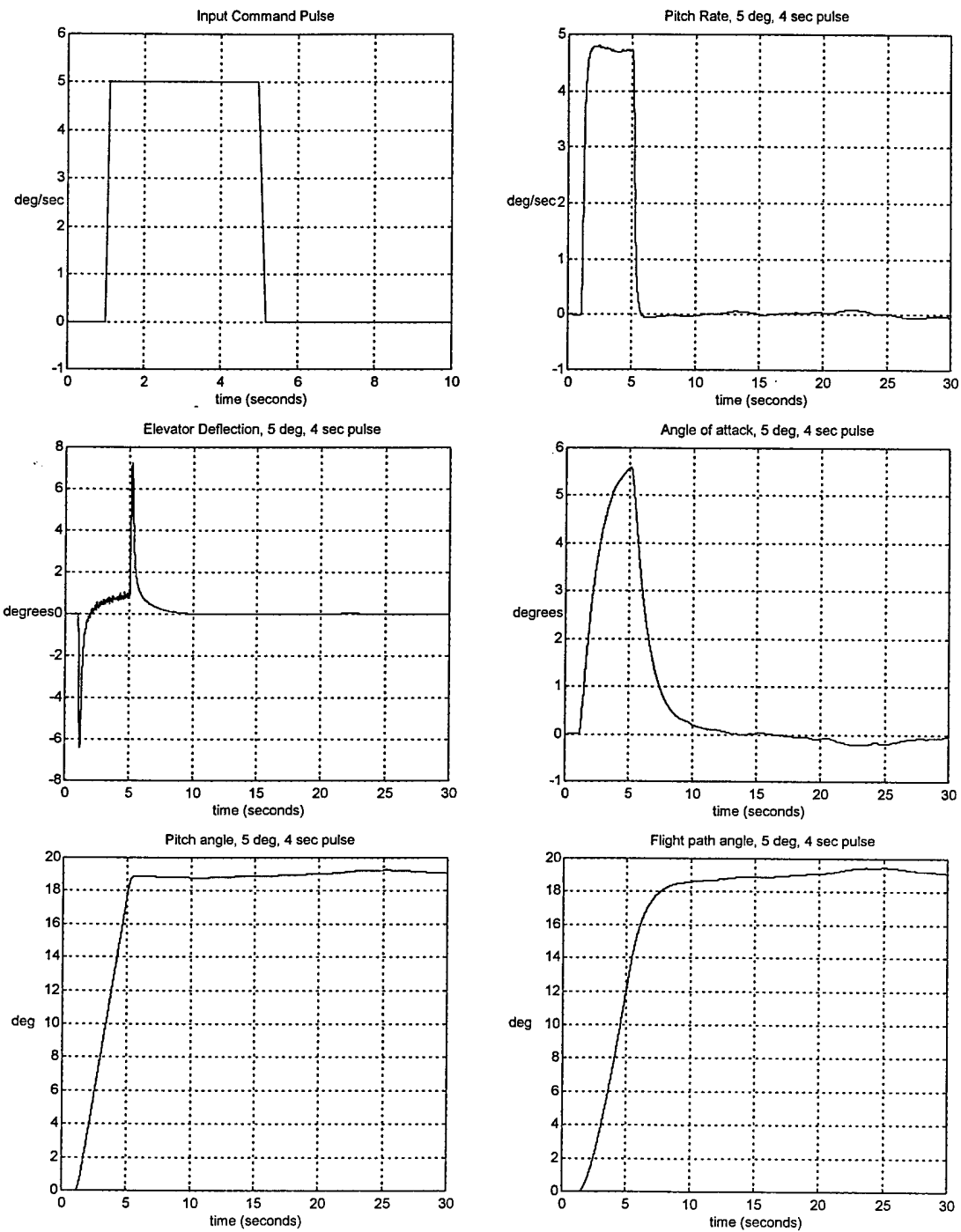
Figure 4.5. Short Period Simulations for Case 1-1 - Noises on
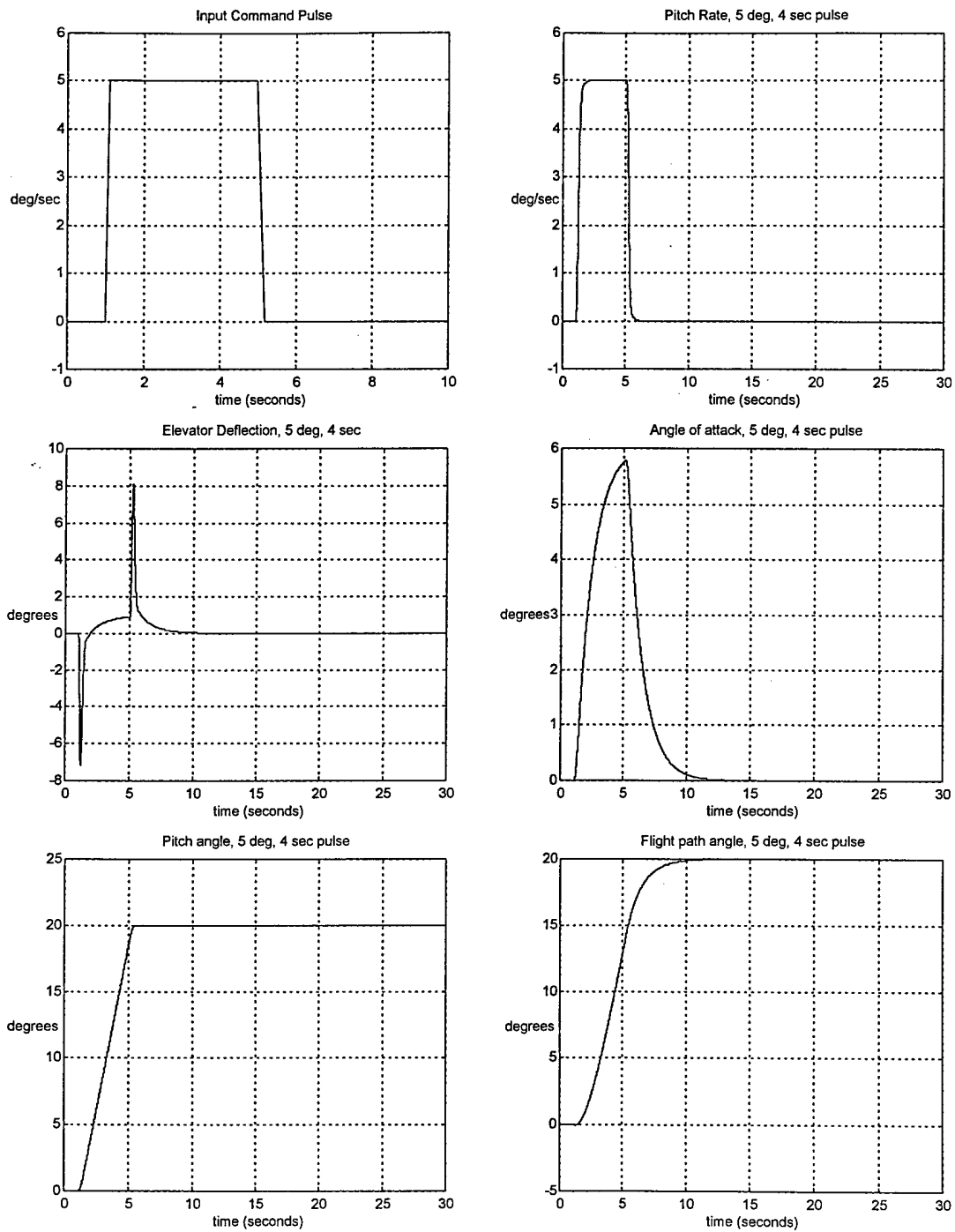
Figure 4.6. Short Period Simulations for Case 1-2 - Noises off
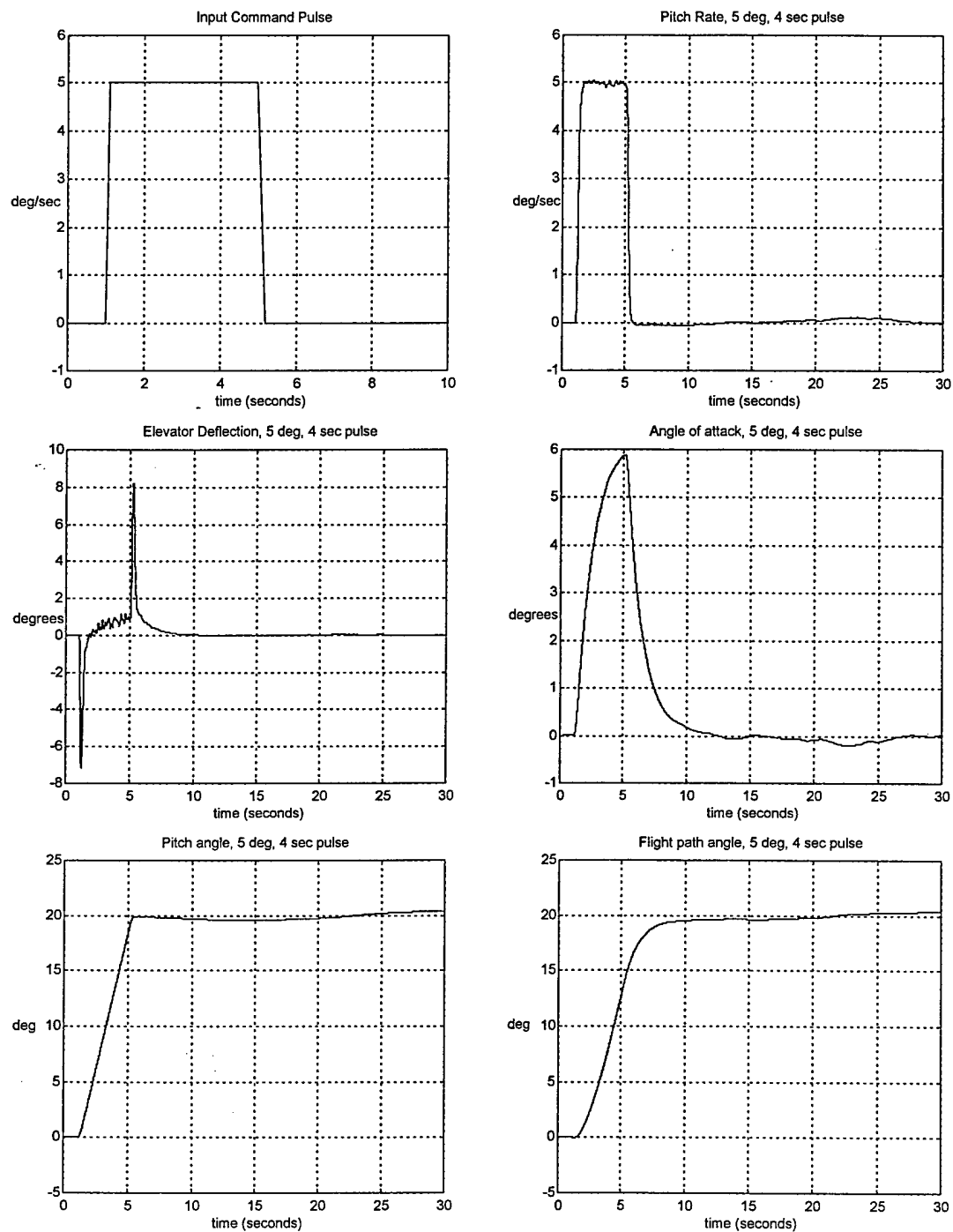
Figure 4.7. Short Period Simulations for Case 1-2 - Noises on
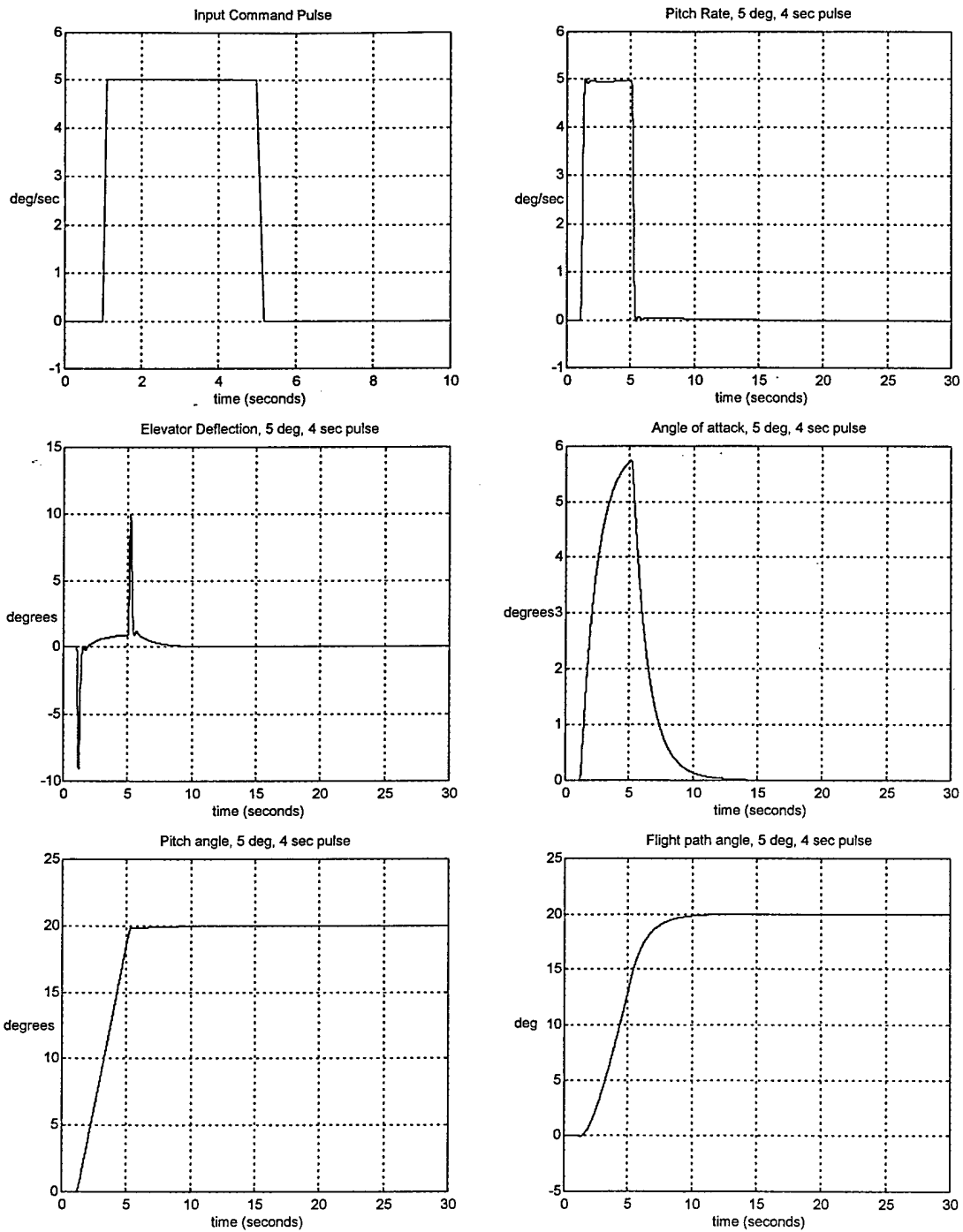
Figure 4.8. Short Period Simulations for Case 1-3 - Noises off
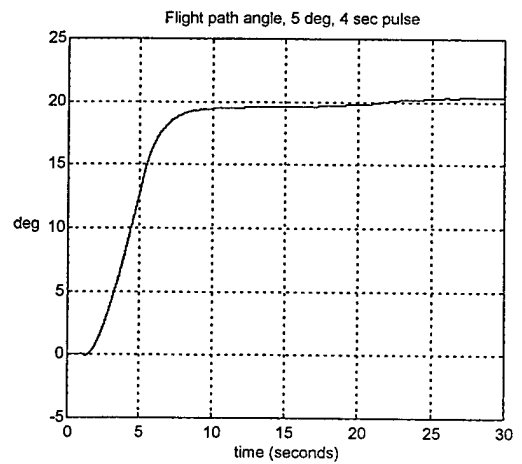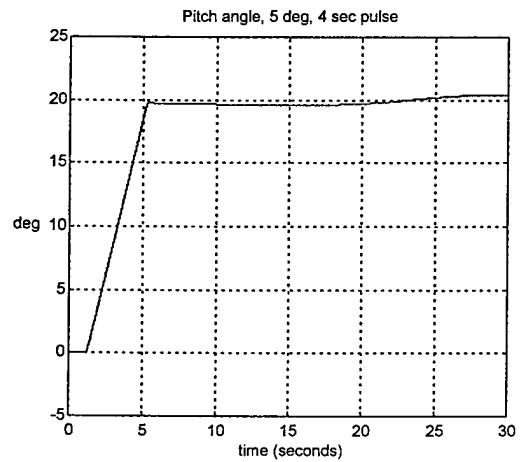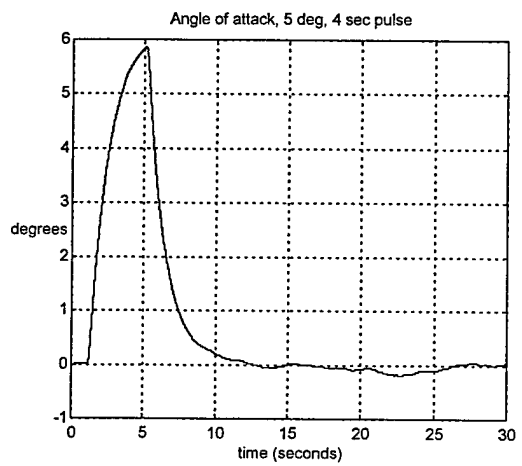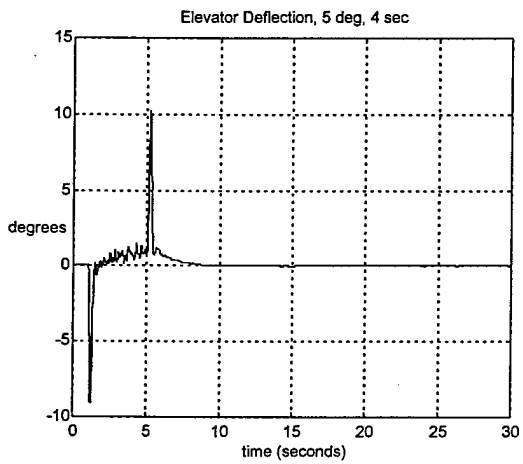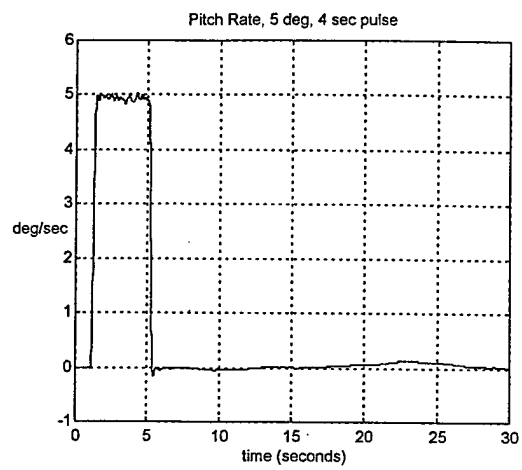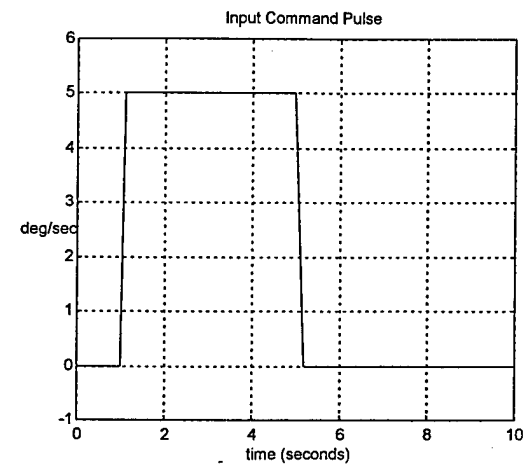
4.9. Short Period Simulations for Case 1-3 - Noises on
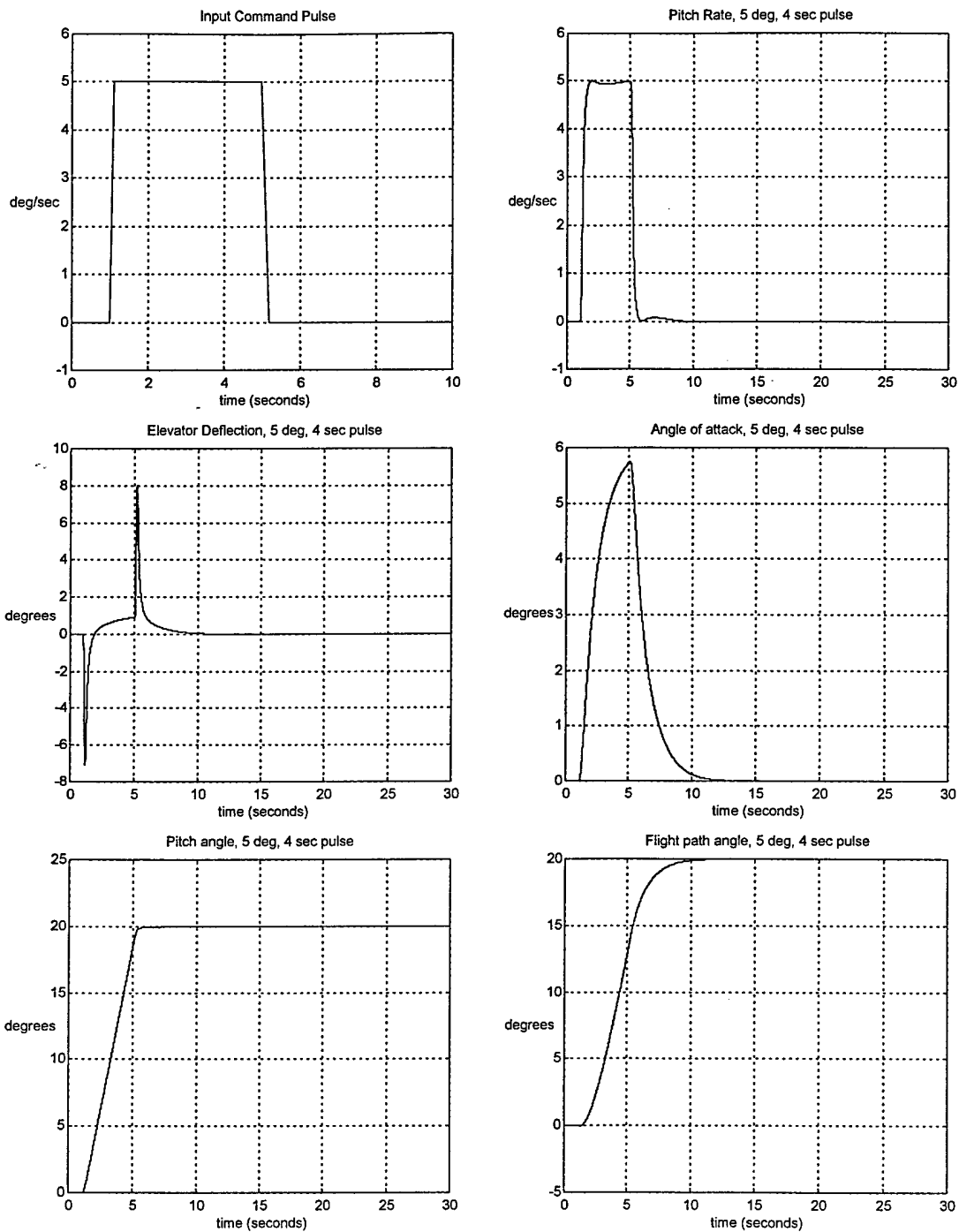
Figure 4.10. Short Period Simulations for Case 1-4 - Noises off
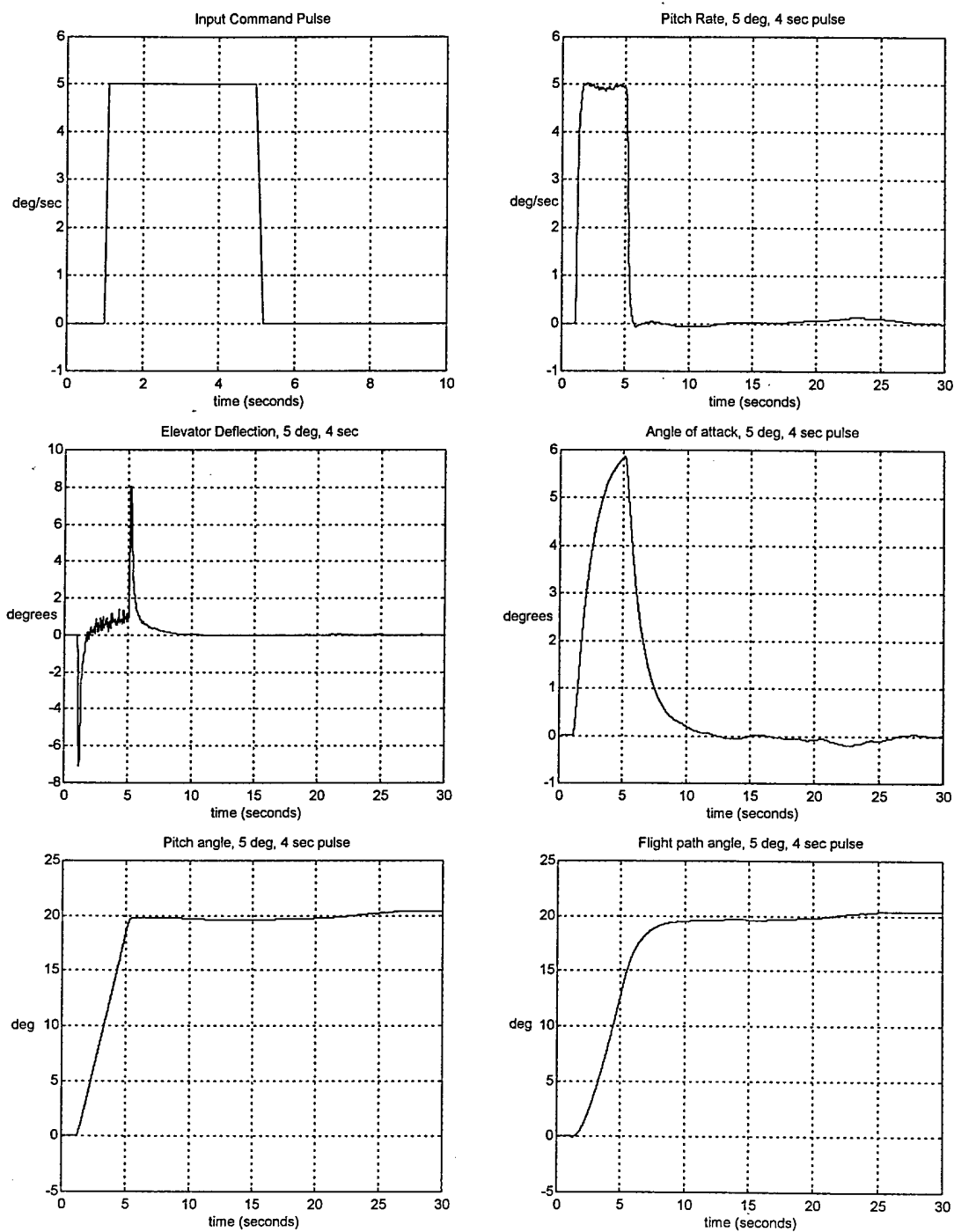
Figure 4.11. Short Period Simulations for Case 1-4 - Noises on
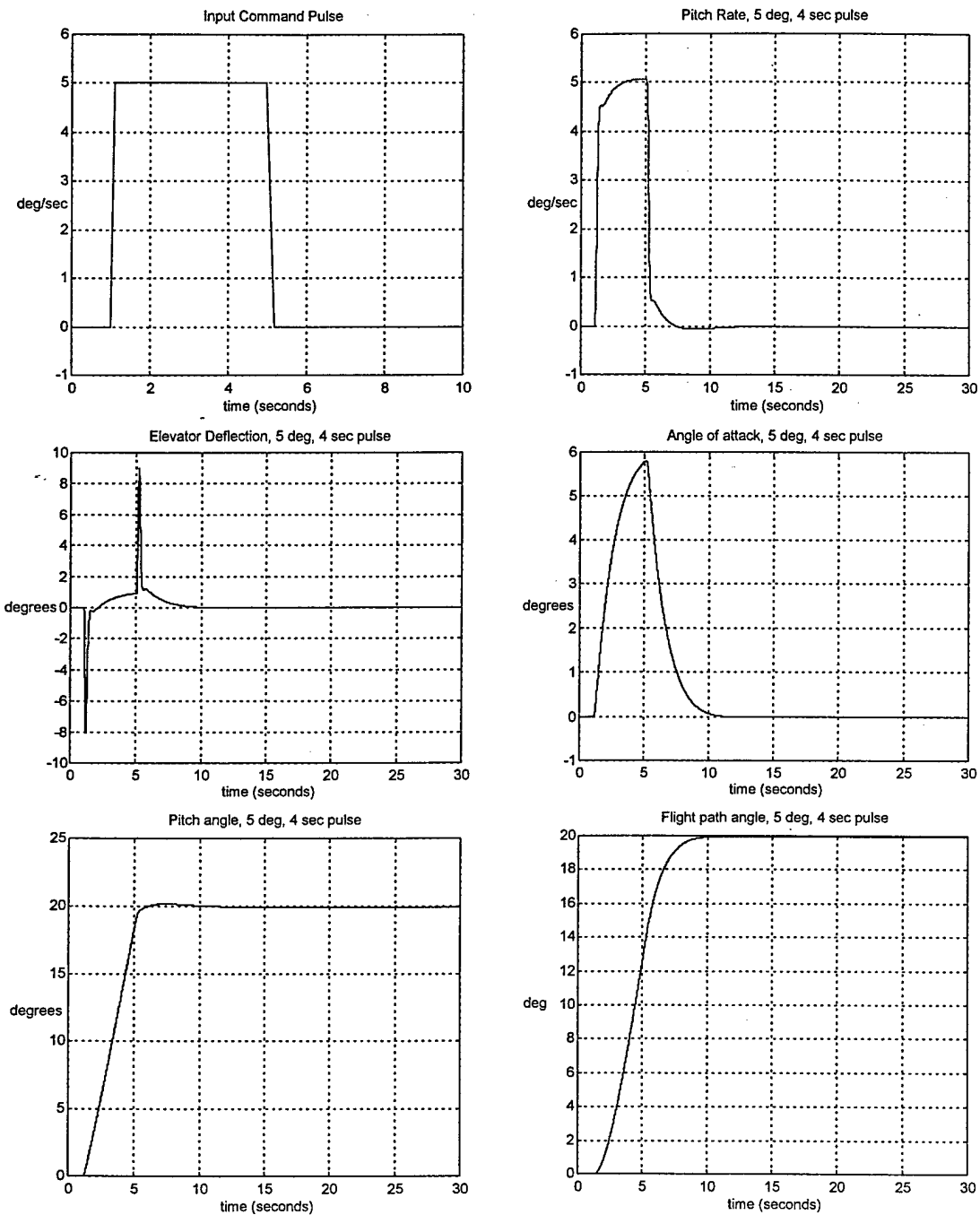
Figure 4.12. Short Period Simulations for case 1-5 - noise off
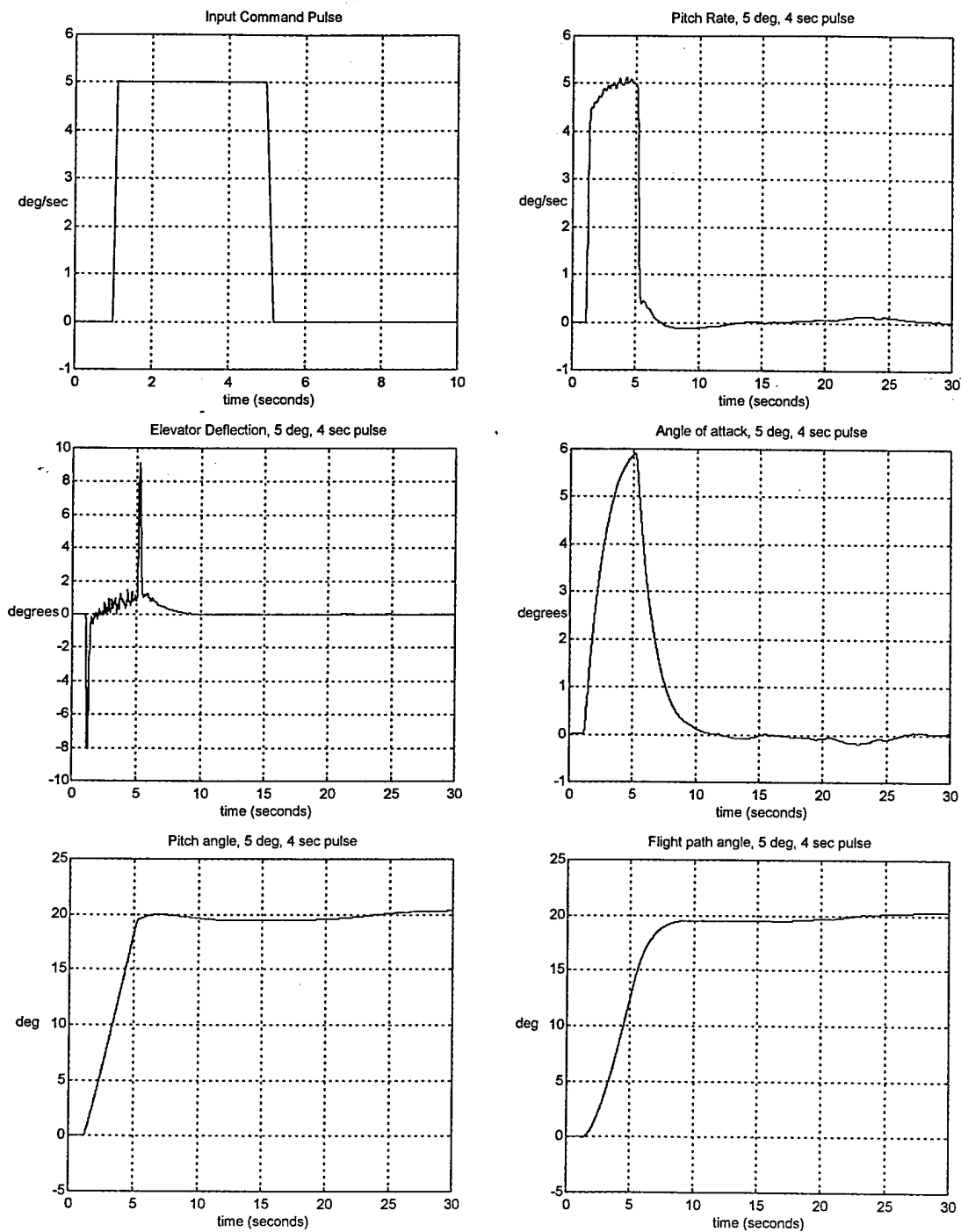
Figure 4.13. Short Period Simulations for case 1-5 - noise on
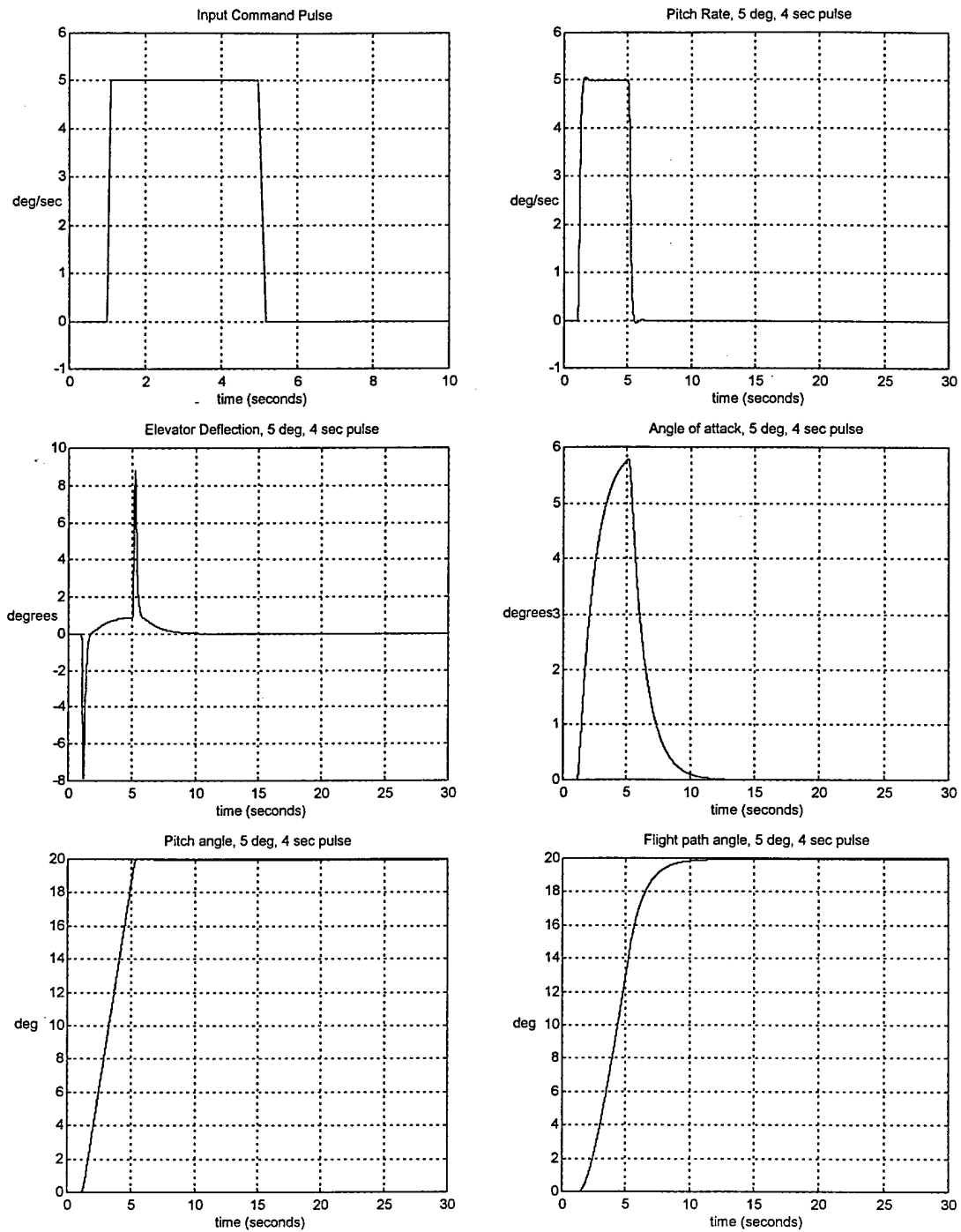
Figure 4.14. Short Period Simulations for case 1-5a- noise off
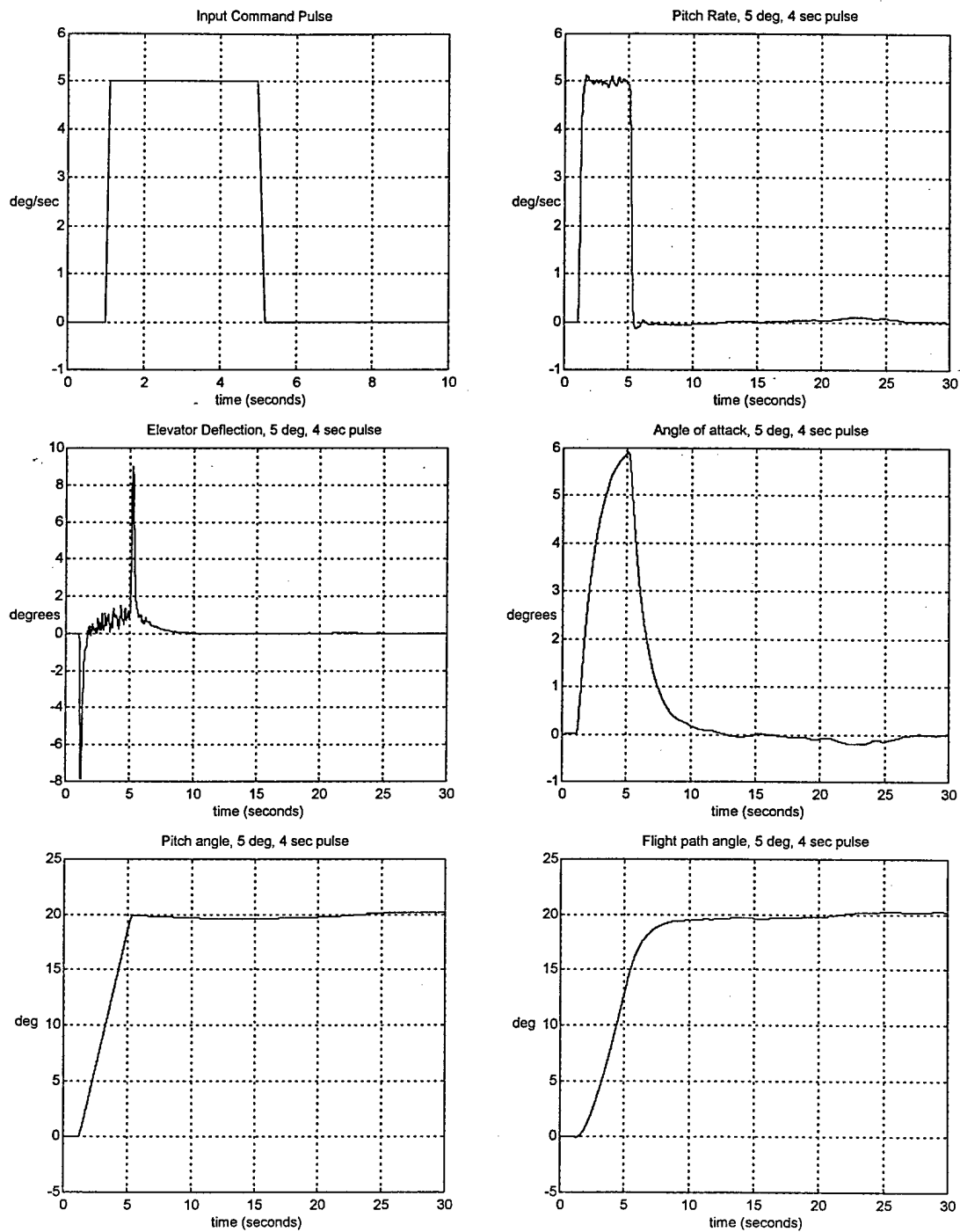
Figure 4.15. Short Period Simulations for case 1-5a- noise on
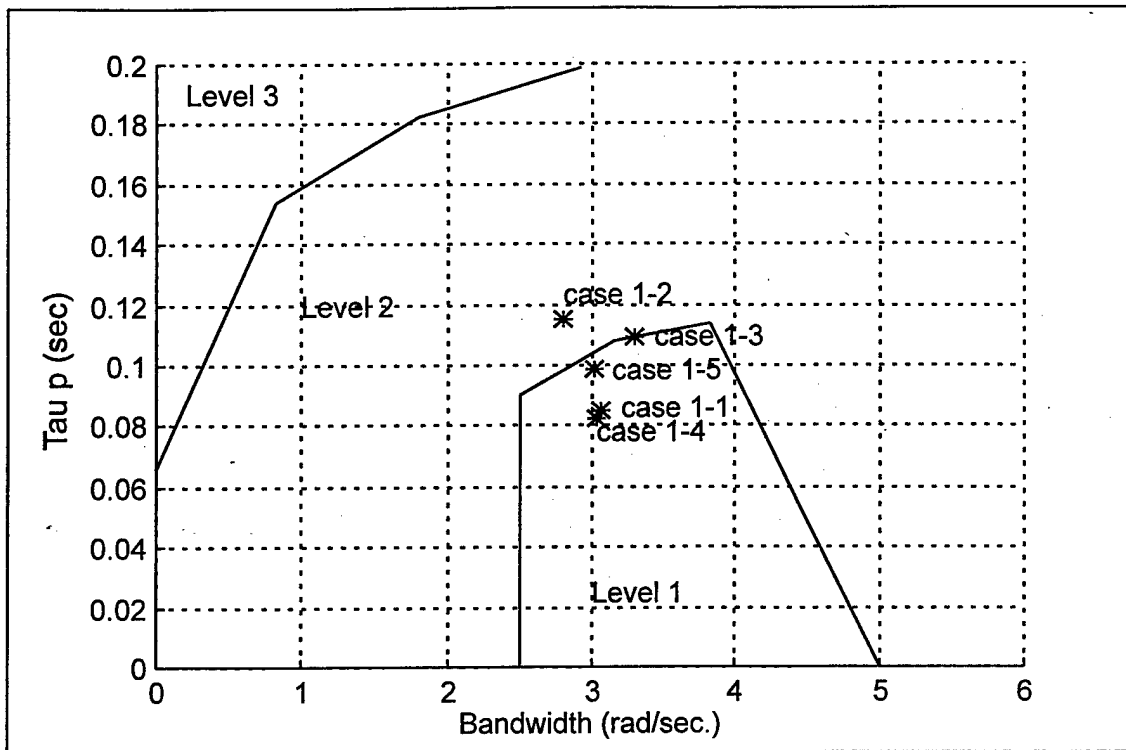
Figure 4.16. Handling Qualities Prediction for Cases 1-1 through 1-5

4.2.1 Simulation Changes.

As was mentioned above, the **only** change required to turn the pitch rate designs into

angle of attack following designs was the addition of a washout filter and lead filter to the

command path of the simulation (see Fig. 4.17). Since these are placed outside the feedback

loop, there are no concerns with regards to changing the overall stability of the system because

it is handled exclusively in the feedback path. These filters will reshape the frequency (and time)

responses of the simulations. Therefore the handling qualities predictions may not be the same

as they are without the filters.

Figure 4.17. SIMULINK Structure for Angle of Attack Following Designs

Figure 4.30 shows the Hoh's Bandwidth handling qualities predictions for the angle of attack following designs. These will be discussed as comments are made on each design. However, before the simulation results are presented, and each design is discussed, it is necessary to discuss the structure of the filters.

The washout filter removes the integral action on pitch rate and pitch angle by placing a zero at the origin. It also gives the pilot the ability to use monotonic stick forces by placing a real pole at typical phugoid magnitudes. The transfer function used the washout filter in Figure 4.17 is given by

$$wofilt = \frac{20s}{20s + 1} \qquad (4.1)$$

The lead filter restores pitch rate overshoot which results in a faster angle of attack response. This is desirable since this an angle of attack following system. The transfer function of the lead filter in Figure 4.17 is

$$lefilt = \frac{1.192s + 1}{.659s + 1} \qquad (4.2)$$

The values for the zero and pole in equation 4.2 move a pole in the q/q_c transfer function from -0.839 to -1.517 which produces the characteristics mentioned above.
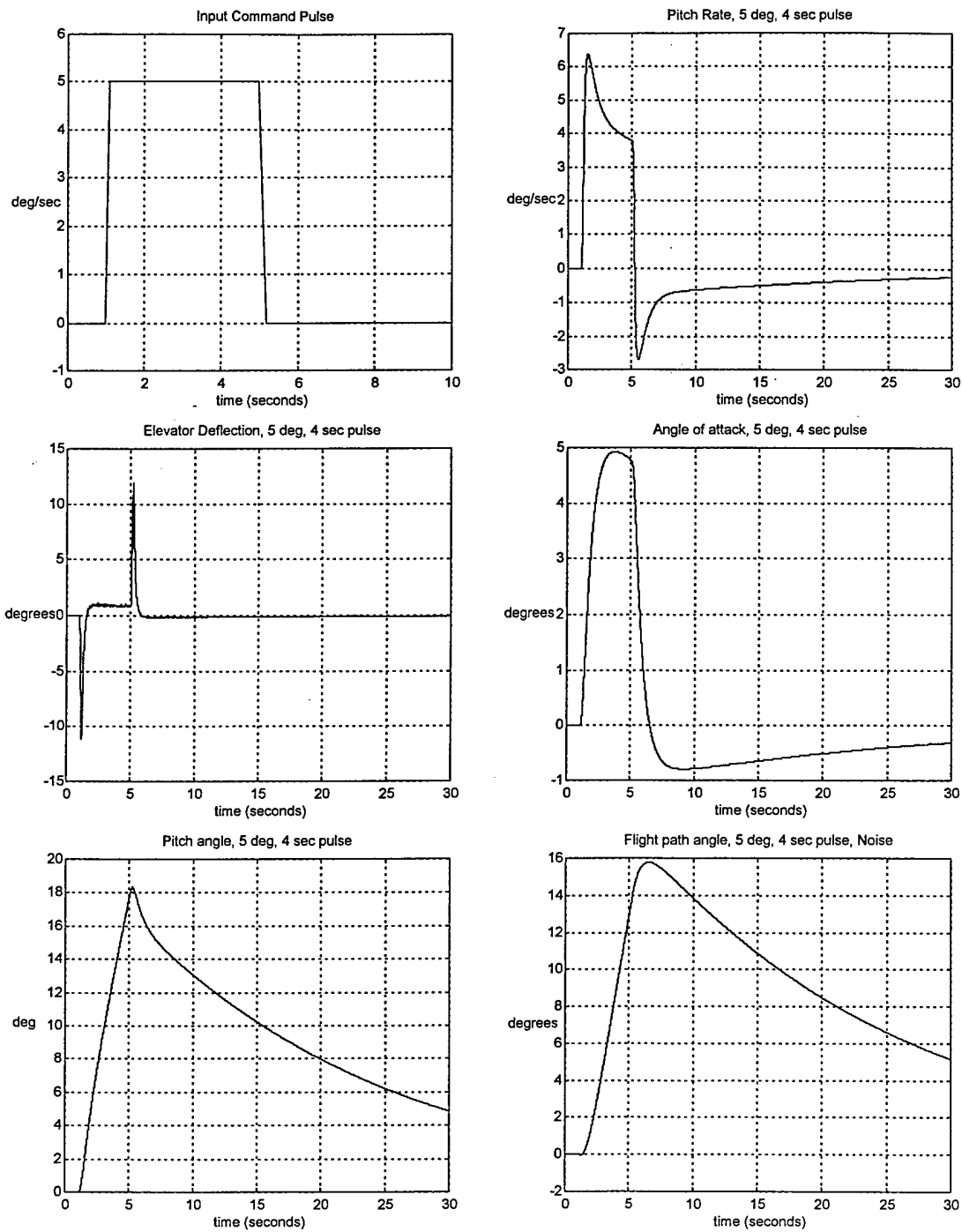
Figure 4.18. Angle of Attack Simulations for Case 1-1 - noises off
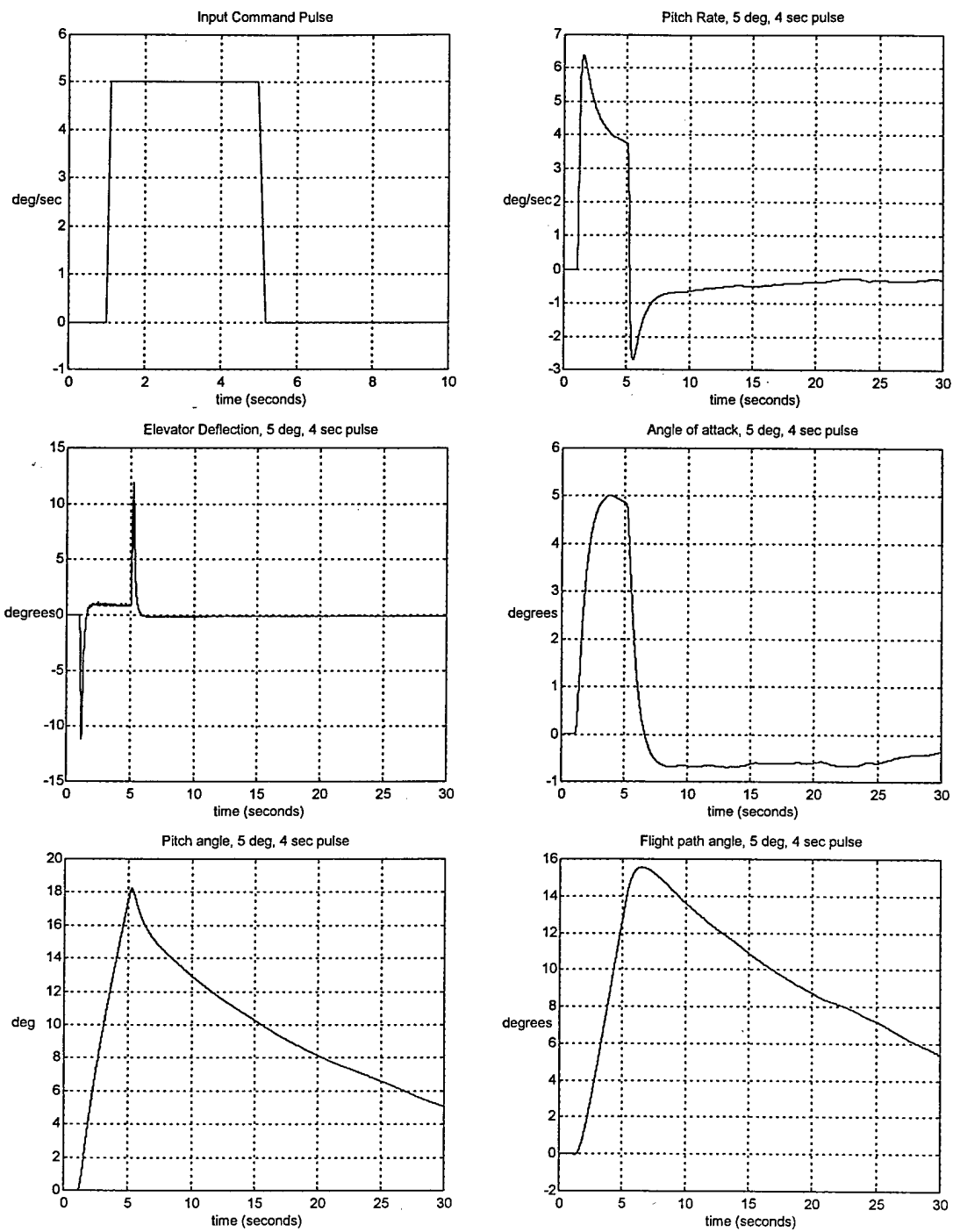
Figure 4.19. Angle of Attack Simulations, Case 1-1 - noises on
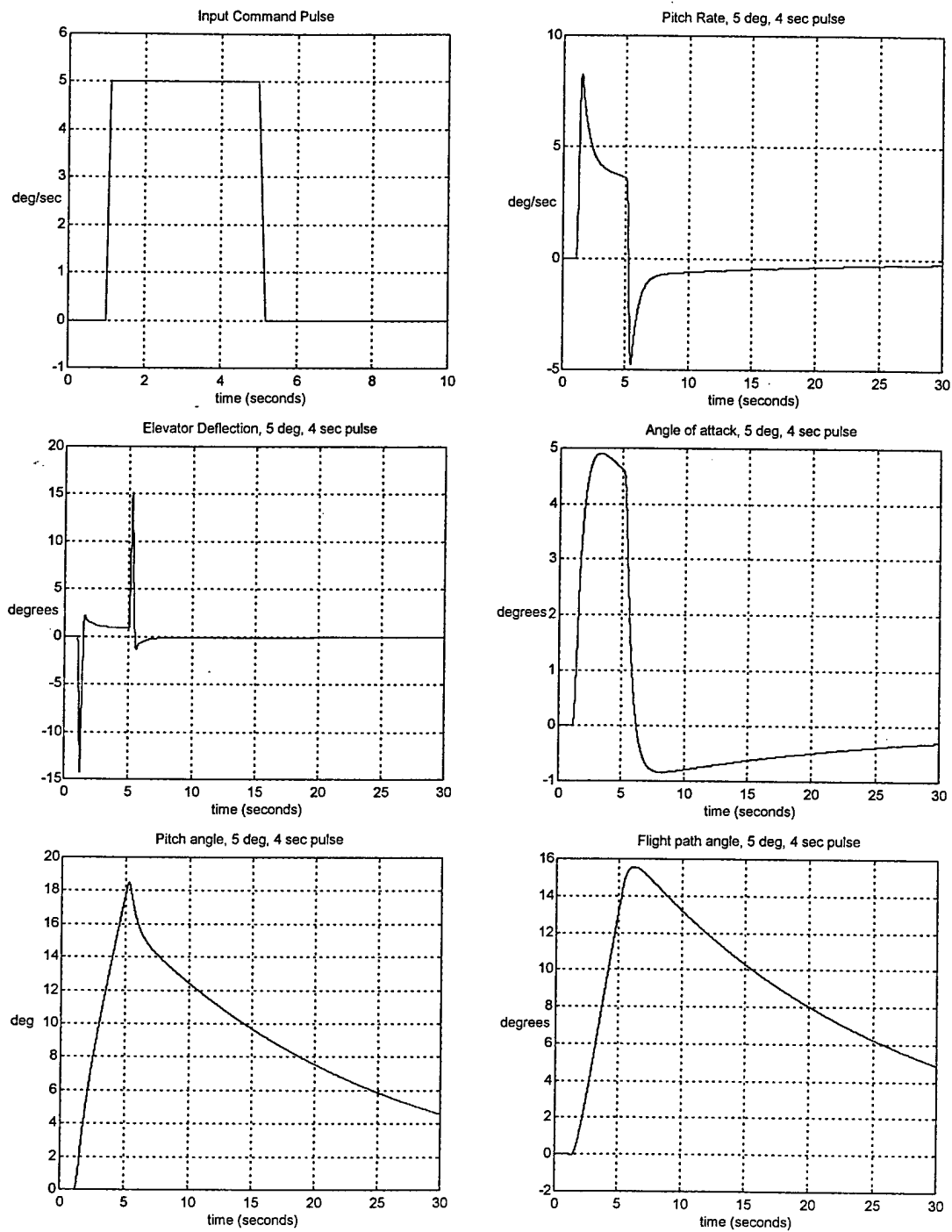
Figure 4.20. Angle of Attack Simulations for Case 1-2 - Noises off
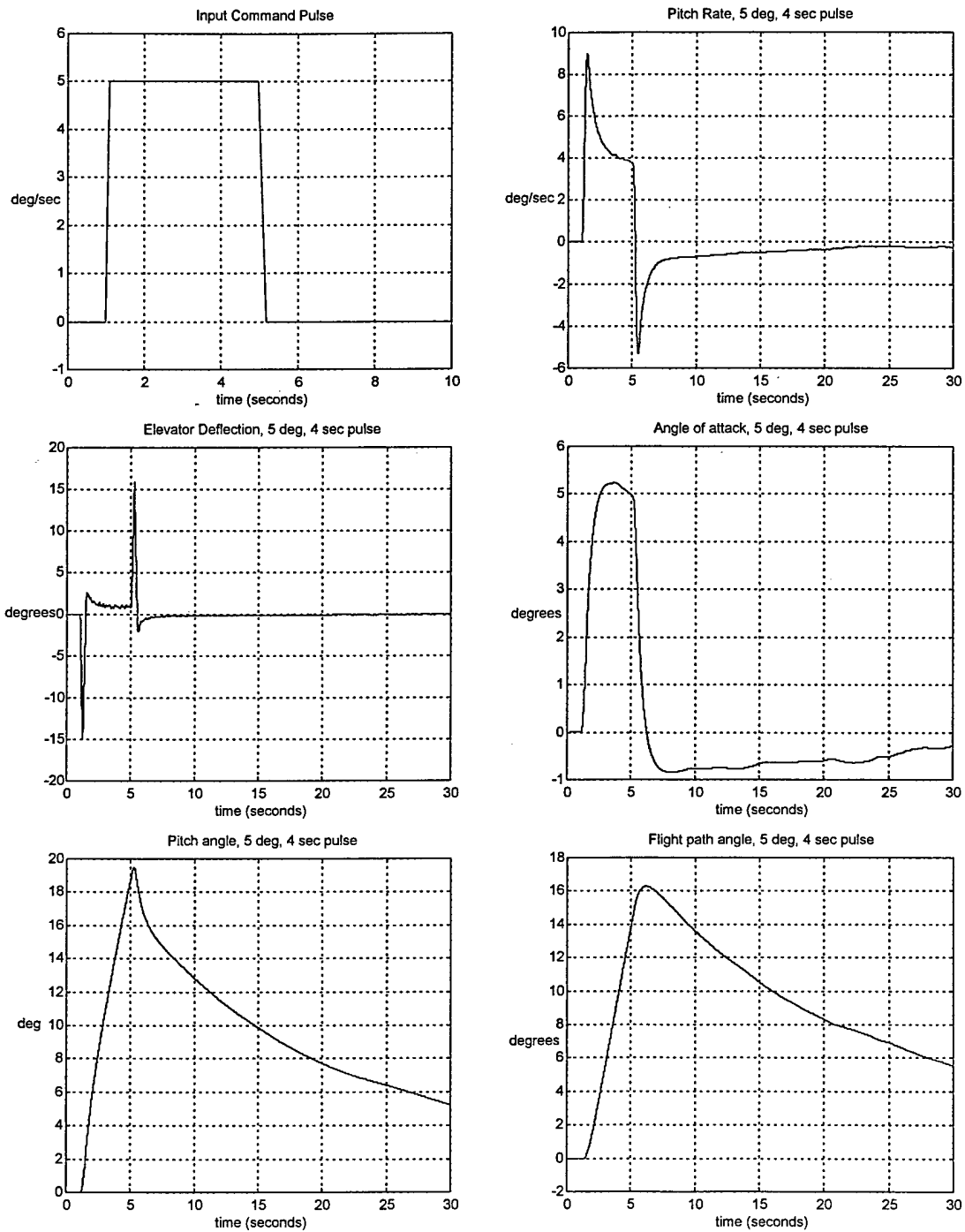
Figure 4.21. Angle of Attack Simulations for Case 1-2 - Noises on
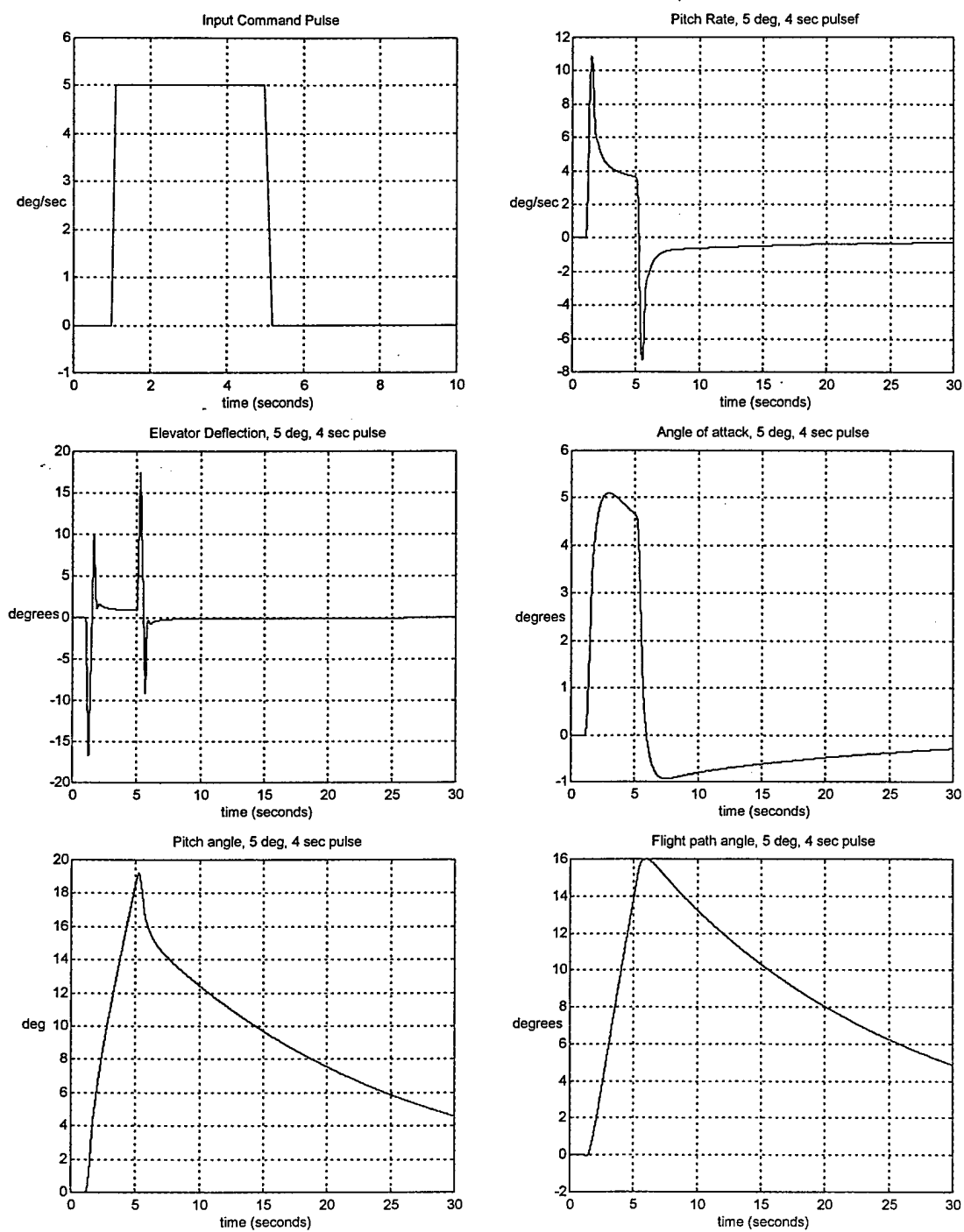
Figure 4.22. Angle of Attack Simulations for Case 1-3 - noise off
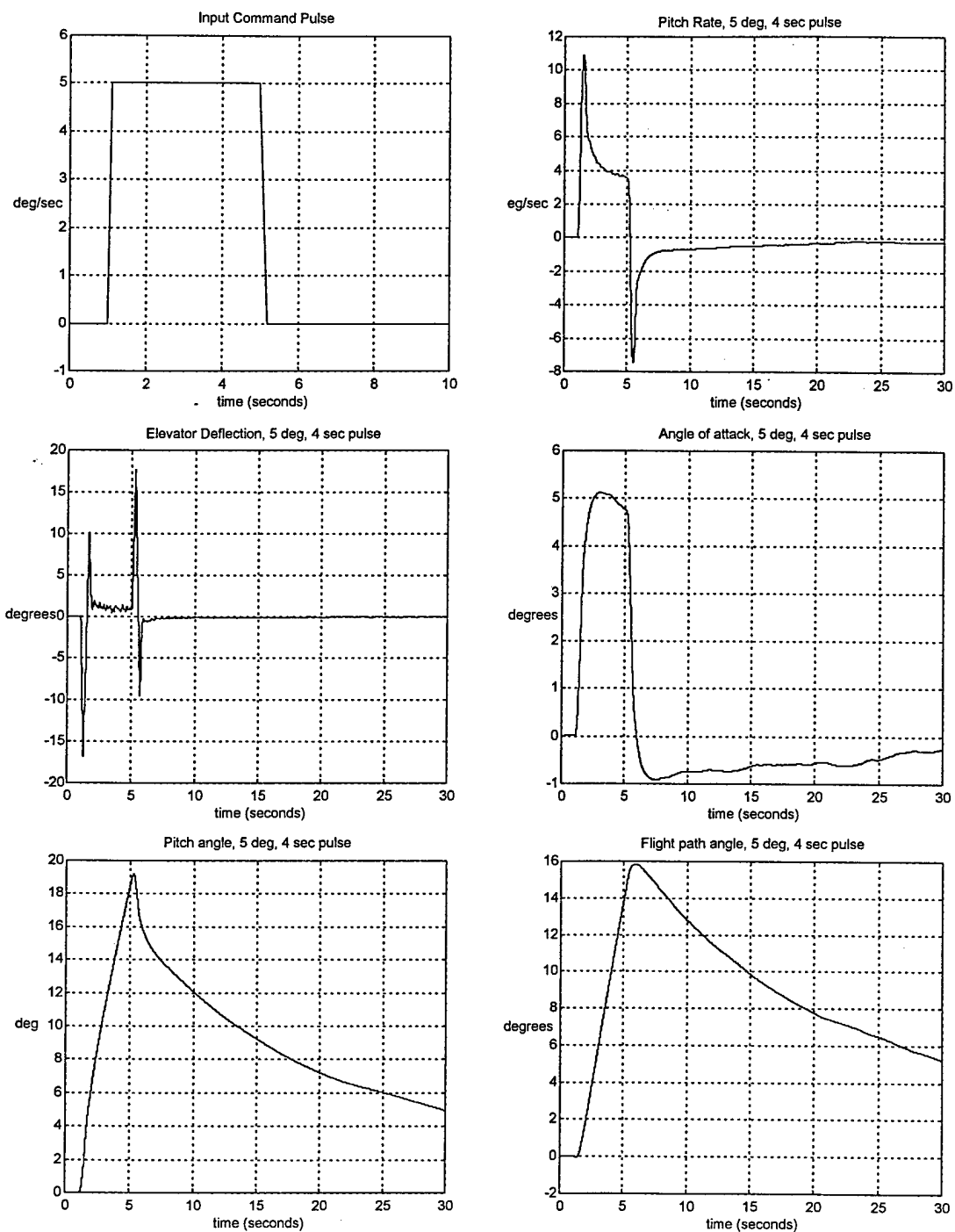
Figure 4.23. Angle of Attack Simulations for Case 1-3 - noise on
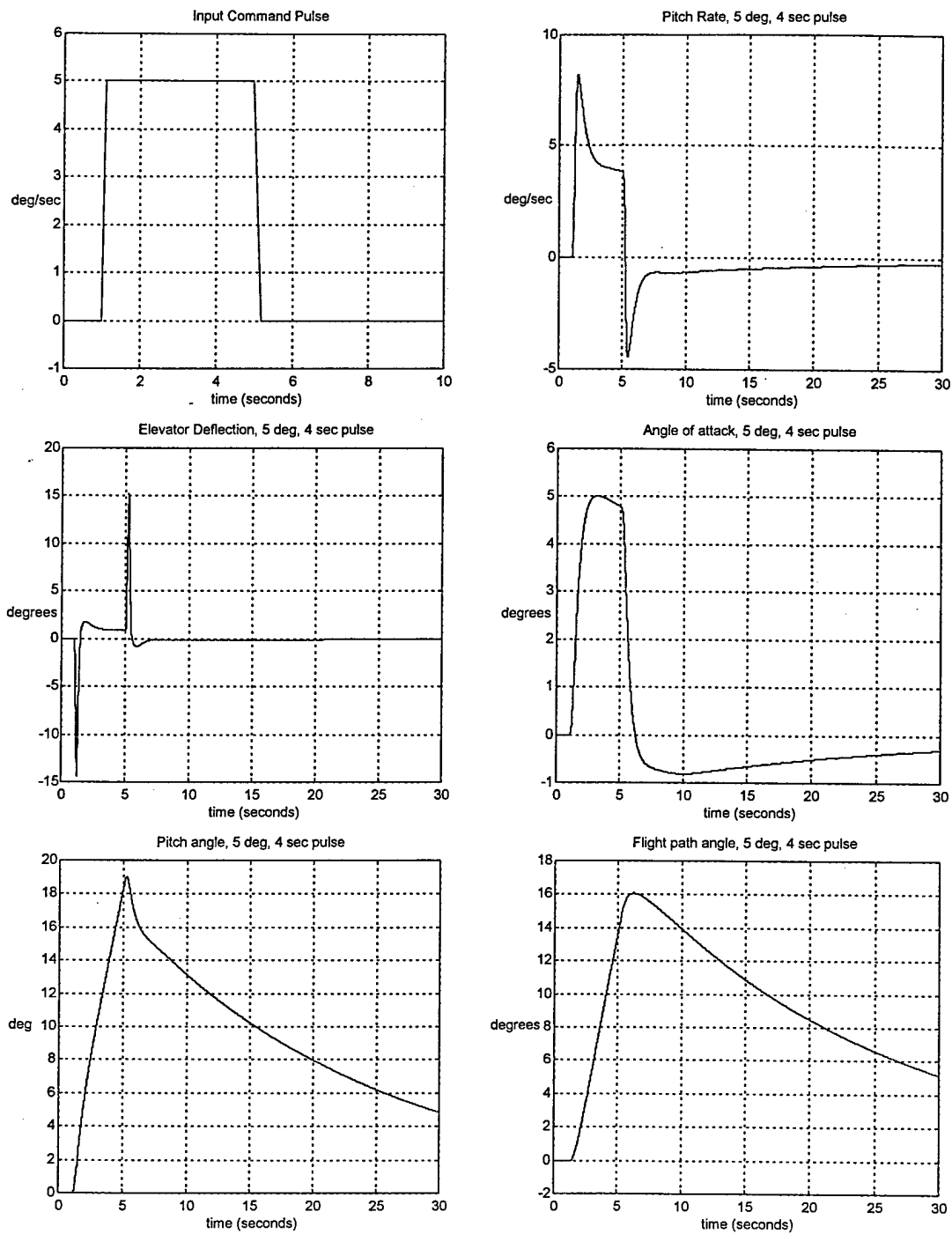
Figure 4.24. Angle of Attack Simulations for Case 1-4 - noise off
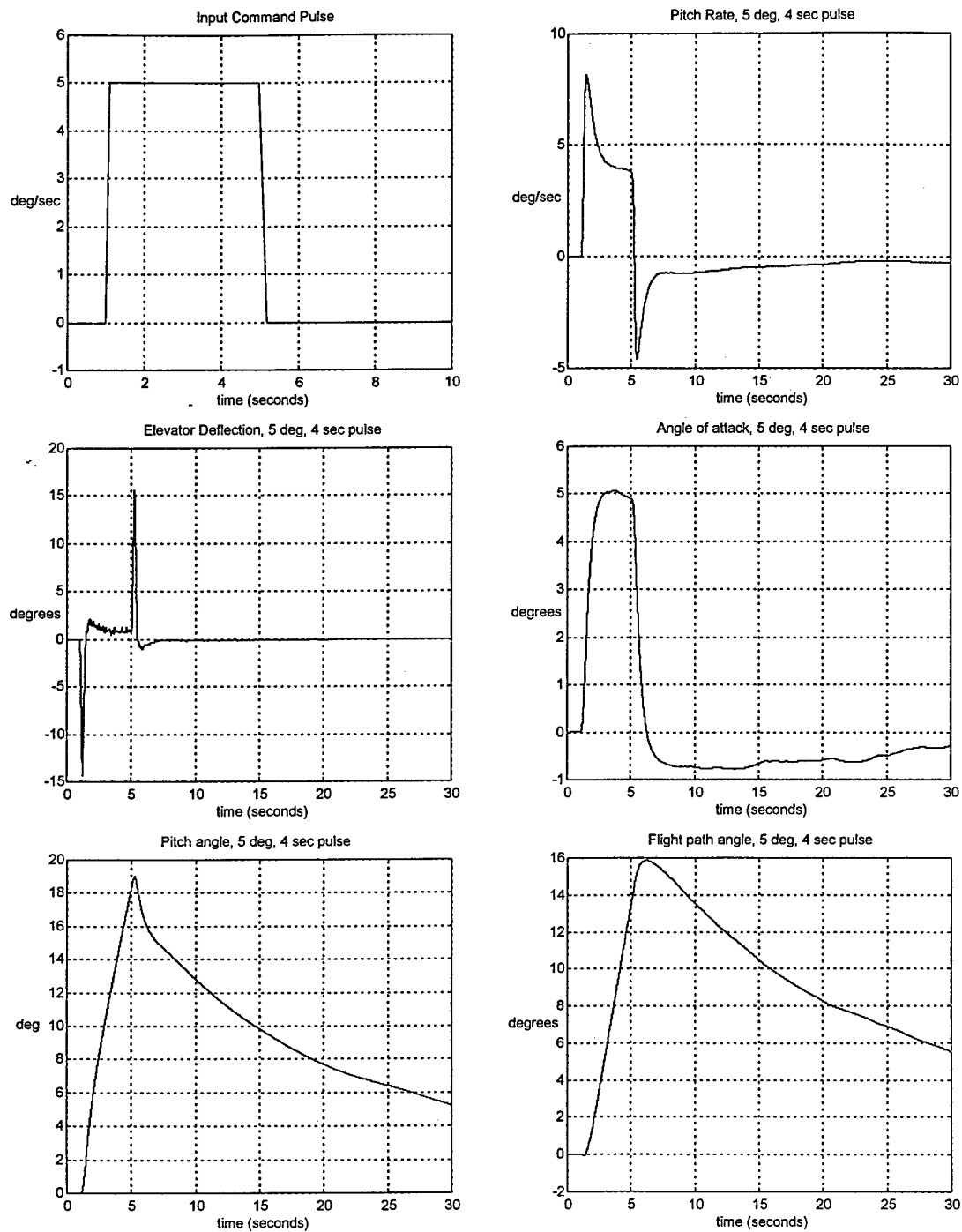
Figure 4.25. Angle of Attack Simulations for Case 1-4 - noise on
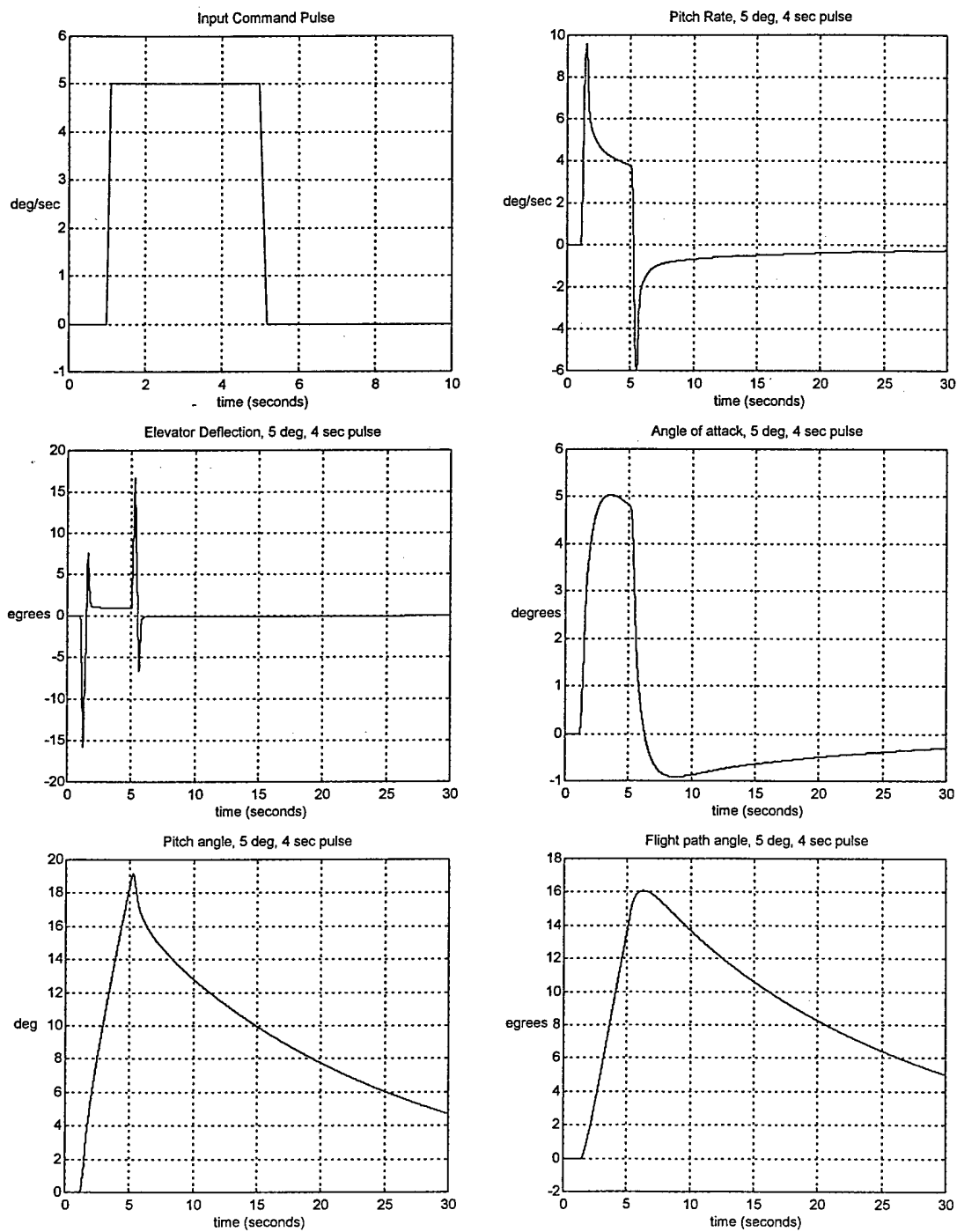
Figure 4.26. Angle of Attack Simulations for Case 1-5 - noise off
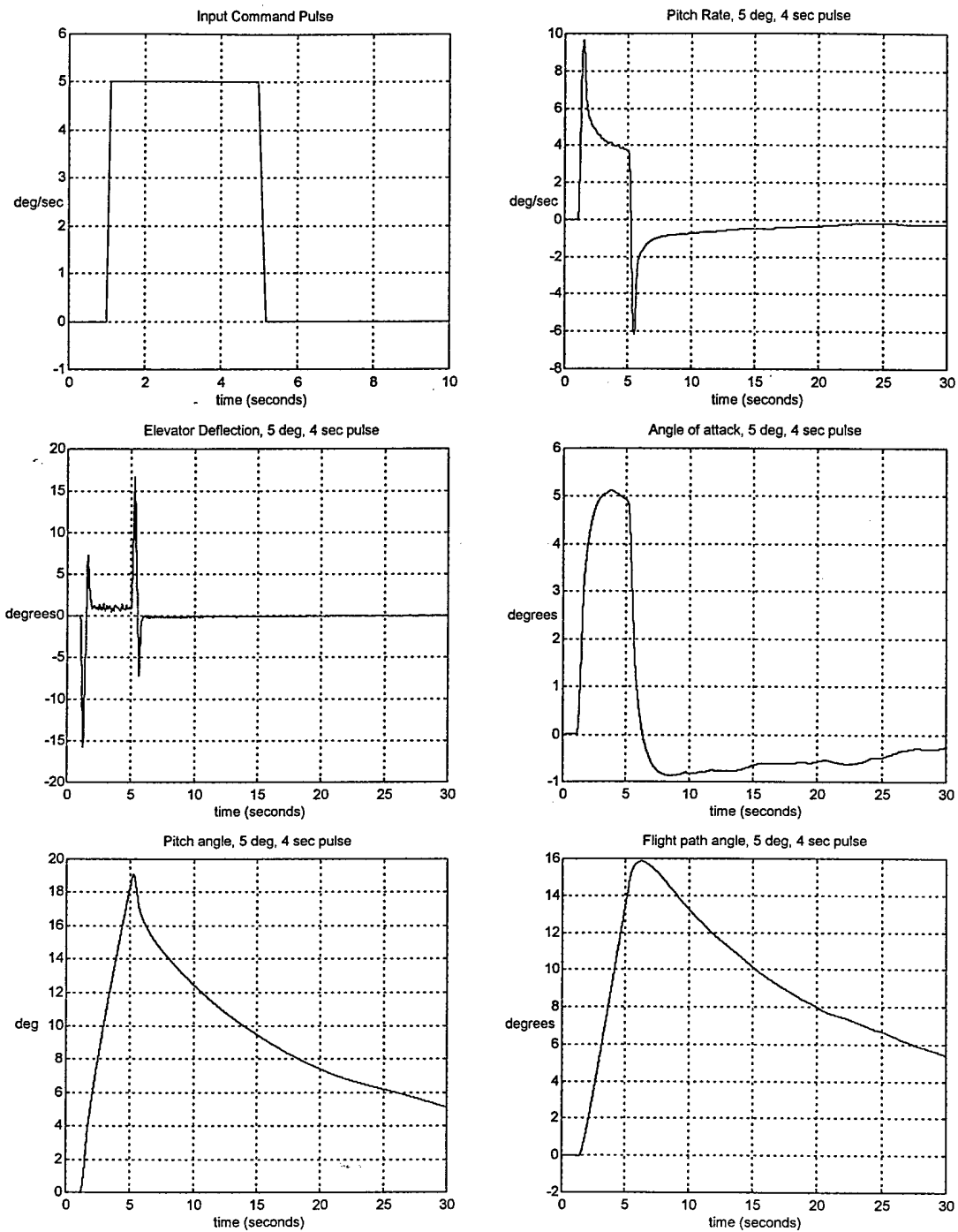
Figure 4. 27. Angle of Attack Simulations for Case 1-5 - noise on
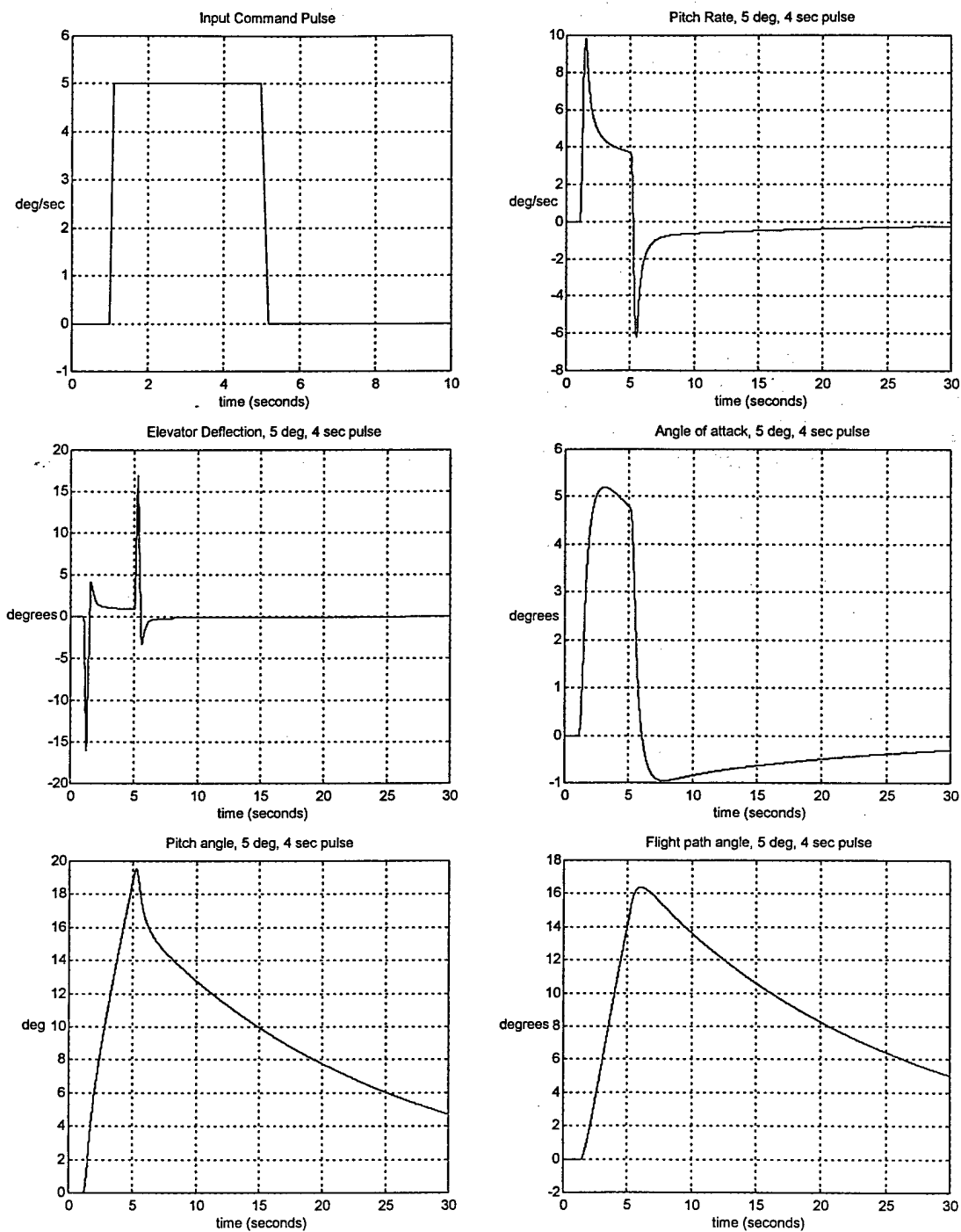
Figure 4.28. Angle of Attack Simulations for Case 1-5a - noise off
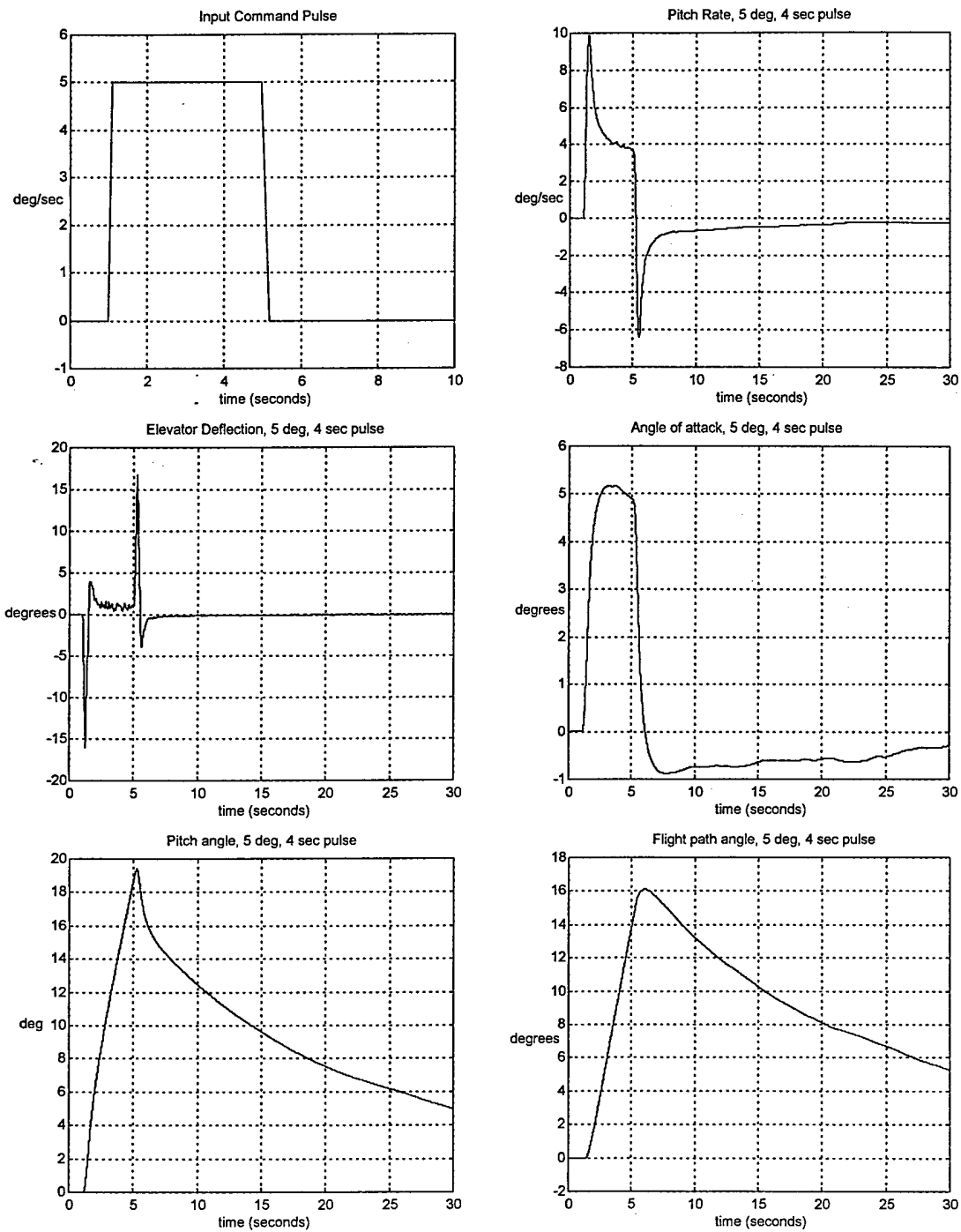
Figure 4.29. Angle of Attack Simulations for Case 1-5a - noise on
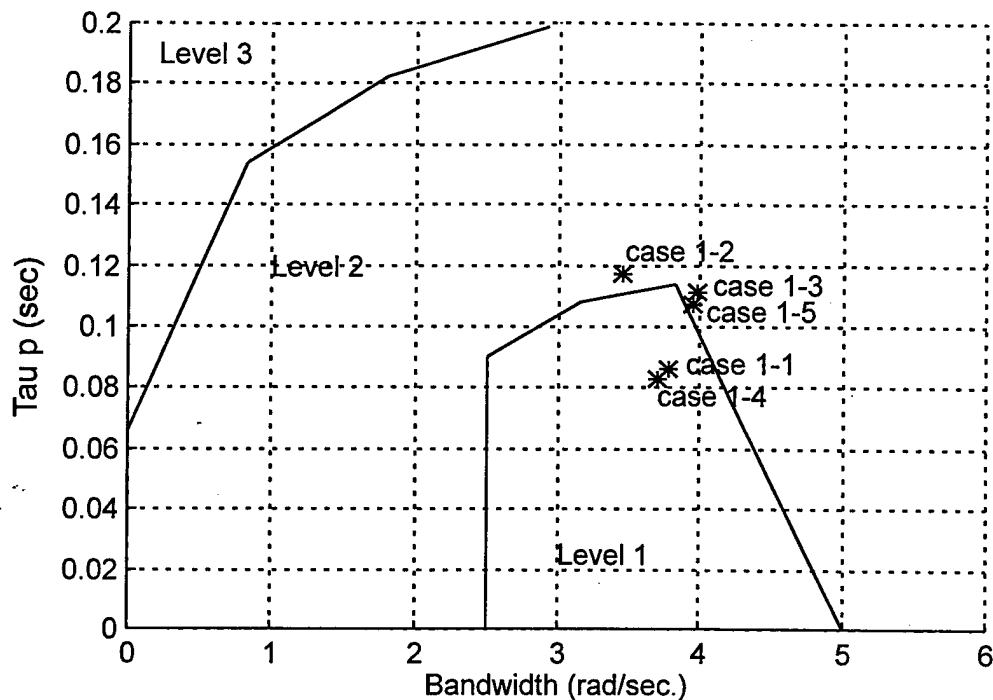
Figure 4.30. Angle of Attack Handling Qualities Predictions for Cases 1-1 through 1-5

The simulation histories are not as straight forward to evaluate as in the pitch rate

designs. This is because we have removed the integral action on the command, and therefore,

the controller is not tracking the command as well. The important factor in these designs is that

they restore conventional response characteristics to the system which should result in good

handling qualities ratings. However, Figure 4.30 does not support this hypothesis very well as

compared to the results for the pitch rate designs in Figure 4.16. In general, the washout and

lead filters have increased the bandwidth of all of the design cases. But, it is important to

remember that there is evidence that the Hoh's Bandwidth handling qualities prediction criteria

do not correlate very well with flight test results, especially in the case of the angle of attack

designs. However, a criteria has been proposed by Berry [24] that shows excellent results. It is

based on the percentage the flight path overshoots when the command is terminated. Flight test

data indicates that a flight path overshoot of less than 20% would be a good metric to predict level 1 pilot ratings. All of the cases in Figures 4.18-4.29 have between a 14-20% flight path overshoot. Case 1-1 is the worst while cases 1-3, 4, and 5 are the best. It is important to note that the flight path overshoot parameter can easily be adjusted by changing the numbers in the washout and lead filters. However, that will be left to Phase II.

4.2.2 Angle of Attack Designs.

An H_2 angle of attack design (case 1-6) and a mixed $H_2 / T_{e_3 d_3} / T_{e_1 d_1}$ angle of attack design (case 1-7) were developed. The only two changes required to convert from a pitch rate problem formulation to an angle of attack problem formulation were to change the command and the ideal model we are attempting to follow. Changing the command does not involve changing the problem formulation as the stick dynamics are the same for both pitch rate and angle of attack commands. The ideal model for these designs is given by

$$Wm = \frac{6.25}{s^2 + 3.5s + 6.25} \qquad (4.3)$$

This model is second order to include some pitch rate overshoot and therefore eliminate the need for the lead and washout filter in the simulation. The only other change made to the original pitch rate problem formulations was to tighten the control rate usage. This is given by

$$Wcr = \begin{bmatrix} .1 & 0 \\ 0 & .1 \end{bmatrix} \qquad (4.4)$$

This was required to prevent destabilizing rate limiting of the system. The stability margin design results are listed in Table 4.4. Norm data is not included because the primary

performance metric other than stability margins will be the flight path angle overshoot from the simulations.

TABLE 4.4

ANGLE OF ATTACK DESIGN DATA - STABILITY MARGIN COMPARISON

Case	Complement. Sensitivity Vector Gain Margins (dB) Input of Plant	Sensitivity Vector Gain Margins (dB) Input of Plant	Phase Margins (deg) Input of Plant	Complement. Sensitivity Vector Gain Margins (dB) Output of Plant	Sensitivity Vector Gain Margins (dB) Output of Plant	Phase Margins (deg) Output of Plant
1-6	[-2.81, 2.12]	[-2.28, 3.10]	17.28	[-2.76, 2.09]	[-2.26, 3.07]	17.10
1-7	[-15.61, 5.27]	[-5.57, 19.98]	53.47	[-11.74, 4.82]	[-4.95, 12.70]	45.19

The stability margins for the H_2 problem are unacceptable at both the input and output of the plant. The controller for this case also has a RHP pole. However, by mixing this design with a tracking constraint $\left(T_{e_3 d_3}\right)$ and an input uncertainty constraint $\left(T_{e_1 d_1}\right)$, we improve the stability margins tremendously and get a controller with all LHP poles. The simulations for these two designs will be presented next followed by a brief discussion of each case's handling qualities.

4.2.3 Angle of Attack Design Simulations.

The simulations are conducted as before with the only difference being that we have no lead filter as shown in Figure 4.30 because these characteristics are accounted for in the ideal model. The washout filter is still used and is the same as equation 4.1.
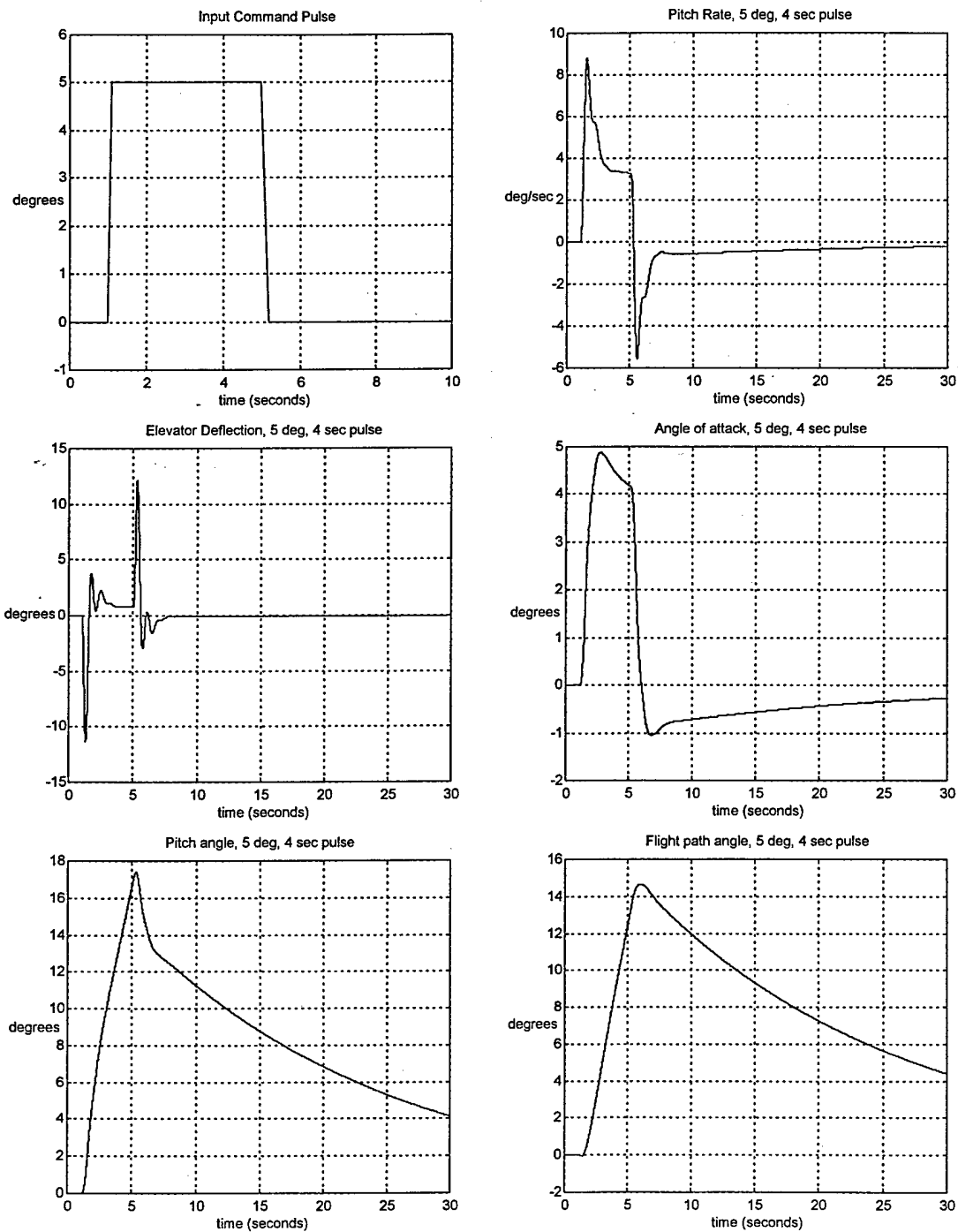
Figure 4.31. Angle of Attack Simulations for Case 1-6 - noise off
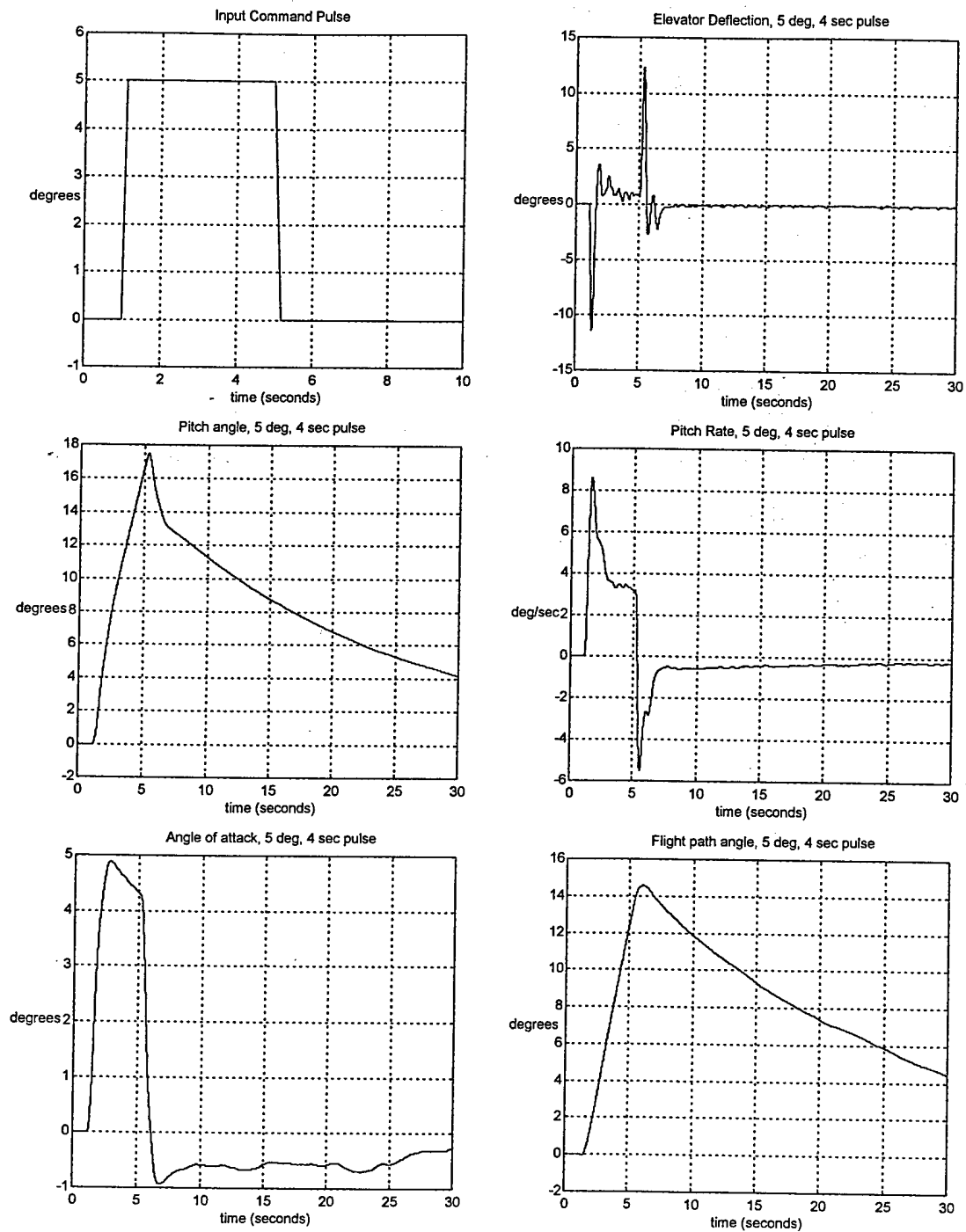
Figure 4.32. Angle of Attack Simulations for Case 1-6 - noise
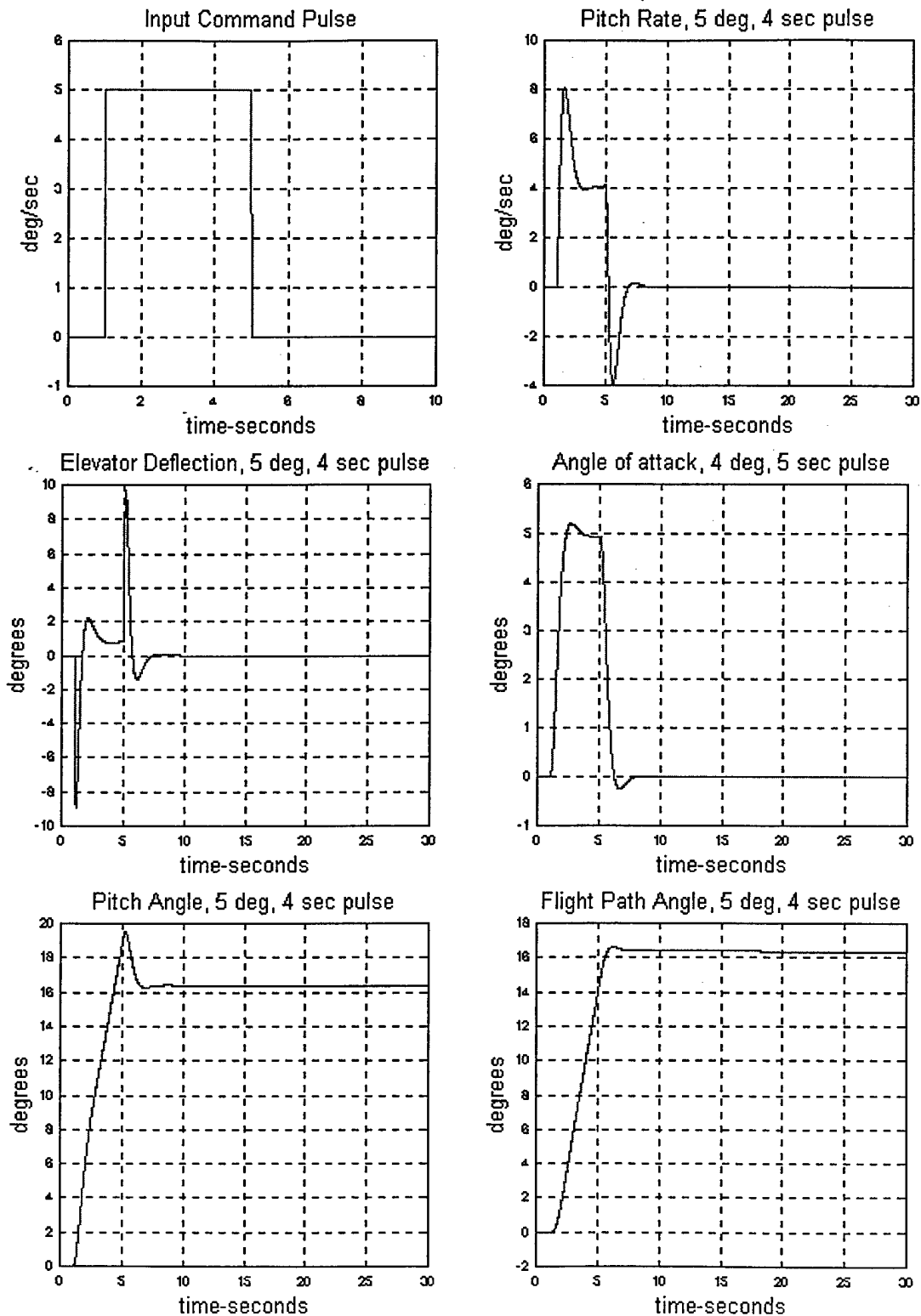
Figure 4.33. Angle of Attack Simulations for Case 1-7 - noise off
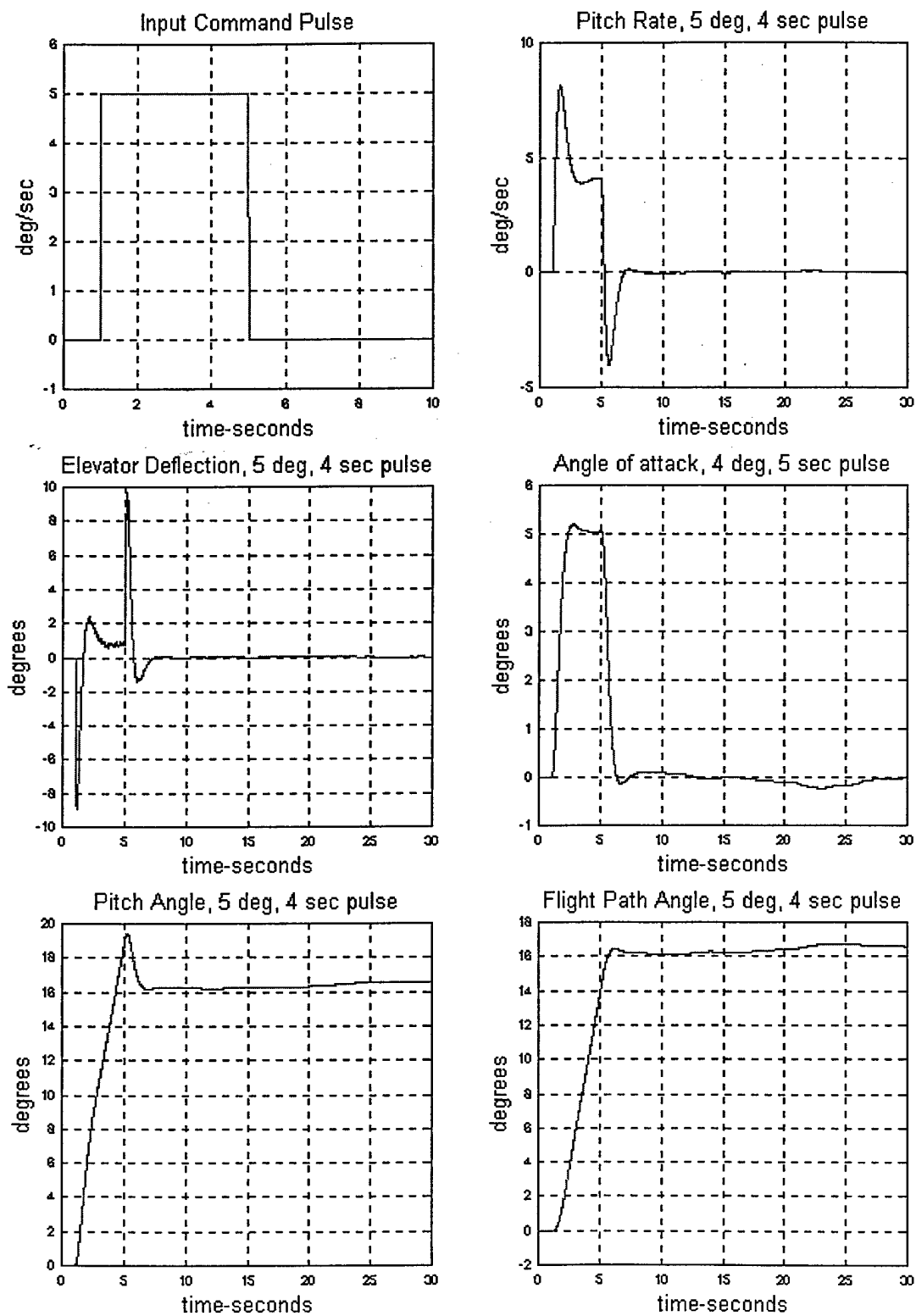
Figure 4.34. Angle of Attack Simulations for Case 1-7 - noise on

The biggest difference between the simulations in Figures 4.31 through 4.34 is that there is much less overshoot of the flight path angle after the command is terminated than in the previous simulations (Figures 4.18-4.29). Both cases here exhibit about 7% overshoot while the minimum before was 12%. This should result in better handling qualities ratings if the flight path overshoot hypothesis is correct. We have gained a fairly significant improvement here in our main handling qualities metric by designing an angle of attack system rather than converting a pitch rate design. . The Hoh's Bandwidth analysis of Case 1-7 predicted Level 1 handling qualities (bandwidth=2.9, tau p=.05 sec., where tau p is a measure of delay in the closed loop response. See [15] for details).

4.3 Summary

Because of the many different flight control designs covered in this chapter, a summary of those that were finally selected for phase II is provided in Table 4.5.

TABLE 4.5

SUMMARY OF FLIGHT CONTROL DESIGNS SELECTED FOR FLIGHT TEST

Case	Method of Design	Type of Design	Hoh's Bandwidth HQ Prediction	Berry Flight Path Overshoot Criteria HQ Prediction
1-1	H_2	Pitch Rate Cmd	Level 1	Level 1
1-1(f)[1]	H_2	AoA Cmd	Level 1	Level 1
1-4	H_2/H_∞	Pitch Rate Cmd	Level 1	Level 1
1-4(f)[1]	H_2/H_∞	AoA Cmd	Level 1	Level 1
1-7	H_2/H_∞	AoA Cmd	Level 1	Level 1

(f) - denotes the pitch rate designs that were changed to AoA by command path filters

All of designs selected for flight test had the best characteristics in terms of having all stable poles, handling qualities predictions, and command tracking. The H_2 design was included along with the mixed norm designs to test the following hypothesis: Given an accurate aircraft model (which was the assumption made with the LearF16), a simple LQG design with good turbulence/noise rejection and command tracking characteristics would be sufficient (eliminating the need to spend the extra time and work to develop a mixed norm design). The accuracy of the findings and hypotheses stated in these first four chapters will be evident in the flight test phase which will begin with the flight test setup in the next chapter.

V. Flight Test Preliminaries

This chapter begins the discussion of the flight test phase of this research. Areas covered will include; a brief discussion of the logistics in setting up the flight test, methodology, procedures of the flight test, implementation and verification, and finally, ground and airborne validation of the control laws. Three new control laws designs that were generated based on implementation and verification results are discussed in the last two sections.

5.1 Flight Test Logistics

All flight test programs are required to have a program name that can be referred to in the documentation required to set up, execute, and report on the program. This research was assigned the name HAVE INFINITY II by the U.S. Air Force Test Pilot School. This point is made to source the references to HAVE INFINITY II in this chapter.

The initial work in setting up this test program dealt with securing the resources, facilities, and aircraft required to perform the flight test program. The HAVE INFINITY II test team (3 pilots, 1 EWO, and 2 Engineers) was responsible (through the USAF TPS Commandant) for all phases of test program management and execution.

5.1.1 Flight Test Resources.

The HAVE INFINITY II program was funded by USAF TPS. The total program budget was $109,000. The major items funded in the program budget included: a two day trip to Calspan facilities in Buffalo, NY; nine 1.0 hour support sorties (3 C-23 and 6 T-38) for the flight test program; and twelve 1.2 hour sorties in the Calspan Variable Stability (VSS) Learjet 24 for the flight test program.

5.1.2 Flight Test Facilities and Procedures

Model verification and validation testing was performed at Calspan facilities in Buffalo, NY and at Edwards AFB, CA. All test program landings were accomplished at Palmdale, CA Regional Airport under a Memorandum of Understanding between USAF TPS and AF Plant 42. Landings were performed at Palmdale to avoid the congestion of the Edwards AFB traffic pattern. The logistics of getting the runway marked for scoring test program landings were also much easier at Palmdale.

5.1.3 Support and Flight Test Aircraft.

The six T-38 support sorties were used to practice and standardize the landing tasks that would later be performed in the Calspan Learjet. The C-23 was used as a target aircraft for the Calspan Learjet to evaluate any PIO tendencies of the HAVE INFINITY II flight control systems during various tracking tasks. The Calspan VSS Learjet served as the test aircraft. The VSS Learjet is a highly modified Learjet Model 24 that functions as a three axis in-flight simulator. The cockpit has two sets of side by side controls. The controls at the left seat, for the safety pilot, maintain the Learjet's conventional flight control system. The evaluation pilot occupies the right seat. Those controls use a fly-by-wire, response feedback, variable stability and variable control system, consisting of: variable feel system, aircraft motion sensors and associated signal conditioning, control system simulation computer, control surface servos, digital configuration control system, engage/disengage and safety monitor logic, and recording/playback capability.

5.2 Flight Test Methodology

Specific methods and procedures had to be established in the planning phase to effectively execute the HAVE INFINITY II flight test program. This section starts by detailing the methodology that was used in the program. The second section covers specific flight test procedures that support the methodology.

5.2.1 Flight Test Methodology.

The flight test methodology can be thought of as a road map that specifies what the test team is going to do to successfully complete the flight test. It starts with an overall purpose and is followed by: specific test objectives, Measures of Performance (MOP's) that outline what is required to meet an objective, success criteria, evaluation criteria, and test methodology.

Purpose. The purpose of the HAVE INFINITY II limited flight test was to evaluate the handling qualities of H_2, mixed H_2/H_∞, and classical longitudinal flight control system designs during the approach and landing phase of flight.

The classical flight control system will be discussed in detail in section 5.4. The test was conducted at Edwards AFB, California from 1 October 1997 to 9 October 1997. The overall test point matrix is shown in Appendix C. The evaluation order of the various flight control configuration was randomized by the TC and referred by the code letter in Table C1 to preserve the integrity of evaluation amongst the test team pilots.

The following paragraphs outline the HAVE INFINITY II specific test objectives, MOPs, success criteria, evaluation criteria, and test methodology that was used to successfully complete this test program.

Test Objective 1 - Flight Control Configuration Evaluations. Evaluate the longitudinal handling qualities of H_2, mixed H_2/H_∞ and classical longitudinal flight control configurations. Measures of Performance (MOP) were:

1. Pilot-in-the-loop Oscillation (PIO) ratings for Handling Qualities During Tracking (HQDT).

2. Cooper-Harper (C-H) ratings, PIO ratings and pilot comments for approach to main wheel touchdown (MWTD).

MOP 1 - PIO Ratings for Handling Qualities During Tracking (HQDT). Susceptibility to PIO of the HAVE INFINITY II flight control configurations was evaluated by performing high bandwidth tracking on an airborne target. A build-up approach was accomplished by performing low bandwidth tracking prior to high bandwidth tracking.

Success Criteria. Collect PIO ratings from 3 pilots for each flight control configuration.

Evaluation Criteria. Each flight control configuration was evaluated against the PIO rating scale (Appendix A). Ratings of 1, 2, and 3 were considered satisfactory. A rating of 4 was considered unsatisfactory, but tolerable. A rating of 5 or 6 was considered unacceptable.

Test Methodology. This test was flown with a C-23 airborne target. The Learjet was in the power approach configuration. Each flight control configuration was evaluated using a buildup approach starting with low bandwidth tracking from a position 1000 feet in trail of the target and progressing to high bandwidth HQDT. Low bandwidth tracking is non-aggressive, gentle maneuvering and open-loop pulses and steps. Handling qualities during tracking (HQDT) is aggressive and assiduous tracking of a precision aimpoint to zero error. During both low bandwidth and high bandwidth tracking, the evaluation pilot attempted to change the desired aim point by 10 mils. If the flight control configuration did not exhibit divergent oscillations during normal control inputs (PIO 6) or divergent oscillations during tight control (PIO 5), close

5-4

formation was performed. In close formation, the evaluation pilot started with low bandwidth tracking and proceeded to HQDT in a buildup fashion. During close formation HQDT, the evaluation pilot attempted to correct the aircraft to a desired position from 10 feet below the desired position. Close formation was accomplished on a 30° line (line up the main wheel of the C-23 with the front antenna) with 10 ft wingtip clearance and nose-tail separation with the C-23. A separate PIO rating was given for the trail position and for the close formation position, if accomplished. Landing tasks were not attempted with any flight control configuration assigned a PIO rating of 5 or 6 during HQDT. The Gibson and Ralph Smith PIO criterion did not predict PIO for any of the HAVE INFINITY II flight test candidates designed during phase I.

MOP 2 - Cooper-Harper (C-H) ratings, PIO ratings and pilot comments for approach to main wheel touchdown (MWTD). The handling qualities of the HAVE INFINITY II flight control configurations were evaluated by performing a series of landings with each configuration. Each configuration started with a straight-in approach to a spot landing and proceeded to offset landing tasks with spot landings if controllability was not in question.

Success Criteria. Collect C-H ratings, PIO ratings and pilot comments from three pilots for each flight control configuration that did not receive a PIO rating of 5 or 6 during MOP 1. The number of ratings given by a pilot for each configuration was determined by the Landing Task Decision Tree, Figure 5.1.

5-5
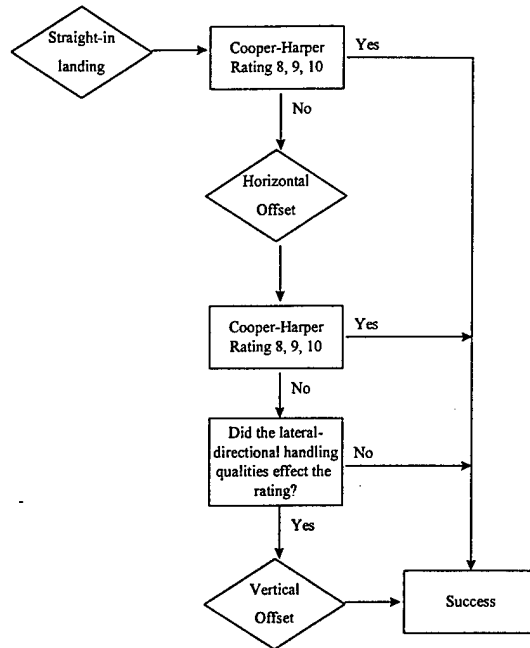
Figure 5.1. Landing Task Decision Tree

Evaluation Criteria. The handling qualities of each flight control configuration were

categorized into one of three levels dependent on landing performance and pilot workload.

Handling qualities were rated using the Cooper-Harper rating scale contained in Appendix A.

Level I was defined as satisfactory, no improvement is necessary. Cooper-Harper ratings of 1, 2

and 3 are Level I. Level II was unsatisfactory, but tolerable, deficiencies warrant improvement.

Cooper-Harper ratings of 4, 5 and 6 are Level II. Level III was unacceptable, deficiencies

require improvement. Cooper-Harper ratings of 7, 8 and 9 are Level III. Histograms of C-H

ratings were analyzed along with PIO ratings and pilot comments. An appropriate handling

qualities level was assigned if the C-H ratings are grouped within one level. If a large dispersion

in ratings was encountered or the ratings were split between levels, it was not possible to assign a

handling qualities level. In these cases pilot comments and engineering judgment were used to

determine an appropriate handling qualities level if possible. PIO ratings were evaluated as described in MOP 1 Test Methodology.

Test Methodology. The goal of this test was to perform one straight-in landing and a horizontal offset landing for each flight control configuration. If controllability was in question (C-H rating of 8, 9, or 10) on any landing, testing of that configuration by that pilot was terminated. If lateral-directional dynamics effect performance during the horizontal offset landing, the pilot performed a vertical offset landing.

This test started by flying a straight-in approach to a spot landing using the 3° Instrument Landing System (ILS) glideslope as described in the next section. The evaluation pilot assigned C-H and PIO ratings and made comments addressing longitudinal handling qualities. If the flight control configuration was not assigned a C-H rating of 8, 9, or 10, a horizontal offset landing was performed. This test technique is described in the next section. If the pilot felt the lateral-directional handling qualities effected the C-H rating for the horizontal offset landing, a vertical offset landing was performed. This test technique is also described in the next section. The vertical offset was only performed if the pilot did not assign a C-H rating of 8, 9, or 10 for the horizontal offset, and the lateral-directional handling qualities effect the C-H rating. This process was completed for each flight control configuration.

Test Objective 2 - Pilot Comments After Main Wheel Touchdown. Collect pilot comments on the longitudinal handling qualities of the flight control configuration after main wheel touchdown.

MOP 1. Collect pilot comments on the longitudinal handling qualities of the flight control configuration after main wheel touchdown.

Success Criteria. Collect pilot comments from all landings.

Evaluation Criteria. None.

Test Methodology. After MWTD, the aircraft stability derivatives are drastically different than the design point of 125 KIAS and 1,000 feet PA. Therefore, this portion of the landing task was evaluated separately. The evaluation pilot lowered the nose wheel to the runway after main wheel touch down. The evaluation continued until the pilot was assured a full stop landing could be accomplished. The pilot made qualitative comments on the longitudinal handling qualities of the flight control configuration during this phase.

This objective was added due to HAVE INFINITY's experience with an uncommanded pitch up in the landing flare for the optimal flight control laws.

5.2.2 Flight Test Procedures

General. Ground testing was accomplished on every flight control configuration prior to in-flight evaluation. Ground testing provided a means of software implementation verification, of the designed configuration, on the Learjet VSS.

Model validation data of the aircraft design model and each flight control configuration was collected at 140 KIAS with the aircraft configured as in the landing task (landing gear down and flaps 20%). Using Programmed Test Inputs, at least three pitch doublets and two frequency sweeps were performed for each configuration.

Each evaluation pilot accomplished high bandwidth HQDT on every flight control configuration, in both 1000 ft trail and close formation, prior to advancing to the landing task. HQDT was accomplished at 140 KIAS and at a minimum altitude of 5,000 ft AGL. The airspeed parameter was established to ensure quality of data between the HQDT phase accomplished up-

and-away and the actual landing phase. Each flight control configuration was evaluated using a buildup approach starting with low bandwidth tracking, from a position 1000 feet in trail of the target, and progressing to high bandwidth tracking (HQDT) as described in the previous section.

The evaluation pilot performed a minimum of one approach and landing with the VSS configured with the baseline Learjet flight control system. This was accomplished during each flight prior to any actual testing with the HAVE INFINITY II flight control configurations installed.

The test conductor configured the Learjet flight control system with the required configuration parameters, and the safety pilot engaged the Variable Stability System. The evaluation pilot took control of the aircraft for the pattern and landing. The safety pilot took control of the aircraft upon the evaluation pilot's determination that a full stop landing could have been accomplished from the current landing. The safety pilot then took control for the remainder of the ground roll, take off, and the climb to pattern altitude. The evaluation pilot provided comments on atmospheric conditions which affected the approach.

Straight-in Landing. Evaluation pilots flew a 3° glide path, using the ILS glideslope to assist with glide path determination, until the decision height of 200 ft AGL, then transitioned visually to consistently flare and touchdown in the desired zone. The approach airspeed was between 125 and 135 KIAS depending on the aircraft weight. The touchdown point should have been in the desired zone described in Figure 5.2. The target airspeed at touchdown was 10 kts less than approach speed (+10/-5 kts). For quality of data, only landings within this touchdown airspeed window were evaluated. The ground test team made a radio call to notify the aircrew of the actual touchdown point, and if desired or adequate performance was attained. The evaluation pilot provided qualitative comments, Cooper-Harper and PIO ratings for the approach to main

wheel touchdown in accordance with Appendix A. After main wheel touchdown, the evaluation pilot provided qualitative comments through nosewheel touchdown and to a point, determined by the evaluation pilot, that a full stop landing could be completed. In accordance with Figure 5.1, if the straight-in landing received a Cooper-Harper rating of other than 8, 9, or 10, this flight control configuration would be evaluated with a Horizontal Offset Landing.

Horizontal Offset Landing. This task forced the pilot to raise his gains by having to concentrate on both longitudinal and lateral control inputs. The Horizontal Offset Landing task was accomplished by flying a visual pattern with a lateral offset of 300 ft from runway centerline. At 200 ft AGL, the evaluation pilot aggressively corrected to the centerline. The correction used an initial bank angle between 30 and 45 degrees within three seconds, and the initial aggressive lateral corrections were completed by 100 ft AGL. A simultaneous correction was made to intercept a visual glide path to touchdown. The desired touchdown point was at the center of the desired zone. Again, the target airspeed at touchdown was 10 kts less than approach speed (+10/-5 kts), and only landings within this touchdown airspeed window were evaluated. Pilot comments and ratings were identical to the straight-in landing. In accordance with Figure 5.1, if the Horizontal Offset Landing received a Cooper-Harper rating of other than 8, 9, or 10 and the lateral-directional handling qualities affected the Cooper Harper rating, this flight control configuration could be evaluated with a Vertical Offset Landing.

Vertical Offset Landing. This task was designed to minimize any lateral-directional handling qualities effects and focus attention on the longitudinal axis. The Vertical Offset Landing was accomplished by flying straight and level at the published Minimum Descent Altitude (MDA - 397' AGL), as if flying a localizer approach. At glideslope intercept (Visual Descent Point), the pilot would aggressively correct to a 3° glide path by 100 ft AGL.

Comments and ratings were identical to those discussed in the straight-in landing. Only landings within the touchdown airspeed window were evaluated.

A landing could be repeated, at the discretion of the TC, based on improper setup, extenuating atmospheric conditions (windshear, etc.), or any factor where a biased rating may have occurred. Test conditions such as minor turbulence or wind variations were documented, but not repeated.

Excessive Tailwind Procedures or Runway Non-Availability. If the tailwind component for runway 25 at Palmdale Airport was greater than 10 kts, runway 07 was used for landing. The precision instrument runway markings depicted in Figure 5.2 were used to help the pilot define the desired and adequate landing zones. Ground spotters were positioned 1200 feet and 1600 feet from the runway threshold to verify landings in the desired zone. If the Palmdale runway was closed or unusable, any other runway in the local flying area could have been used with a published instrument precision approach using the same procedures described for runway 07.

Figure 5.2. Touchdown Zone

5.3 Control Law Implementation and Verification

The HAVE INFINITY II control laws were implemented by converting the state space

representation to a transfer function format for each channel of the control laws (which is the

standard implementation for Calspan). This implementation differed from the HAVE INFINITY

implementation. The HAVE INFINITY program was forced to use a state space implementation

due to instabilities in their control laws. The Calspan VSS computer used MATLAB™ and

SIMULINK™ to implement and simulate the HAVE INFINITY II control configurations. All of

the control laws had three input channels (command, along with q and α feedback) and one

output channel (elevator command). This is shown in the SIMULINK™ block diagram in

Figure 5.3. The command channel implementation model follows in Figure 5.4.

Figure 5.3. Three Channel Control Law Implementation Model
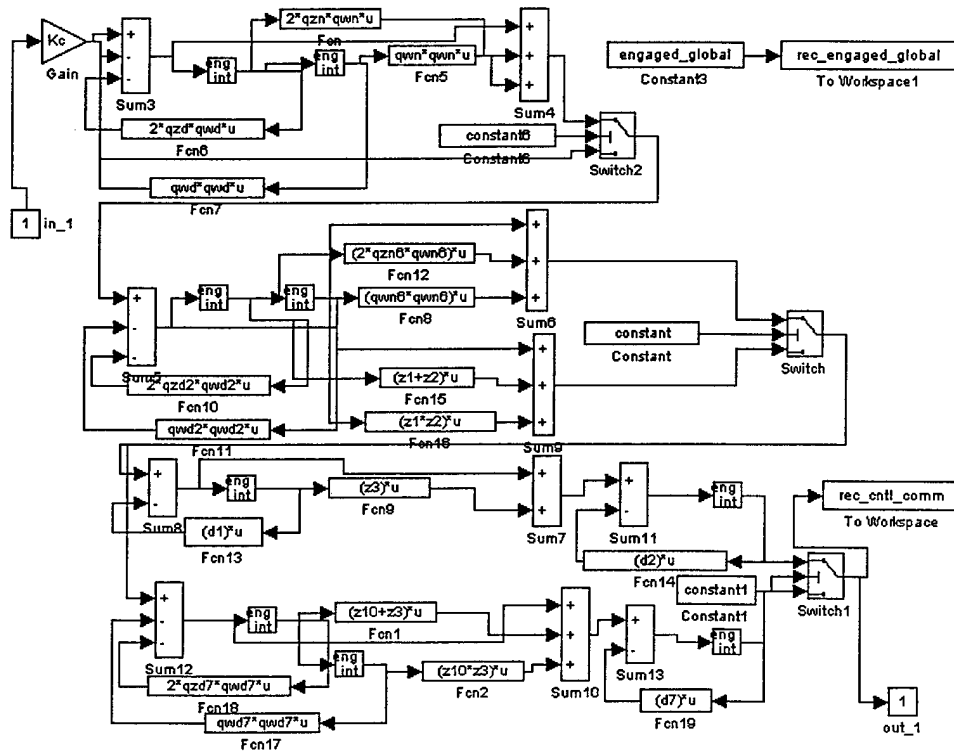
Figure 5.4. Command TF Channel Implementation Model

The q and α transfer function implementation models are very similar. The structure of the implementation models did not change between HAVE INFINITY II flight control configurations. Differences in controller order and structure of the dynamics of the pole/zeros between control configurations were accounted for by activating/deactivating the necessary transfer function loops within each channel. This was done with the software switches that are apparent in Figure 5.4. Initial HAVE INFINITY II control law verification and simulation was accomplished when integration and debugging of the control implementation architecture, with the rest of the Learjet VSS, was completed. The first verification work dealt with making sure the aircraft model was correctly implemented. Verification of the aircraft poles and zeros is in Table D1, Appendix D. The implementation transfer functions for each of the control laws from Table 4.5 are shown in Tables 5.1-5.3. The format of the transfer functions is described in the first paragraph of Appendix D.

TABLE 5.1
COMMAND CHANNEL IMPLEMENTATION TRANSFER FUNCTION

Case	Command Channel
1-1	$\dfrac{-2291.2359[0.7000,60.000](21.4843)(1.5171)(0.2990)}{[0.7189,277.1040][0.9999,31.6083][6.0000)(0.8405)}$
1-4	$\dfrac{-1693.5630[0.8361,73.6640](18.3649)[0.7060,1.0943]}{[0.7250,276.6304](35.2238)(32.6059)[0.3659,1.4619]}$
1-5	$\dfrac{-36.8823(53.0559)[0.7064,24.8286](1.3192)(0.8195)(0.4175)}{(85.4428)[0.6456,25.3192][0.9375,5.1344][0.9454,0.3811]}$

TABLE 5.2
PITCH RATE CHANNEL IMPLEMENTATION TRANSFER FUNCTION

Case	q Feedback Channel
1-1	$\dfrac{1252.4538[0.7000,60.0000](6.0000)(4.0809)(1.4402)}{[0.7189,277.1040][0.9999,31.6083](6.0000)(0.8405)}$
1-4	$\dfrac{1223.7806[0.9171,89.9112](16.5553)[0.7593,0.9092]}{[0.7250,276.6304](35.2238)(32.6059)[0.3659,1.4619]}$
1-5	$\dfrac{43.4441[0.7898,34.0126][0.8267,5.3258](0.8936)(0.4391)}{(85.4428)[0.6456,25.3192][0.9375,5.1344][0.9454,0.3811]}$

TABLE 5.3
AOA CHANNEL IMPLEMENTATION TRANSFER FUNCTION

Case	α Feedback Channel
1-1	$\dfrac{10.6641[0.7000,60.000](6.0000)(4.0809)(1.4402)}{[0.7189,277.1040][0.9999,31.6083](6.0000)(0.8405)}$
1-4	$\dfrac{147.8755(168.6614)(37.9513)(22.9369)[0.7248,1.9879]}{[0.7250,276.6304](35.2238)(32.6059)[0.3659,1.4619]}$
1-5	$\dfrac{3.5357(60.5737)[0.6775,24.5839](4.9107)[0.9705,0.4375]}{(85.4428)[0.6456,25.3192][0.9375,5.1344][0.9454,0.3811]}$

Recall that case 1-1 and 1-4 also had AOA versions. This was done by placing the filters described in chapter IV in the command path prior to the controller. A software switch was also placed in this path so these filters could be bypassed when the pitch rate versions and case 1-5 were being tested. Initial verification and simulation took place at Calspan facilities in Buffalo, NY from 3 to 5 August 1997. The HAVE INFINITY II test team felt it was important to be able to address any implementation problems early in the program. This would allow time to make any necessary design adjustments prior to flight test. It turns out that both case 1-1 and case 1-4 had implementation problems.

The problems in both cases dealt with high frequency modes. Calspan had recommended using Euler Integration with a 0.01 sec step time (100 Hz sample rate) for both desktop and airborne SIMULINK™ simulations. This integration routine was used by Calspan

because of its speed and simplicity. While the Euler method was the simplest and fastest integration routine offered in SIMULINK™, it was also the most inaccurate. Cases 1-1 and 1-4 (both AoA and pitch rate versions) were numerically unstable when simulated with Euler Integration. However, they were numerically stable when simulated using the 'linsim' and 'rk45' integration routines. Upon consultation with Calspan engineers during phase I, they stated that the 'rk45' integration routine had been used successfully in the Learjet. It was agreed that 'rk45' could also be used on this flight test program. However, when the control laws were implemented on the Learjet, it was discovered that 'rk45' could not be used as an integration routine. It introduced too much computational delay into the system and caused the VSS to continually trip off when any control inputs were made. Consequently the decision was made to use Euler Integration and try to reconfigure cases 1-1 and 1-4 to work with this integration method.

Case 1-1. Reconfiguring this case to work with Euler Integration was successful. Analysis of the transfer functions for each channel revealed that there were zeros in this control law that were canceling the actuator poles. There was also a set of very high frequency poles at 277 radians/sec. It appeared that the control law had canceled the actuator dynamics and put in its own to meet the tight tracking constraint on the first order 6/(s+6) model. This hypothesis was confirmed by pole-zero canceling these high frequency dynamics from each channel and making the corresponding gain adjustment. The Euler SIMULINK™ time responses were now stable, and still matched very closely to those in Figures 4.4/4.5. The only difference noted was that the rise time on the pitch rate response increased slightly. This was considered an improvement as the Calspan test pilots felt the original response would have been rated as too

abrupt. The stability margins, and handling qualities predictions were unchanged. The 2-norm increased from 2.518 to 5.1, reflecting the "slower" response.

It is appropriate to note here that there was of some confusion amongst HAVE INFINITY II team members and Calspan engineers regarding the naming conventions used for the control laws. Cases 1-1/1-1(f), and 1-4/1-4(f) were easily confused when collecting verification and initial simulation data. Hence, the names were changed from "cases" to the script file name that was used to create each design. The new names are shown in Table 5.4 and will be used from this point forward.

TABLE 5.4
NEW HAVE INFINITY II CONTROL LAW NAMING CONVENTIONS

Old Name	New Name
Case 1-1	H2INI
Case 1-1(f)	H2AIN
Case 1-4	MXINI
Case 1-4(f)	MXAIN
Case 1-5	MXAOA

Verification of the implementation of the "new" poles and zeros of the H2INI/H2AIN control law is in Table D2, Appendix D. Verification of the implementation of the MXAOA control law poles and zeros is in Table D3, Appendix D.

MXINI/MXAIN. Reconfiguring this transfer function was not successful. The high frequency dynamics that caused the numerical instability with Euler Integration could not be pole-zero canceled in the AOA channel without making this transfer function improper (see Table 5.3). This rendered the MXINI/MXAIN control laws unfit for implementation and disqualified it from further consideration.

At this point, the HAVE INFINTY II test team felt it had time to replace the two control configurations lost with the disqualification of MXINI/MXAIN, in addition to designing a classical feedback gain configuration. The classical configuration was suggested by Calspan as a simple design that would have known level I handling qualities. This design could then be used as a baseline to compare the handling qualities of the multiobjective designs. The test team also decided to produce an H_2 AOA command design and a mixed H_2/H_∞ pitch rate command design. The H_2 AOA design would be fast to produce and add a single norm AOA command design to the filtered pitch rate configuration (H2AIN). The mixed H_2/H_∞ pitch rate design replaced MXINI. MXAIN was not replaced because MXAOA already represented a mixed H_2/H_∞ AOA command design.

Classic Feedback Gain Design. This design was produced using only simple q and α feedback gains. The aircraft dynamics The pitch rate feedback gains, K_q, = 0.441, and the AOA feedback gain, K_α, = 1.60, were provided by Calspan. These gains were known to produce Level I handling qualities for the Learjet (simulating an F-16) based on previous flight test experience.

This control design was given the name CLASSIC. H_2 and H_∞ norms were not computed for CLASSIC. Vector margins are shown in Table 5.5.

TABLE 5.5

CLASSIC STABILITY MARGINS

Name	Complement. Sensitivity Vector Gain Margins (dB) Input of Plant	Sensitivity Vector Gain Margins (dB) Input of Plant	Phase Margins (deg) Input of Plant	Complement. Sensitivity Vector Gain Margins (dB) Output of Plant	Sensitivity Vector Gain Margins (dB) Output of Plant	Phase Margins (deg) Output of Plant
CLASSIC	[-∞, 6.02]	[-6.02, ∞]	60.00	[-5.02, 3.16]	[-3.02, 4.66]	25.37

While the stability margins at the output of the plant are lower than desired, they are better than the H2INI/H2AIN configurations. This design had also been proven in previous flight test by

Calspan, so the lower stability margins were considered acceptable. Time histories for this

design are shown in Figure 5.5 and 5.6.

Figure 5.5. Short Period Simulations for CLASSIC - Noises off

Figure 5.6. Short Period Simulations for CLASSIC - Noises on

Handling qualities predictions for this design were calculated using the Hoh's Bandwidth and Berry Flight Path Overshoot Criteria. The Hoh's bandwidth criteria predicted level I with a delay parameter (tau p) of 0.02 and a bandwidth of 2.9 rad/sec. The Berry Criteria also predicted level I with a 19% overshoot.

Implementing the CLASSIC control law was very easy since no dynamics were involved in the control law. Simple gain blocks were placed at the appropriate place in the control law path of the VSS software architecture. The gains were then simply defined as the values selected when needed, and zero when evaluating a different control law. Verification of the implementation of the CLASSIC control gains is in Table D4, Appendix D.

H_2 Angle of Attack Command Design. This design was produced so a single norm AOA command system would be tested in addition to the existing pitch rate design (H2INI). It was hoped that some handling qualities preferences might be distinguished between the AOA and pitch rate designs. The problem setup for this AOA design was the same as described in section 3.2, except that the output variable being differenced with the ideal model is α rather than q. Some of the constraint and performance weightings have also been changed from previous designs.

The ideal model used in this design was chosen to have the same dynamics as the CLASSIC design since they had known level I handling qualities. The dynamics of this ideal model worked out to be

$$Wm = \frac{5.29}{s^2 + 2.43s + 5.29} \tag{5.1}$$

Other constraint and performance weight changes include the tracking performance weight, *Wp,* the control use constraint, *Wcu,* and the control rate usage constraint, *Wcr.* A static

weight of 20 was chosen for *Wp*. Recall that this weighting will actually be the inverse of the value chosen. Therefore it will allow up to a 5% tracking error over all frequencies. The control rate and control use weights were set equal to 1. This removed any control use/rate restrictions from the problem. Since the ideal model is a second order system with relatively slow rise time, rate limiting and running out of control authority was not a problem..

The plant, actuator, turbulence, state weighting, and sensor noise models all remained unchanged from previous designs.

This control design was given the name H2AOA. H_2 and H_∞ norms are shown in Table 5.6 and vector stability margins are shown in Table 5.7.

TABLE 5.6

NORM DATA FOR H2AOA DESIGN

Name	$\|T_{zw}\|_2$	$\|T_{e_3d_{31}}\|_\infty$	$\|T_{e_1d_1}\|_\infty$	$\|T_{e_2d_2}\|_\infty$
H2AOA	5.90	2490	0.31	2.52

TABLE 5.7

H2AOA STABILITY MARGINS

Name	Complement. Sensitivity Vector Gain Margins (dB) Input of Plant	Sensitivity Vector Gain Margins (dB) Input of Plant	Phase Margins (deg) Input of Plant	Complement. Sensitivity Vector Gain Margins (dB) Output of Plant	Sensitivity Vector Gain Margins (dB) Output of Plant	Phase Margins (deg) Output of Plant
H2AOA	[-8.75, 4.27]	[-5.27, 15.57]	49.36	[-4.57, 2.98]	[-3.28, 5.34]	26.54

The high norm for the tight tracking constraint ($T_{e_3d_3}$) indicates this design does not tightly track command inputs. This correlates with the 5% tracking error at all frequencies that was accepted in the design setup. Figures 5.9 and 5.10 show that the time histories for this design do look similar to the CLASSIC (as intended). The stability margins for this design are

similar to the CLASSIC design. This is not surprising since the H2AOA design was supposed to

have the same response (and therefore same handling qualities) as the CLASSIC.
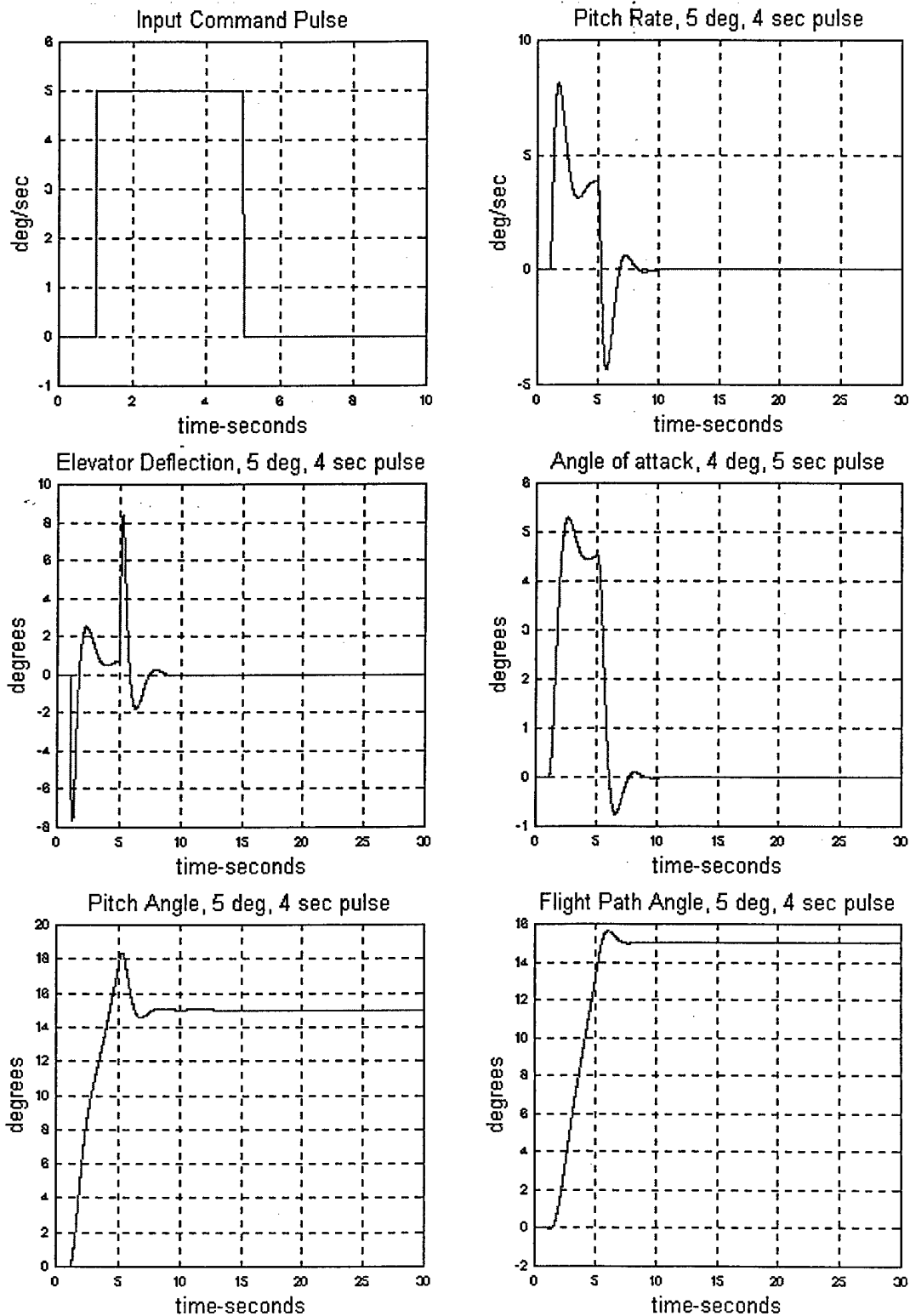
Figure 5.7. Short Period Simulations for H2AOA - Noises off
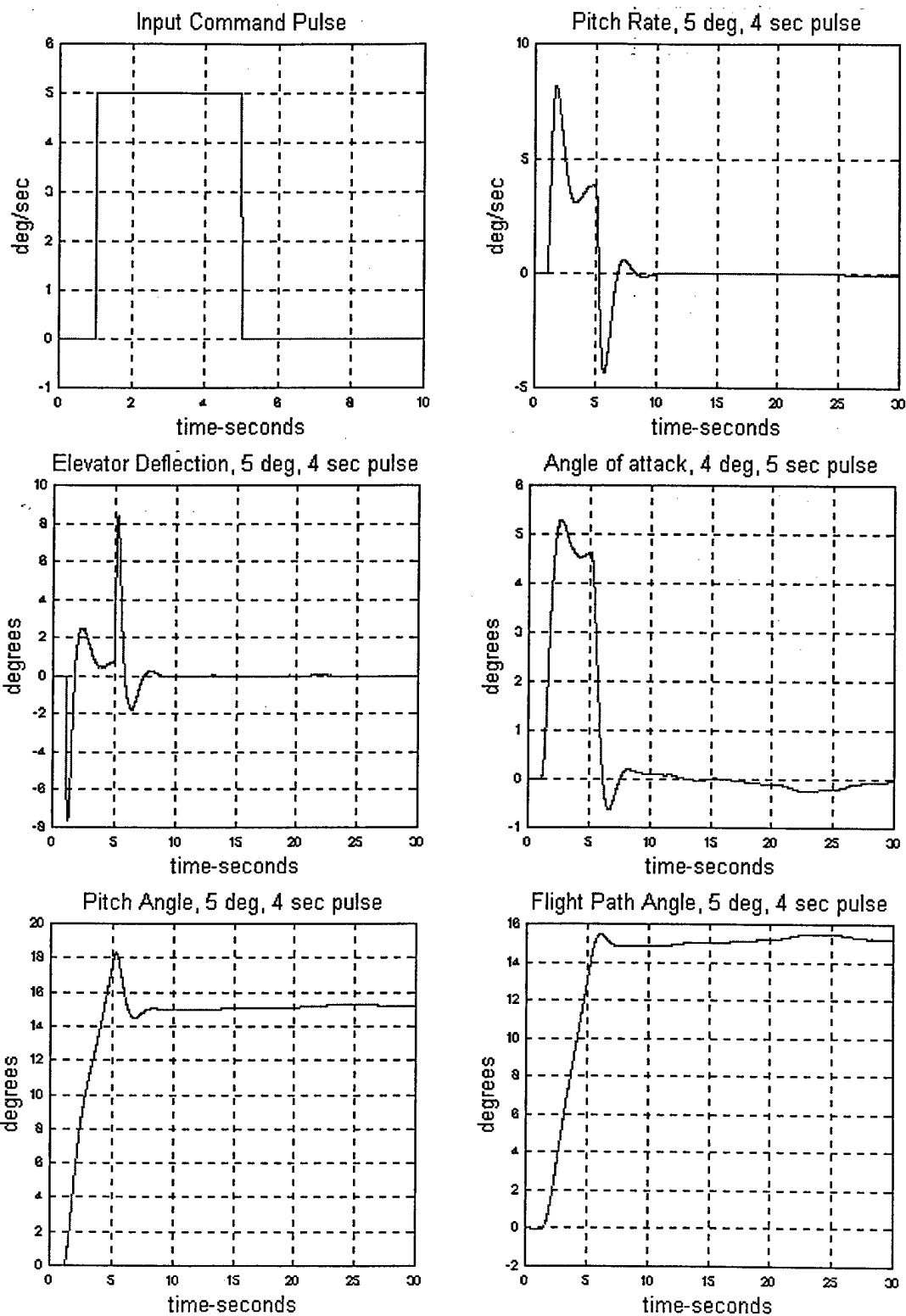
Figure 5.8. Short Period Simulations for H2AOA - Noises on

Handling qualities predictions for this design were calculated using the Hoh's Bandwidth and Berry Flight Path Overshoot Criteria. The Hoh's bandwidth criteria predicted borderline level I/II with a delay parameter (tau p) of 0.10 and a bandwidth of 2.7 rad/sec. The Berry Criteria predicted level I with a 19% overshoot. Consideration was given to trying to tune this design (by adjusting control use weights, ideal model, etc.) to get a better handling qualities prediction. However the test team pilot comments from initial ground simulation indicated that they liked the response of the design. Therefore no changes were made.

The dynamics of the H2AOA control law and verification of their implementation is found in Table D5, Appendix D.

Mixed H_2/H_∞ Angle of Pitch Rate Command Design. This design was a tradeoff of noise rejection/tracking with output stability margins. It was comprised of the same H_2 problem design formulation as for the H2AOA design, and the output stability margin constraint, $T_{e_2 d_2}$. However, the ideal model for this design was changed somewhat from the H2AOA configuration after some discussion with Calspan test pilots. They indicated that ideal model natural frequencies of as low as 2 rad/sec should result in good handling qualities for the landing task. Hence an ideal model with a natural frequency of 2 rad/sec was chosen for this design. The transfer function is given by

$$Wm = \frac{4}{s^2 + 2s + 4} \tag{5.2}$$

The tracking performance weight, *Wp,* the control use constraint, *Wcu,* and the control rate usage constraint, *Wcr,* were reset to the values in section 3.3. This was done because these weights worked for that pitch rate design.

The plant, actuator, turbulence, state weighting, and sensor noise models all remained unchanged from previous designs.

This control design was again given the name MXINI. H_2 and H_∞ norms are shown in Table 5.8 and vector stability margins are shown in Table 5.9.

TABLE 5.8

NORM DATA FOR MXINI DESIGN

Name	$\|T_{zw}\|_2$	$\|T_{e_3 d_3}\|_\infty$	$\|T_{e_1 d_1}\|_\infty$	$\|T_{e_2 d_2}\|_\infty$
MXINI	1.63	261.20	0.26	3.15

TABLE 5.9

MXINI STABILITY MARGINS

Name	Compliment. Sensitivity Vector Gain Margins (dB) Input of Plant	Sensitivity Vector Gain Margins (dB) Input of Plant	Phase Margins (deg) Input of Plant	Compliment. Sensitivity Vector Gain Margins (dB) Output of Plant	Sensitivity Vector Gain Margins (dB) Output of Plant	Phase Margins (deg) Output of Plant
H_2 Subproblem	[-5.86, 28.48]	[-5.86, 3.47]	57.53	[-3.30, 2.39]	[-2.66, 3.86]	20.66
MXINI	[-12.28, 4.96]	[-5.41, 17.39]	51.25	[-8.97, 4.32]	[-4.87, 12.13]	44.21

The high norm for the tight tracking constraint ($T_{e_3 d_3}$) indicates this design does not tightly track command inputs. However, recall that this design has given up some tracking performance for better stability margins by virtue of the mixed problem formulation. A comparison between the stability margins for the H_2 portion of the problem and the MXINI in Table 5.9 shows that the output margins are significantly improved (as intended). Figures 5.9 and 5.10 show the time histories for this design.
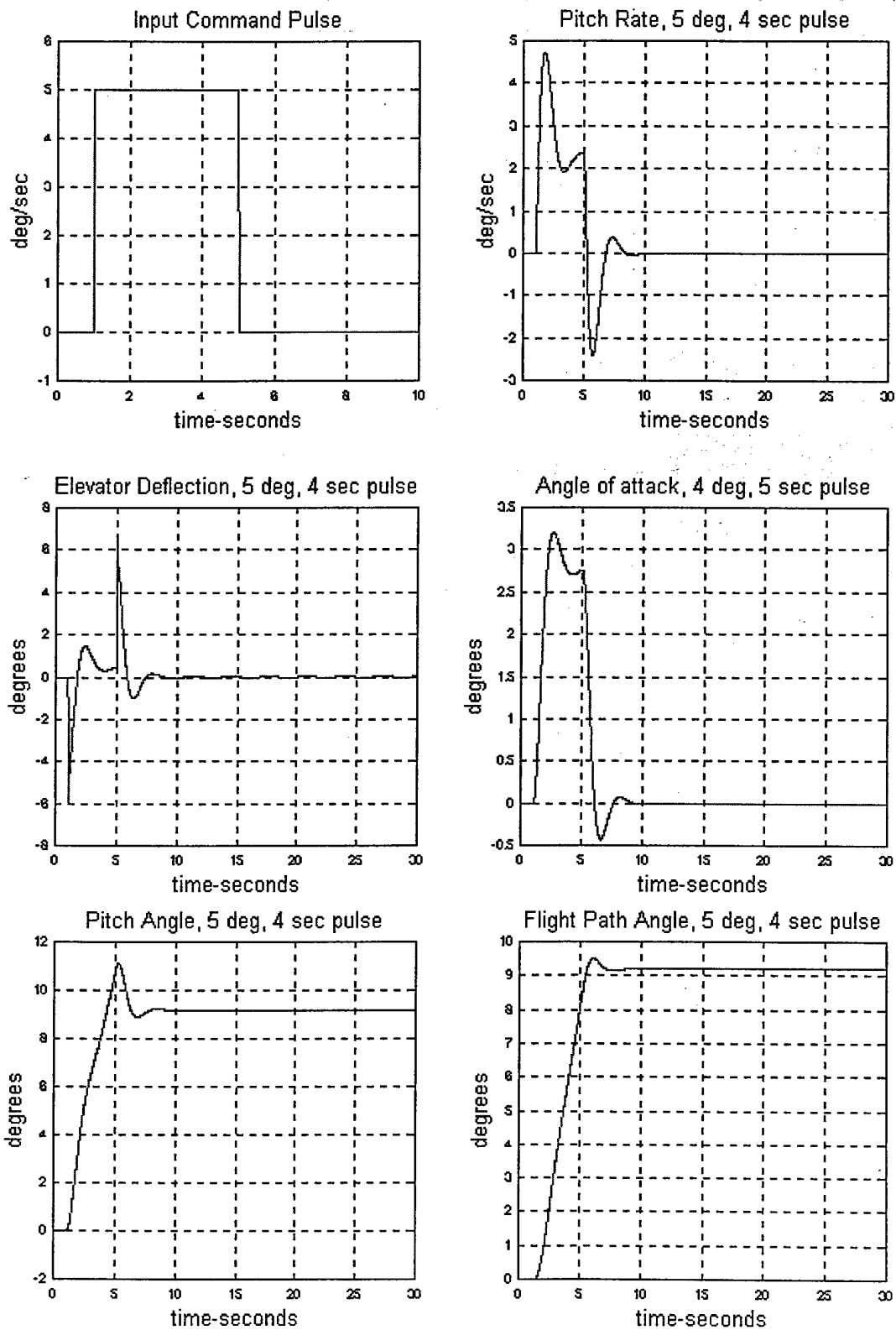
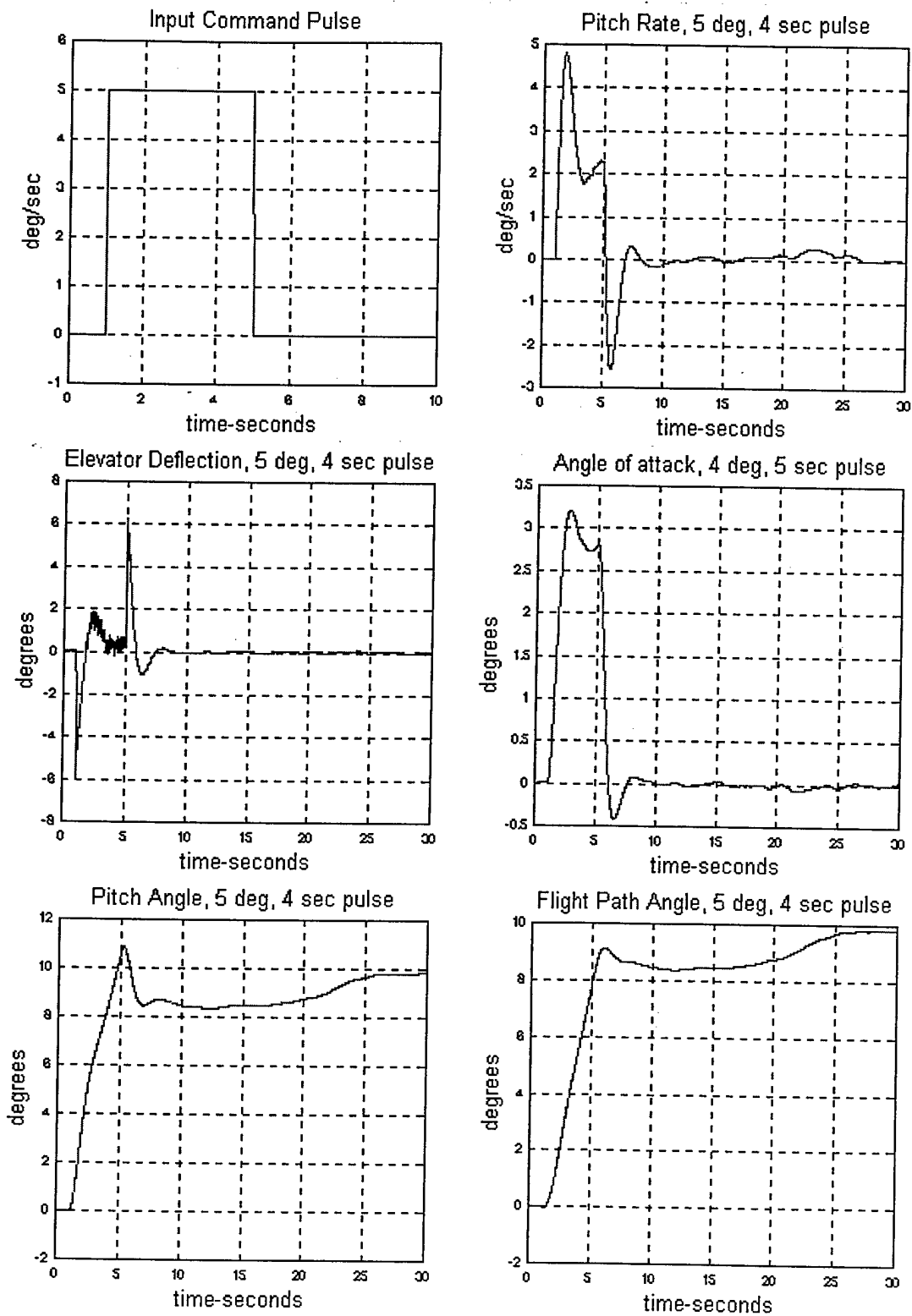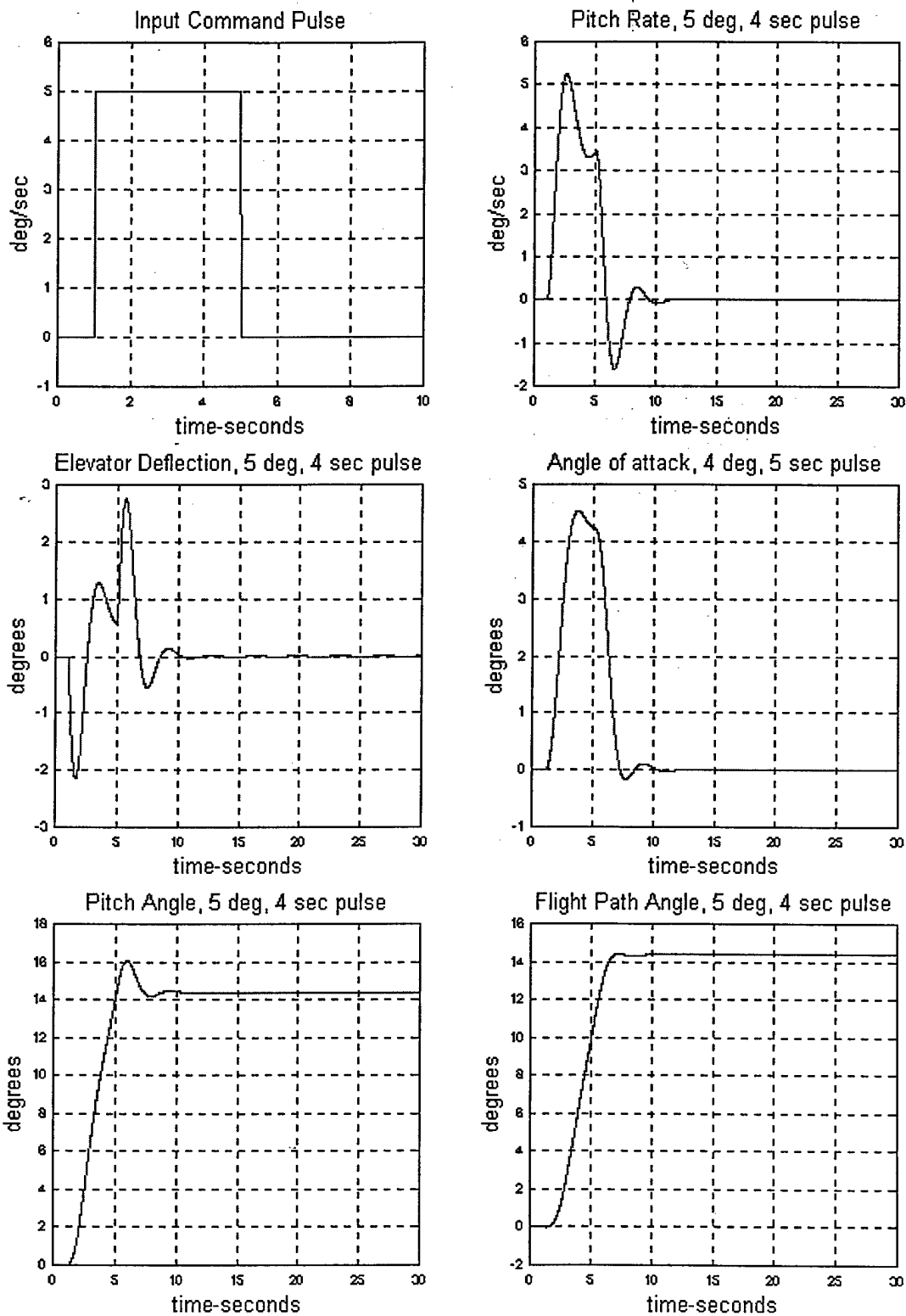Figure 5.9. Short Period Simulations for MXINI - Noises off
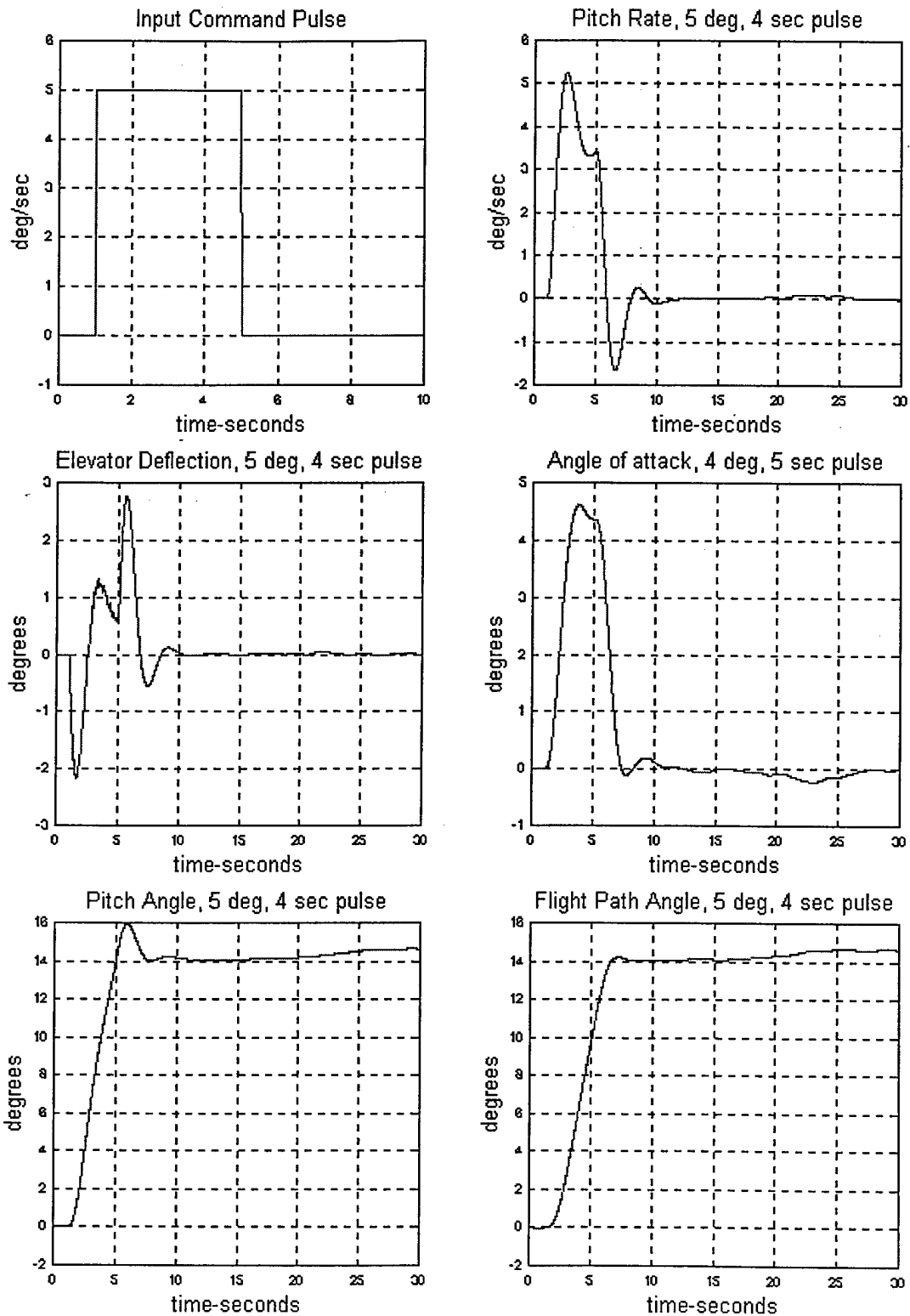
Figure 5.10. Short Period Simulations for MXINI - Noises on

Handling qualities predictions for this design were calculated using the Hoh's Bandwidth and Berry Flight Path Overshoot Criteria. The Hoh's bandwidth criteria predicted solid level I handling qualities with a delay parameter (tau p) of 0.025 and a bandwidth of 3.2 rad/sec. However, the Berry Criteria predicted level II with a 40% overshoot.

This design was produced in the time period between initial implementation verification in Buffalo and the final verification at Edwards AFB 1 day prior to flight test. Consequently the implementation could not be verified until the final verification simulation. It turned out that there was an error in the script file that implemented the MXINI control law. The pole-zero mismatch is shown in Table D6, Appendix D. A simple fix to the script file within the established SIMULINK™ control law architecture was attempted at the end of the ground simulation period at Edwards AFB. However, complete verification of the fix was not made prior to the first HQDT sortie due to time constraints.

5.4 Ground and Airborne Flight Control Law Validation

Validation testing was accomplished during ground test by comparing the closed-loop time responses to a PTI pulse input at the control stick. The comparison was made between each control system coded on the VSS computer to those generated in the design process. Since the design model was a short period approximation of the F-16, only the pitch rate and the AOA responses were examined. The linear time history response matches had some discrepancies, but were considered an acceptable validation of the closed loop response. See Figures D1-D5 in Appendix D for ground time history validation plots. Recall that no time history validation was done for the MXINI configuration due to time constraints.

In addition to comparing PTI time responses for validation, the test team pilots were able to "fly" simulated approaches with each flight control configuration using an integrated synthetic horizon, Attitude-Direction Indicator (ADI), and flight path marker display. This not only gave them a feel for how each control configuration might fly, but provided valuable qualitative validation information that was not obtained from the time response matches. The pilots noticed an apparent negative speed stability behavior in the aircraft for the H2INI, H2AIN, and H2AOA configurations which had not been noticed previously. Upon discussion with Calspan, it was explained that the VSS computer modified the Learjet's short period dynamics to look like F-16 short period dynamics, but did not eliminate or modify the actual Learjet phugoid that would be present inflight. Consequently, when the Learjet phugoid mode was included in the simulation, which had not been done previously, three of the configurations appeared to have negative speed stability. The Learjet phugoid mode was not considered in the design process upon the advice of the AFIT faculty and Calspan. They felt this mode would not have a significant effect on handling qualities and would add unnecessary complexity and increased order to the resulting flight control designs. In actuality, it appeared that leaving the Learjet phugoid mode out of the design process might have an impact on the handling qualities of the flight control designs. The CLASSIC and MXAOA control configurations did not exhibit any negative speed stability characteristics during piloted ground simulations. The CLASSIC control configuration may have handled the additional dynamics well because it only involved a small amount of gain on the AOA and pitch rate feedback paths. Unlike all of the other flight control configurations, there were no controller dynamics interacting with the phugoid mode in the CLASSIC configuration. The MXAOA controller was dynamic (i.e., a transfer function); however, it was also designed to handle model uncertainty. Thus, the MXAOA control configuration also performed as expected.

Inflight model validation results closely matched the ground model validation results (Figures D6-D10) and were considered acceptable. The pilots again noticed the apparent negative speed stability characteristic in the H2INI, H2AIN, and H2AOA configurations. Some of the discrepancies in the latter portions of the time histories for the H2INI, H2AIN, and H2AOA configurations were attributed to the apparent negative speed stability. Again, the MXAOA and CLASSIC configurations performed as expected with no apparent instabilities.

The fix of the MXINI configuration was spot checked during this flight. This configuration caused a small, bounded PIO. Analysis of the implementation revealed the intended fix had not worked. Furthermore, a simple fix within the existing VSS software architecture was not possible. The decision was made to drop MXINI from subsequent flight evaluation.

Post-flight analysis using the design controller and aircraft dynamics revealed that one of the low frequency poles in the H2INI, H2AIN, and H2AOA control law configurations became unstable in the closed loop dynamics when the Learjet phugoid was included in the aircraft dynamics (See Tables D7-D11 in Appendix D). This indicates that these designs were not robust to the addition of unmodeled, low frequency dynamics such as the phugoid.

5.5 Summary

Taking care of the logistics and setting the methodology/procedures to be used in this flight test program was they key to the successful verification and implementation of the HAVE INFINITY II control laws. It was this process that produced the decision to make a trip Calspan facilities two months prior to flight test for the purpose of initial verification and validation of the control laws. The early discovery of problems with the implementation of the H2INI/H2AIN

and MXINI/MXAIN control laws allowed time for redesign and supplemental implementation of the new designs (CLASSIC, H2AOA and (new) MXINI).

Ultimately, the verification and validation phase of the test program confirmed the flight control laws implemented, and flown, were the same as those designed, except for the MXINI configuration. The dynamics of the actual aircraft were different than the dynamics of the design model due to the exclusion of the phugoid mode from the design model. As a result, the H2INI, H2AIN, and H2AOA control configurations were negatively impacted due to a lack of robustness to low frequency differences between the design model and the actual aircraft. The system should have been tested with the phugoid mode early in the design process. Then, if a stability problem was found, a redesign could have been accomplished by adding additional uncertainty to the short period model or simply including the phugoid mode in the design. The bottom line is that early FCS ground tests should be conducted with the highest fidelity aircraft model available to allow time for required redesigns prior to flight test.

Table 5.10 provides a summary of the designs that were successfully implemented, verified, and validated for flight test.

TABLE 5.10

SUMMARY OF VERIFIED AND VALIDATED FLIGHT CONTROL DESIGNS SELECTED FOR HANDLING QUALITIES FLIGHT TEST

Name	Method of Design	Type of Design	Hoh's Bandwidth HQ Prediction	Berry Flight Path Overshoot Criteria HQ Prediction
CLASSIC	Feedback Gain	AOA & Pitch rate feedback	Level 1	Level 1
H2AOA	H_2	AOA Cmd	Level 1	Level 1
H2INI	H_2	Pitch Rate Cmd	Level 1	Level 1
H2AIN	H_2	AOA Cmd	Level 1	Level 1
MXAOA	H_2/H_∞	AOA Cmd	Level 1	Level 1

VI. Flight Test Results

This chapter reviews the handling qualities results of the five configurations flight tested based on the test team's analysis of the quantitative and qualitative data. All of the raw quantitative and qualitative handling qualities data is presented in Appendix E. The final section is an overall summary comparing handling qualities flight test data to their respective predictions. Table 6.1 summarizes the test team pilots' experience.

TABLE 6. 1

EVALUATION PILOT EXPERIENCE

Pilot	Primary A/C	Flight Hours
Boe (USAF)	F-15C	1,500
Stevenson (USN)	F-14A/B	1,300
Cantiello (ItAF)	F-3 TORNADO	1,100

6.1 CLASSIC Flight Control Configuration

The evaluation pilots performed four straight-in and four horizontal offset landings with the CLASSIC flight control configuration. See Figures E1 through E4 (Appendix E) for Cooper-Harper (C-H) and PIO histograms. Level I C-H ratings were given for each landing with one exception that received C-H 4. All Level I ratings were associated with PIO 1, and the C-H 4 received a PIO 3. All the C-H and PIO ratings were unaffected by differences in wind conditions (Appendix E).

All pilots agreed that the CLASSIC flight control configuration provided a predictable, linear initial response, although the response was somewhat slower than several of the other configurations. The majority of Level I ratings confirmed the satisfactory handling qualities of

this configuration; however, while performing HQDT, pilot two noted that the aircraft response was not linear with respect to the size of the input. If the aircraft response was truly linear, a larger input should result in a larger output over the same period of time. In other words, a faster initial response should occur with a larger input. Pilot two found that large stick inputs did not produce a faster pitch rate response than smaller inputs. While pilot two saw this problem consistently during the HQDT tasks, he did not notice it during any of the landing tasks. On one landing, however, pilot three downgraded the configuration to C-H 4 because he had to sacrifice desired performance when he encountered an unexpected pitch response in the flare. Postflight analysis showed that pilot three increased the size and rate of his stick inputs at the initiation of the flare, but the aircraft did not respond faster to these inputs. This forced pilot three to lower his gains and accept a long landing. Both pilot two and pilot three's comments about the pitch response were consistent with a rate limitation problem in the flight control system; however, flight data evaluation did not support a rate limitation problem. No other explanation for the nonlinear pitch response was found. Inputs large enough to uncover the nonlinear pitch response were not required on a majority of the landings so the problem had little impact on the C-H and PIO ratings. Overall, the CLASSIC flight control configuration was rated Level I.

6.2 H2AOA Flight Control Configuration

The evaluation pilots performed four straight-in and four horizontal offset landings with the H2AOA flight control configuration. See Figures E5 through E8 (Appendix E) for C-H and PIO histograms. The H2AOA flight control configuration received the worst ratings of all the configurations flown in the landing tasks. Level II C-H ratings were given for all landings with one exception that received C-H 3. Two landings were given C-H 6 ratings with PIO 4. Another

landing was given a C-H 6 rating with a PIO 3. In general, the ratings for the horizontal offset

landing task were better than the ratings for the straight-in landing task, although one of the C-H

6 ratings was given for a horizontal offset task. The ratings of this configuration also worsened

with higher winds. The only Level I rating (C-H 3) was given during very light winds

(Appendix E).

All three pilots agreed the long-term pitch axis response was slowly divergent. A

deviation in airspeed started a pitching moment, resulting in slowly increasing stick forces that

continued to build in the initial direction until the pilot retrimmed the aircraft. The pitching

moment was opposite of what was expected. When the airspeed slowed from a trimmed

condition, forward stick pressure was required to keep the nose from rising. The amount of

disturbance required to start a divergence was very small. A 1-knot deviation in airspeed was

enough to initiate the slow buildup of stick force. The small size of the disturbance, required to

initiate the divergence, made the direction unpredictable to the pilot; such that the pilot had no

indication whether the divergence would result in a slow buildup of push or pull force. One pilot

commented that flying the configuration "felt like trying to balance on a bowling ball." This

problem increased pilot workload because the pilots had to pay constant attention to airspeed and

pitch attitude, and continually retrim the aircraft. These characteristics became less apparent

during the offset landing tasks when the pilots were exercising tighter control of the aircraft.

Under tight control, the aircraft was not allowed to diverge from trim, and the C-H and PIO

ratings improved. Regardless of task, all pilots felt the nose pitch down after main wheel

touchdown. The pilots were unable to keep the nose from dropping with a reasonable amount of

stick force and did not attempt to use large displacements of aft stick to arrest the nose

movement. Pilot two felt the stick forces increase dramatically in the flare on both a straight-in

task and a horizontal offset task, which made the pitch attitude very hard to control. This characteristic generated the two PIO 4 ratings given by pilot two. The small amplitude pitch oscillations caused pilot two to freeze the stick and he achieved desired performance only because the PIO occurred very late in the flare. Overall, the long-term divergent response of this flight control system had a large impact on the majority of the landings. The H2AOA flight control configuration was rated Level II.

The divergent nature of the H2AOA flight control configuration was not completely unexpected. As discussed in Chapter V (section 5.4), ground simulations completed just prior to flight test revealed that the system had a slowly divergent first order mode. This problem was not predicted with the short period approximation of the aircraft model used in design and during initial ground tests. The problem was only found when the phugoid mode was included during the final ground simulation 1 day prior to the start of flight test.

6.3 H2INI Flight Control Configuration

The evaluation pilots performed eight straight-in and eight horizontal offset landings with the H2INI flight control configuration. See Figures E9 through E12 (Appendix E) for C-H and PIO histograms. Pilot one consistently rated this configuration Level II while pilot three consistently rated this configuration Level I. Pilot two rated the configuration Level I for the straight-in task, but gave both Level I and Level II ratings for the horizontal offset task. The PIO ratings by all the pilots fell between PIO 1 and PIO 3 with the majority of the ratings PIO 1 or PIO 2. The C-H and PIO ratings were worse for the horizontal offset task than they were for the straight-in task. This configuration also received poorer ratings under higher winds (Appendix E).

All the pilots liked the short-term pitch response, describing it as smooth and predictable. All three pilots could change the pitch attitude rapidly; however, pilot one commented on one of his four landings that the response felt sluggish. No explanation was found for this comment. All three pilots flew this configuration with winds from 8 knots to 20 knots. During these flights, each pilot noticed an airspeed sensitivity and divergence similar to the H2AOA configuration, but not as objectionable. Under these windy conditions, pilot three also noticed "negative speed stability" during the go-around portion of a low approach. Pilot Two's second look at the configuration occurred on a day when the winds varied from calm to 10 knots. During this sortie, pilot two only noticed the divergent characteristics when the wind was above 5 knots. Pilot two gave the configuration Level II ratings during the windy conditions due to the increased workload required to maintain airspeed. Pilot one was able to consistently achieve desired performance with this configuration but he found the divergent nature of the system to be objectionable enough to warrant Level II ratings. All the pilots noticed a slight tendency for the nose to pitch down during the landing roll. This pitching moment was more benign than the H2AOA configuration. Like the H2AOA design, the slight divergent nature of the aircraft with this flight control configuration was predicted during the final ground test. Overall, the slight divergent nature of the pitch response had an impact on the landing tasks. The H2INI configuration was rated between Level I and Level II.

6.4 H2AIN Flight Control Configuration

The evaluation pilots performed six straight-in and six horizontal offset landings with the H2AIN flight control configuration. See Figures E13 through E16 (Appendix E) for C-H and PIO histograms. The C-H ratings for this configuration ranged from C-H 3 to C-H 5 with the

majority of the ratings being C-H 4. The PIO ratings for this configuration ranged from PIO 1 to PIO 3 with the majority of ratings being PIO 2. Although each pilot's C-H and PIO ratings varied, the overall distribution of the ratings were virtually the same for both the straight-in and horizontal offset tasks. None of the ratings were affected by the winds (Appendix E).

The H2AIN flight control configuration exhibited many of the same characteristics as the H2INI flight control configuration, although to a greater degree. This similarity was logical as the only difference between H2AIN and H2INI was a filter placed in the command channel of the H2AIN configuration. This filter was designed to make the original pitch rate tracking system behave more like an AOA tracking system. While this objective was achieved, the filter made the initial pitch response more sluggish. The pilots did not like this sluggishness and commented that the pitch response "takes a while to get going." The sluggishness was very noticeable when the stick was displaced slightly and held while the pitch response was observed. The pitch rate accelerated slowly until it stabilized at a steady state value. The added filter in the H2AIN design may have caused the divergent nature of the system to be more noticeable. All the pilots felt that the long-term pitch axis response diverged in a manner similar to the H2AOA configuration, although at a slower rate. This divergence made the configuration very sensitive to airspeed deviations from trim, therefore pilot workload increased trying to maintain airspeed. Pilot two commented that he was 5 KIAS below his trim airspeed during the approach and had to push on the stick; however, during the flare, all the pilots commented that the nose felt heavy. This made the aircraft hard to control precisely in the flare and forced the pilots to adopt a low-gain technique to obtain desired performance. The pilots were unable to keep the nose from dropping after landing due to the heavy stick forces. This nose down motion was worse than H2INI, but not as bad as H2AOA. Like the H2AOA and H2INI configurations, the H2AIN

system was found to be divergent during the final ground test. Both the sluggishness of the pitch response and the divergent nature of the system had an impact on the landing tasks. The H2AIN configuration was rated between Level I and Level II.

6.5 MXAOA Flight Control Configuration

The evaluation pilots performed 11 straight-in and 10 horizontal offset landings with the MXAOA flight control configuration. See Figures E17 through E20 (Appendix E) for C-H and PIO histograms. Pilots one and two consistently rated this configuration Level I while pilot three consistently rated this configuration Level II. PIO ratings ranged from PIO 1 to PIO 3. The winds did not have an effect on the C-H and PIO ratings (Appendix E).

The MXAOA flight control configuration was stable with no tendency for a long-term pitch divergence. Stability was predicted for this configuration during the final ground test. While the long-term pitch response was acceptable, the pilots felt that the short-term pitch response was fast and too lightly damped. Each of the pilots noticed a small overshoot in the aircraft's pitch response which they described as a "pitch bobble." This bobble could be eliminated by anticipating the aircraft's response and adjusting the size of the input accordingly. Pilots one and two were able to eliminated this pitch overshoot with what they considered to be minimal compensation and gave the configuration Level I C-H ratings. Pilot three, however, found the pitch bobble objectionable during the flare and had to sacrifice desired performance on several landings. During these landings, the pilot cautiously delayed the power reduction until the pitch bobble damped out. This caused Pilot Three to carry excess power into the flare and float beyond the desired touchdown point. On the landings, when pilot three was able to achieve desired performance; he still felt the workload was high enough to warrant Level II ratings. The

pitch sensitivity was also noted during HQDT. Both pilot two and three gave the configuration PIO 4 ratings during HQDT tasks. The HQDT results indicate that this configuration was PIO prone to large amplitude, high frequency inputs. This tendency may have been the cause of the unwanted pitch motions seen by pilot three. Overall, the pitch sensitivity of this flight control system had an impact on some of the landings and the MXAOA flight control configuration was rated between Level I and Level II.

6.6 Summary

Overall the handling qualities results were excellent. Most of the Level II comments related to the instability in the H2INI, H2AIN, and H2AOA designs were attributed to the phugoid mode. The H2INI, H2AIN, and H2AOA designs produced acceptable, but unsatisfactory, handling qualities, and may have been closer to satisfactory had the phugoid mode been included in the design aircraft model. The results of this program simply reinforce that early verification and validation of design models through the use of the highest fidelity simulation possible, must be supported and required by the Responsible Test Organization (RTO).

It should also be pointed out here that the variation in the number of landings for each flight control configuration was intentional. The requirement for success was that each pilot evaluate the flight control configuration twice in the landing phase (1 straight-in, 1 offset), unless the configuration received a C-H 8, 9, or 10 (in which case it would be dropped). Beyond that, the configurations evaluated were determined by the TC. The borderline Level I/II configurations got more landings in an attempt to eliminate this ambiguity. While not successful in that respect, the added data was helpful in confirming previous pilot comments and ratings.

Table 6.2 compares the flight test handling qualities results with the designs predictions.

TABLE 6.2

HANDLING QUALITIES RESULTS VS. PREDICTIONS

Name	Type of Design	Hoh's Bandwidth HQ Prediction	Berry Flight Path Overshoot Criteria HQ Prediction	Flight Test Results
CLASSIC	AOA & Pitch rate feedback gain	Level 1	Level 1	Level 1
H2AOA	H_2 AOA Cmd	Level 1	Level 1	Level 2
H2INI	H_2 Pitch Rate Cmd	Level 1	Level 1	Level 1/2
H2AIN	H_2 AOA Cmd	Level 1	Level 1	Level 1/2
MXAOA	H_2/H_∞ AOA Cmd	Level 1	Level 1	Level 1/2

Since the actual aircraft included a mode not present in the design model, the comparison in Table 6.2 is "apples to oranges". To remedy this, the handling qualities predictions were recomputed with the phugoid mode included in the aircraft design model. The plots of the Hoh's Bandwidth Criteria and time history predictions are in Appendix F. A plot of the Hoh's Bandwidth predictions, for each configuration without the phugoid is included for ease of reference. These results are summarized in Table 6.3.

TABLE 6.3

HANDLING QUALITIES RESULTS VS. PREDICTIONS WITH PHUGOID MODE

Name	Type of Design	Hoh's Bandwidth HQ Prediction (w/phugoid)	Berry Flight Path Overshoot Criteria HQ Prediction (w/phugoid)	Flight Test Results
CLASSIC	AOA & Pitch rate feedback gain	Level 1	Level 1	Level 1
H2AOA	H_2 AOA Cmd	Level 2	Divergent[1]	Level 2
H2INI	H_2 Pitch Rate Cmd	Level 2	Divergent[1]	Level 1/2
H2AIN	H_2 AOA Cmd	Level 2	Divergent[1]	Level 1/2
MXAOA	H_2/H_∞ AOA Cmd	Level 1	Level 1	Level 1/2

1. Handling qualities prediction were not possible from the Berry criteria for the divergent control laws.

The data in Table 6.3 show good correlation between the predictions and actual results. Moreover, these results would tend to nullify the hypothesis made earlier that the Hoh's bandwidth criteria would not do a good job of predicting handling qualities. While it cannot be concluded from these results that the Hoh's criteria will work will give good predictions in all cases (history has proven that [23]), it did do a good job here. Of course the borderline Level I/II ratings make it much easier to correlate the flight test data with predictions!

The borderline ratings are important in that they indicate there are a lot of good characteristics about the designs. They also indicate there are some bad characteristics, but not so bad such that the design should be scrapped. The problems caused by the negative speed stability could be fixed by simply re-running the H_2 designs with the phugoid mode included in the aircraft model. The sluggishness of the H2AIN configuration was likely caused by the filter dynamics (since it was the only difference from H2INI). This problem could be easily remedied by taking the filter out which would leave H2INI! The split in MXAOA came down to pilot

preference. However, the fact that a slight pitch bobble was noticed by all pilots increasing the

ideal model damping would probably eliminate the problem.

VII. Conclusions and Recommendations

7.1 Conclusions

The overall objective of this research was to perform an inflight handling qualities evaluation of several multiobjective, optimal flight control designs. This objective was met.

Overall the results were good and indicate that the multiobjective, optimal model following design techniques used in this research can produce at least Level I/II (acceptable) handling qualities.

Specific objectives were categorized into two phases: development and simulation phase (phase I), and the flight test phase (phase II).

Phase I specific objectives included the development and simulation of H_2, H_∞, μ, mixed H_2/H_∞, and mixed H_2/μ problems. All of these objectives were met.

Selection of the ideal model used for model following in the designs was based on handling qualities predictions using Hoh's Bandwidth Criteria and academic knowledge of what a good closed loop model would be. Initially, it was thought that the ideal model would be the sole determinant of handling qualities for all of the designs produced. However within the context of a specific ideal model, it was found that the selection of the control rate usage and tracking performance weights could significantly influence the Hoh's handling qualities predictions of a given H_2 design by changing the bandwidth of the closed loop system.

Increases to control rate limiting weight degraded handling qualities predictions by

producing systems with smaller bandwidth that rolled off rapidly in phase at frequencies above the bandwidth frequency. This became important because of the selection of the tracking weights. The higher the DC gain of the tracking weight, the better the tracking performance. However, demanding tight tracking many times caused rate limiting. The solution to this was to increase the rate limit weight. The bottom line was that there was a tradeoff between these two weights in the designs considered in this study. This resulted in a fair amount of iteration during the design process to get level I handling qualities predictions. While this finding may be specific to the work done here, it serves as a place to start when the designer is looking to manipulate the handling qualities of a model following design.

The final objective of phase I was to pick the best design candidates for flight test. Designs were selected for flight test based on the following criteria and constraints:

1. The compensator was stable (All poles in LHP).

2. Design handling qualities must have been predicted Level I using the Hoh's Bandwidth Criteria (Landing Phase). The Berry Flight Path Overshoot Criteria was also considered, but not used as a primary criteria for flight test selection.

3. Designs were desired to have 6 dB of gain margin and 45° of phase margin.

4. Designs should have good command tracking characteristics.

All of the desired design types were completed and evaluated for flight test in phase I. The designs selected for flight test had the best overall combination of characteristics for the criteria listed. There weren't any μ designs or single norm H_∞ designs represented in the flight

test candidates. The μ designs evaluated were disqualified as not implementable because of RHP compensator poles. All of the H_∞ formulations were used solely as singular constraints for the mixed H_2/H_∞ problems and never intended to be stand alone designs. This was done to allow the designer to better manage the tradeoff process thereby facilitating the development of designs having the desired properties.

Limitations associated with the Calspan Learjet led to the use of the Euler integration routine in MATLAB™ SIMULINK™ for inflight simulation of the control laws. This in turn led to changes in the H2INI/H2AIN configuration and disqualified the MXINI/MXAIN configuration. Three new designs were generated (CLASSIC, H2AOA, and MXINI) to replace the two that were disqualified. The optimal design ideal models were based on dynamics that had proven good handling qualities from previous Calspan flight test.

Phase II objectives were to flight test the control designs selected for flight test from phase I, collect Cooper-Harper handling qualities ratings, compare those ratings with the design phase predictions, and draw conclusions with regards to any apparent trends in predictions vs. actual ratings.

Proper model verification, validation on the ground and inflight was a critical step that allowed for a satisfactory evaluation of the handling qualities of the HAVE INFINITY II flight control system designs. The Calspan Learjet did an excellent job of simulation on the ground and in the air. This was confirmed by the correlation of the ground and flight test time response matches and pilot qualitative comments. Handling qualities results indicate that the optimal design methods used gave Level II or borderline Level I/II handling qualities. Most of the Level II comments related to the instability in the H2INI, H2AIN, and H2AOA designs caused by the

phugoid mode that was unaccounted for in the design process. These designs may have been rated closer to Level I if the phugoid had been included in the design aircraft model.

Design handling qualities predictions of the Hoh criteria and flight test handling qualities ratings correlated very well after the phugoid mode was included in the aircraft model (Tables 6.2 and 6.3).

The negative speed stability and inability to properly implement MXINI obscured any possible comparisons of pilot preferences between AOA and pitch rate command systems.

7.2 Recommendations

- Further flight test of multiobjective, optimal control designs (like those produced in this research) should emphasize testing some the purported benefits of these design techniques such as turbulence rejection and design robustness once Level I handling qualities are established. This will be the true measure of whether or not these methods offer any advantages over more simple conventional methods like feedback gains and root locus techniques. Evaluating turbulence rejection could be done by performing the same task in calm and turbulent conditions and comparing the handling qualities. Evaluating design robustness would be done by systematically varying the aircraft dynamics off nominal (for a given task in the same flight conditions) and documenting at what level of deviation the handling qualities degraded.

- Involve the organization that will be implementing and flying the control designs (in this case Calspan) in the concept phase of the research. These organizations

usually have volumes of practical experience that can save research time and positively influence the outcome of the results. Additionally, the contractor can get a clear appreciation of what the project's goals and methods are. They can then clarify implementation limitations so that research time will not be wasted producing something that can't be implemented (as was done with the SIMULINK™ integration routines). The bottom line is that all significant players in the research program should be involved from the beginning.

- Early FCS ground tests should be conducted with the highest fidelity aircraft model available to allow time for required redesigns prior to flight test. This lesson was learned by both the HAVE INFINITY in the verification phase and the HAVE INFINITY II test team in the validation phase.

- The model following technique should be used when designing an aircraft flight control law that will be subject to handling qualities evaluations. The experience in this research shows that the optimal multiobjective methods do a good job of model following when a reasonable tracking constraint is included. By taking advantage of this fact, and following an ideal model with known good handling qualities, the handling qualities "unknown" in the flight control design can be eliminated. This leaves the designer the flexibility to use weights and constraints to build in other capabilities in the control law (turbulence rejection, robustness to uncertainty, better stability margins, etc.).

Appendix A

Cooper-Harper and PIO Rating Scales

A.1 Cooper-Harper Rating

A Cooper-Harper (C-H) rating was given for each landing task. Figure B4 was used by the test conductor to aid the pilot in determining the appropriate C-H rating.
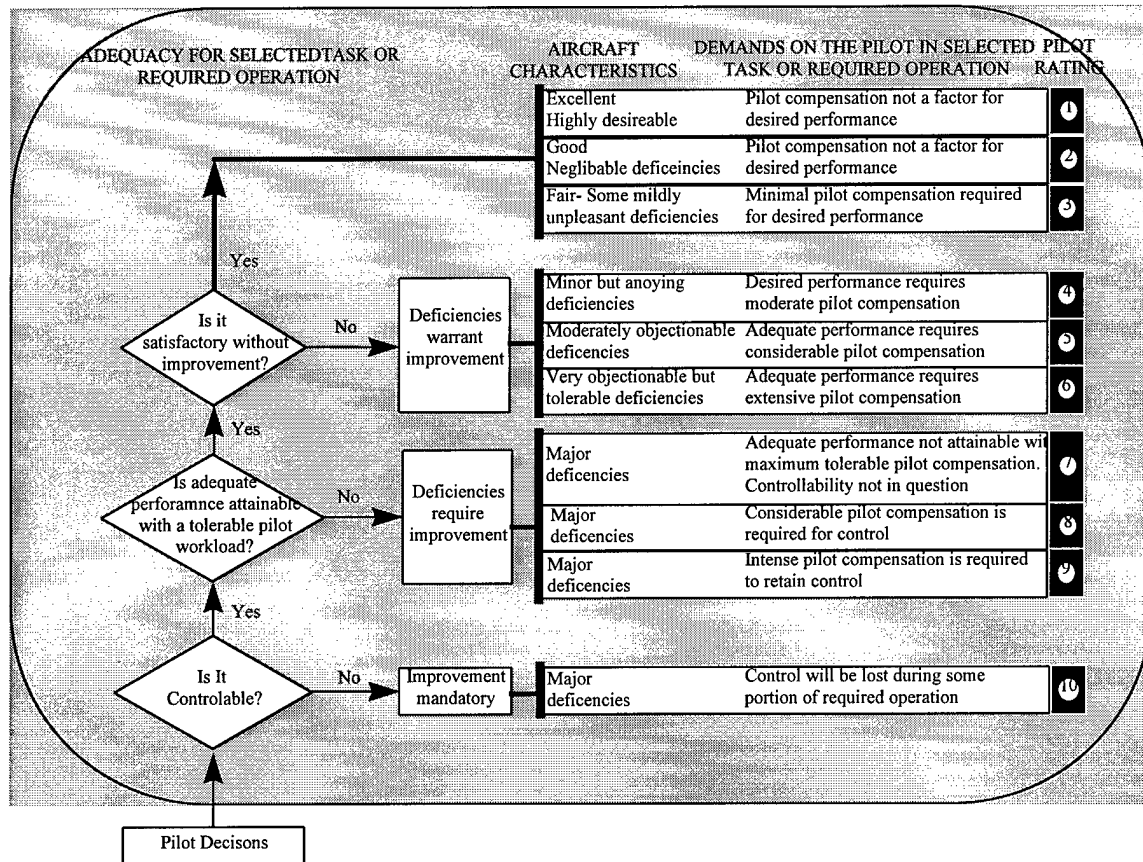
Figure A1. Cooper-Harper Rating Scale

A.2 Pilot-in-the-loop Oscillation Rating

A pilot-in-the-loop oscillation PIO rating was given for handling qualities during tracking (HQDT) with an C-23target aircraft, and for each landing task. Figure A2 was used by the test conductor to aid the pilot in determining the appropriate PIO rating. Descriptions for the

PIO ratings are shown in Figure A3.
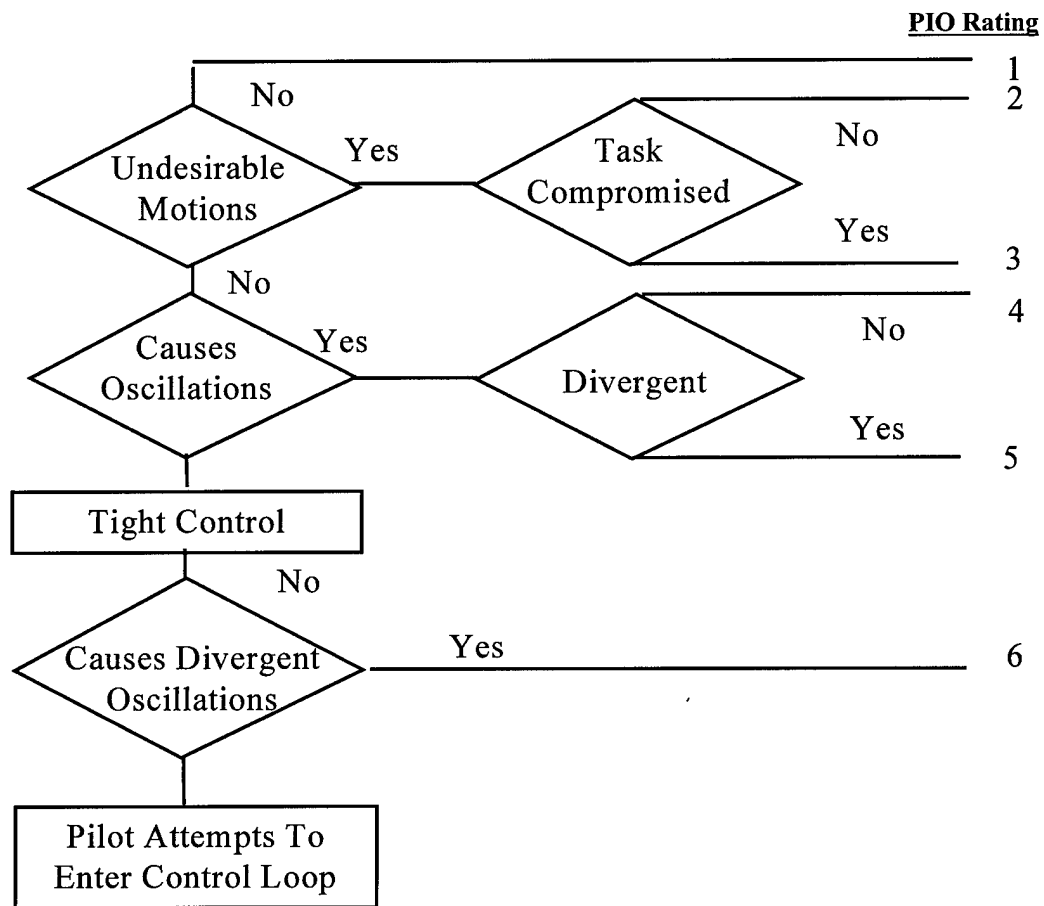
Figure A2. Pilot-in-the-Loop Oscillation Rating Decision Tree

Pilot-in-the-loop Oscillation (PIO) Scale	
Description	Numerical Rating
No tendency for pilot to induce undesirable motions.	1
Undesirable motions tend to occur when pilot initiates abrupt maneuvers or attempts tight control. These motions can be prevented or eliminated by pilot techniques.	2
Undesirable motions easily induced when pilot initiates abrupt maneuvers or attempts tight control. These motions can be prevented or eliminated, but only at sacrifice to task performance or through considerable pilot attention and effort.	3
Oscillations tend to develop when pilot initiates abrupt maneuvers or attempts tight control. Pilot must reduce gain or abandon task to recover.	4
Divergent oscillations tend to develop when pilot initiates abrupt maneuvers or attempts tight control. Pilot must open loop by releasing or freezing the stick.	5
Disturbance or normal pilot control may cause divergent oscillation. Pilot must open control loop by releasing or freezing the stick.	6

Figure A3. Pilot-in-the-Loop Oscillation Rating Scale

Appendix B

Mathematical Development

B. 1 Detailed H_2 Mathematical Development

In mathematical shorthand, H_2 optimization can be written as: Determine a compensator $K(s)$ such that

(1)

$$\alpha_0 = \inf_{K(s) Stabilizing} \|z\|_2 = \|T_{zw}\|_2 \tag{2}$$

$$= \inf_{K(s) Stabilizing} \|F_\ell(P,K)\|_2 \tag{3}$$

$$= \inf_{K(s) Stabilizing} \|P_{zw} + P_{zu}K(I - P_{yu}K)^{-1}P_{yw}\|_2$$

where α_0 is the minimum achievable two-norm.

A state space realization of P is represented by

$$\dot{x} = A_2 x + B_w w + B_2 u \tag{4}$$

$$z = C_z x + D_{zw} w + D_{zu} u \tag{5}$$

$$y = C_2 x + D_{yw} w + D_{yu} u \tag{6}$$

The "2" subscript indicates that this is H_2 optimization and will become important later when mixed H_2 / H_∞ optimization is discussed. The following assumptions apply to H_2 optimization:

(i) $D_{zw} = 0$

(ii) $D_{yu} = 0$

(iii) (A_2, B_2) is stabilizable and (C_2, A_2) is detectable

(iv) $D_{zu}^T D_{zu} = I$ and $D_{yw} D_{yw}^T = I$

(v) $\begin{bmatrix} A_2 - j\omega I & B_2 \\ C_z & D_{zu} \end{bmatrix}$ has full column rank for all ω.

(vi) $\begin{bmatrix} A_2 - j\omega I & B_w \\ C_2 & D_{yw} \end{bmatrix}$ has full row rank for all ω.

Condition (i) is imposed to ensure the two-norm of T_{zw} is finite. Condition (ii) is included to simplify the problem; however, it is not formally required. Condition (iii) is necessary for a stabilizing solution to exist. Condition (iv) is required for regularity. It ensures that there is a direct penalty on control use and no perfect measurements. This condition can be relaxed to a full rank condition through scaling [9]. Finally, conditions (v) and (vi) are required to ensure existence of stabilizing solutions to the two ARE's used in solving the H_2 problem.

The controller that minimizes (1) is unique and will be denoted K_{2opt}, with a corresponding minimum two-norm α_0. It is desired to parameterize the family of stabilizing sub-optimal H_2 controllers for the purpose of trading off H_2 performance for H_∞ performance. This family of controllers can be parameterized through an LFT of a transfer function J and a constrained freedom parameter $Q \in H_2$, as shown in Figure B1. A particular form of J is expressed as

$$J(s) = \begin{bmatrix} J_{uy} & J_{ur} \\ J_{vy} & J_{vr} \end{bmatrix} = \left[\begin{array}{c|cc} A_J & K_f & K_{fl} \\ \hline -K_c & 0 & I \\ K_{cl} & I & 0 \end{array} \right] \tag{7}$$

Figure B1. H_2 System with Parameterized Controller

where

$$A_J = A_2 - K_f C_2 - B_2 K_c \qquad (8)$$

$$K_c = B_2^T X_2 + D_{zu}^T C_z \qquad (9)$$

$$K_f = Y_2 C_2^T + B_w D_{yw}^T \qquad (10)$$

$$K_{cl} = -C_2 \qquad (11)$$

$$K_{fl} = B_2 \qquad (12)$$

where X_2 and Y_2 real, unique, positive semidefinite solution to the following AREs

$$(A_2 - B_2 D_{zu}^T C_z)^T X_2 + X_2 (A_2 - B_2 D_{zu}^T C_z) - X_2 B_2 B_2^T X_2 + \hat{C}_z^T \hat{C}_z = 0 \qquad (13)$$

where

$$\hat{C}_z = (I - D_{zu} D_{zu}^T) C_z \qquad (15)$$

and

$$(A_2 - B_w D_{yw}^T C_2)^T Y_2 + Y_2 (A_2 - B_w D_{yw}^T C_2) - Y_2 C_2^T C_2 Y_2 + \hat{B}_w \hat{B}_w^T = 0 \qquad (16)$$

where

$$\hat{B}_w = B_w (I - D_{yw}^T D_{yw}) \qquad (17)$$

The family of controllers that produce $\|T_{zw}\|_2 \leq \alpha$ can now be parameterized by

$$K(s) = F_\ell [J(s), Q(s)] \qquad (18)$$

where Q can be chosen to be any $Q \in H_2$ such that

$$\|Q\|_2^2 \leq \alpha^2 - \alpha_0^2 \qquad (19)$$

The optimal H_2 controller is obtained from the above parameterization when Q is chosen equal to zero. The resulting optimal controller is given by

$$K_{2opt} = \begin{bmatrix} A_J & K_f \\ -K_c & 0 \end{bmatrix} \qquad (20)$$

B.2 Detailed H_∞ Mathematical Development

This can be expressed in mathematical shorthand as: Determine the compensator $K(s)$ such that

$$\inf_{Kstabilizing} \sup_{\|d\|_2 \leq 1} \|e\|_2 := \inf_{Kstabilizing} \|T_{ed}\|_\infty \equiv \gamma_0 \tag{21}$$

$$= \inf_{Kstabilizing} \|F_\ell(P,K)\|_\infty \tag{22}$$

$$= \inf_{Kstabilizing} \|P_{ed} + P_{eu}K(I - P_{yu}K)^{-1}P_{yd}\|_\infty \tag{23}$$

where γ_0 is the minimum achievable infinity-norm. Recall that the infinity-norm of T_{ed} can be calculated by finding the maximum singular value, $\bar{\sigma}$. The mathematical expression is

$$\|T_{ed}\|_\infty = \sup_\omega \bar{\sigma}[T_{ed}] \tag{24}$$

A state space realization of (2.13) is expressed as

$$\dot{x} = A_\infty x + B_d d + B_\infty u \tag{25}$$

$$d = C_e x + D_{ed} d + D_{eu} u \tag{26}$$

$$y = C_\infty x + D_{yd} d + D_{u\infty} u \tag{27}$$

It should be noted that D_{yu} here is the same D_{yu} as in the H_2 problem, if the plants are the same. This fact will be very important later when the mixed H_2 / H_∞ problem is discussed. The ∞ subscript indicates the problem is setup for H_∞ optimization. As with H_2 optimization, there are several assumptions that are made:

(i) $D_{ed} = 0$

(ii) $D_{yu} = 0$

(iii) (A_∞, B_∞) is stabilizable and (C_∞, A_∞) is detectable

(iv) $D_{eu}^T D_{eu} = I$ and $D_{yd} D_{yd}^T = I$

(v) $\begin{bmatrix} A_\infty - j\omega I & B_\infty \\ C_e & D_{eu} \end{bmatrix}$ has full column rank for all ω

(vi) $\begin{bmatrix} A_\infty - j\omega I & B_d \\ C_\infty & D_{yd} \end{bmatrix}$ has full row rank for all ω

Conditions (i) and (ii) are included to simplify the problem; however, they are not necessary for

a solution to exist. Condition (iii) is necessary for a stabilizing solution to exist. Condition (iv)

is required for regularity. It ensures that there is a direct penalty on control use and no perfect

measurements. This condition can be relaxed to a full rank condition through scaling[9].

Finally, conditions (v) and (vi) are required to ensure existence of stabilizing solutions to the two

ARE's used in solving the H_∞ problem.

While the conditions above are similar to H_2 optimization, there are major differences

associated with the solution to the H_∞ optimization problem. In general, the controller that

achieves γ_0 in equation (21) is not unique. Furthermore, γ_0 is found through an iterative

method based on the solution to two AREs and a coupling condition. This method is based on

the parameterization of all suboptimal controllers where

$$\|T_{ed}\|_\infty < \gamma \tag{28}$$

for some $\gamma < \gamma_0$. Note that (28) excludes γ_0, but allows it to be approached to any desired tolerance. The family of all admissable controllers that satisfy (28) is illustrated by the LFT shown in Figure B2.
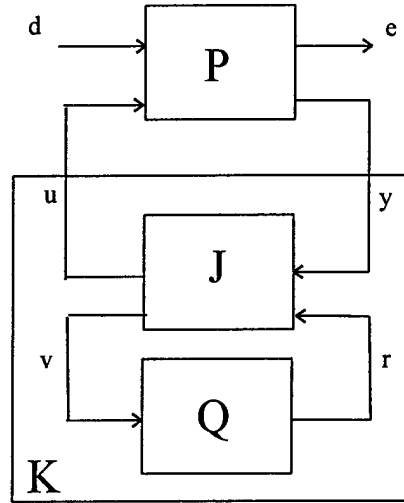
Figure B2. H_∞ System with Parameterized Controller

Even though there are major differences in the solution to the H_∞ optimization problem, the H_∞ optimal controller, $K_{\infty opt}$, can still be found by applying equation (7), which is repeated below for convenience. Of course, the elements in (7) are defined differently, so that

$$J(s) = \begin{bmatrix} J_{uy} & J_{ur} \\ J_{vy} & J_{vr} \end{bmatrix} = \left[\begin{array}{c|cc} A_J & K_f & K_{fl} \\ \hline -K_c & 0 & I \\ K_{cl} & I & 0 \end{array} \right]$$
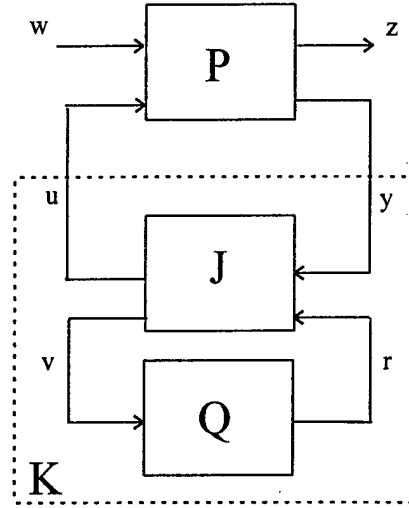
where

$$A_J = A_\infty - K_f C_\infty - B_\infty K_c + \gamma^{-2} Y_\infty C_e^T (C_e - D_{eu} K_c) \qquad (29)$$

$$K_c = (B_\infty^T X_\infty + D_{eu}^T C_e)(I - \gamma^{-2} Y_\infty X_\infty)^{-1} \qquad (30)$$

$$K_f = Y_\infty C_\infty^T + B_d D_{yd}^T \qquad (31)$$

$$K_{cl} = -(\gamma^{-2} D_{yd} B_d^T X_\infty + C_\infty)(I - \gamma^{-2} Y_\infty X_\infty)^{-1} \qquad (32)$$

$$K_{fl} = \gamma^{-2} Y_\infty C_e^T D_{eu} + B_\infty \qquad (33)$$

where X_∞ and Y_∞ are symmetric, positive semidefinite solutions to the following AREs

$$(A_\infty - B_\infty D_{eu}^T C_e)^T X_\infty + X_\infty (A_\infty - B_\infty D_{eu}^T C_e) + X_\infty (g^{-2} B_d B_d - B_\infty B_\infty^T) X_\infty + \hat{C}_e^T \hat{C}_e = 0 \qquad (34)$$

where

$$\hat{C}_e = (I - D_{eu} D_{eu}^T) C_e \qquad (35)$$

and

$$(A_\infty - B_d D_{yd}^T C_\infty) Y_\infty + Y_\infty (A_\infty - B_d D_{yd}^T C_\infty)^T + Y_\infty (\gamma^{-2} C_e^T C_e - C_\infty^T C_\infty) Y_\infty + \hat{B}_d \hat{B}_d^T = 0 \qquad (36)$$

where

$$\hat{B}_d = B_d (I - D_{yd}^T D_{yd}) \qquad (37)$$

Finally, Q can be chosen to be any $Q \in H_\infty$ such that

$$\|Q\|_\infty < \gamma \qquad (38)$$

Notice that Q does not have to be chosen equal to zero to get an optimal controller here, as was

the case in H_2 optimization.

B.3 Detailed Mathematical Development for the Structured Singular Value.

The structured singular value is a matrix function based on the underlying structure of a set of block diagonal matrices

$$\Delta := \left\{ diag\left[\delta_1 I_{r1}, \ldots, \delta_S I_{rS}, \Delta_1, \ldots, \Delta_F \right] \middle| \delta_i \in C, \ \Delta \in C^{m_j \times m_j} \right\} \tag{39}$$

where $\delta_i I_{ri}$ is the ith scalar block of order r_i and Δ_j is the jth full block of order m_j. For simplicity, we will assume that Δ is square, but the theory applies for no-square perturbations as well. The dimension n of $\Delta \in \Delta$ is given by

$$n = \sum_{i=1}^{S} r_i + \sum_{j=1}^{F} m_j \tag{40}$$

We will want to place a limit on the maximum infinity-norm that Δ can have. To do this, we define a set of block diagonal matrices that have an infinity-norm bounded by γ^{-1} as

$$\mathbf{B}\Delta := \left\{ \Delta \in \Delta \ \middle| \overline{\sigma}(\Delta) \le \gamma^{-1} \right\} \tag{41}$$

The structured singular value of a complex matrix M defined over a set of perturbations Δ is

$$\mu_\Delta(M) := \frac{1}{\min\left\{ \overline{\sigma}(\Delta) \ \middle| \Delta \in \Delta, \det(I - M\Delta) = 0 \right\}} \tag{42}$$

unless there is no $\Delta \in \Delta$ which makes $I - M\Delta$ singular, in which case $\mu_\Delta(M) = 0$.

From the definition of $\mu_\Delta(M)$, it can be seen that the maximum singular value of M is always an upper bound. However, this bound is conservative when we have more than one Δ block.

One method of reducing this conservativeness of the upper bound is to consider some transformation that does not affect the value of $\mu_\Delta(M)$ but does affect the value of $\bar{\sigma}(M)$. We do this by defining a set of scaling transfer functions D which has the same block structure as the perturbations Δ. These transfer functions are given by

$$\mathbf{D} := \left\{ \left[D_1, \ldots, D_S, d_1 I_{M_1}, \ldots, d_F I_{mF} \right] \middle| D_i \in C^{r_i \times r_i}, D_i = D_i^* > 0, d_j \in C, d_j > 0 \right\} \quad (43)$$

Now, an upper bound is given by the following:

Theorem B.1 *Assume* $M \in C^{n \times n}$, Δ *is defined by (39), and* **D** *is defined by (43). Then*

$$\mu_\Delta(M) \leq \inf_{D \in \mathbf{D}} \bar{\sigma}(DMD^{-1}) \quad (44)$$

Proof: See [11], Theorem 2.3.3.

Therefore, we can reduce the calculation of an upper bound on μ to computing the maximum singular value of a matrix. The next step is to take the system in Figure 2.3 and put it into the P-K form that is shown in Figure 2.1. This is shown in Figure B2.

Next we define the M transfer function matrix that will allow us to calculate μ.

$$M = F_\ell(P, K) \quad (45)$$
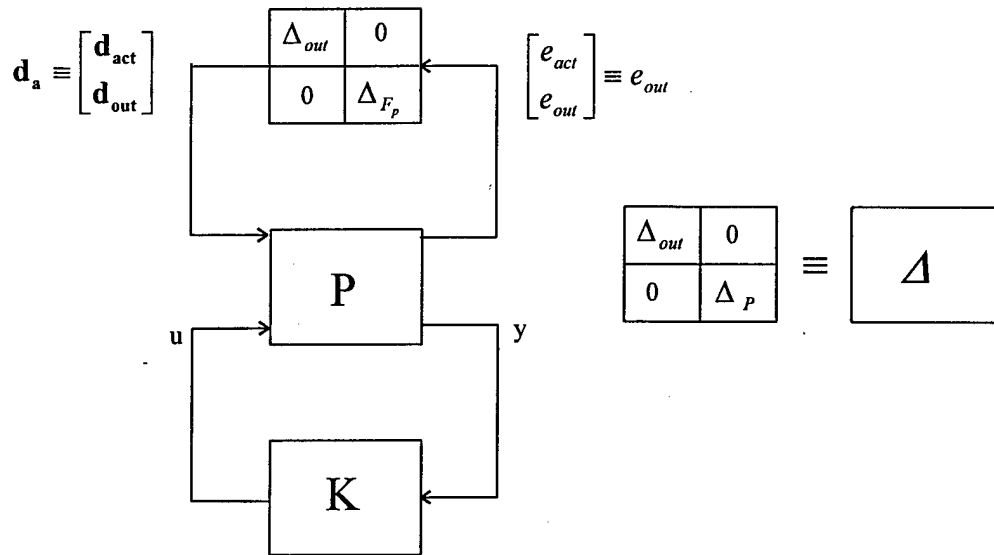
Figure B3. P-K Diagram of System with Uncertainty

Using equation (45), Figure B2 reduces to the $M - \Delta$ system shown below.
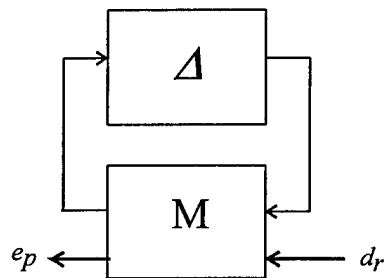
Figure B4. $M - \Delta$ System

Now M and Δ can be partitioned as

$$M = \begin{bmatrix} M_{11} & M_{12} \\ M_{21} & M_{22} \end{bmatrix} \qquad (46)$$

B-12

$$\Delta \in \varDelta = \left\{ \begin{bmatrix} \Delta_{out} & 0 \\ 0 & \Delta_P \end{bmatrix} \middle| \Delta_{out} \in \varDelta_{out}, \Delta_P \in \varDelta_P \right\} \tag{47}$$

The main result of μ theory can now be stated as follows.

Theorem B.2 (Main Loop Theorem) *The following are equivalent:*

   i. $\mu_\Delta(M) < \gamma$

   ii.   *(a)* $\mu_{\Delta_{out}}(M_{11}) < \gamma$, *and*

          (b) $\displaystyle \max_{\Delta_{out} \in B\Delta_{out}} \mu_{\Delta_P}\left[F_\ell(M, \Delta_{out})\right] < \gamma$

Proof: [11], Corollary 4.7.   ■

The importance of this theorem is that we now have a single test on M that will provide us with information about the system response to each perturbation block. Let $\mu_{\Delta_{out}}(M_{11}) < \gamma$ be a requirement for stability and $\mu_{\Delta_P}(M) < \gamma$ be a desired measure of performance. Then from the Main Loop Theorem, $\mu_\Delta(M) < \gamma$ implies our performance condition is satisfied and the system is robustly stable. The theorem also allows us to exchange Δ_{act} *and* Δ_{out}. Now $\mu_\Delta(M) < \gamma$ implies that our system has robust performance for **all** perturbations. The development to this point has only considered the case where M is a constant matrix. Next we expand these concepts to include dynamic matrices.

   B.3.1 Frequency Domain μ-synthesis. Let $M(s)$ be a MIMO transfer function with n_d inputs and n_e outputs. Assume $\varDelta \subset C^{n_d \times n_e}$ has the block structure given in (39). Now define the set of all dynamic perturbations which have the desired diagonal structure as

$$M(\Delta) := \left\{ \Delta(s) \in \Re H_\infty \mid \Delta(s_0) \in \Delta \quad \text{for all } s_0 \in \overline{C}^+ \right\} \tag{48}$$

where $\overline{C}^+$ is the extended closed right-half complex plane.

Now we can define the complex structured singular value of the dynamic transfer matrix $M(s)$ over the structured perturbations $\Delta(s) \in M(\Delta)$ as

$$\|G(s)\|_\mu = \sup_{\omega \in \Re} \mu[G(j\omega)] \tag{49}$$

Note that the structured singular value is not really a norm. The notation above is used only for convenience. Next we define the set **D** of scaling transfer functions which have the same block diagonal structure as Δ, where each block is a stable perturbation. Then an upper bound on the structured singular value of the transfer matrix, $G(s)$, is given by

$$\|G(s)\|_\mu \le \sup_{\omega \in \Re} \inf_{D \in D} \overline{\sigma}(DMD^{-1}) \tag{50}$$

$$= \inf_{D \in D} \|DMD^{-1}\|_\infty \tag{51}$$

Equation (51) converts the μ problem into an H_∞ problem that includes the selection of the scaling matrix D. We can now perform μ-synthesis by the following process:

(1) Determine the closed-loop transfer function M by performing a standard H_∞ optimization on some open-loop plant, P.

(2) Select an order of scaling matrix D, that best fits the singular values of Δ over a large frequency range and solve the H_∞ optimization problem again.

(3) Iterate on (1) and (2) until the value of μ stops decreasing.

This method is known as *D-K Iteration* and is mechanized in MATLAB™ (see [12] for details). This method is not guaranteed to converge to the optimal scaling D or the optimal controller K, but in practice the method works well. The D-K iteration method results in a controller order equal to the plant order plus twice the order of the D scales. This implies that there is a tradeoff between controller order and the accuracy of the D scale fits. Also of note is that since μ - synthesis is based on designing an H_∞ controller, it can result in a non-strictly proper controller (ie, one with a non-zero D matrix).

B.4 Detailed Mathematical Development for the Mixed H_2 / H_∞ Problem.

B.4.1 State Space Formulation. The development that follows was taken from [4]. The mixed H_2 / H_∞ problem is shown graphically in Figure B5. This system has exogenous inputs w and d. The controlled outputs of the system are z and e. The measured output is y and the control is u. These definitions are the same as those in Figures B1 and B2. However, P is now a combination of the P matrices from the H_2 and H_∞ subproblems.
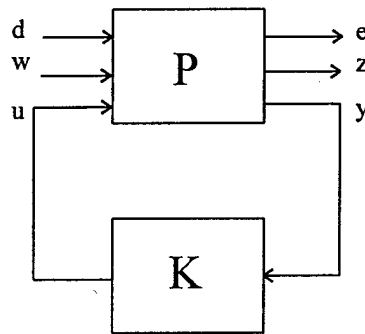
Figure B5. Block Diagram for the Mixed H_2 / H_∞ Problem

The resulting state space representation of P is given by

$$\dot{x} = \tilde{A}x + \tilde{B}_d d + \tilde{B}_w w + \tilde{B}_u u \tag{52}$$

$$e = \tilde{C}_e x + \tilde{D}_{ed} d + \tilde{D}_{ew} w + \tilde{D}_{eu} u \tag{53}$$

$$z = \tilde{C}_z x + \tilde{D}_{zd} d + \tilde{D}_{zw} w + \tilde{D}_{zu} u \tag{54}$$

$$y = \tilde{C}_y x + \tilde{D}_{yd} d + \tilde{D}_{yw} w + \tilde{D}_{yu} u \tag{55}$$

The transfer function form is

$$P = \left[\begin{array}{c|ccc} \tilde{A} & \tilde{B}_d & \tilde{B}_w & \tilde{B}_u \\ \hline \tilde{C}_e & \tilde{D}_{ed} & \tilde{D}_{ew} & \tilde{D}_{eu} \\ \tilde{C}_z & \tilde{D}_{zd} & \tilde{D}_{zw} & \tilde{D}_{zu} \\ \tilde{C}_y & \tilde{D}_{yd} & \tilde{D}_{yw} & \tilde{D}_{yu} \end{array} \right] \tag{56}$$

We can also represent (56) by its individual H_2 and H_∞ problems. These are given by equations (4-6) and (25-27) respectively. The assumptions for the mixed H_2 / H_∞ problem are:

(i) $D_{yw} = 0$

(ii) $D_{yu} = 0$

(iii) (A_2, B_u) is stabilizable and (C_y, A_2) is detectable

(iv) $D_{zu}^T D_{zu} = I$ and $D_{yw} D_{yw}^T = I$

(v) $\begin{bmatrix} A_2 - j\omega I & B_{u2} \\ C_z & D_{zu} \end{bmatrix}$ has full column rank for all ω.

B-16

(vi) $\begin{bmatrix} A_2 - j\omega I & B_w \\ C_{y2} & D_{yw} \end{bmatrix}$ has full row rank for all ω.

Note that these assumptions are the same ones that were used for the H_2 problem. There are no assumptions included dealing with the H_∞ part of the mixed problem because it is a constraint. No H_∞ optimization will be performed and as such, we will not have to solve any H_∞ Riccati equations. We can also allow perfect measurements and no control penalty in the H_∞ portion of the problem. This will be handled by the H_2 part of the problem since the controller energy will be constrained by the H_2 part of the problem. We are also guaranteed to have a stabilizing controller since the plant is the same for both problems. A state space representation of the controller in Figure B5 is

$$\dot{x}_c = A_c x_c + B_c y \tag{57}$$

$$u = C_c x_c + D_c y \tag{58}$$

Combining (4-6) and (57-58) produces the closed loop state space equation for T_{zw}

$$\dot{x}_2 = \left(A + B_2 D_c C_2\right) x_2 + B_2 C_c x_c + \left(B_w + B_2 D_c D_{yw}\right) w \tag{59}$$

$$\dot{x}_c = B_c C_2 x_2 + A_c x_c + B_c D_{yw} w \tag{60}$$

$$z = \left(C_z + D_{zu} D_c C_2\right) x_2 + D_{zu} C_c x_c + D_{zu} D_c D_{yw} w \tag{61}$$

Notice that $D_{zu} D_c D_{yw}$ must be equal to zero based on assumption (i), for the two-norm of T_{zw} to be finite. Also notice that this combined with assumption (iv) implies that $D_c = 0$. Thus, the only way this problem has a solution is for the controller K to be strictly proper. If we close the loop on our mixed H_2 / H_∞ system with the controller represented in (59-61), we get

$$\dot{\mathbf{x}}_2 = \mathcal{A}_2\,\mathbf{x}_2 + \mathcal{B}_w\,w \tag{62}$$

$$z = \mathcal{C}_e\,\mathbf{x}_\infty \tag{63}$$

and

$$\dot{\mathbf{x}}_\infty = \mathcal{A}_\infty\,\mathbf{x}_\infty + \mathcal{B}_d\,d \tag{64}$$

$$e = \mathcal{C}_e\,\mathbf{x}_\infty + \mathcal{D}_{ed}\,d \tag{65}$$

where

$$\mathbf{x}_2 = \begin{bmatrix} x_2 \\ x_c \end{bmatrix} \tag{66}$$

$$\mathbf{x}_\infty = \begin{bmatrix} x_\infty \\ x_c \end{bmatrix} \tag{67}$$

$$A_2 = \begin{bmatrix} A_2 & B_2 C_c \\ B_c C_2 & A_c \end{bmatrix} \tag{68}$$

$$A_\infty = \begin{bmatrix} A_\infty & B_\infty C_c \\ B_c C_\infty & A_c \end{bmatrix} \tag{69}$$

$$\mathcal{B}_w = \begin{bmatrix} B_w \\ B_c D_{yw} \end{bmatrix} \tag{70}$$

$$\mathcal{B}_d = \begin{bmatrix} B_d \\ B_c D_{yd} \end{bmatrix} \tag{71}$$

$$C_z = \begin{bmatrix} C_z & D_{zu} C_c \end{bmatrix} \tag{72}$$

$$C_e = \begin{bmatrix} C_e & D_{eu} C_c \end{bmatrix} \tag{73}$$

$$\mathcal{D}_{ed} = D_{ed} \qquad (74)$$

The following definitions are to simplify the subsequent development:

$$\underline{\alpha} \equiv \inf_{K_{adm}} \|T_{zw}\|_2$$

$K_{2_{opt}} \equiv$ the unique K(s) that makes $\|T_{zw}\|_2 = \underline{\alpha}$

$K_{mix} \equiv$ a solution to the H_2 / H_∞ problem for some γ

$$\underline{\gamma} \equiv \inf_{K_{adm}} \|T_{ed}\|_\infty$$

$\bar{\gamma} \equiv \|T_{ed}\|_\infty$ when $K = K_{2_{opt}}$

$\gamma^* \equiv \|T_{ed}\|_\infty$ when $K(s) = K_{mix}$

$\alpha^* \equiv \|T_{zw}\|_2$ when $K(s) = K_{mix}$

$\gamma \equiv$ the constraint which γ^* must stay less than or equal to $\left(\gamma^* \leq \gamma\right)$

The mixed H_2 / H_∞ problem can now be restated as follows: determine a $K(s)$ such that

(i) The underlying H_2 and H_∞ problems are stable, i.e., $\mathcal{A}_2$ and $\mathcal{A}_\infty$ are stable

(ii) $\gamma^* \leq \gamma$ for some given $\gamma > \underline{\gamma}$

(iii) $\|T_{zw}\|_2$ is minimized.

Walker [4] introduced the following theorem to develop this problem:

Theorem B.4.1.1 *Let $\left(A_c . B_c . C_c\right)$ be given and assume there exists a $Q_\infty = Q_\infty^T \geq 0$ satisfying*

$$\mathcal{A}_\infty Q_\infty + Q_\infty \mathcal{A}_\infty^T + (Q_\infty \mathcal{C}_e^T + \mathcal{B}_d \mathcal{D}_{ed}^T) R^{-1} (Q_\infty \mathcal{C}_e^T + \mathcal{B}_d \mathcal{D}_{ed}^T)^T + \mathcal{B}_d \mathcal{B}_d^T = 0 \qquad (75)$$

where $R = \left(\gamma^2 I - \mathcal{D}_{ed} \mathcal{D}_{ed}^T \right) > 0$. Then the following are equivalent:

(i) $(\mathcal{A}_\infty, \mathcal{B}_d)$ is stabilizable

(ii) $\mathcal{A}_2$ is stable

(iii) $\mathcal{A}_\infty$ is stable.

Moreover, if the above hold then the following are true:

(iv) $\|T_{ed}\|_\infty \leq \gamma$

(v) the two-norm of the transfer function T_{zw} is given by

$$\|T_{zw}\|_2^2 = tr\left[C_z \, Q_2 \, C_z^T \right] = tr\left[Q_2 \, C_z^T C_z \right]$$

where $Q_2 = Q_2^T \geq 0$ is the solution to the Lyapunov equation

$$\mathcal{A}_2 \, Q_2 + Q_2 \, \mathcal{A}_2^T + \mathcal{B}_w \mathcal{B}_w^T = 0$$

(vi) all real symmetric solutions Q_∞ of Equation (75) are positive semidefinite

(vii) there exists a unique minimal solution Q_∞ to Equation (75) in the class of real symmetric

solutions

(viii) Q_∞ is the minimal solution of equation (75) if and only if

$$\Re e\left[\lambda_i \left(\mathcal{A}_\infty + \mathcal{B}_d \mathcal{D}_{ed}^T \, R^{-1} \, \mathcal{C}_e + Q_\infty \, \mathcal{C}_e^T \, R^{-1} \, \mathcal{C}_e \right) \right] \leq 0 \text{ for all } i \qquad (76)$$

(ix) $\|T_{ed}\|_\infty < (\leq) \; \gamma$ iff $\Re e \left[\lambda_i \left(\mathcal{A}_\infty + \mathcal{B}_d \mathcal{D}_{ed}^T \, R^{-1} \, \mathcal{C}_e + Q_\infty \, \mathcal{C}_e^T \, R^{-1} \, \mathcal{C}_e \right) \right]$ $(<) \; \leq 0$ where Q_∞ is

the minimal solution to Equation (75).

The main result from this theorem is that, given a controller that is closed-loop stable for the H_2 problem, we can determine the minimum level of the H_∞ constraint, $\underline{\gamma}$, by determining the minimum value of γ for which a positive semidefinite solution to (75) exists.

Using Theorem B.4.1.1 the mixed problem can now be restated as: Determine the $K(s)$ which minimizes the objective function

$$J\left(A_c, B_c, C_c\right) = tr\left[Q_2 C_z^T C_z\right] \tag{77}$$

where Q_2 is the real, symmetric, positive semidefinite solution to

$$\mathcal{A}_2 Q_2 + Q_2 \mathcal{A}_2^T + \mathcal{B}_w \mathcal{B}_w^T = 0 \tag{78}$$

and satisfying the constraint

$$\mathcal{A}_\infty Q_\infty + Q_\infty \mathcal{A}_\infty^T + \left(Q_\infty \mathcal{C}_e^T + \mathcal{B}_d \mathcal{D}_{ed}^T\right) R^{-1} \left(Q_\infty \mathcal{C}_e^T + \mathcal{B}_d \mathcal{D}_{ed}^T\right)^T + \mathcal{B}_d \mathcal{B}_d^T = 0 \tag{79}$$

where Q_∞ is the real, symmetric, positive semidefinite solution.

This is a minimization problem with two equality constraints and will be solved using a Lagrange multiplier approach. An excellent discussion of this method can be found in Arora [13]. The Lagrangian for the mixed problem is

$$\begin{aligned}
L = {}& tr\left[Q_2 C_z^T C_z\right] + tr\left\{\left[A_2 Q_2 + Q_2 A_2^T + B_w B_w^T\right] X\right\} \\
& + tr\left\{\left[A_\infty Q_\infty + Q_\infty A_\infty^T + (Q_\infty C_e^T + B_d D_{ed}^T) R^{-1} (Q_\infty C_e^T + B_d D_{ed}^T)^T\right.\right. \\
& \left.\left. + B_d B_d^T\right] Y\right\}
\end{aligned} \tag{80}$$

where $\mathcal{X}$ and $\mathcal{Y}$ are symmetric Lagrange multiplier matrices.

The first order necessary conditions for the minimum of this Lagrangian are

$$\frac{\partial \mathcal{L}}{\partial A_c} = X_{12}^T Q_{12} + X_2 Q_2 + Y_{12}^T Q_{ab} + Y_2 Q_b = 0 \tag{81}$$

$$\frac{\partial \mathcal{L}}{\partial B_c} = X_{12}^T Q_1 C_{y2}^T + X_2 Q_{12}^T C_{y2}^T + X_{12}^T V_{12} + X_2 B_c V_2 + Y_{12}^T Q_a C_{y\infty}^T + Y_2 Q_{ab}^T C_{y\infty}^T$$
$$+ Y_{12}^T V_{ab} + Y_2 B_c V_b + \left(Y_{12}^T Q_a + Y_2 Q_{ab}^T\right) C_e^T M + \left(Y_{12}^T Q_{ab} + Y_2 Q_b\right) C_c^T D_{eu}^T M = 0 \tag{82}$$

$$\frac{\partial \mathcal{L}}{\partial C_c} = B_{u2}^T X_1 Q_{12} + B_{u2}^T X_{12} Q_2 + R_{12}^T Q_{12} + R_2 C_c Q_2 + B_{u\infty}^T Y_1 Q_{ab} + B_{u\infty}^T Y_{12} Q_b$$
$$+ R_{ab}^T Q_a Y_1 Q_{ab} + R_{ab}^T Q_{ab} Y_{12}^T Q_{ab} + R_{ab}^T Q_{ab} Y_2 Q_b + R_b C_c Q_{ab}^T Y_1 Q_{ab} + R_b C_c Q_b Y_{12}^T Q_{ab}$$
$$+ R_b C_c Q_{ab}^T Y_{12} Q_b + R_b C_c Q_b Y_2 Q_b + P_1\left(Y_1 Q_{ab} + Y_{12} Q_b\right) + P_2\left(Y_{12}^T Q_{ab} + Y_2 Q_b\right) = 0 \tag{83}$$

$$\frac{\partial \mathcal{L}}{\partial \mathcal{X}} = \mathcal{A}_2 Q_2 + Q_2 \mathcal{A}_2^T + \mathcal{B}_w \mathcal{B}_w^T = 0 \tag{84}$$

$$\frac{\partial \mathcal{L}}{\partial Q_2} = \mathcal{A}_2^T \mathcal{X} + \mathcal{X} \mathcal{A}_2 + \mathcal{C}_z^T \mathcal{C}_z = 0 \tag{85}$$

$$\frac{\partial \mathcal{L}}{\partial \mathcal{Y}} = \mathcal{A}_\infty Q_\infty + Q_\infty \mathcal{A}_\infty^T + (Q_\infty \mathcal{C}_e^T + \mathcal{B}_d \mathcal{D}_{ed}^T) R^{-1} (Q_\infty \mathcal{C}_e^T + \mathcal{B}_d \mathcal{D}_{ed}^T)^T + \mathcal{B}_d \mathcal{B}_d^T = 0 \tag{86}$$

$$\frac{\partial \mathcal{L}}{\partial Q_\infty} = \left(\mathcal{A}_\infty + \mathcal{B}_d \mathcal{D}_{ed}^T R^{-1} \mathcal{C}_e + Q_\infty \mathcal{C}_e^T R^{-1} \mathcal{C}_e\right)^T \mathcal{Y}$$
$$+ \mathcal{Y}\left(\mathcal{A}_\infty + \mathcal{B}_d \mathcal{D}_{ed}^T R^{-1} \mathcal{C}_e + Q_\infty \mathcal{C}_e^T R^{-1} \mathcal{C}_e\right) = 0 \tag{87}$$

where

$$M = R^{-1} D_{ed} D_{yd}^T \tag{88}$$

$$P_1 = D_{eu}^T R^{-1} D_{ed} B_d^T \tag{89}$$

$$P_2 = D_{eu}^T M B_c^T \tag{90}$$

B-22

$$Q_2 = \begin{bmatrix} Q_1 & Q_{12} \\ Q_{12}^T & Q_2 \end{bmatrix} \tag{91}$$

$$\mathcal{X} = \begin{bmatrix} X_1 & X_{12} \\ X_{12}^T & X_2 \end{bmatrix} \tag{92}$$

$$Q_\infty = \begin{bmatrix} Q_a & Q_{ab} \\ Q_{ab}^T & Q_b \end{bmatrix} \tag{93}$$

$$\mathcal{Y} = \begin{bmatrix} Y_1 & Y_{12} \\ Y_{12}^T & Y_2 \end{bmatrix} \tag{94}$$

$$B_w B_w^T = \begin{bmatrix} B_w \\ B_c D_{yw} \end{bmatrix} \begin{bmatrix} B_w^T & D_{yw}^T B_c^T \end{bmatrix}$$
$$= \begin{bmatrix} V_1 & V_{12} B_c^T \\ B_c V_{12}^T & B_c V_2 B_c^T \end{bmatrix} \tag{95}$$

$$B_d \left(D_{ed}^T R^{-1} D_{ed} + I \right) B_d^T = \begin{bmatrix} B_d \\ B_c D_{yd} \end{bmatrix} \left(D_{ed}^T R^{-1} D_{ed} + I \right) \begin{bmatrix} B_d^T & D_{yd}^T B_c^T \end{bmatrix}$$
$$= \begin{bmatrix} V_a & V_{ab} B_c^T \\ B_c V_{ab}^T & B_c V_b B_c^T \end{bmatrix} \tag{96}$$

$$C_z^T C_z = \begin{bmatrix} C_z^T \\ C_c^T D_{zu}^T \end{bmatrix} \begin{bmatrix} C_z & D_{zu} C_c \end{bmatrix}$$
$$= \begin{bmatrix} R_1 & R_{12} C_c \\ C_c^T R_{12}^T & C_c^T R_2 C_c \end{bmatrix} \tag{97}$$

$$C_e^T R^{-1} C_e = \begin{bmatrix} C_e^T \\ C_c^T D_{eu}^T \end{bmatrix} R^{-1} \begin{bmatrix} C_e & D_{eu} C_c \end{bmatrix}$$
$$= \begin{bmatrix} R_a & R_{ab} C_c \\ C_c^T R_{ab}^T & C_c^T R_b C_c \end{bmatrix} \tag{98}$$

These equations have not been solved analytically but do provide some insight into the nature of the solution. Equation (86) implies either $\mathcal{Y}=0$ or $\left(\mathcal{A}_\infty + \mathcal{B}_d \mathcal{D}_{ed}^T R^{-1} \mathcal{C}_e + Q_\infty \mathcal{C}_e^T R^{-1} \mathcal{C}_e\right)$ is neutrally stable. The first condition means that the solution is off the boundary of the H_∞ constraint (where the boundary is defined as the constraint being satisfied at equality). The second condition implies that the solution lies on the boundary of the constraint and Q_∞ is a neutrally stabilizing solution for the H_∞ Riccati equation (78). Since Walker was not able to solve the problem analytically, a numerical approach was taken.

Note that Equation (78) has the form

$$A_y^T \mathcal{Y} + \mathcal{Y} A_y = 0 \qquad (99)$$

where $A_y = \left(\mathcal{A}_\infty + \mathcal{B}_d \mathcal{D}_{ed}^T R^{-1} \mathcal{C}_e + Q_\infty \mathcal{C}_e^T R^{-1} \mathcal{C}_e\right)$.

There are two theorems from Snyders and Zakai [15] that are useful at this point:

Theorem B.4.1.2 *If A_y is stable, then $\mathcal{Y} = 0$ is the only solution to Equation (99).*

Recall Theorem B.4.1.1 (ix) says that if A_y is not neutrally stable, Q_∞ is not the minimal solution to (74). Since $\mathcal{Y}=0$, the Lagrangian (80) reduces to

$$\mathcal{L} = tr\left[Q_2 C_z^T C_z\right] + tr\left\{\left[\mathcal{A}_2 Q_2 + Q_2 \mathcal{A}_2^T + \mathcal{B}_w \mathcal{B}_w^T\right]\mathcal{X}\right\} \qquad (100)$$

This is the Lagrangian associated with the H_2 problem (note we still have to solve the Lyapunov equation in the constraint to evaluate the objective function). The other theorem applicable to (99) is:

Theorem B.4.1.3 *Let A_y be neutrally stable. Then (79) has infinitely many $\mathcal{Y} \geq 0$ solutions of possibly varying ranks.*

However; theorem B.4.1.1 (ix) says that Q_∞ is the minimal solution. In order to relate this to the original $\gamma^* \leq \gamma$ constraint, Walker states the following theorem:

Theorem B.4.1.4 *Assume $\mathcal{A}_\infty$ is stable and $R = \left(\gamma^2 I - D_{ed}D_{ed}^T\right) > 0$. If there exists a $Q_\infty \geq 0$ satisfying*

$$\mathcal{A}_\infty Q_\infty + Q_\infty \mathcal{A}_\infty^T + \left(Q_\infty \mathcal{C}_e^T + \mathcal{B}_d\mathcal{D}_{ed}^T\right)R^{-1}\left(Q_\infty \mathcal{C}_e^T + \mathcal{B}_d\mathcal{D}_{ed}^T\right)^T + \mathcal{B}_d\mathcal{B}_d^T = 0$$

then the following are equivalent:

(i) $\left\|T_{ed}\right\|_\infty = \gamma$

(ii) $\left(\mathcal{A}_\infty + \mathcal{B}_d\mathcal{D}_{ed}^T R^{-1} \mathcal{C}_e + Q_\infty \mathcal{C}_e^T R^{-1} \mathcal{C}_e\right)$ *is neutrally stable*

Furthermore, in this case Q_∞ is unique.

Thus we can discern two things from Equation (79). If $\mathcal{Y} = 0$ we have an unconstrained H_2 problem. If $A_y = \left(\mathcal{A}_\infty + \mathcal{B}_d\mathcal{D}_{ed}^T R^{-1} \mathcal{C}_e + Q_\infty \mathcal{C}_e^T R^{-1} \mathcal{C}_e\right)$ is neutrally stable, we are on the boundary of the original $\gamma^* \leq \gamma$ constraint and Q_∞ is the neutrally stabilizing solution to (79). At this point, Walker fixed the order of the controller to the order of the H_2 subproblem or greater. This led to the following theorem:

Theorem B.4.1.5 *Assume $n_c \geq n_2$. Then the following hold:*

(i) If $\gamma < \underline{\gamma}$, no solution to the mixed H_2 / H_∞ problem exists

(ii) If $\underline{\gamma} < \gamma \leq \overline{\gamma}$, K_{mix} is such that $\gamma^* = \gamma$

(iii) If $\gamma \geq \overline{\gamma}$, K_{2opt} is the solution to the mixed H_2 / H_∞ problem.

Proof: See [4]. ∎

For a controller with order greater than equal to the order of the H_2 problem, the solution to the mixed H_2 / H_∞ problem with $\underline{\gamma} < \gamma \leq \overline{\gamma}$ lies on the boundary of the H_∞ constraint, $\gamma^* = \gamma$. Thus, in this region, α^* is a montonically decreasing function of γ as shown in Figure B6. This curve is called a Pareto optimal curve. In general, points on a Pareto curve represent an optimal tradeoff between an objective and a constraint. Unfortunately, since the solution to (75) must be the neutrally stabilizing solution, (87) becomes very difficult to handle as we move to the left on the curve.
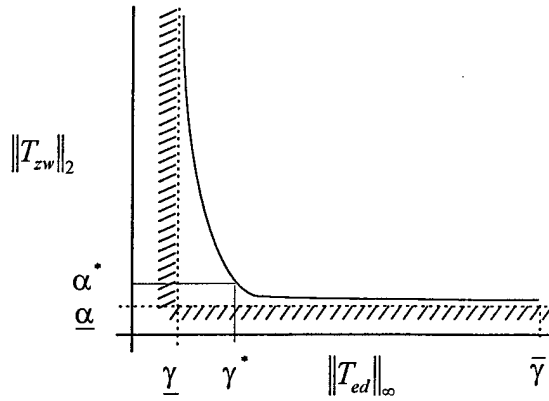
Figure B6. Typical Mixed H_2 / H_∞ γ vs. α Curve

Appendix C

Flight Test Matrix

TABLE C1

HAVE INFINITY II PROFILE TEST MATRIX

MISSION PROFILE	TEST POINT	CONFIG.	TASK	PRIORITY	COMMENTS
1*		A	HQDT - 1000' Trail	1	Each pilot flies
			HQDT - Formation	2	Profile 1 first
		B	HQDT - 1000' Trail	1	
			HQDT - Formation	2	
		C	HQDT - 1000' Trail	1	* Airborne model
			HQDT - Formation	2	validation
		D	HQDT - 1000' Trail	1	will be performed
			HQDT - Formation	2	by the
		E	HQDT - 1000' Trail	1	first pilot to fly
			HQDT - Formation	2	profile 1
		F	HQDT - 1000' Trail	1	
			HQDT - Formation	2	
2	1	A	Straight-in Landing	1	Profile Order
	2	A	Horizontal Offset Landing	1	Pilot 1-2, 3, 4
	3	A	Vertical Offset Landing	2	Pilot 2-3, 4, 2
	4	B	Straight-in Landing	1	Pilot 3-4, 2, 3
	5	B	Horizontal Offset Landing	1	
	6	B	Vertical Offset Landing	2	
	7	C	Straight-in Landing	2	
	8	C	Horizontal Offset Landing	2	
	9	C	Vertical Offset Landing	3	
	10	D	Straight-in Landing	2	
	11	D	Horizontal Offset Landing	2	
	12	D	Vertical Offset Landing	3	
	13	E	Straight-in Landing	3	
	14	E	Horizontal Offset Landing	3	
	15	E	Vertical Offset Landing	4	
	16	F	Straight-in Landing	3	
	17	F	Horizontal Offset Landing	3	
	18	F	Vertical Offset Landing	4	

Configurations (In evaluation priority order)
A - Classic Design   D - H2/H-Infinity Pitch Rate Design
B - H2 AOA Design   E - H2 Pitch Rate Design
C - H2/H-Infinity AOA Design   F - H2 AOA Filter

Note: Pilots will not be informed of configurations so as to minimize rating biases.

PROFILE	TEST POINT	CONFIG.	TASK	PRIORITY	COMMENTS
3	1	C	Straight-in Landing	1	
	2	C	Horizontal Offset Landing	1	
	3	C	Vertical Offset Landing	2	
	4	D	Straight-in Landing	1	
	5	D	Horizontal Offset Landing	1	
	6	D	Vertical Offset Landing	2	
	7	E	Straight-in Landing	2	
	8	E	Horizontal Offset Landing	2	
	9	E	Vertical Offset Landing	3	
	10	F	Straight-in Landing	2	
	11	F	Horizontal Offset Landing	2	
	12	F	Vertical Offset Landing	3	
	13	A	Straight-in Landing	3	
	14	A	Horizontal Offset Landing	3	
	15	A	Vertical Offset Landing	4	
	16	B	Straight-in Landing	3	
	17	B	Horizontal Offset Landing	3	
	18	B	Vertical Offset Landing	4	
4	1	E	Straight-in Landing	1	
	2	E	Horizontal Offset Landing	1	
	3	E	Vertical Offset Landing	2	
	4	F	Straight-in Landing	1	
	5	F	Horizontal Offset Landing	1	
	6	F	Vertical Offset Landing	2	
	7	A	Straight-in Landing	2	
	8	A	Horizontal Offset Landing	2	
	9	A	Vertical Offset Landing	3	
	10	B	Straight-in Landing	2	
	11	B	Horizontal Offset Landing	2	
	12	B	Vertical Offset Landing	3	
	13	C	Straight-in Landing	3	
	14	C	Horizontal Offset Landing	3	
	15	C	Vertical Offset Landing	4	
	16	D	Straight-in Landing	3	
	17	D	Horizontal Offset Landing	3	
	18	D	Vertical Offset Landing	4	

Configurations (In evaluation priority order)
A - Classic Design   D - H2/H-Infinity Pitch Rate Design
B - H2 AOA Design   E - H2 Pitch Rate Design
C - H2/H-Infinity AOA Design   F - H2 AOA Filter

Note: Pilots will not be informed of configurations so as to minimize rating biases.

Appendix D

Ground and Flight Test Verification and Validation Data

D.1 Pole-Zero Format

The pole-zero notation used in Chapter IV and Tables C1-C7 is standard Test Pilot School (TPS) shorthand for expressing the poles and zeros of a transfer function. This notation lists first order poles and zeros as positive if they are stable, and negative if they are unstable. For example; (2.0) expresses the s-domain monomial s+2. Setting this expression equal to zero results in a pole of s = -2. Second order pole and zero pairs are expressed as an ideal damping ratio (ζ) and the pole or zero natural frequency (ω_n) in brackets. For example; [0.5 4] would express the s-domain polynomial $s^2+4s+16$, which is of the form $s^2+2\zeta\omega_n+\omega_n^2$. The gain is the result setting s=0 in the numerator and denominator of the transfer function. The optimal control transfer functions are divided into the three input channels of the control law; command, pitch rate (q), and angle of attack (α).

TABLE D1

POLE-ZERO VERIFICATION-AIRCRAFT

	Design Model	Implementation Model
Poles (rad/sec)	(0.3029) (-1.4971)	(0.3028) (-1.4970)
Zeros (rad/sec)	(-0.8329) (-70.2309)	(-0.8329) (-70.2310)

TABLE D2

POLE-ZERO VERIFICATION - H2INI/H2AIN

	Design Model	Implementation Model
Poles (rad/sec) Command Channel	(6.0) (0.8405) [0.9999, 31.6083]	(6.0) (0.8405) [0.9999, 31.6083]
Zeros (rad/sec) Command Channel	(21.4843) (1.5171) (0.2990)	(21.4843) (1.5171) (0.2990)
Gain Command Channel	-107.42	-107.42
Zeros (rad/sec) Pitch Rate Channel	(6.0) (4.0809) (1.4402)	(6.0) (4.0809) (1.4402)
Gain - q Channel	58.71	58.71
Zeros (rad/sec) AOA Channel	(6.0) (3.9061) (1.5840)	-0.8329 -70.2310
Gain - α Channel	0.50	0.4999

TABLE D3

POLE-ZERO VERIFICATION - MXAOA

	Design Model	Implementation Model
Poles (rad/sec) Command Channel	(85.4428) [0.6456, 25.3192] [0.9375, 5.1344] [0.9454, 0.3811]	(85.4428) [0.6456, 25.3192] [0.9375, 5.1344] [0.9454, 0.3811]
Zeros (rad/sec) Command Channel	(53.0559) (1.3192) (0.8195) (0.4175) [0.7064, 24.8286]	(53.0559) (1.3192) (0.8195) (0.4175) [0.7064, 24.8286]
Gain Command Channel	-36.8823	-36.8823
Zeros (rad/sec) Pitch Rate Channel	(0.8936) (0.4391) [0.7898, 34.0126] [0.8267, 5.3258]	(0.8936) (0.4391) [0.7898, 34.0126] [0.8267, 5.3258]
Gain - q Channel	43.4441	43.4441
Zeros (rad/sec) AOA Channel	(60.5737) (4.9107) [0.6775, 24.5839] [0.9705, 0.4375]	(60.5737) (4.9107) [0.6775, 24.5839] [0.9705, 0.4375]
DC Gain - α Channel	3.5357	3.5357

TABLE D4

POLE-ZERO VERIFICATION-CLASSIC

	Design Model	Implementation Model
Gain - Kq Pitch Rate Feedback Loop	0.441	0.441
Gain - Ka AoA Feedback Loop	1.60	1.60

NOTES - There was no dynamic compensation used in this design. Only the feedback gains shown above were used to produce the Classic design.

TABLE D5

POLE-ZERO VERIFICATION - H2AOA

	Design Model	Implementation Model
Poles (rad/sec) All Channels	(7.2304) (4.4631) [0.53, 2.30]	(7.2304) (4.4631) [0.53, 2.30]
Zeros (rad/sec) Command Channel	(6.6167) (1.5171) (0.2990)	(6.6167) (1.5171) (0.2990)
Gain Command Channel	-14.5252	-14.5252
Zeros (rad/sec) Pitch Rate Channel	(1.5461) [0.53, 2.30]	(1.5461) [0.53, 2.30]
Gain - q Channel	11.0656	11.0656
Zeros (rad/sec) AOA Channel	(1.4962) [0.53, 2.30]	(1.4962) [0.53, 2.30]
Gain - α Channel	0.1054	0.1054

TABLE D6

POLE-ZERO VERIFICATION - MXINI

	Design Model	Implementation Model
Poles (rad/sec) Command Channel	(1.9051) (84.9036) [0.6906, 29.4591] [0.1563, 1.3921]	(1.9051) (84.9036) [0.6906, 29.4591] [0.1563, 1.3921]
Zeros (rad/sec) Command Channel	(1.8081) (0.7184) (216.1494) [0.3888, 28.1514]	(1.8081) (0.7184) (216.1494) [0.3888, 28.1514]
Gain Command Channel	-0.5776	-0.5776
Zeros (rad/sec) Pitch Rate Channel	(2.4557) [0.8242, 55.7059] [0.6217, 1.1901]	(2.4557) [0.8242, 55.7059] [0.6217, 1.1901]
Gain - q Channel	15.6905	15.6905
Zeros (rad/sec) AoA Channel	(6.3463) [0.2511, 1.6603] [0.6896, 44.3650]	[0.2511, 1.6603] [0.6896, 44.3650]
Poles (rad/sec) α poles	(1.9051) (84.9036) [0.6906, 29.4591] [0.1563, 1.3921]	(0.8015) (2.4179) (1.0) [0.6905, 29.4951]
Gain - α Channel	1.5090	1.5090

Test Aircraft: Lear 24, N101VS   Task: PTI Pulse
Configuration: Ground Simulation   (1/2 inch defl, 3 sec dur.)
Flight Control Config: CLASSIC   Date: 01 October 97
Source: Ground Test
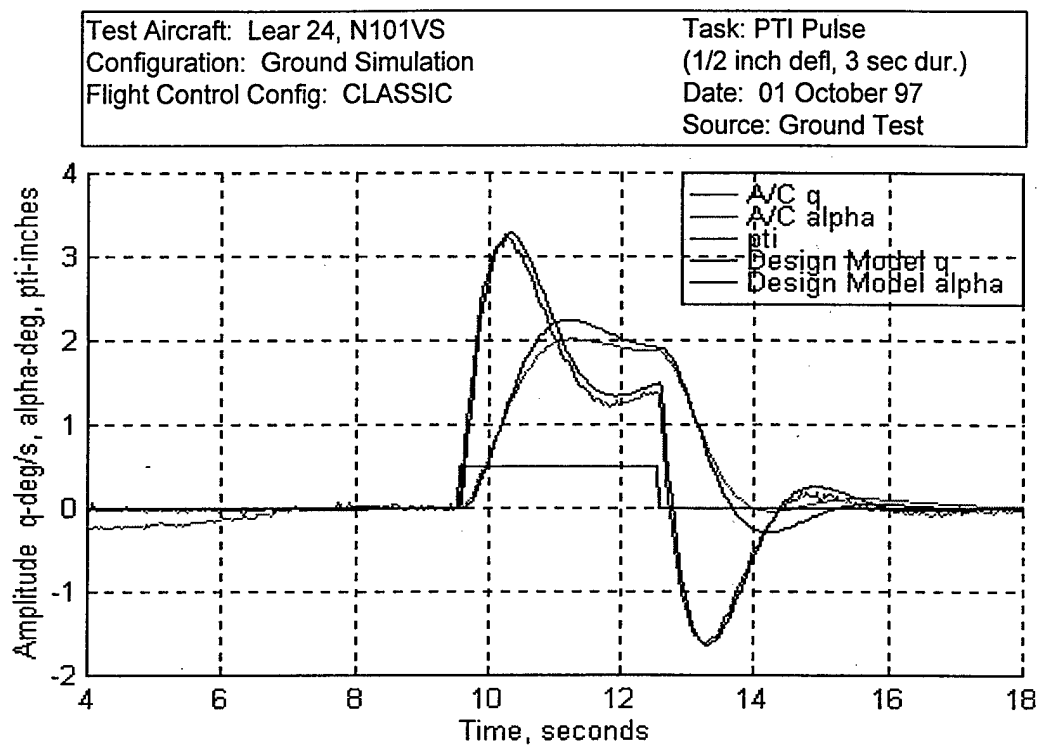
Figure D1. Ground Test Closed-Loop q and α Time Responses – CLASSIC

Test Aircraft: Lear 24, N101VS   Task: PTI Pulse
Configuration: Ground Simulation   (1/2 inch defl, 3 sec dur.)
Flight Control Config: H2AOA   Date: 01 October 97
Source: Ground Test
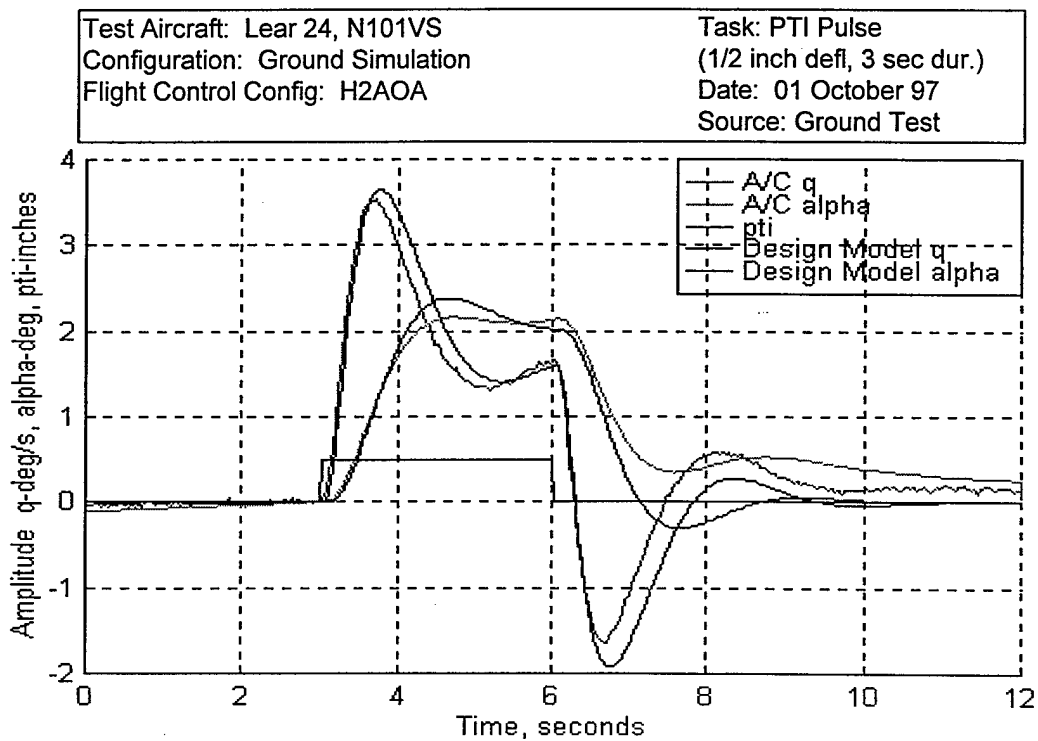
Figure D2. Ground Test Closed-Loop q and α Time Responses – H2AOA

Test Aircraft: Lear 24, N101VS	Task: PTI Pulse
Configuration: Ground Simulation	(1/2 inch defl, 3 sec dur.)
Flight Control Config: H2INI	Date: 01 October 97
	Source: Ground Test
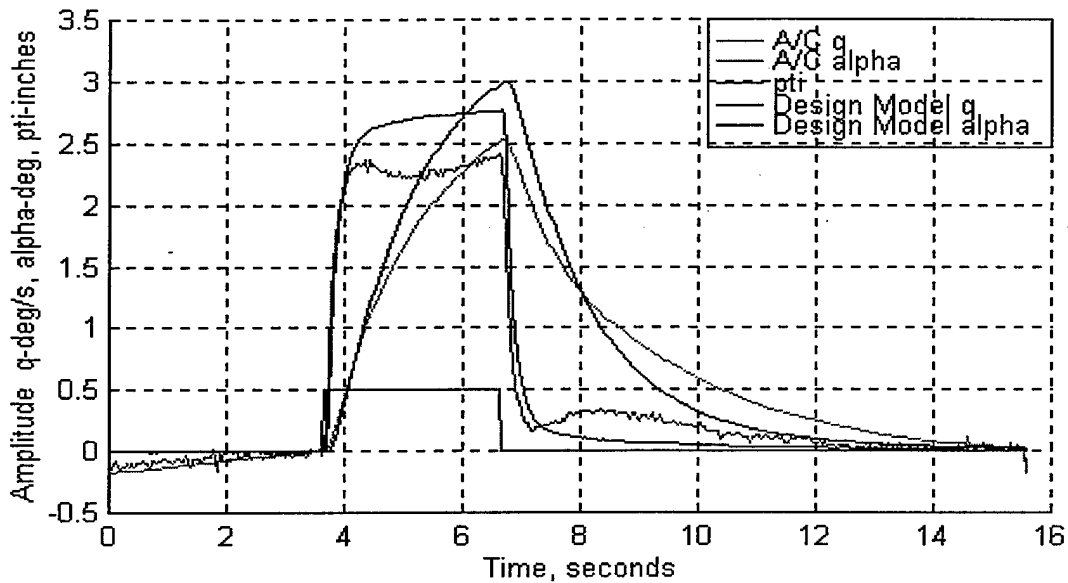
Figure D3. Ground Test Closed-Loop q and α Time Responses – H2INI

Test Aircraft: Lear 24, N101VS	Task: PTI Pulse
Configuration: Ground Simulation	(1/2 inch defl, 3 sec dur.)
Flight Control Config: H2AIN	Date: 01 October 97
	Source: Ground Test
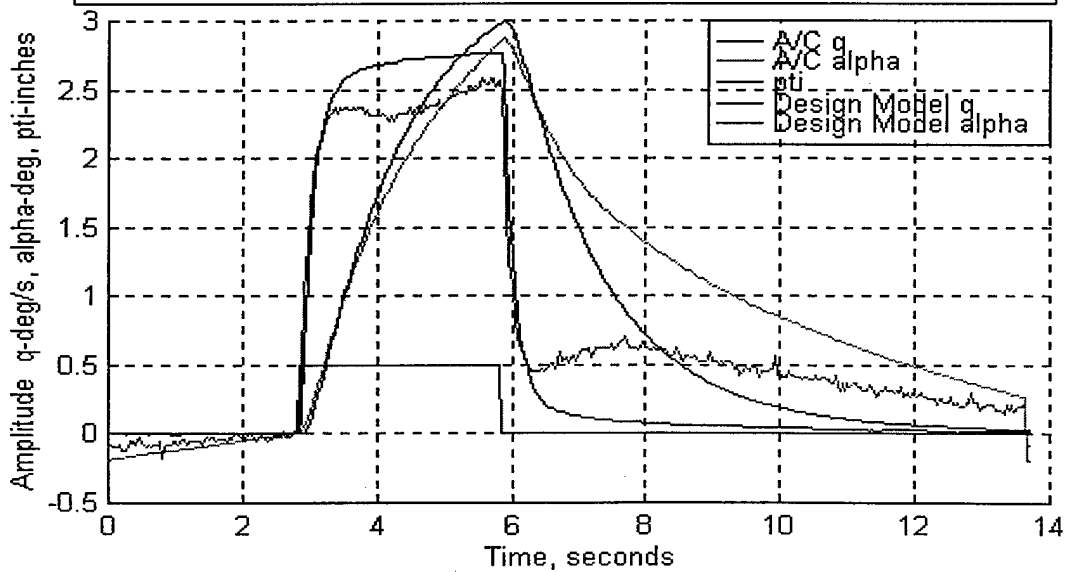
Figure D4. Ground Test Closed-Loop q and α Time Responses – H2AIN

Test Aircraft: Lear 24, N101VS   Task: PTI Pulse
Configuration: Ground Simulation   (1/2 inch defl, 3 sec dur.)
Flight Control Config: MXAOA   Date: 01 October 97
                                         Source: Ground Test

Figure D5. Ground Test Closed-Loop q and α Time Responses – MXAOA

Test Aircraft: Lear 24, N101VS   Task: PTI Pulse
Configuration: 140 KIAS, 8K MSL   (1/2 inch, 3 sec dur.)
        Gear Down, Flaps 20°   Date: 02 October 97
Flight Control Config: CLASSIC   Source: Flight Test
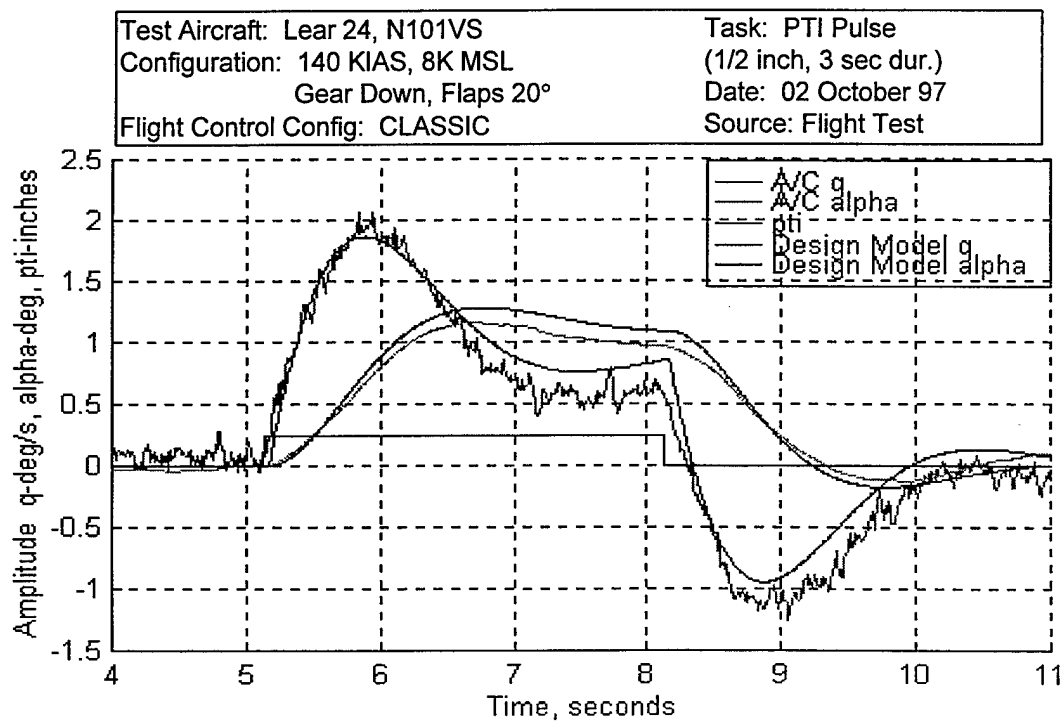
Figure D6. Flight Test Closed-Loop q and α Time Responses – CLASSIC

D-9

Test Aircraft: Lear 24, N101VS   Task: PTI Pulse
Configuration: 140 KIAS, 8K MSL   (1 inch, 3 sec dur.)
                Gear Down, Flaps 20°   Date: 02 October 97
Flight Control Config: H2AOA   Source: Flight Test
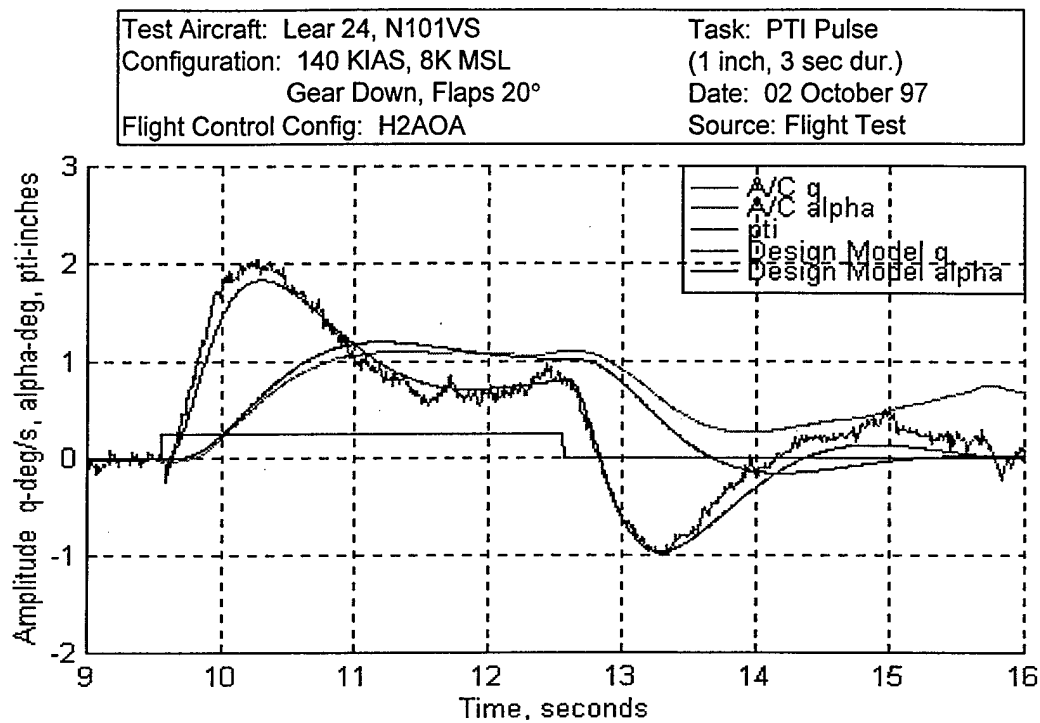
Figure D7. Flight Test Closed-Loop q and α Time Responses – H2AOA

Test Aircraft: Lear 24, N101VS   Task: PTI Pulse
Configuration: 140 KIAS, 8K MSL   (1 inch, 3 sec dur.)
                Gear Down, Flaps 20°   Date: 02 October 97
Flight Control Config: H2INI   Source: Flight Test
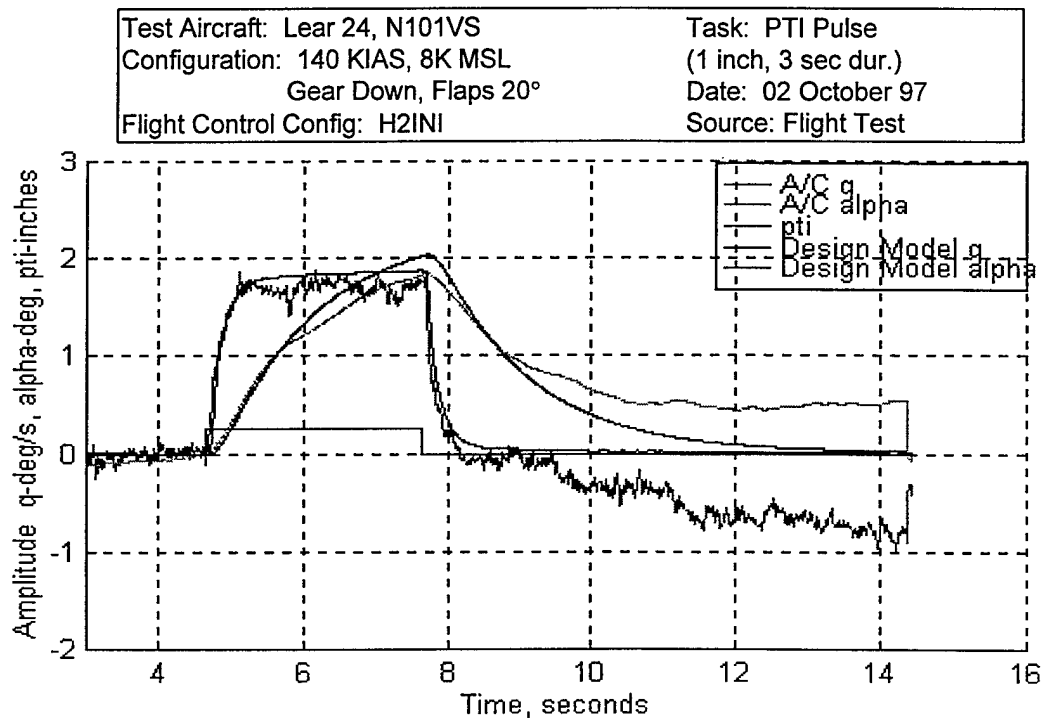
Figure D8. Flight Test Closed-Loop q and α Time Responses – H2INI

D-10
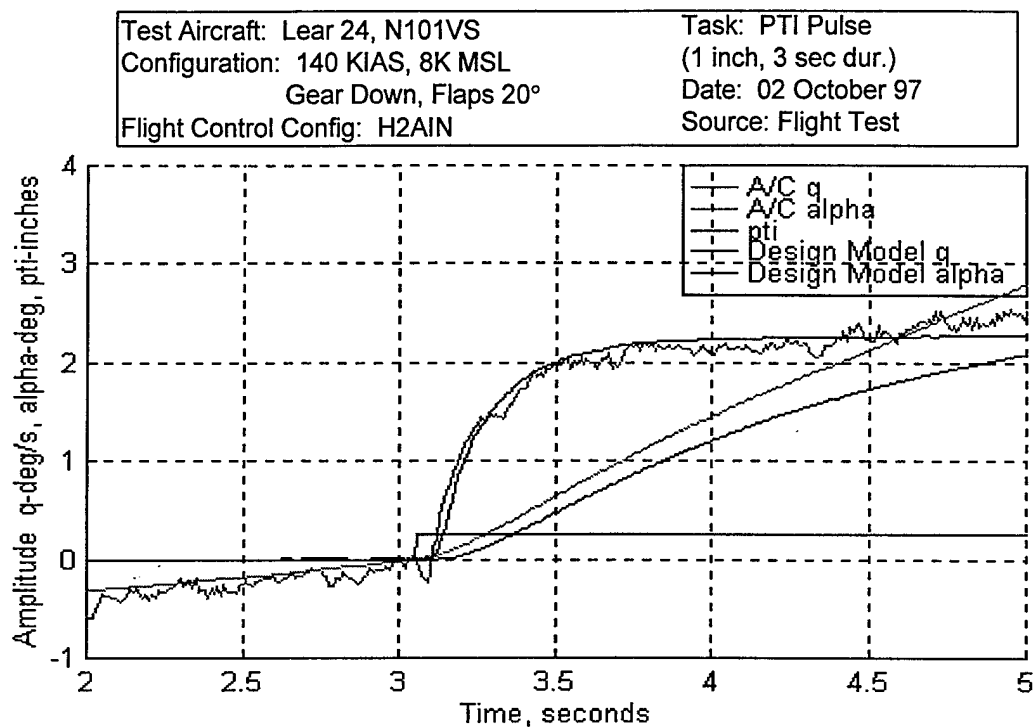
Figure D9. Flight Test Closed-Loop q and α Time Responses – H2AIN
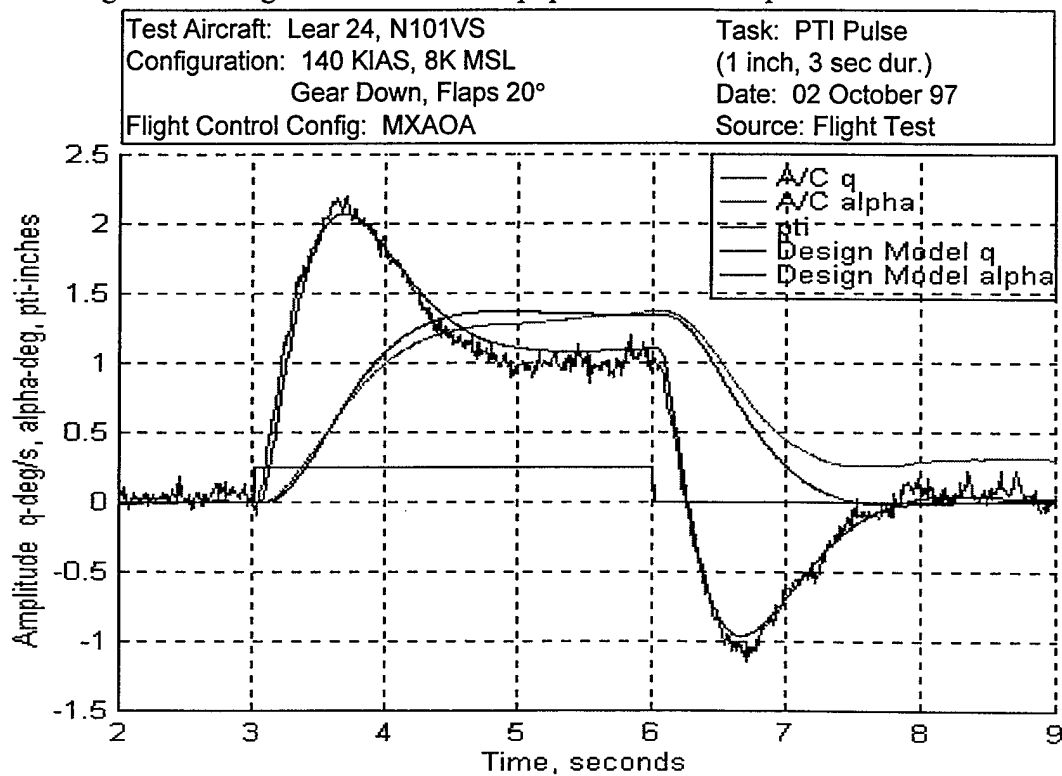
Figure D10. Flight Test Closed-Loop q and α Time Responses – MXAOA

TABLE D7

CLOSED LOOP POLE ANALYSIS - CLASSIC

Closed Loop System Poles without Phugoid Mode	Closed Loop System Poles with Phugoid Mode
[0.7001, 59.1105] [0.5322, 2.2772]	[0.7002, 59.1573] [0.5192, 2.2702] [0.1424, 0.1698]

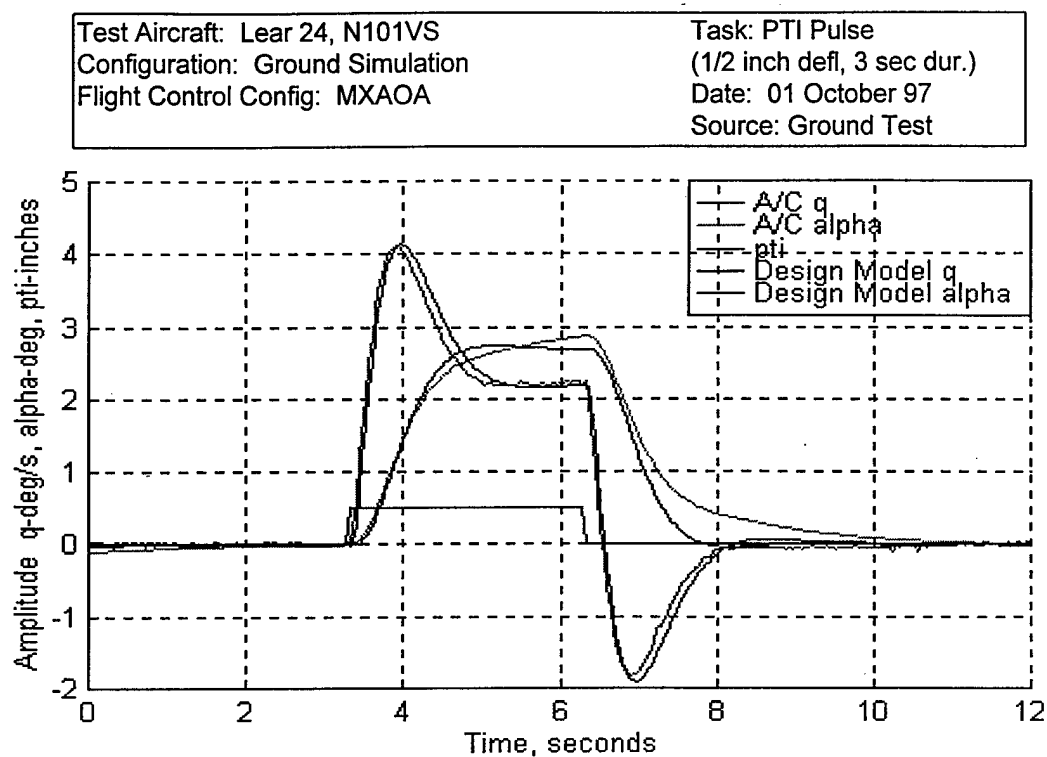## TABLE D8

CLOSED LOOP POLE ANALYSIS - H2AOA

Closed Loop System Poles without Phugoid Mode	Closed Loop System Poles with Phugoid Mode
[0.7038, 60.2400] [0.6921, 7.4210] (1.5176) [0.5300, 2.3000] (0.3013)	[0.7038, 60.2399] [0.6921, 7.4256] (1.5127) [0.5300, 2.3000] [0.7308, 0.3161] (-0.1123)

TABLE D9

CLOSEDLOOP POLE ANALYSIS - H2AIN

Closed Loop System Poles without Phugoid Mode	Closed Loop System Poles with Phugoid Mode
[0.72, 277.41] [0.70, 60.00] [0.92, 33.43] (6.00) (1.52) (0.84) (0.30)	[0.72, 277.41] [0.70, 60.00] [0.92, 33.43] (6.00) (1.51) (0.88) [0.66, 0.35] (-0.14)

TABLE D10

CLOSED LOOP POLE ANALYSIS - H2INI

Closed Loop System Poles without Phugoid Mode	Closed Loop System Poles with Phugoid Mode
[0.72, 277.41]	[0.72, 277.41]
[0.70, 60.00]	[0.70, 60.00]
[0.92, 33.43]	[0.92, 33.43]
(6.00)	(6.00)
(1.52)	(1.51)
(0.84)	(0.88)
(0.30)	[0.66, 0.35]
	(-0.14)

TABLE D11

CLOSED LOOP POLE ANALYSIS - MXAOA

Closed Loop System Poles without Phugoid Mode	Closed Loop System Poles with Phugoid Mode
(84.3732)	(84.3735)
[0.7115, 59.5679]	[0.7115, 59.5672]
[0.6186, 24.3357]	[0.6186, 24.3363]
(6.8060)	(6.8240)
[0.8230, 2.6992]	[0.8247, 2.6746]
(2.0367)	(2.0477)
(0.7097)	(0.6733)
(0.4358)	(0.4345)
	[0.6605, 0.0697]

Appendix E

Handling Qualities Rating Data

Test Aircraft: Lear 24, N101VS
Configuration: Gear Down, Flaps 20%, FCS CLASSIC
Altitude/Airspeed: 4,300 ft MSL/130 KIAS

Task: Straight In Landing
Dates: 6 to10 October 1997
Data Source: Flight Test

Legend:
■ Pilot 1
□ Pilot 2
▤ Pilot 3

Y-axis: Number of Occurrences (0 to 7)
X-axis: Cooper-Harper Rating (1 to 10)
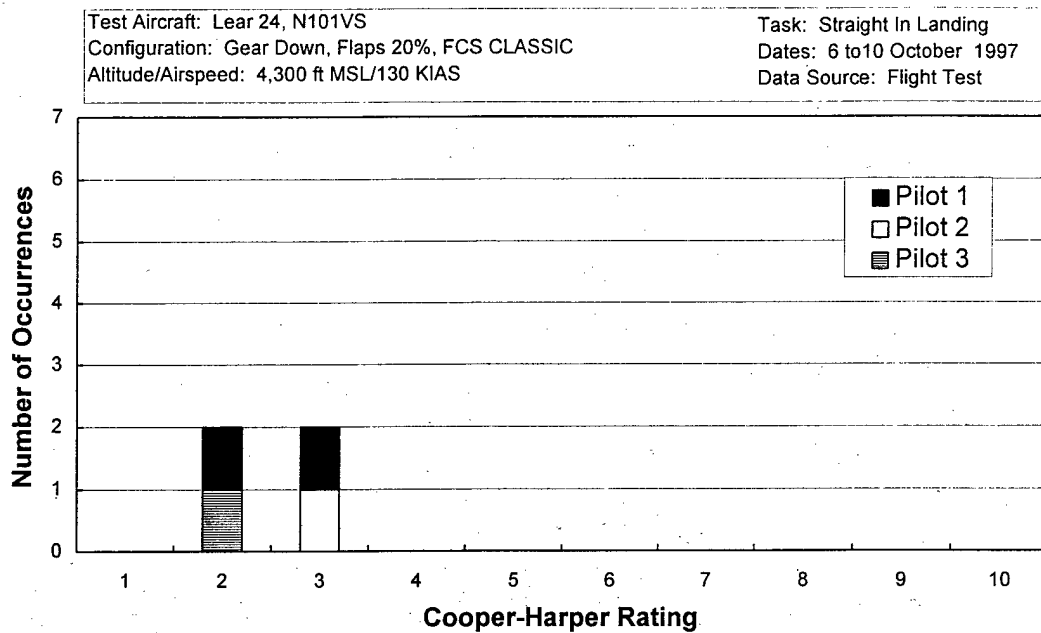
Figure E1. Straight-In Landing Cooper-Harper Ratings -- CLASSIC

Test Aircraft: Lear 24, N101VS
Configuration: Gear Down, Flaps 20%, FCS CLASSIC
Altitude/Airspeed: 4,300 ft MSL/130 KIAS

Task: Straight In Landing
Dates: 6 to10 October 1997
Data Source: Flight Test

Legend:
■ Pilot 1
□ Pilot 2
▤ Pilot 3

Y-axis: Number of Occurrences (0 to 7)
X-axis: PIO Rating (1 to 6)
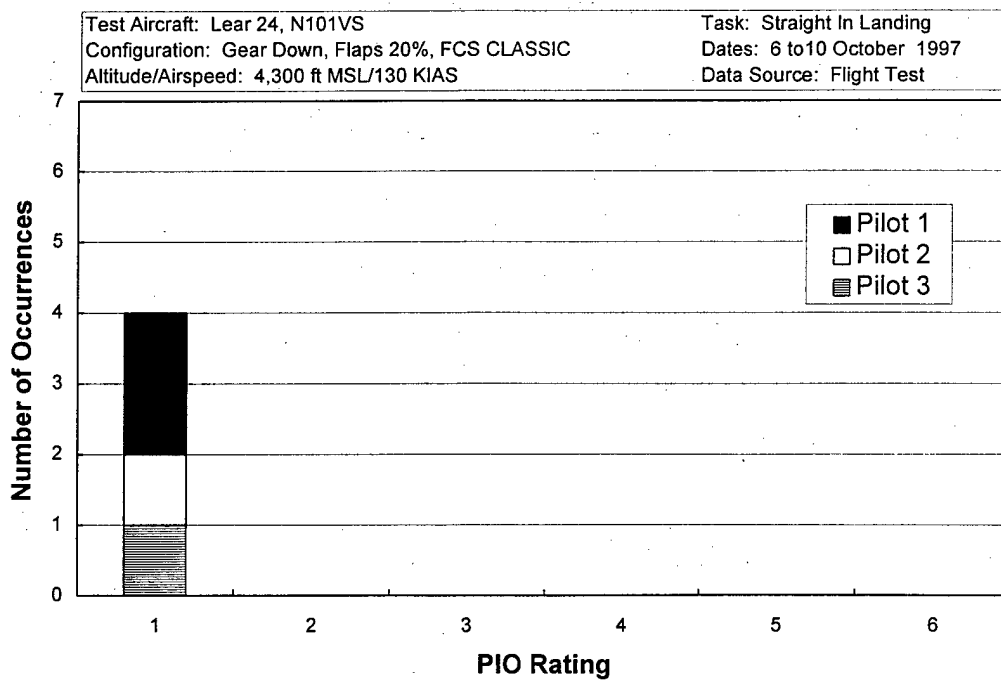
Figure E2. Straight-In Landing PIO Ratings -- CLASSIC
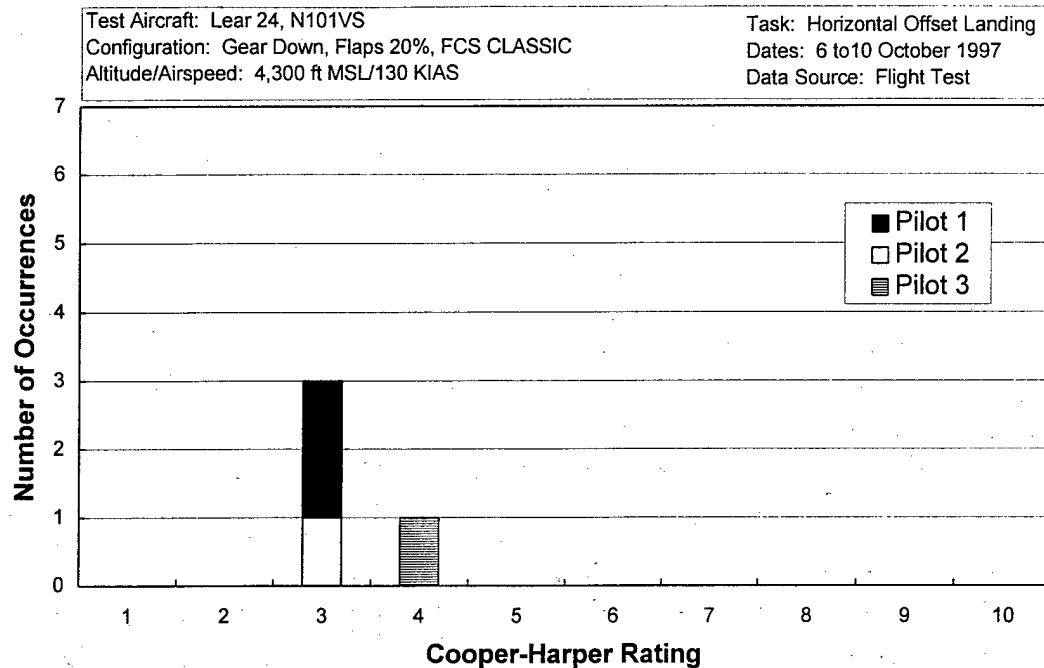
Figure E3. Horizontal Offset Landing Cooper-Harper Ratings -- CLASSIC
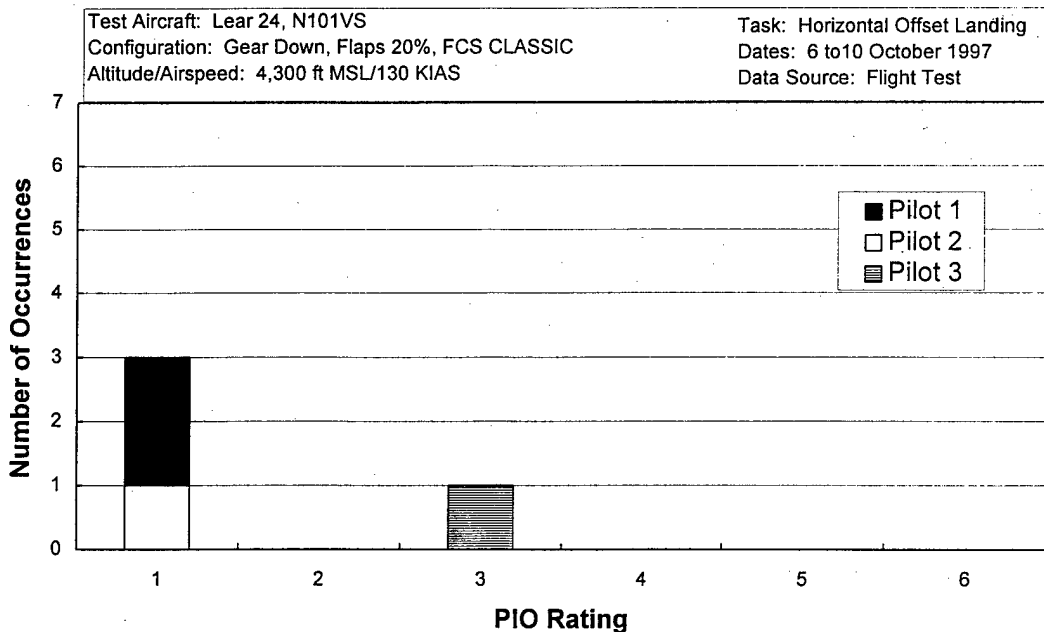
Figure E4. Horizontal Offset Landing PIO Ratings -- CLASSIC

Test Aircraft: Lear 24, N101VS
Configuration: Gear Down, Flaps 20%, FCS H2AOA
Altitude/Airspeed: 4,300 ft MSL/130 KIAS

Task: Horizontal Offset Landing
Dates: 6 to10 October 1997
Data Source: Flight Test
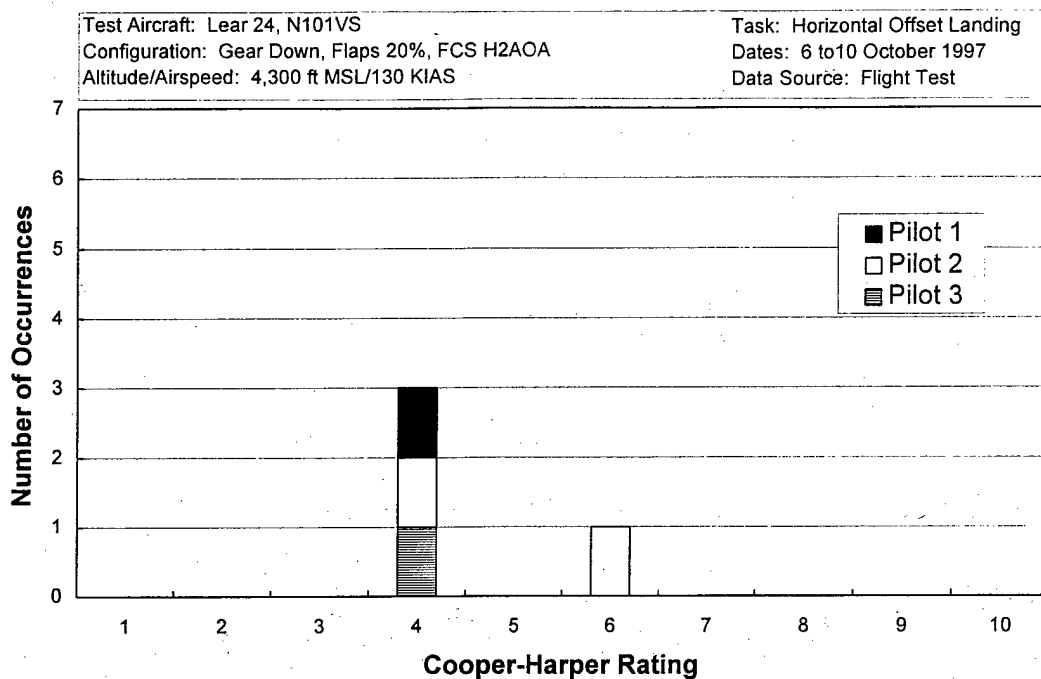
Figure E7. Horizontal Offset Landing Cooper-Harper Ratings -- H2AOA

Test Aircraft: Lear 24, N101VS
Configuration: Gear Down, Flaps 20%, FCS H2AOA
Altitude/Airspeed: 4,300 ft MSL/130 KIAS

Task: Horizontal Offset Landing
Dates: 6 to10 October 1997
Data Source: Flight Test

Figure E8. Horizontal Offset Landing PIO Ratings -- H2AOA

Test Aircraft: Lear 24, N101VS   Task: Straight In Landing
Configuration: Gear Down, Flaps 20%, FCS H2INI   Dates: 6 to10 October 1997
Altitude/Airspeed: 4,300 ft MSL/130 KIAS   Data Source: Flight Test

Figure E9. Straight-In Landing Cooper-Harper Ratings -- H2INI

Test Aircraft: Lear 24, N101VS   Task: Straight In Landing
Configuration: Gear Down, Flaps 20%, FCS H2INI   Dates: 6 to10 October 1997
Altitude/Airspeed: 8,000 ft MSL/140 KIAS   Data Source: Flight Test
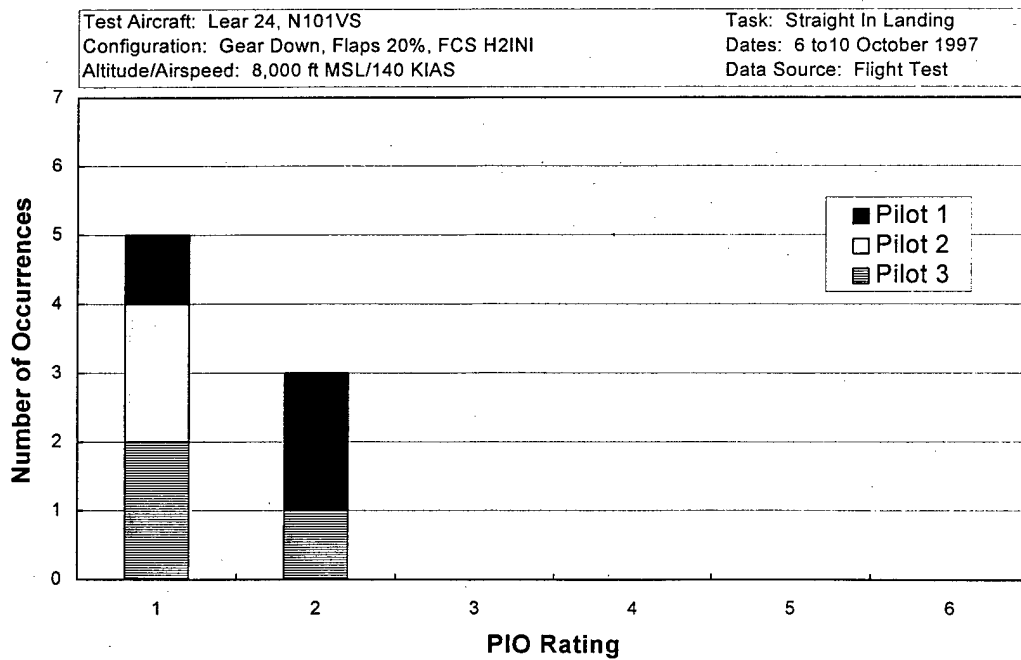
Figure E10. Straight-In Landing PIO Ratings -- H2INI

Test Aircraft: Lear 24, N101VS
Configuration: Gear Down, Flaps 20%, FCS H2INI
Altitude/Airspeed: 4,300 ft MSL/130 KIAS

Task: Horizontal Offset Landing
Dates: 6 to 10 October 1997
Data Source: Flight Test

Figure E11. Horizontal Offset Landing Cooper-Harper Ratings -- H2INI

Test Aircraft: Lear 24, N101VS
Configuration: Gear Down, Flaps 20%, FCS H2INI
Altitude/Airspeed: 8,000 ft MSL/140 KIAS

Task: Horizontal Offset Landing
Dates: 6 to10 October 1997
Data Source: Flight Test

Figure E12. Horizontal Offset Landing PIO Ratings -- H2INI
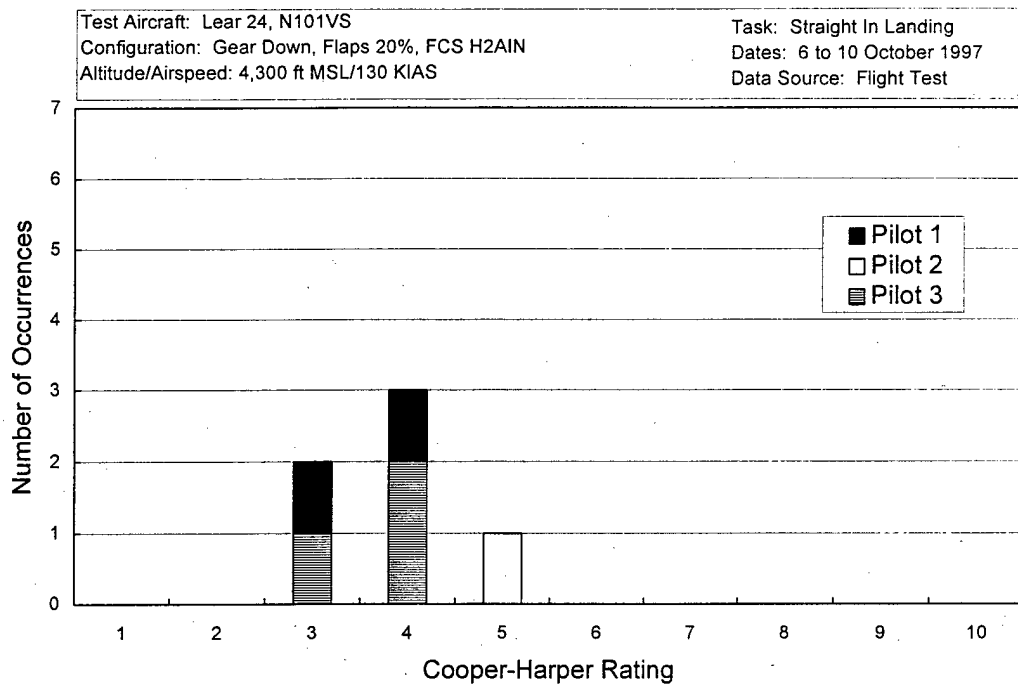
Figure E13. Straight-In Landing Cooper-Harper Ratings -- H2AIN
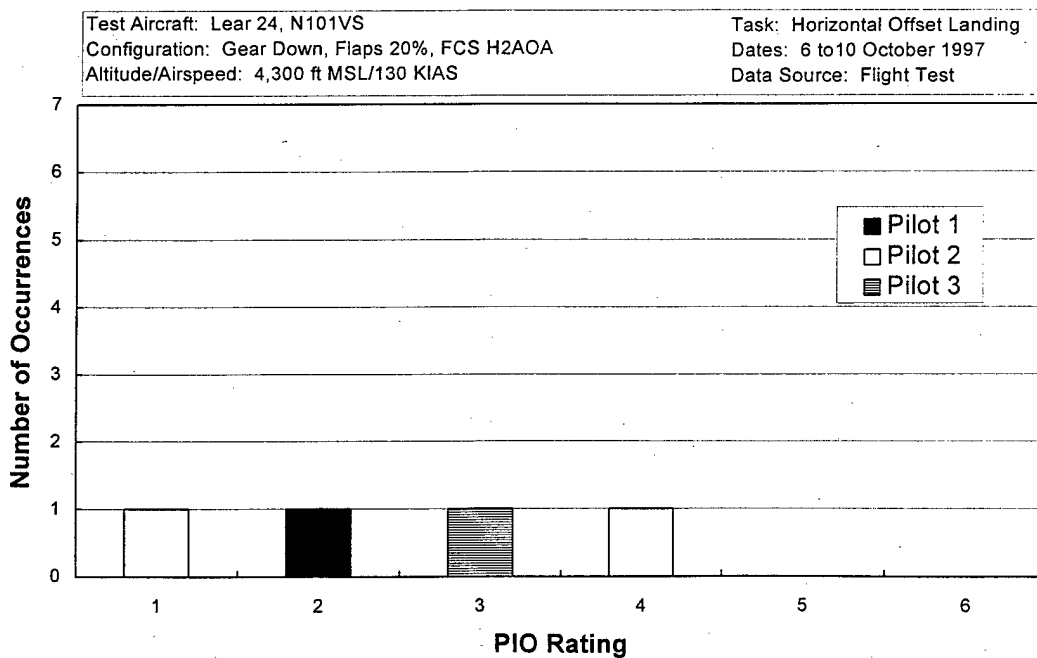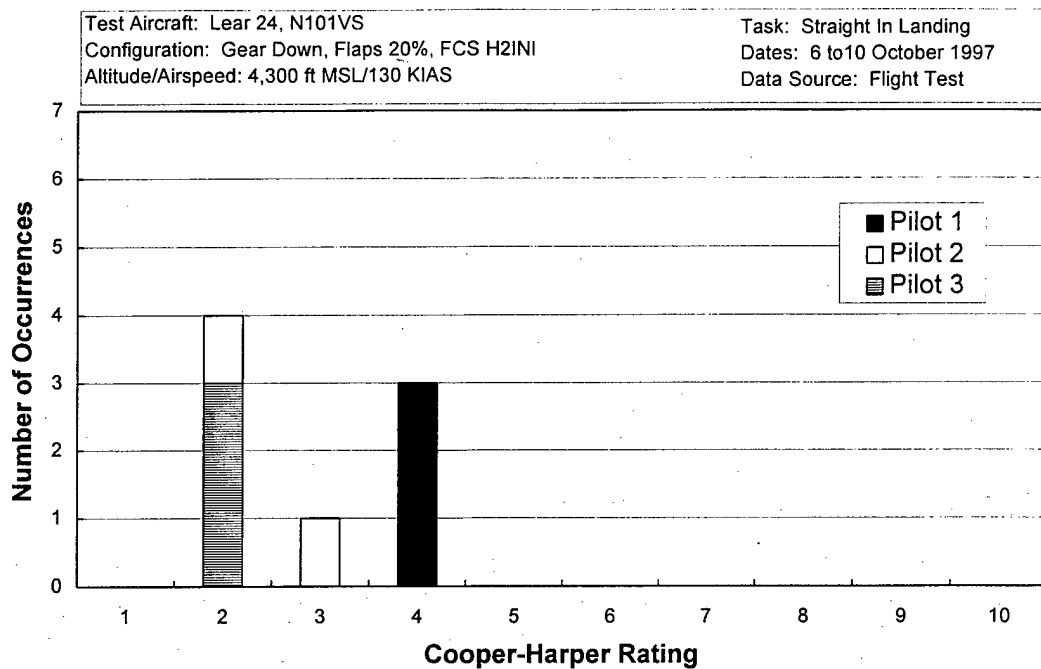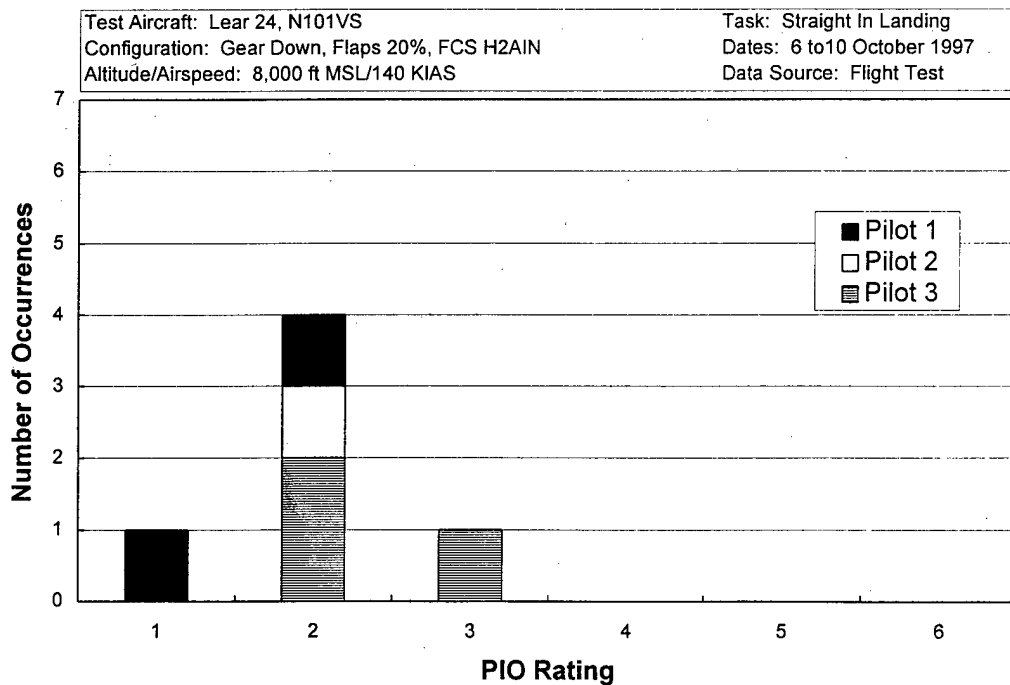

Figure E14. Straight-In Landing PIO Ratings -- H2AIN

Test Aircraft: Lear 24, N101VS
Configuration: Gear Down, Flaps 20%, FCS H2AIN
Altitude/Airspeed: 4,300 ft MSL/130 KIAS

Task: Horizontal Offset Landing
Dates: 6 to10 October 1997
Data Source: Flight Test
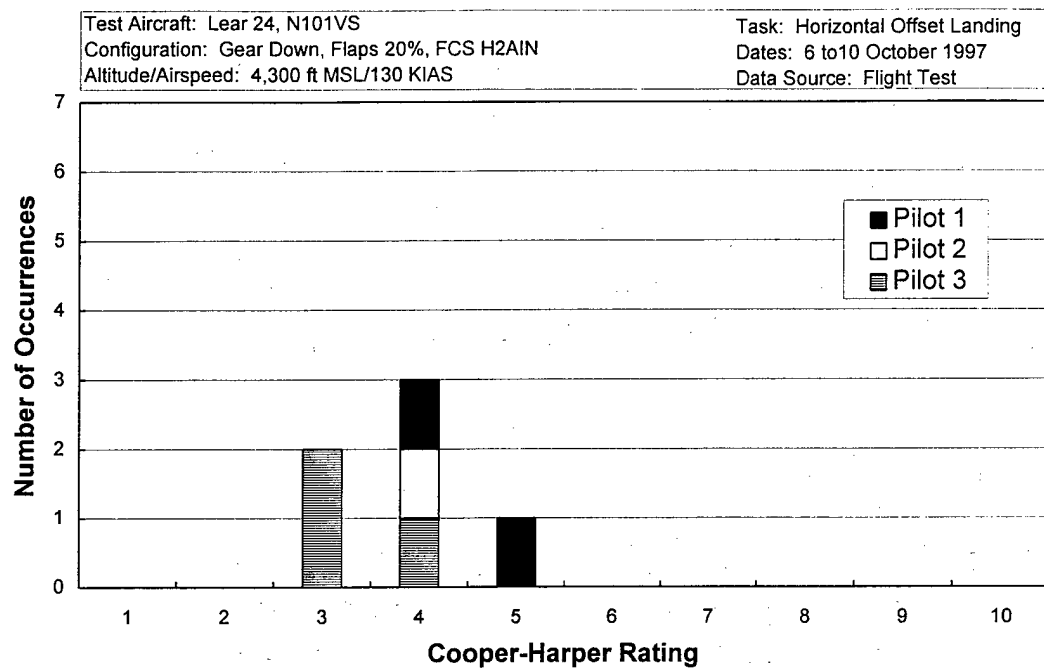
Figure E 15. Horizontal Offset Landing Cooper-Harper Ratings -- H2AIN

Test Aircraft: Lear 24, N101VS
Configuration: Gear Down, Flaps 20%, FCS H2AIN
Altitude/Airspeed: 8,000 ft MSL/140 KIAS

Task: Horizontal Offset Landing
Dates: 6 to10 October 1997
Data Source: Flight Test
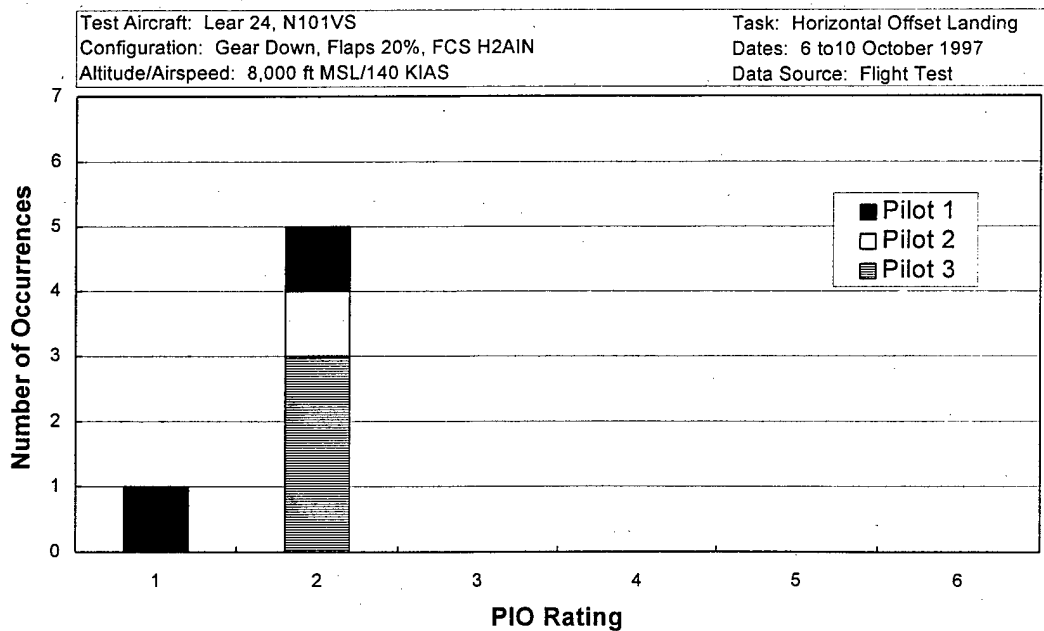
Figure E16. Horizontal Offset Landing PIO Ratings -- H2AIN

E-9
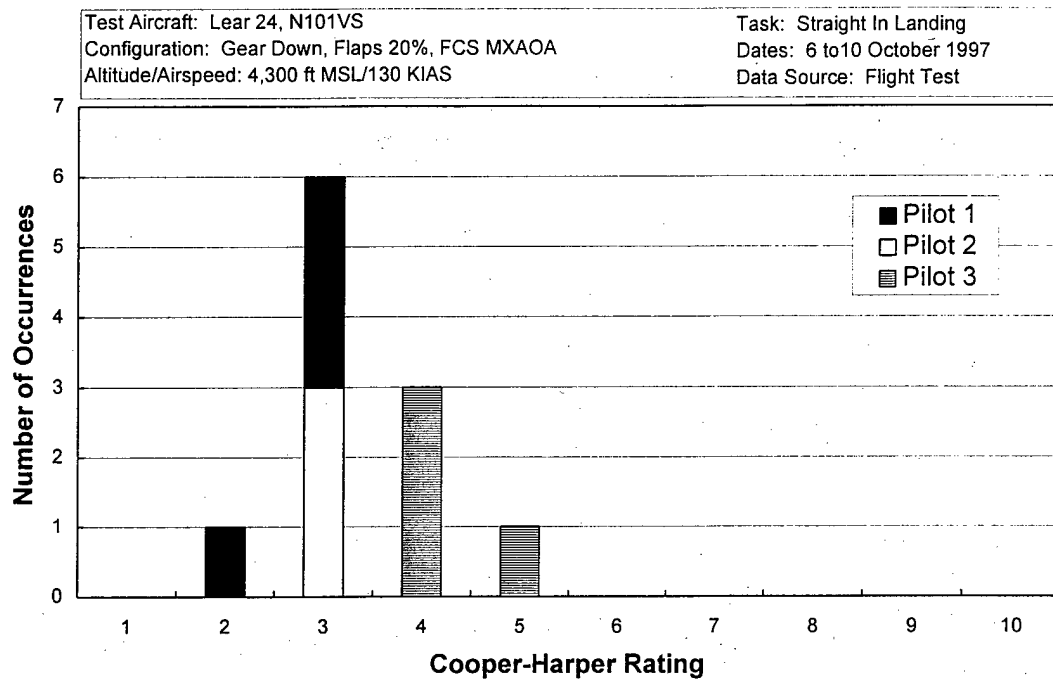
Figure E17. Straight-In Landing Cooper-Harper Ratings -- MXAOA

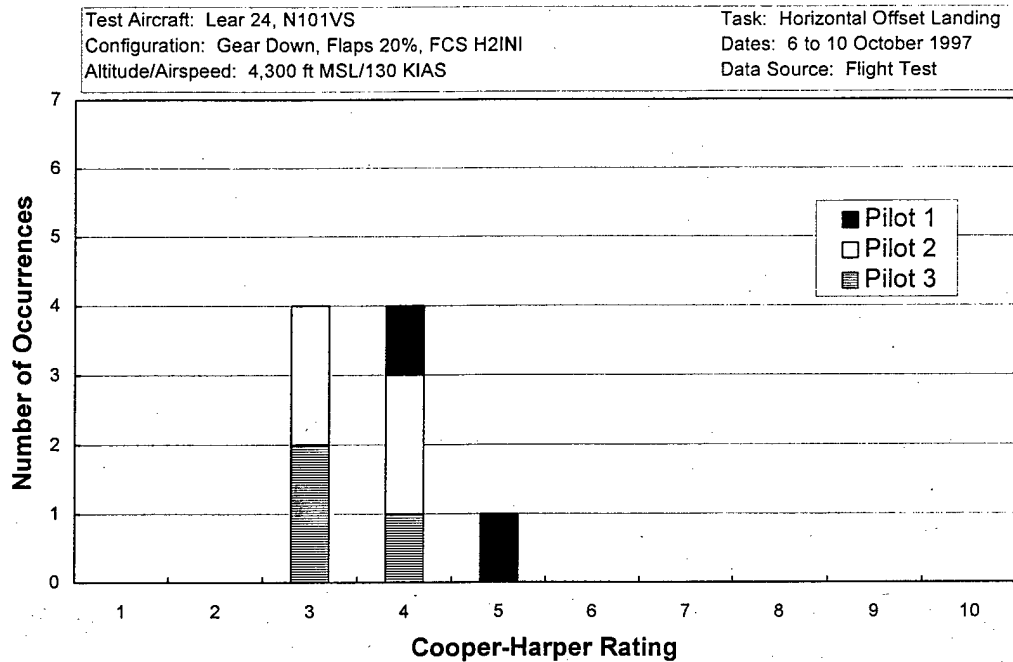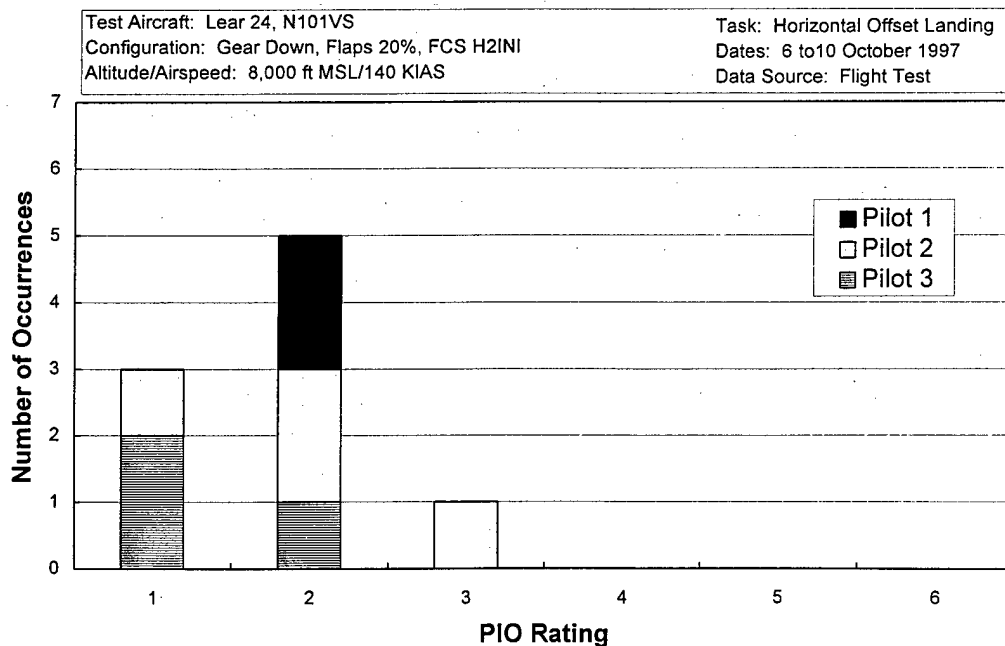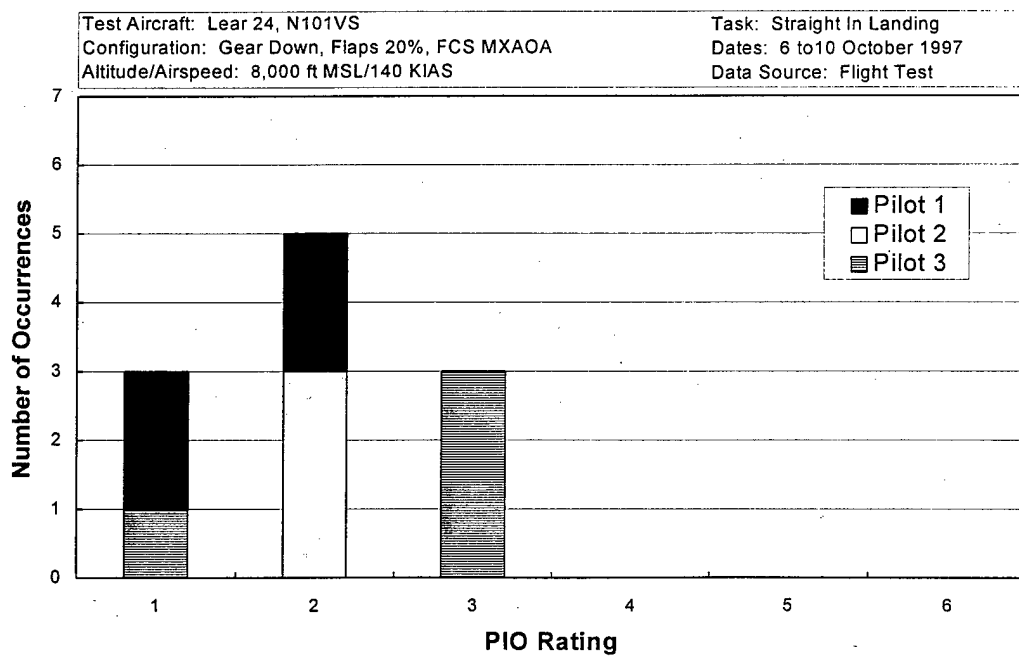Figure E18. Straight-In Landing PIO Ratings -- MXAOA

Test Aircraft: Lear 24, N101VS
Configuration: Gear Down, Flaps 20%, FCS MXAOA
Altitude/Airspeed: 4,300 ft MSL/130 KIAS

Task: Horizontal Offset
Dates: 6 to10 October 1997
Data Source: Flight Test
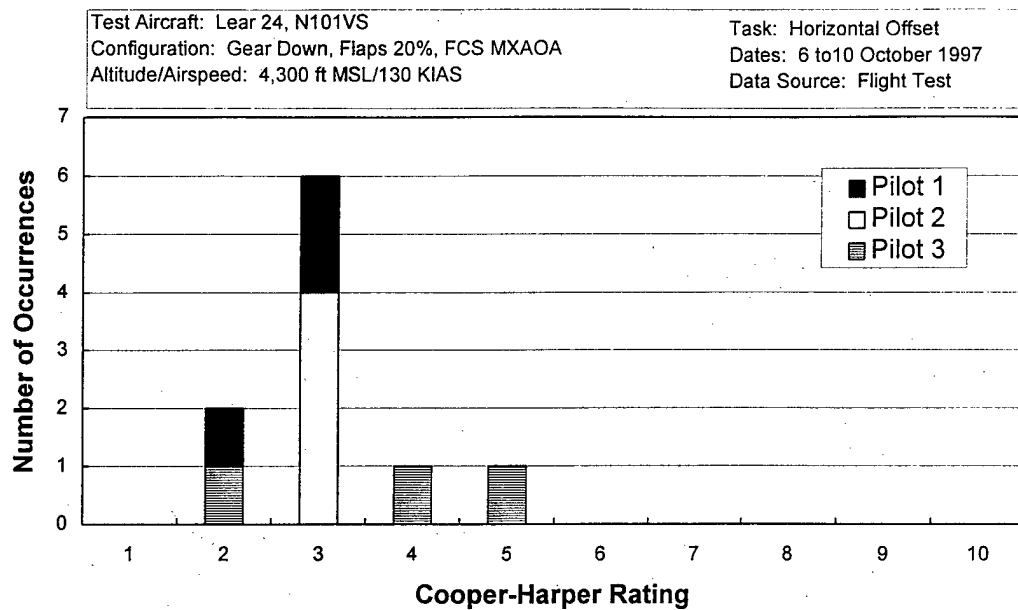
Figure E19. Horizontal Offset Landing Cooper-Harper Ratings -- MXAOA

Test Aircraft: Lear 24, N101VS
Configuration: Gear Down, Flaps 20%, FCS MXAOA
Altitude/Airspeed: 8,000 ft MSL/140 KIAS

Task: Horizontal Offset
Dates: 6 to 10 Oct ober 97
Data Source: Flight Test

Figure E20. Horizontal Offset Landing PIO Ratings – MXAOA

Flight #1   **Mission date:** 6 Oct 97   **Eval Pilot:** Pilot #1 (Boe)
Winds: 240/10

Appr	Task	Configuration	Landing Zone	C-H	PIO	Comments
1	St-In	H2INI	Desired	4	1	minor pitch deficiencies/heavy nose after touchdown
2	St-In	CLASSIC	Desired	3	1	could put the aircraft where the pilot wanted
3	St-In	MXAOA/H_∞ AOA Cmd	Desired	2	1	easy to set pitch picture/very good flying qualities
4	Horiz	H2INI	Desired	5	2	stick force change for a given displacement
5	Horiz	CLASSIC	Desired	-	-	no grade - pilot unsure of workload
6	Horiz	CLASSIC	Desired	3	1	good flying qualities
7	Horiz	MXAOA/H_∞ AOA Cmd	Desired	2	1	best of all 3 flight control systems tested today/ negligible deficiencies

Flight #2   **Mission date:** 6 Oct 97   **Eval Pilot:** Pilot #3 (Cantiello)
Winds: 240/15G25

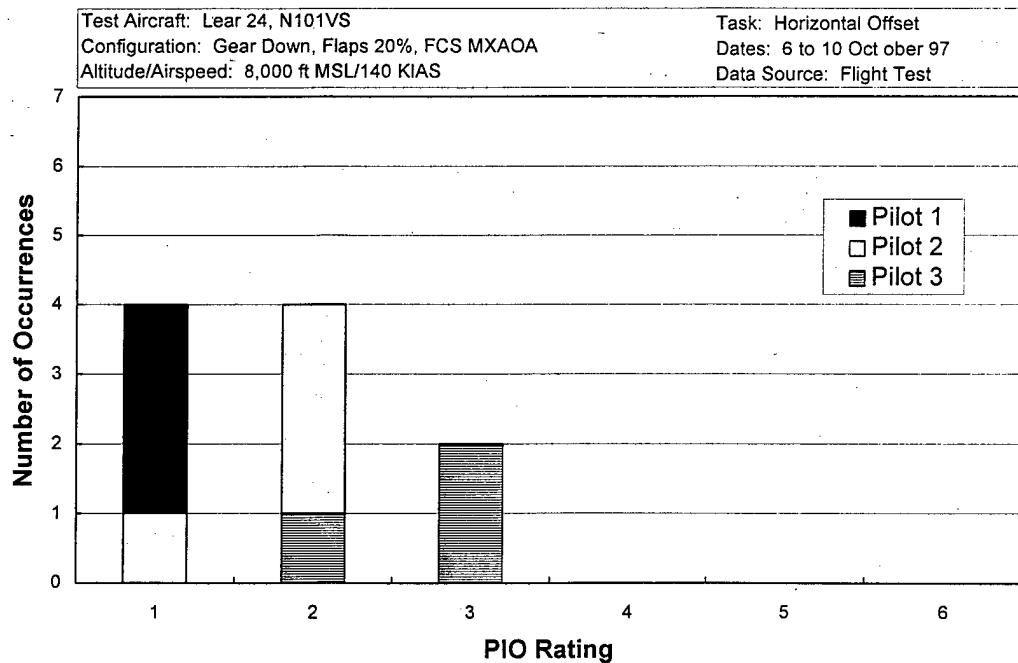| Appr	Task	Configuration	Landing Zone	C-H	PIO	Comments
1	St-In	H2AIN	Desired	4	2	trimming continuously / pitch sensitivity in the flare/ nose heavy after touchdown
2	St-In	H2AOA	Desired	5	3	hard to trim/very sensitive in pitch/heavy nose after touchdown
3	St-In	MXAOA	Desired	4	3	pitch "bobble" in the flare
4	St-In	H2INI	Desired	2	1	not affected by gusts/ very good flying qualities
5	Horiz	H2AIN	Desired	4	2	higher workload due to gusty winds
6	Horiz	H2AOA	Desired	4	3	trimming continuously/ pitch sensitivity in the flare/ nose heavy after touchdown
7	Horiz	MXAOA	Adequate	5	3	pitch sensitive in the flare/ light turbulence
8	Horiz	H2INI	Desired	4	2	mild undesirable motion and pitch sensitivity in the flare/ nose heavy after touchdown

Flight #3   **Mission date:** 7 Oct 97   **Eval Pilot:** Pilot #2 (Stevenson)
Winds: 280/18

Appr	Task	Configuration	Landing Zone	C-H	PIO	Comments
1	St-In	MXAOA	Desired	4	2	tendency to overshoot desired pitch attitude
2	St-In	H2AOA	Desired	6	4	small amplitude pilot-in-the-loop oscillation (PIO) in flare/ heavy nose on landing
3	St-In	H2AIN	Adequate	5	2	sluggish initial response
4	Horiz	MXAOA	Desired	3	2	predictable/no speed stability feedback/easy to fly
5	Horiz	H2AOA	Desired	4	1	divergent when off trim airspeed
6	Horiz	H2AIN	Desired	4	2	nose pitch up below trim airspeed/higher workload due to constant trim
7	Horiz	H2AOA	Desired	6	4	heavy stick in flare led to PIO/ sensitive to pilot bandwidth

Flight #4   **Mission date:** 7 Oct 97   **Eval Pilot:** Pilot #2 (Stevenson)
Winds: 270/20

Appr	Task	Configuration	Landing Zone	C-H	PIO	Comments
1	St-In	CLASSIC	Desired	3	1	predictable and responsive
2	St-In	H2INI	Desired	3	1	predictable/rapid initial pitch response
3	St-In	MXAOA	Desired	3	1	linear response/slight pitch overshoot in the flare
4	Horiz	CLASSIC	Desired	3	1	rapid initial response
5	Horiz	H2INI	Desired	4	2	sensitive to airspeed/high workload to maintain airspeed
6	Horiz	MXAOA	Desired	3	2	small pitch overshoot in flare (turbulence)
7	Horiz	H2INI	Desired	4	3	airspeed pitch sensitivity required higher workload
8	Horiz	MXAOA	Desired	3	1	precise pitch attitude changes required lower gain pilot technique

Flight #5 **Mission date:** 8 Oct 97 **Eval Pilot:** Pilot #3 (Cantiello)
Winds: Calm

Appr	Task	Configuration	Landing Zone	C-H	PIO	Comments
1	St-In	CLASSIC	Desired	2	1	beautiful, very good flying qualities
2	St-In	H2INI	Desired	2	1	very good flying qualities/ easy to trim
3	St-In	MXAOA	Desired	4	3	more sensitive in the flair/tendency to float
4	St-In	H2AIN	Desired	4	3	pitch sensitive in the flair/had to stay low gain
5	St-In	H2AOA	Desired	3	2	heavy nose in the flare
6	Horiz	H2INI	Desired	3	1	very nice to fly/nice control harmony and response
7	Horiz	CLASSIC	Desired	4	3	moderate workload due to sensitivity in pitch and mild undesirable motion
8	Horiz	MXAOA	Desired	4	3	mild undesirable motion/ tendency to float in flare
9	Horiz	H2AIN	Desired	3	2	slightly sensitive in the flare

Flight #6 **Mission date:** 8 Oct 97 **Eval Pilot:** Pilot #1 (Boe)
Winds: Calm

Appr	Task	Configuration	Landing Zone	C-H	PIO	Comments
1	St-In	H2AIN	Desired	3	1	no trim problems
2	St-In	H2AOA	Desired	6	3	divergent/worst flown configuration/ heavy stick forces for small speed changes
3	St-In	CLASSIC	Desired	2	1	very good flying qualities
4	St-In	MXAOA	Desired	3	2	pitch "bobble" in flare
5	Horiz	H2AOA	Desired	4	2	hard to trim/heavy nose after touchdown
6	Horiz	H2AIN	Desired	4	2	continuously trimming/ heavy nose in flare
7	Horiz	MXAOA	Desired	3	1	no trim problems
8	Horiz	CLASSIC	Desired	-	-	no grade - pilot unsure of workload
9	Horiz	CLASSIC	Desired	3	1	good flying qualities/light turbulence

E-14

Flight #9   **Mission date:** 9 Oct 97   **Eval Pilot:** Pilot #3 (Cantiello)
                      Winds: 230/10

Appr	Task	Configuration	Landing Zone	C-H	PIO	Comments
1	St-In	H2INI	Desired	2	2	very good fly qualities
2	St-In	MXAOA	Desired	4	1	pitch sensitivity in the flare/ light stick forces/tendency to float
3	St-In	MXAOA	Desired	4	3	undesirable motions which compromised the task
4	St-In	H2AIN	Desired	3	2	hard to trim precisely/small pitch "bobble" in flare
5	Horiz	H2INI	Desired	3	1	good control harmony
6	Horiz	MXAOA	Desired	2	2	no trim problems/easy to fly
7	Horiz	H2AIN	Desired	3	2	slight trim compensation

Appendix F
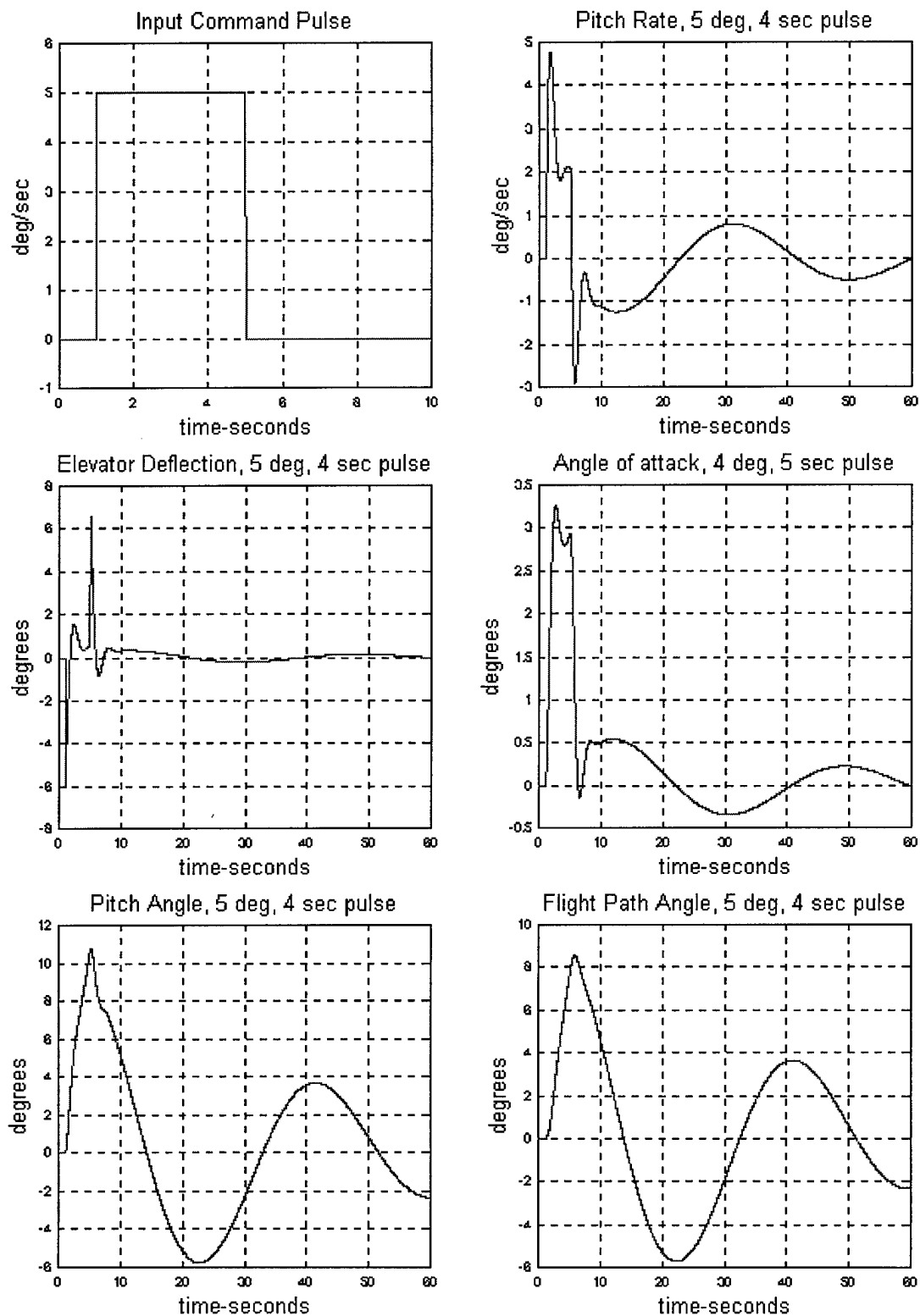
Handling Qualities Prediction Data

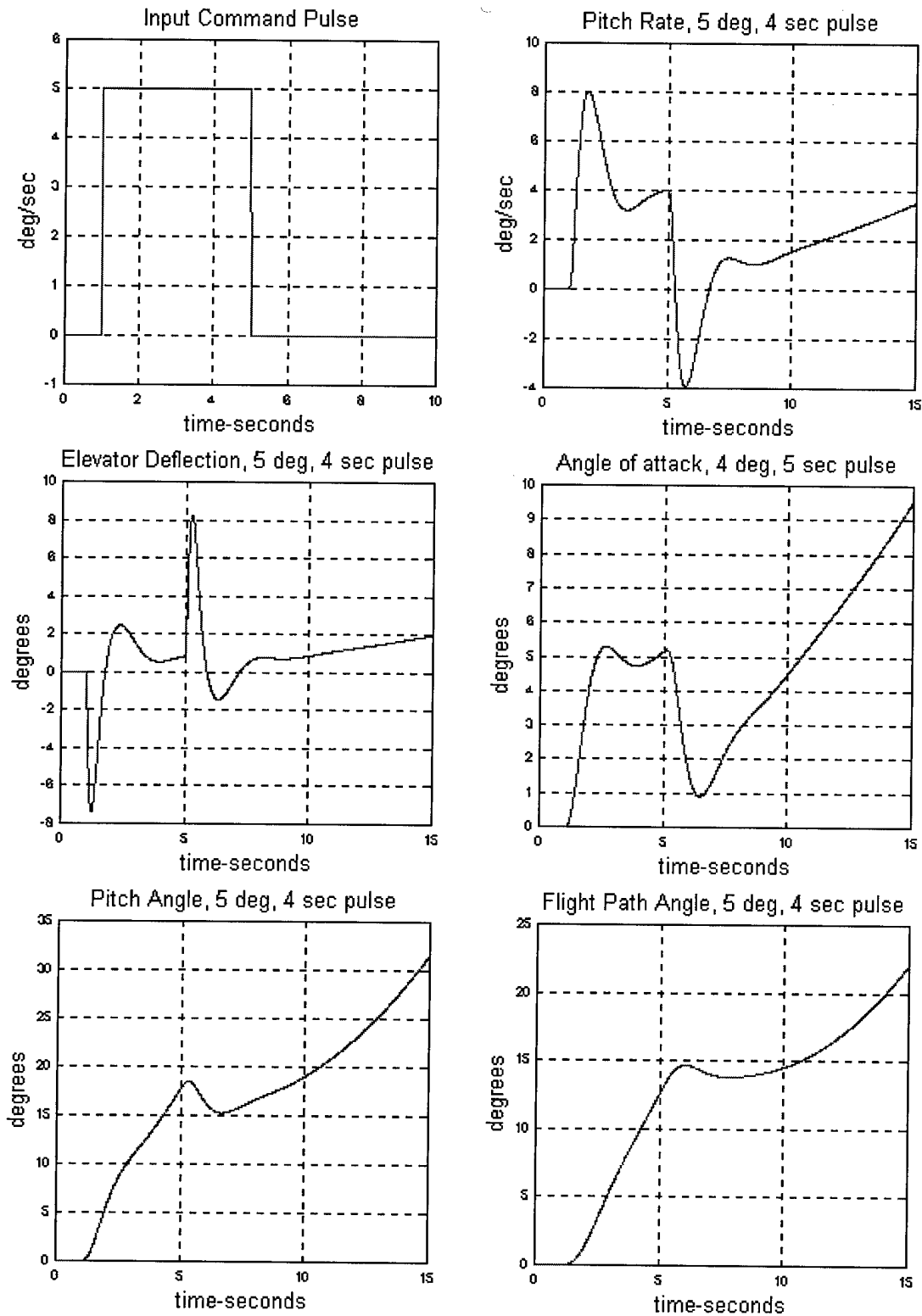Figure F1. CLASSIC Configuration Time Histories with Phugoid Mode-Noise Off

Figure F2. H2AOA Configuration Time Histories with Phugoid Mode-Noise off

Input Command Pulse

Pitch Rate, 5 deg, 4 sec pulse

Elevator Deflection, 5 deg, 4 sec pulse

Angle of attack, 4 deg, 5 sec pulse

Pitch Angle, 5 deg, 4 sec pulse

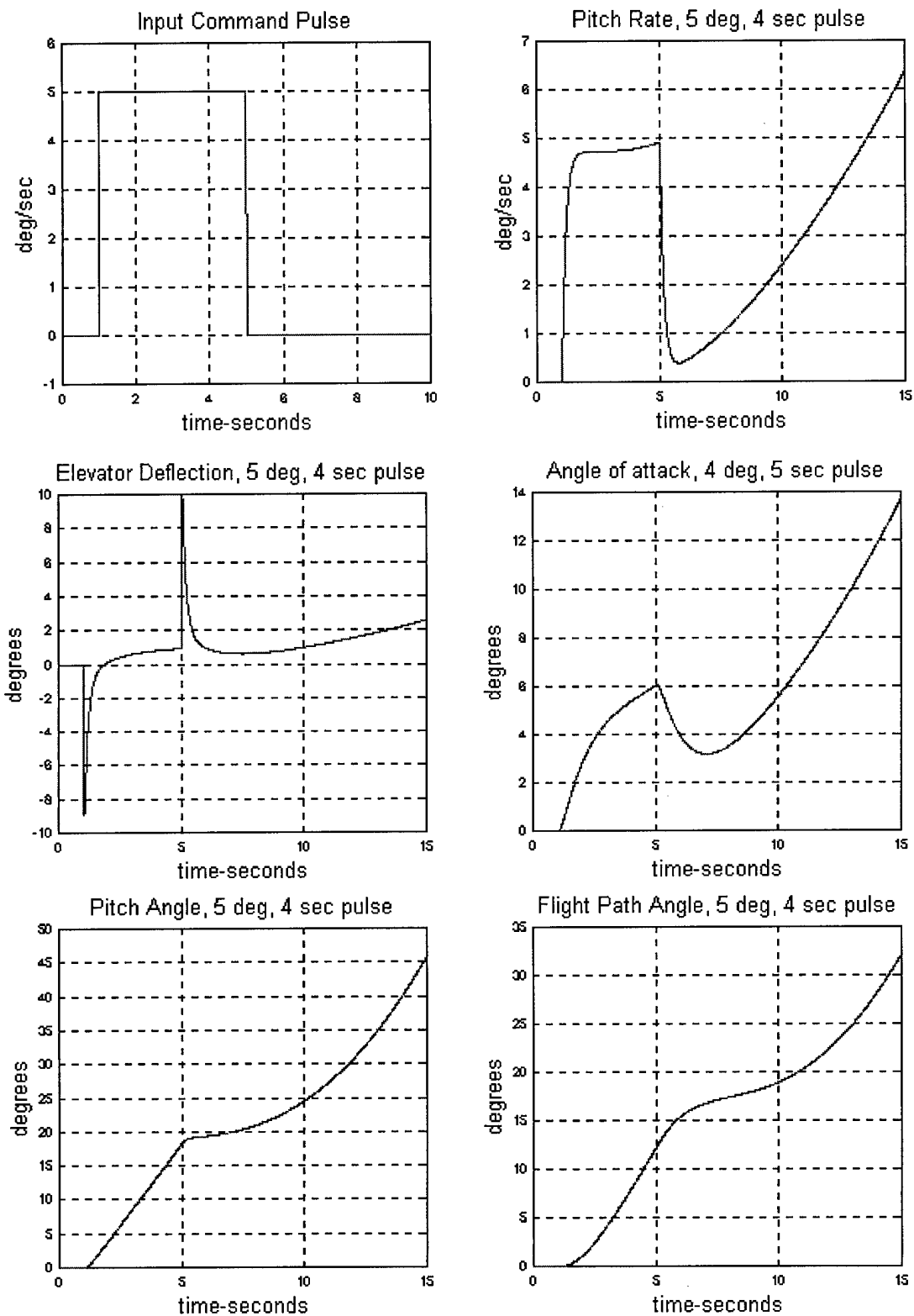## Flight Path Angle, 5 deg, 4 sec pulse

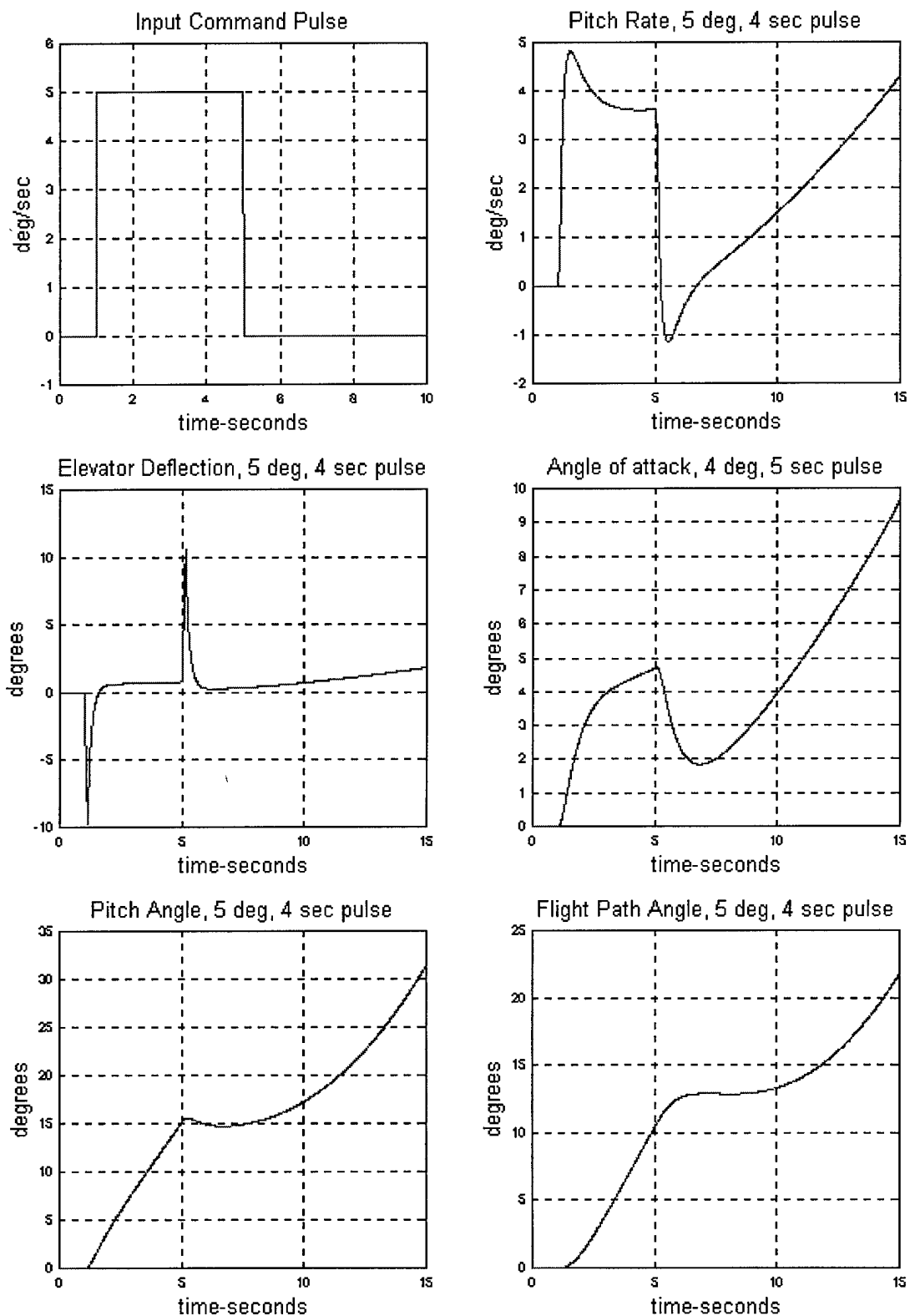Figure F3. H2INI Configuration Time Histories with Phugoid-Noise off

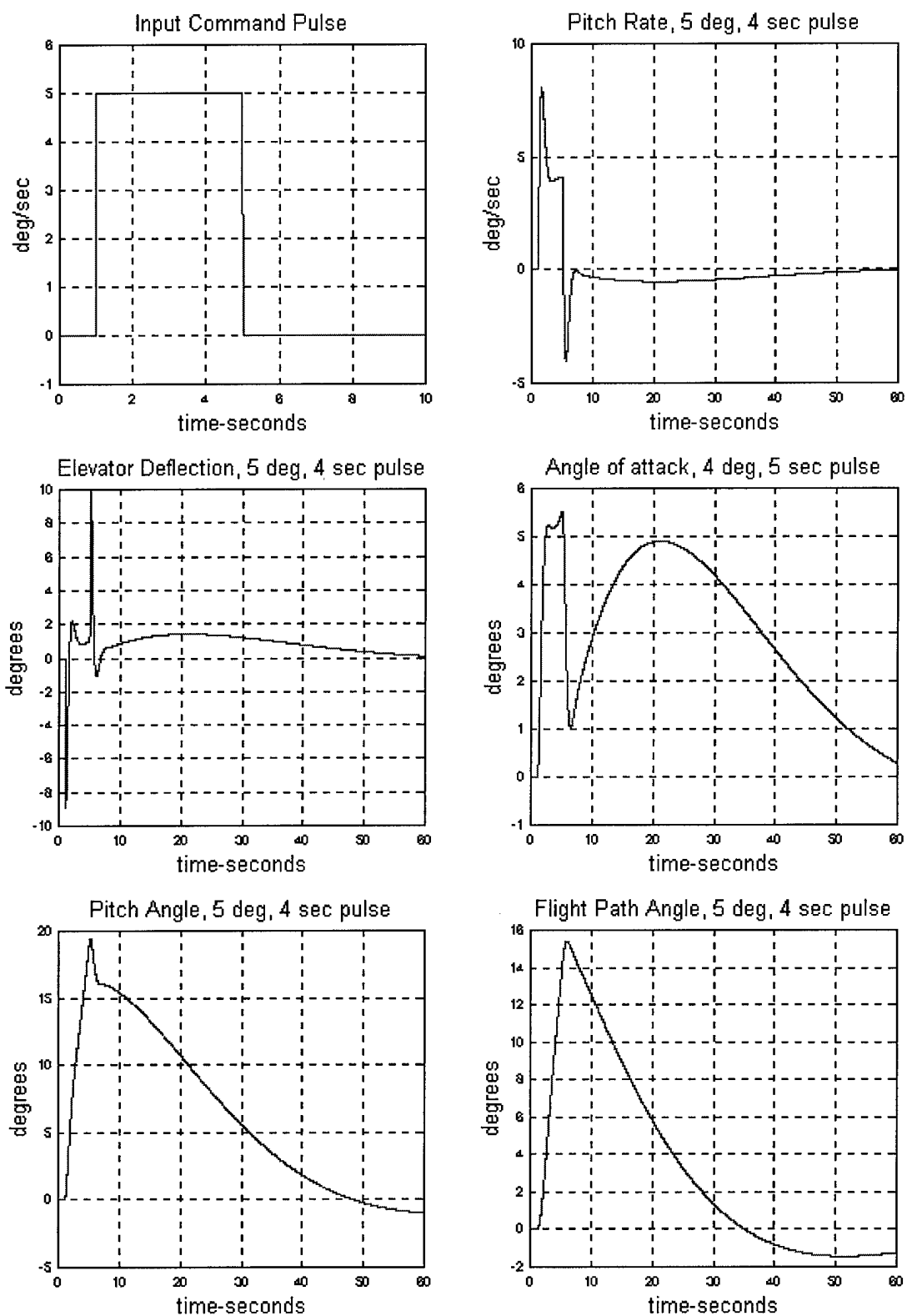Figure F4. H2AIN Configuration Time Histories with Phugoid-Noise off

Figure F5. MXAOA Configuration Time Histories with Phugoid-Noise off
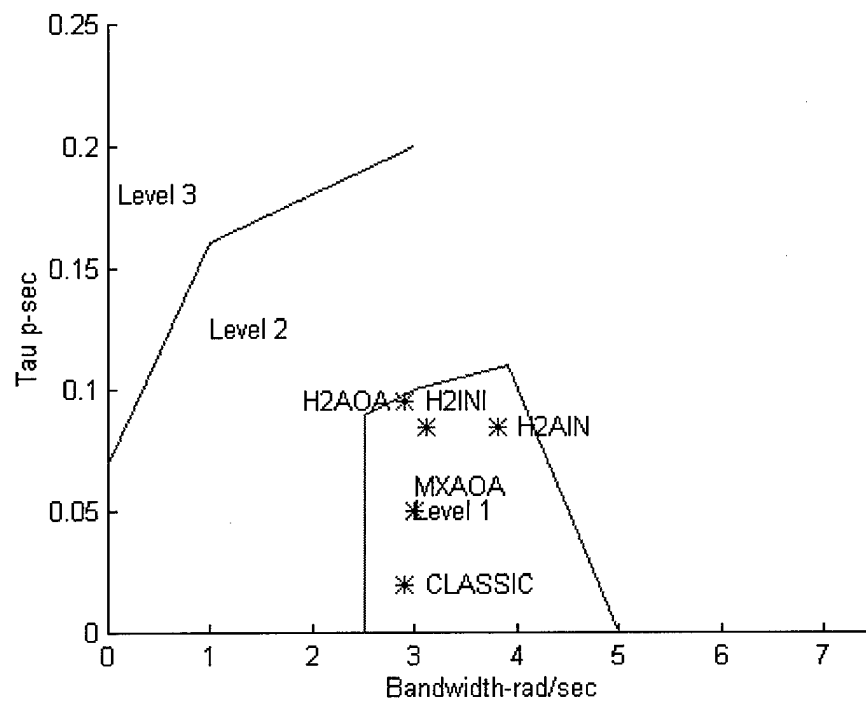
F-6

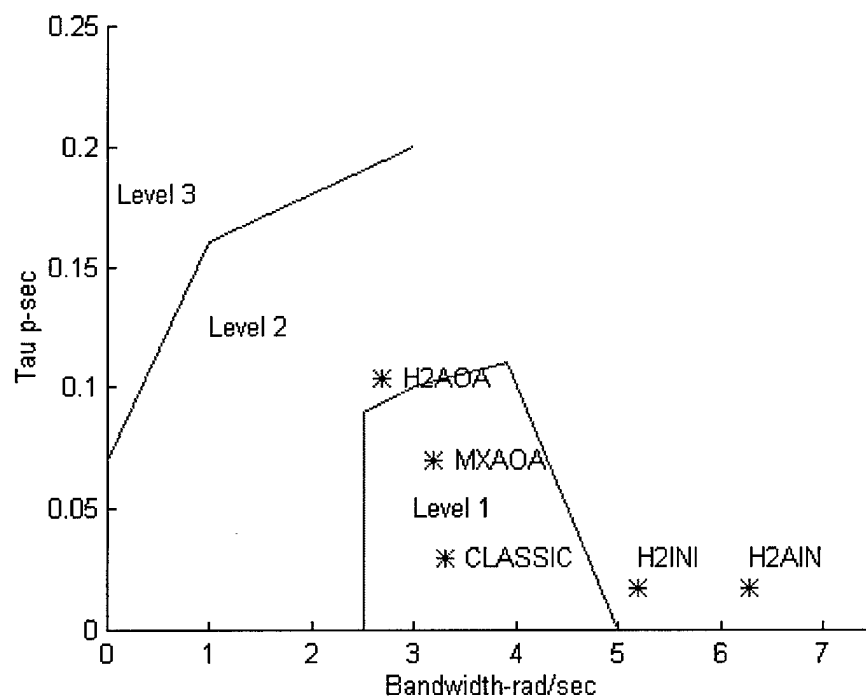Figure F6. Hoh's Bandwidth Handling Qualities Predictions without Phugoid

Figure F7. Hoh's Bandwidth Handling Qualities Predictions with Phugoid

1. D. S. Bernstein and W. H. Haddad. LQG Control with an H_∞ Performance Bound: A Riccati Equation Approach. *IEEE Trans. Auto. Control*, AC-34(3):293-305, March 1989.

2. D. B. Ridgely, L. Valavani, M. Dahleh, and G. Stein. Solution to the General Mixed H_2 / H_∞ Control Problem-Necessary Conditions for Optimality. *Proceedings of the American Control Conference,* 1348-1352, Chicago, IL, June 1992.

3. D. B. Ridgely, C. P. Mracek, and L. Valavani. Numerical Solution to the Mixed H_2 / H_∞ Optimization Problem. *Proceedings of the American Control Conference*, 1353-1357, Chicago IL, June 1992.

4. D. E. Walker. H_2 *Optimal Control with* H_∞, μ, L_1 *Constraints*. PhD Thesis, Air Force Institute of Technology, Dayton, OH, 1994.

5. A. Megretski. On the Order of Optimal Controllers in the Mixed H_2 / H_∞ Control. *Proceedings of the 33rd Conference on Decision and Control*, Lake Buena Vista, FL, December 1994.

6. D. R. Jacques, R. A. Canfield, D. B. Ridgely, M.S., Spillman. A MATLAB Toolbox for Fixed-Order Mixed-Norm Control Synthesis. *IEEE Control Systems*, Vol 16(5):36-44, October 1996.

7. P.T. Edwards, *Modern Flight Control Design, Implementation and Flight Test.* Masters Thesis, air Force Institute of Technology, Dayton, OH, 1007.

8. Military Standard, *Flying Qualities of Piloted Aircraft*. MIL-STD-1797A. Wright-Patterson Air Force Base, OH, January 1990.

9. K. Zhou, J. C. Doyle, K. Glover. *Robust and Optimal Control.* Prentice Hall, Upper Saddle River, NJ, 1996.

10. R. L. Daily. Lecture Notes for the Workshop on H_∞ and μ Methods of Robust Control. In conjunction with the *American Control Conference*, San Diego, CA, 1990.

11. A. Packard and J. Doyle. The Complex Structured Singular Value. *Automatica*, 29:71-109, 1993.

12. G. J. Balas, J. C. Doyle, K. Glover, A. Packard, and R. Smith. μ *-Analysis and Synthesis Toolbox.* The Mathworks. Inc., 1991.

13. J. S. Arora *Introduction to Optimum Design.* McGraw-Hill, Inc., New York, NY, 1989.

14. Snyders and M. Zakai. On Nonnegative Solutions of the Equation $AD + DA^T = -C^*$. *SIAM Journal of Applied Mathematics*, 18(3):704-714, May 1970.

15. R. H. Hoh, T. T. Myers, I. L. Ashkenas, R. F. Ringland, and S. J. Craig. *Development of Flying Quality Criteria for Aircraft with Independent Control of Six Degrees of Freedom.* AFWAL-TR-81-3027. Air Force Flight Dynamics Laboratory, Wright-Patterson Air Force Base, OH, April 1981.

16. D. A. Kivioja. *Comparison of the Control Anticipation Parameter and the Bandwidth Criterion During the Landing Task.* Master's Thesis, Air Force Institute of Technology, Dayton, OH, 1996.

17. G. F. Franklin, J. D. Powell, and A. Emami-Naeini. *Feedback Control of Dynamic Systems.* Addison-Wesley, second edition, 1991.

18. Milam and E. A. Thomas. F-16 Power Approach Handling Qualities Improvements. *Proceedings of the Society of Experimental Test Pilots*, 90-105, Beverly Hills, CA, September 1982.

19. D. B. Ridgely. Lecture Notes on Aircraft Control, Air Force Institute of Technology, Winter 1996.

20. SIMULINK: Dynamic System Simulation Software. The Mathworks, Inc., Natick, MA, 1992.

21. F. M. Hoblit. *Gust Loads on Aircraft: Concepts and Applications.* American Institute of Aeronautics and Astronautics, Inc., Washington, D. C., 1988.

22. D. McClean. *Automatic Flight Control Systems.* Prentice Hall, 1990.

23. C. J. Berthe, C. R. Chalk, and S. Sarrafian. An In Flight Investigation of Pitch Rate Flight Control Systems and Application of Frequency and Time Domain Predictive Criteria. *Journal of the American Institute of Aeronautics and Astronautics*, 84-1897, October 1984.

24. D. T. Berry. A Flight Path Overshoot Flying Qualitie metric for the Landing Task. *Journal of Guidance of the American Institute of Aeronautics and Astronautics,* Vol 9, No. 6, Nov-Dec 1986.

Vita

Captain John R. Anderson was born on 10 March 1966 in Albert Lea, Minnesota. He graduated from Glenville High School, Glenville, Minnesota in 1984. Captain Anderson attended the Illinois Institute of Technology in Chicago, Illinois where he earned his commission through AFROTC and a Bachelor of Science degree in Mechanical and Aerospace Engineering in 1988. He attended Undergraduate Navigator Training and Electronic Warfare Officer Training at Mather AFB, CA, where he received his wings in October, 1989. He was assigned to the 343rd Strategic Reconnaissance Squadron (SRS), Strategic Air Command (SAC), Offutt AFB, NE, flying the RC-135 V/W Rivet Joint. While at Offutt, Captain Anderson served as a flight instructor, flight evaluator, and mission director. Captain Anderson was reassigned to Las Vegas, NV for a data masked assignment in February 1994. Captain Anderson was selected for the Joint Air Force Institute of Technology/USAF Test Pilot School Program in February 1995. He graduated from the Experimental Test Navigator course in December 1997. Upon completion of his studies, he will be assigned to the 413th Flight Test Squadron at Edwards AFB, California, flight testing electronic warfare systems.

Permanent Address: Rural Route #1, Box 223
Glenville, MN 56036

REPORT DOCUMENTATION PAGE

Public reporting burden for the collection of information is estimated to average 1 hour per response, including the time for reviewing instructions, searching existing data sources, gathering and maintaining the data needed, and completing and reviewing the collection of information. Send comments regarding this burden estimate or any other aspect of this collection of information, including suggestions for reducing this burden, to Washington Headquarters Services, Directorate for information Operations and Reports, 1215 Jefferson Davis Highway, Suite 1204, Arlington, VA 22202-4302, and to the Office of Management and Budget, Paperwork Reduction Project (0704-0188), Washington, DC 20503.

1. AGENCY USE ONLY *(Leave blank)*	2. REPORT DATE March 1998	3. REPORT TYPE AND DATES COVERED Master's Thesis

4. TITLE AND SUBTITLE Flight Test and Handling Qualities Evaluation of a Longitudinal Flight Control System Designed Using Multiobjective Control Design Techniques	5. FUNDING NUMBERS JON: M96J0200 PEC: 65807
6. AUTHOR(S) John R. Anderson, Capt, USAF	

7. PERFORMING ORGANIZATION NAME(S) AND ADDRESS(ES Air Force Institute of Technology 2950 P Street Wright-Patterson OH 45433-6583	8. PERFORMING ORGANIZATION REPORT NUMBER AFIT/GAE/ENY/98M-01

9. SPONSORING / MONITORING AGENCY NAME(S) AND ADDRESS(ES) USAF Test Pilot School 220 S. Wolfe Ave Edwards AFB CA 93524 (805) 277-3000	10. SPONSORING / MONITORING AGENCY REPORT NUMBER N/A

11. SUPPLEMENTARY NOTES

12a. DISTRIBUTION / AVAILABILITY STATEMENT Approved for public release; distribution unlimited	12b. DISTRIBUTION CODE A

13. ABSTRACT *(Maximum 200 words)*

This thesis addresses the application of optimal, multiobjective control theory control theory to flight control design for the approach and landing phase of flight. Five flight control systems were designed using classical, H_2, H_∞ and Mixed H_2/H_∞ methods. The MATLAB™ MUTOOLS™ and AFIT MXTOOLS toolboxes were used to produce the optimal, multiobjective designs. These designs were implemented for flight test on the Calspan VSS I Learjet, simulating the unstable longitudinal dynamics of an F-16 type aircraft. A limited handling qualities investigation was performed. Model following was used in the design phase to meet handling qualities specifications. The designs were successfully implemented and verified on the Calspan Learjet prior to flight test. An unmodeled aircraft mode was discovered just prior to flight test that made three of the designs slightly unstable. However, all of the designs achieved Level II or better Cooper-Harper handling qualities ratings for the landing tasks performed illustrating that the optimal multiobjective methods used can give acceptable or better handling qualities.

14. SUBJECT TERMS Mixed H_2/H_∞ Optimization			15. NUMBER OF PAGES 217
handling qualities	flight control systems	VSS II Learjet	
variable stability	optimal control theory	H_2 Optimization	16. PRICE CODE
landing tasks	state-space optimization techniques	H_∞ Optimization	

17. SECURITY CLASSIFICATION OF REPORT	18. SECURITY CLASSIFICATION OF THIS PAGE	19. SECURITY CLASSIFICATION OF ABSTRACT	20. LIMITATION OF ABSTRACT
UNCLASSIFIED	UNCLASSIFIED	UNCLASSIFIED	SAR

NSN 7540-01-280-5500